MATHEMATICAL MODELING TO STUDY TRANSMISSION DYNAMICS OF HIV/AIDS, MALARIA AND DENGUE FEVER

Thesis

Submitted for the Award of the Degree of

DOCTOR OF PHILOSOPHY

in

Mathematics

By

SHOKET ALI

Registration Number: 41700199

Supervised By

Dr. Preety Kalra

Mathematics (Associate Professor)

Lovely Professional University,

Punjab (India)

Co-Supervised by

Dr. Ather Aziz Raina

Mathematics (Head & Assistant Professor)

Government Degree College Thannamandi,

Jammu & Kashmir (India)

LOVELY PROFESSIONAL UNIVERSITY, PUNJAB

2024

DECLARATION

I, hereby declared that the presented work in the thesis entitled **"Mathematical Modeling to Study Transmission Dynamics of HIV/AIDS, Malaria and Dengue Fever"** in fulfillment of the degree of **Doctor of Philosophy (Ph.D.)** is the outcome of research work carried out by me under the supervision of Dr. Preety Kalra (Supervisor), working as Associate Professor, in the Department of Mathematics, School of Chemical Engineering and Physical Sciences of Lovely Professional University, Punjab (India) and Dr. Ather Aziz Raina (Co-Supervisor), working as Head & Assistant Professor, in the Department of Mathematics, Govt. Degree College Thannamandi, Jammu & Kashmir (India). In keeping with the general practice of reporting scientific observations, due acknowledgements have been made whenever work described here has been based on findings of other investigator. This work has not been submitted in part or full to any other University or Institute for the award of any degree.

Signature:

Name of the Scholar: Shoket Ali
Registration No.: 41700199
Department: Mathematics
Lovely Professional University, Punjab (India)
Date: 6th August 2024

CERTIFICATE

This is to certify that the work reported in the Ph.D. thesis entitled **"Mathematical Modeling to Study Transmission Dynamics of HIV/AIDS, Malaria and Dengue Fever"** submitted in fulfillment of the requirement for the reward of the degree of **Doctor of Philosophy (Ph.D.)** in Mathematics, is a research work carried out by Shoket Ali (41700199), is a bonafide record of his original work carried out under my supervision and that no part of this thesis has been submitted for any other degree, diploma or equivalent course.

Signature

Dr. Preety Kalra

Associate Professor
Department of Mathematics
Lovely Professional University,
Punjab (India)
Date: 6th August 2024

Signature

Dr. Ather Aziz Raina

Head & Assistant Professor
Department of Mathematics
Govt. Degree College Thannamandi,
Jammu & Kashmir (India)

Abstract

The application of mathematical modeling in understanding diseases such as HIV/AIDS, Malaria and Dengue fever represents a cornerstone in the synergy between the fields of Mathematics, Biology and Medicine. Expanding on the existing trajectory in mathematical biology, this research endeavors to push the boundaries by not only formulating diverse mathematical models but also unraveling intricate mechanisms that govern disease progression. By employing differential equations, partial differential equations, and difference equations, this study aims to delve deeper into the dynamics of disease transmission and discern the nuanced response to therapeutic interventions, thereby bolstering our arsenal against these afflictions.

Furthermore, the integration of various mathematical approaches not only augments our comprehension of disease dynamics but also fosters the development of targeted strategies for disease control and management. The challenges inherent in deciphering the intricate biological complexities within the human system have prompted a reliance on computational techniques. The advent of high-speed computing has alleviated significant computational burdens, enabling the widespread application of these techniques to address physiological complexities that elude traditional analytical methods.

Dedicated to constructing specific mathematical models tailored to the complexities of HIV/AIDS, Malaria and Dengue fever, this thesis is structured into six chapters. Beginning with a comprehensive ‘General Introduction’, the groundwork is laid by introducing fundamental concepts crucial for understanding the subsequent chapters. Each subsequent chapter delves deeply into individual diseases, presenting a synthesis of analytical discoveries validated through meticulous numerical simulations. These numerical results, meticulously encapsulated in tables and graphs, serve as robust validations substantiating the analytical outcomes expounded upon throughout the thesis.

The comprehensive exploration of these diseases within this thesis transcends mere theoretical constructs, aiming to bridge the gap between mathematical abstraction and real-world clinical applicability. By synthesizing intricate mathematical models with empirical data, this research endeavors to not only elucidate disease dynamics but also pave the way for the translation of these findings into actionable insights for healthcare practitioners and policymakers. Moreover, the integration of empirical observations with mathematical formulations serves as a pivotal step toward personalized medicine, potentially tailoring treatment strategies according to the nuanced variations observed in different patient cohorts.

Furthermore, the thesis extends its scope by exploring the potential implications of the derived mathematical models beyond disease dynamics. It delves into the realms of epidemiological forecasting, offering a glimpse into the potential trajectories of these diseases under varying conditions and interventions. This predictive aspect stands as a testament to the versatility of mathematical modeling in not only understanding the present state but also in projecting future scenarios, thereby aiding in the proactive design of public health policies and interventions.

The intended research on disease dynamics will employ mathematical modeling to accomplish the following objectives:

1. To develop mathematical models for the analysis of severe human physiological problems like HIV/AIDS, malaria and dengue fever.
2. To find the solution of the developed models by using analytical as well as numerical techniques like Runge-Kutta method, finite difference method, etc. The soft computing techniques will also used to study complex models of severe human diseases.
3. To investigate various parameters like reproduction number, rate of spread of an infection, epidemic trends, the effects of treatment and vaccination, etc., which play an important role in understanding the transmission dynamics of the above-mentioned human diseases.
4. Validation of the solution of purposed models in the study with the previous published research work/literature.

Chapter 1: General Introduction

This chapter serves as a comprehensive introduction, covering fundamental concepts and mathematical models pertaining to severe human diseases like HIV/AIDS, Malaria and Dengue fever, supplemented by relevant literature. Within the realm of epidemiology, several successful applications of mathematical models are explored.

The introduction driving this study is delineated in Section 1.1, outlining the specific objectives and purposes. A review of the literature is in Section 1.2 and the objectives of the proposed work are in Section 1.3. Moving forward, Section 1.4 focuses on fundamental models concerning population dynamics in infectious diseases such as HIV/AIDS. Section 1.5 delves into the modeling intricacies of Malaria. Highlighting the specifics of Dengue fever, Section 1.6 delves into its modeling intricacies and Section 1.7 refers to the main terms used in the thesis. Mathematical preliminaries are discussed in Section 1.8. Some numerical methods have been elaborated on in Section 1.9.

Chapter 2: Stability Analysis of HIV/AIDS Transmission: A Mathematical Model for Sex Labourers

In this particular chapter, we proceed to develop a nonlinear mathematical framework that elucidates the transmission dynamics pertaining to HIV/AIDS within the community of women engaged in sex work by categorizing the population into male, female, and sex worker compartments. The formulated model delineates four distinct groups: susceptible, slowly infectious, rapidly infectious, and full-blown AIDS categories. Our investigation focuses on the fundamental reproduction number (R_0), which determines disease eradication. Moreover, we demonstrate that when (R_0) falls below one, the disease ceases, whereas when (R_0) surpasses one, the disease proliferates. Additionally, we conduct a stability analysis of both disease-free equilibrium (DFE) and endemic equilibrium (EE).

Chapter 3: Study of HIV Transmission Dynamics using SEIRS Epidemic Model

This chapter thoroughly explores disease transmission dynamics in two parts. The first Section-3(A) focuses on the intricate relationship between media awareness and HIV transmission, which is crucial for targeted prevention strategies. Section-3(B) examines the co-infection dynamics of HIV/AIDS and TB, considering the influence of media awareness. The overall aim is to contribute to a holistic understanding of disease transmission and the impact of media awareness on tailored public health strategies for these critical health challenges.

Section 3(A): Analyzing HIV Transmission Dynamics with Media Awareness

In this section, an analysis of the transmission dynamics of an SEIRS epidemic model for HIV is conducted through the utilization of a mathematical model. The focus of this analysis is on the impact of media. The research involves the development of a system of differential equations for each population group, which includes the susceptible, exposed, infected, and recovered classes. By employing rigorous mathematical analysis, the study presents a comprehensive understanding of the dynamics involved in the spread of the disease. The fundamental reproduction number (R_0) is performed and the examination of two equilibria, namely the endemic and disease-free states, offers valuable insights. Notably, it is established that the disease-free equilibrium is both locally and globally asymptotically stable. In order to verify the findings, numerical simulations are carried out using an innovative hybrid soft computing approach called the Adaptive Neuro-Fuzzy Inference System (ANFIS).

Section 3(B): Analyzing the Co-infection Dynamics of HIV/AIDS-TB with Media Awareness

This section extends the SEIRS epidemic framework to examine the specialized dynamics of co-infection among HIV and tuberculosis (TB). It emphasizes the nuanced understanding of this co-infection, focusing solely on HIV/AIDS and TB dynamics without the broader epidemic model structure. A literature review underscores the heightened vulnerability of HIV-infected individuals to TB, highlighting the critical role of treatment. The primary contribution lies in refining this specialized model and incrementally unraveling co-infection transmission and treatment outcomes. Future research directions emphasize exploring media awareness's influence within this specialized framework, aiming to pave the way for targeted interventions and further investigations into this intricate health challenge among diverse populations.

Chapter 4: Mathematical Analysis of Malaria Transmission: SEIRS Model with Mosquito Vector Dependency

This chapter introduces a mathematical model SEIRS illustrating how malaria spreads. Mosquitoes as carriers depend on humans for survival. Environmental factors contribute to malaria's spread. Managing and controlling malaria effectively reduces its transmission. The sensitivity analysis highlights that targeting pesticide use and improving drainage systems are crucial in combating the disease.

Chapter 5: The Study of Dengue Transmission Dynamics through the SEIR Model

This chapter introduces a mathematical model that delves into the transmission dynamics of dengue through an SEIR (Susceptible, Exposed, Infectious and Recovered) framework. Within this model, a logistic function is employed to depict the growth and persistence of the mosquito population, acting as the vector and relying on the human population for sustenance. The determination of the basic reproduction number R_0, serves to evaluate the disease transmission potential. Findings indicate that when $R_0 < 1$, the disease-free equilibrium is locally stable, whereas instability arises when R_0 exceeds one. Additionally, the stability analysis extends to both endemic and disease-free equilibria. The outcomes of this study offer valuable insights into dengue transmission dynamics, contributing to the formulation of effective disease control and prevention strategies.

Chapter 6: Conclusion and Future Scope

In this chapter, the culmination of this research unfolds as the conclusion encapsulates the key findings and implications of our mathematical modeling exploration into diseases like HIV/AIDS, Malaria and Dengue fever. Furthermore, the chapter outlines a compelling future scope, delineating avenues for continued research and the potential impact on public health strategies, limitations & areas for improvement.

The thesis contains a comprehensive and up-to-date bibliography.

I express my utmost gratitude to **Almighty Allah,** for His mercy and grace, guiding me through every challenge in life. His blessings provided the strength necessary to overcome the hardships encountered during this research journey. It's His guidance that steered me towards the right path and His pleasure remains my ultimate aspiration.

The completion of this thesis stands as a collective effort, drawing immense inspiration, encouragement, and support from esteemed teachers, parents, colleagues and friends. I am indebted to those who played pivotal roles in the successful completion of this project.

At this moment of accomplishment, I wish to extend my deepest gratitude and heartfelt thanks to my Supervisor, **Dr. Preety Kalra,** Associate Professor at the Department of Mathematics, Lovely Professional University, Punjab, India. Her guidance and motivation at every stage of my research have been instrumental. Her mentorship not only taught me to appreciate science and conduct research but also provided invaluable personal support, welcoming scientific discussions and attentively listening to my concerns.

Additionally, I owe a profound debt of gratitude to my Co-Supervisor, **Dr. Ather Aziz Raina,** Head and Assistant Professor at the Department of Mathematics, Govt. Degree College Thannamandi, Rajouri (J&K). Dr. Raina, a true gentleman, stands as a testament to hard work and intelligence. Without his invaluable help and unwavering support, the completion of this work wouldn't have been possible. His guidance and dedication have been indispensable in shaping this endeavor.

I am delighted to acknowledge the enthusiastic support and encouragement extended by the esteemed faculty of the University throughout this research endeavor.

Heartfelt gratitude extends to Dr. Madhu Jain, Associate Professor at the Department of Mathematics, Indian Institute of Technology Roorkee, for her consistent scholarly guidance, unwavering support and inspirational motivation. Dr. Jain's innovative ideas and positive criticism propelled me to perform at my best. Her sincere help and guidance were pivotal in shaping this endeavor.

I extend sincere thanks to Dr. Chandra Shekhar (Professor) and Dr. Rakhee (Professor) at Birla Institute of Technology and Science, Pilani, Rajasthan, for unwavering support, technical guidance and prompt assistance.

Special appreciation goes to Dr. Ram Singh and Dr. Rinku Mathur for their cooperation and critical evaluation of my research, which were crucial in shaping the presentation of my work.

I am indebted to Lovely Professional University, Punjab, for providing an excellent platform for my doctoral pursuits. Gratitude also extends to the libraries of IIT Kanpur and IIT Roorkee for granting access to relevant literature.

My heartfelt thanks to my wife, Tubassam Naz, for her unwavering support and encouragement throughout this research journey. I express my love and gratitude to my son, Mohammed Aahil, whose cheerful presence provided solace during moments of fatigue.

I owe immense gratitude to my parents, Shri Mir Wali and Smt. Maqsood Begum, for their unending blessings and unwavering support, which serve as a constant source of inspiration. I dedicate this thesis to them, acknowledging their love, support and sacrifices that paved my path to success.

Gratitude to my fellow researchers and friends, Dr. Rustam Abass and Dr. Anees Akbar, for their solidarity and collective support during my research period.

Finally, my heartfelt thanks to my younger brothers, Mr. Shahid Rabbani and Mr. Mohd Arif, for their inspiration and unwavering support, which were instrumental in successfully completing this work.

(Shoket Ali)

Contents

R_0	Basic Reproduction Number
WHO	World Health Organization
HIV	Human Immunodeficiency Virus
HIV-1	Human Immunodeficiency Virus type 1
AIDS	Acquired Immunodeficiency Syndrome
HCV	Hepatitis C Virus
WBCs	White Blood Cells
STDs	Sexually Transmitted Diseases
ART	Antiretroviral Therapy
SARS	Severe Acute Respiratory Syndrome
ANFIS	Adaptive Neuro-Fuzzy Inference System
COVID-19	Corona Virus Disease 2019
ODEs	Ordinary Differential Equations
TV	Television
mTB	Micro Tuberculosis
DFE	Disease Free Equilibrium
EE	Endemic Equilibrium
GDP	Gross Domestic Product
MSM	Men who have Sex with Men

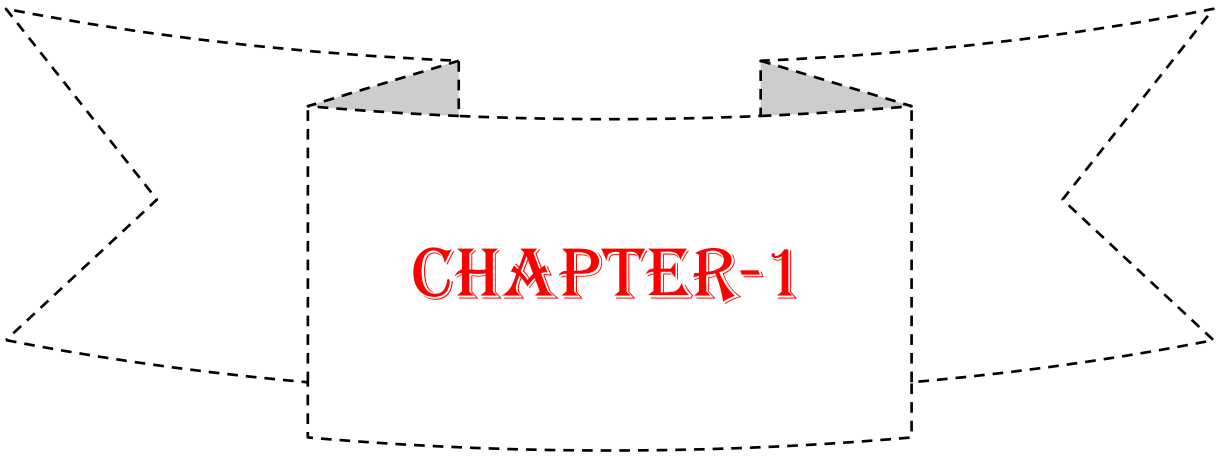

General Introduction

Keywords: Disease Dynamics, HIV/AIDS Modeling, Malaria Transmission, Dengue Fever and Mathematical Epidemiology.

Chapter 1: General Introduction

1.1. Introduction

Severe diseases wield a profound influence on human populations, causing immense suffering and imposing significant social and economic burdens. These diseases are among the leading causes of mortality, affecting millions worldwide and straining healthcare systems, especially in developing nations. Mathematical modeling emerges as an invaluable tool for delving deep into the vitals of these ailments. The primary goals of mathematical modeling in the context of severe diseases, whether examined over time or across geographical regions, are twofold: to uncover the basic procedure of ailment transference and the most influential factors driving their spread, thus facilitating predictive capabilities; and to devise and assess strategies for their control. Mathematical modeling of severe diseases has a rich history, resulting in a diverse array of models that shed light on the causes and patterns of epidemic outbreaks.

The realm of mathematical modeling is not only vast but also awe-inspiring in its application across biology, genetics and the medical sciences. It has established itself as a critical instrument for analyzing how infectious diseases spread and is controlled. Mathematical models possess the unique power to translate complex real-world disease scenarios into manageable mathematical structures, allowing for theoretical and numerical analyses that yield valuable insights and practical applications. Model formulation plays a crucial role in clarifying assumptions, identifying variables and parameters, and deriving key metrics, including thresholds, basic reproduction numbers and contact numbers.

The mathematical modeling process of human disease is depicted in Figure 1.1, demonstrating how mathematical modeling serves as a bridge between complex real-world scenarios and actionable insights.

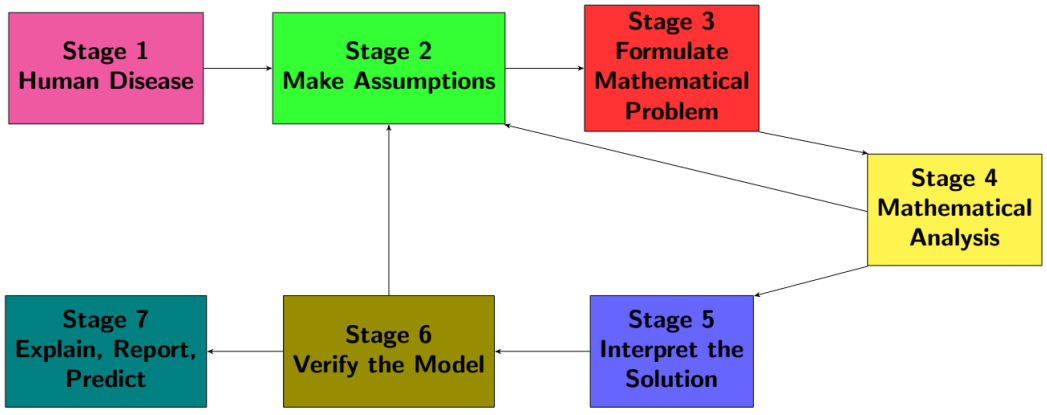

Figure 1.1: Human disease mathematical modeling procedure.

In the field of medical sciences, mathematical modeling, in conjunction with physiological fluid dynamics, plays a critical role. It has unraveled longstanding mysteries in biology, leveraging the computational power of computers to reveal insights previously hidden from researchers. Mathematical models and computer simulations play a crucial role as essential tools for experimentation, enabling the development and validation of theories, conducting sensitivity analyses and deriving key parameter estimates from empirical data. Carefully constructed mathematical models can be potent instruments for unraveling the intricate mechanisms underpinning various severe diseases.

Gaining insights into the spread patterns of communicable diseases across communities, regions and nations is crucial in the field of biosciences. Mathematical models play a vital role in facilitating the comparison, planning, implementation, evaluation and optimization of diverse programs related to detection, prevention, therapy and control. Epidemiological modeling contributes to the planning and analysis of epidemiological surveys by identifying crucial data needs, recognizing trends, providing overarching predictions and quantifying uncertainties in forecasted outcomes.

In this thesis, we focus on the spread dynamics of severe diseases, particularly employing ordinary differential equations (ODEs), compartmental models and related methodologies. Given the vast scope of mathematical modeling in the realm of diseases, it is impractical to undertake an exhaustive mathematical and computational analysis of all severe diseases and physiological challenges. Biological systems are intricate, making the construction of precise models a formidable task. This study aims to explore various facets of severe illnesses and physiological hurdles, focusing on developing models that elucidate the spread dynamics of diseases like HIV/AIDS, malaria and dengue fever. This thesis aims to provide a comprehensive exploration of fundamental concepts and modeling considerations relevant to our research.

1.2. Review of Literature

There are many serious diseases that spread globally through infections and sexual contact. One of the most severe and deadly diseases is HIV/AIDS, leading to millions of fatalities in both developed and developing countries. Researchers have used mathematical models to study HIV/AIDS, as over 35 million people worldwide live with this virus. In 2013, approximately 2.1 million new infections were documented, reflecting a 38% reduction compared to 2001. Moreover, HIV infections in children have declined by 58% since 2001. However, tuberculosis remains a primary cause of death in HIV patients. Research on this topic has advanced over the last three decades.

AIDS mainly spreads through bodily fluids, such as blood transfusions, physical contact and the use of infected needles. Researchers like Cai *et al.,* (2009) have used ordinary differential equations to create models for HIV/AIDS. Tan (1991) explored stochastic models to simulate AIDS and other infectious diseases. Ida *et al.,* (2007) described HIV infection using non-linear differential equations, which were solved numerically. Mukandavire and Garira (2007) introduced a mathematical framework for HIV/AIDS, integrating a distinct incubation period in the structure of a system comprising discrete time delay differential equations. The related infection of the Hepatitis C Virus (HCV) and HIV is a notable public safety concern, especially focused on preventing transmission among high-risk populations like injecting drug users. Yovanna *et al.,* (2013) reported an elevated risk of developing HCV-related liver disease, cirrhosis and liver cancer in individuals co-infected with both HIV and HCV.

Various approaches have been proposed to model HIV/AIDS among intravenous drug users. For example, Haynatzki *et al.,* (2000) suggested a new approach. Wu and Tan (2000) proposed a steady-state approach to modeling the HIV epidemic, assessing the quantities of AIDS cases and infectious individuals across various stages. Mathematical models were employed by Hyman and Stanley (1988) to comprehend the dynamics of the AIDS outbreak. Shen *et al.,* (2015) scrutinized the model and conducted an extensive analysis of global dynamics. They utilized Lyapunov functionals to confirm the worldwide stability of both disease-free and endemic equilibria. The essential reproduction number represented as R_0, is instrumental in determining the potential for the disease to ultimately dissipate.

Huo and Feng (2013) were instrumental in the development of a comprehensive model that integrates both slow and fast-latent sections. Simultaneously, Okosun *et al.,* (2013) delved into the realm of HIV/AIDS treatment and the testing of unknowingly infected individuals within a homogeneous population. In another notable contribution, Defeng and Wang (2013) introduced a time consuming mathematical model, aiming to evaluate the impact of vaccination and Antiretroviral Therapy (ART) on HIV/AIDS. Their model accounted for two distinct groups: individuals cognizant of their infected status and those oblivious to it.

Turning to the correlation between HIV/AIDS & the hepatitis C virus, Bhunu and Mushayabasa (2013) devised a meticulous mathematical model, while Cai *et al.,* (2014) explored the intricacies of an HIV/AIDS cured model that encompassed numerous infection stages and incorporated density-dependent infection dynamics. Kaur *et al.,* (2014) shifted the focus to a nonlinear model, investigating the transmission dynamics of the HIV/AIDS outbreaks with specific attention to the involvement of women hooker.

In the qualitative exploration of HIV dynamical models, Elaiw and Almuallem (2015) took on the challenge of understanding three models involving two sorts of co-circulating selected cells. Meanwhile, Wang *et al.,* (2015) conducted an analysis of the global stability of an HIV viral infection model that featured a continuous age structure. Huo *et al.,* (2016) contributed to the field by formulating a mathematical model of the HIV/AIDS epidemic that incorporated a treatment class. Notably, the fundamental reproduction number assumed a pivotal role in discovering the overarching global dynamics in their model.

In the early stages, many researchers worldwide began focusing on HIV/AIDS care, prevention and treatment. This disease has become a global challenge, leading to increased funding for HIV/AIDS over the past 15 years. Smith and Wahl (2005) devised an SIR model to characterize the immunological aspects of HIV dynamics. This model not only considered the standard elements but also incorporated the impact of reverse transcriptase inhibitors and other drugs designed to impede cellular contaminated. Sani *et al.,* (2007) developed various stochastic models to investigate HIV spread in a mobile heterosexual population, analyzing both deterministic and diffusion analogs of these models. Meanwhile, Naresh *et al.,* (2009) introduced an arithmetical replica, delving into the influence of tuberculosis on the dissemination of HIV contaminated within a person's inhabitants undergoing logistic growth. Addressing the broader spectrum of infectious diseases, Sing *et al.,* (2013) investigated the transmission dynamics of malaria, tuberculosis, HIV/AIDS and their co-infection, shedding light on the intricate interplay of these health challenges. Song *et al.,* (2010) scrutinized a classical arithmetical replica, incorporating a contrast reaction of the HIV-contaminated rate with a time hold-up, contributing to the refinement of our understanding.

In a nonlinear approach, Biswas and Pal (2017) devised a comprehensive HIV/AIDS mathematical model, examining transmission dynamics across four population compartments, incorporating factors such as vaccination and antiretroviral therapy. Turning to the broader dynamics, Jia and Qin (2017) formulated a model that delved into the intricate facets of the HIV/AIDS epidemic. Their approach featured a generalized nonlinear incidence rate, accounting for treatment alternatives. Employing a geometric method, they conducted a thorough analysis of the firmness of both ailment-free & native parity within the framework of ordinary differential equations.

In the tough of complex networks, Yuan *et al.,* (2018) proposed an SIR model, introducing birth and death rates to categorize contaminated humans into categories based on their ulceration status. This comprehensive approach added valuable insights to our understanding of the

dynamics within complex networks. Zhang and Guo (2018) developed a multi-phase SEIR model designed for infectious diseases, incorporating a continuous age structure for each consecutive infectious stage over an extended infective duration. The model is capable of illustrating the advancement of diseases across various infectious stages, resembling conditions such as HIV, hepatitis B & C. In the year 2018, Huo *et al.,* proposed a novel SEIS epidemic model that took into account the impact of media influence. The researchers employed the characteristic equation of equilibrium to derive the basic reproduction number, providing a quantitative measure of the disease's potential for spread and further developing steady-state stability within the model.

Malaria, caused by the Plasmodium parasite, remains a pressing global health challenge. The disease is primarily transmitted to humans through mosquito vectors, resulting in a spectrum of symptoms and complications. Mathematical models, such as the one initially presented by Ross in 1916, represented some of the earliest attempts to explore the dynamics of malaria transmission. Since then, numerous researchers, including Ngwa and Shu (2000) and Ngwa (2004), have formulated deterministic differential equation models to unravel the intricacies of endemic malaria, accounting for variations in both human and mosquito populations. Their work has been pivotal in identifying the primary drivers of disease transmission. Building on these foundations, Chitnis *et al.,* (2012) introduced models that incorporated factors such as immigration and disease-induced mortality, shedding light on the influence of these variables in the context of infectious agents and malaria transmission. These models provided valuable insights into the multifaceted factors affecting disease spread.

In the year 2017, Cai *et al.,* broadened the scope of research by developing a malaria model that introduced an asymptomatic category within the human population. Notably, their model incorporated exposed classes in both human populations and vector populations. An innovative aspect of their work proposed the potential for asymptomatic individuals to experience reinfection and transition to symptomatic states, contributing to a more comprehensive understanding of malaria dynamics. Similarly in 2018, Bakary *et al.,* contributed to the field by presenting a mathematical model that took into consideration the age distribution of the vector population and the periodic biting rate of female Anopheles mosquitoes. This approach added a layer of complexity, providing a more nuanced perspective on the intricate dynamics involved in the transmission of malaria.

Sing *et al.,* (2019) explored the stability of malaria transmission dynamics, with a specific focus on the mosquito-dependent coefficient for the human population. Their work shed light on

the complex interplay between human and vector factors. In 2020, Ibrahim *et al.,* presented an innovative model that intricately divided the infected population into two distinct segments: individuals who were unaware of their infection and those who were cognizant of it. The model introduced a novel perspective by asserting that the rate of expansion of cognizance was intricately linked to the number of creatures who remained unmindful of their infection. This novel approach provided a fresh and insightful outlook on potential strategies for disease control.

Al Basir *et al.,* (2021) designed a comprehensive mathematical model that investigated malaria dynamics while considering the impact of interventions based on awareness levels. Their concept suggested that the level of awareness could significantly influence disease transmission rates between vectors and humans and vice versa. It also explored how control methods could enhance awareness. Subsequently, Ndii and Adi (2021) introduced an innovative mathematical framework that divided the susceptible population into two distinct sub-groups: those who possessed awareness and those who lacked awareness. The model included a consistent consciousness estimate, suggesting that a segment of the initially uninformed vulnerable persons would shift into the category of informed creatures over time. Additionally, the model incorporated practical optimal control theory for vector management, taking into consideration the expenses linked to awareness campaigns.

In a recent advancement, Al Basir and Abraha (2023) introduced a foreordained arithmetical design to explore the vitals of malaria and assess the effects of interference like drift nets and germicides. Significantly, their model regarded awareness as a dynamic variable that undergoes changes over time, acknowledging the evolving nature of awareness campaigns and their impact. Lastly, Tchoumi *et al.,* (2023) put forth an arithmetical design that specifically addressed the vitals of malaria transmission, taking into account host susceptibility and specifically addressing the partial immunity acquired after infection. Researchers have broadened the scope of their malaria models by incorporating additional elements. These include assessing the evaluation of jungle fever resistance to mepacrine medications and the investigation of approaches such as mass treatment and the utilization of insecticides. For example, researchers such as Forouzannia and Gumel (2015) have examined the impact of anti-malarial drugs on malaria transmission, further enriching the field of malaria modeling.

Dengue Hemorrhagic Fever (DHF), first identified in the 1950s, poses a serious threat to children in the Americas and Asia. This virus, transmitted by female Aedes aegypti mosquitoes, leads to symptoms like bleeding and cardiovascular collapse. Unfortunately, there are currently no vaccines or targeted treatments available for dengue fever and it continue to spread globally,

with two of its four serotypes causing severe often fatal infections. Gubler (2002) highlighted the public health, social and economic issues related to dengue and DHF. Researchers like Augiar *et al.,* (2013) have used mathematical modeling to distinguish between primary and secondary infections, with implications for disease management. Smith and Mercer (2014) have examined dengue models that account for factors like seasonal influences and various subclasses.

The intricate connection between climate change and the transmission of dengue has attracted considerable attention. Bal and Sodoudi (2020) investigated how climate factors affect dengue occurrences in Kolkata, India, using modeling and prediction techniques. In contrast, Butterworth *et al.,* (2017) examined the possible impacts of weather change on the transmission of dengue in the southeastern United States, underscoring the importance of acknowledging local variations in climate. Caldwell *et al.,* (2021) broadened their scope to analyze mosquito-borne disease dynamics across continents using climate data. Davis *et al.,* (2021) presented a regional index for suitable situation to forecast the influence of weather change on the transmission of dengue. Ebi and Nealon (2016) underscored the need to adapt public health strategies to combat the increasing risks of dengue in a changing climate. Gutierrez *et al.,* (2022) supplied information on the meteorological factors associated with dengue outbreaks in the non-endemic area of Northwest Argentina. Huber *et al.,* (2018) highlighted the seasonality of dengue risk in relation to seasonal temperature variation and climate suitability. Kakarla *et al.,* (2020) evaluated the appropriateness and transmission capabilities of dengue in India under both current and anticipated climate change conditions, carrying implications for prevention and control. In a separate study, Mordecai *et al.,* (2017) employed mechanistic models to investigate how temperature affects the transmission of various mosquito-borne diseases. Ngonghala *et al.,* (2021) delved into the complex dynamics of vector-borne diseases in response to temperature changes. Nuraini *et al.,* (2021) developed a climate-based dengue model for Semarang, Indonesia, highlighting the importance of localized models. Taghikhani and Gumel (2018) enriched the theoretical foundation of dengue modeling by considering vector vertical transmission and temperature fluctuations. Wang *et al.,* (2022) provided insights into the vulnerability of dengue transmission to extreme weather conditions. Finally, Xu *et al.,* (2020) forecasted the outlook of dengue within the context of climate change scenarios, emphasizing the necessity for continuous research to tackle the evolving dynamics of dengue in a changing climate. These studies collectively underscore the critical relationship between climate change and dengue transmission, emphasizing the need for region-specific models and strategies to address the increasing threat of dengue in the circumstances of a varying climate.

Mathematical models play a vital role in understanding diseases like malaria and dengue. These models rely on mathematical equations, often in the form of differential equations and partial differential equations. They assist us in comprehending the conditions necessary for disease transmission and the dynamics associated with the spread of diseases. These models offer estimates of disease transmission and incidence under various scenarios, aiding us in predicting and combating these infectious diseases.

Incorporating factors like temperature fluctuations and vector parameters is crucial in these models. Research indicates that daily and seasonal temperature changes significantly impact the transmission of diseases such as dengue. These studies are essential for our improved comprehension and management of these diseases. Dengue in particular remains a global health concern and mathematical modeling can aid in exploring solutions to mitigate its impact.

In conclusion, mathematical modeling has significantly advanced our understanding the transmission dynamics of diseases like Dengue fever, HIV/AIDS & malaria. Researchers utilize these models to investigate the various factors influencing disease spread, assess the impact of interventions and treatments, and enhance our ability to control and manage these diseases on a global scale.

1.3. Objectives of the Proposed Work

Objectives of research proposal are given below.

1. To develop the mathematical models for the analysis of severe human physiological problems like HIV/AIDS, malaria and dengue fever.
2. To find the solution of the developed models by using analytical as well as numerical techniques like Runge-Kutta method, finite difference method, etc. The soft computing techniques will also used to study complex models of severe human diseases.
3. To investigate various parameters like reproduction number, rate of spread of an infection of epidemic trends, the effects of treatment and vaccination, etc., which play an important role in understanding the transmission dynamics of above mentioned human diseases.
4. Validation of the solution of purposed models in the study with the previous published research work/literature.

1.4. Modeling of HIV/AIDS

Even with advanced medicines and vaccines, some diseases remain deadly worldwide. Human Immunodeficiency Virus (HIV) is known for causing the dangerous Acquired Immune Deficiency Syndrome (AIDS). HIV primarily targets the immune system of the body, particularly CD cells that originate in the bone marrow. Within this group of cells, certain ones

are specifically targeted by the virus and become infected. T-cells a subset of lymphocytes, which are a type of white blood cells (WBCs), are among the key components affected by HIV infection. These WBCs protect the body from infections and T-cells are the front-line soldiers that fight against infections. There are various types of T-cells, each with its own role in identifying, attacking and destroying harmful agents. Alongside other WBCs, they play a critical role in the immune system, safeguarding the body from infections. These cells mature and develop in an organ in the chest called the thymus because they are initially produced in the bone marrow.

The transmission of AIDS has been a subject of debate. It is now widely accepted that bodily fluids, like blood transfusions, close physical contact, the use of infected needles and childbirth, are the primary ways this deadly disease spreads. Jones and Perelson (2005) conducted experiments that showed that when awake antiretroviral therapy is consistently given to HIV-1 contaminated patients for extended periods, almost all victim reach viral loads that standard tests cannot detect.

In their study, Cai *et al.*, (2009) formulated an ODEs model related to HIV/AIDS, focusing on the transitions of infected individuals from the symptomatic to the asymptomatic stage while considering different treatment options. Meanwhile, the significance of systematic reviews and meta-analyses in identifying risk factors for infections is growing, exerting influence on global policy decisions (cf. Tacconelli and Cataldo, 2009; Smallbone and Simeonidis, 2009).

1.4.1. Basic Model of HIV/AIDS

Let the entire sexually active population be denoted as N, which is further classify into two class: the vulnerable (HIV-negative) denoted as S, and the infected denoted as I. Λ is commonly understood as the rate at which individuals join the sexually active population over a specific period, while the departure of individuals from this population is indicated by the rate μ. Moreover, β represents the likelihood of contracting HIV in a single sexual partnership with an HIV-positive human and c denotes the rate at which new partnerships are formed. It is hypothesized that individuals who contract HIV experience an increased probability rate equal to α.

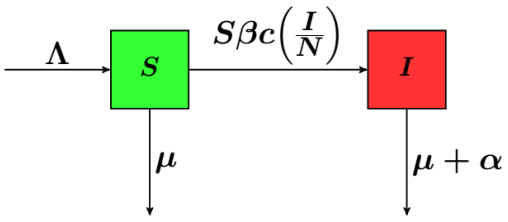

Figure 1.2: Transition diagram illustrates the dynamics of HIV.

The rate of new infections is calculated by multiplying the estimate at which recently developed association are formed (c), the rate at which the single sexual partnerships with an HIV-positive (β), and the chance that the partner is HIV-positive $\left(\frac{I}{N}\right)$. The following is an expression of the model in terms of differential equations:

$$S' = \Lambda - S\beta c\left(\frac{I}{N}\right) - \mu S \tag{1.1}$$

$$I' = S\beta c\left(\frac{I}{N}\right) - (\mu + \alpha)I \tag{1.2}$$

Notations:

Λ: Individuals entering the sexually active population at rate of μ.

β: Likelihood of contracting HIV from a single sexual partner.

c: The rate at which new alliances are established.

α: Rate of increase of HIV infected individuals.

1.5. Modeling of Malaria

The word malaria comes from the Latin word "malaria". The Romans observed illness after night air walks. Dr. Ronald Ross, a British medical officer in Hyderabad, India, first identified mosquitoes as malaria transmitters about a century ago. His Nobel Prize-winning research in 1902 discovered that the black pigment found in human disease also exists in mosquito bellies. He developed the traditional Ross model, a foreordained distinctive calculative replica for malaria that includes susceptible (S_h) and infected (I_h) compartments. Mosquitoes with compartments (S_m, I_m) adhere to the SI structure due to their inability to recover from infection. Ross investigated the evolution of infected class fractions (I_h, I_m) using two differential equations, one for humans and one for mosquitoes.

One in every five children in Africa dies before the age of five, with a malaria parasite taking a kid every 30 seconds and causing over a million deaths each year. Malaria impacts 300 million individuals' worldwide, killing 1-1.5 million people each year. Malaria, which is caused by Plasmodium parasites and spread by female Anopheles mosquitoes, was mathematically modeled by Ross in 1911. Factors influencing infected vector movement effect disease transmission, which is shaped by parasite, vector and host interactions. The first models were

two-dimensional and represented humans and mosquitoes. Mathematics, notably in the SIR model plays a significant role in infectious diseases, categorizing states as susceptible, infectious and recovered.

The model, which investigates malaria control through mass treatment and insecticides, takes into account sensitive and resistant parasite strains. Malaria-induced human mortality is linked to the backward bifurcation phenomena. Humans enter the system in a susceptible state at birth β_1, move to an infectious state when contracting the disease α_1 and can recover α_2 or exit via death d. Immigration and natural death occur at rates β_2, with the total population denoted as N (Forouzannia and Gumel, 2014; Erin *et al.*, 2013). Mathematical modeling facilitates the examination of malaria indicators, translating measurable data into transmission measures, addressing concerns with traditional methods and allowing direct comparisons across transmission intensities and seasonal patterns.

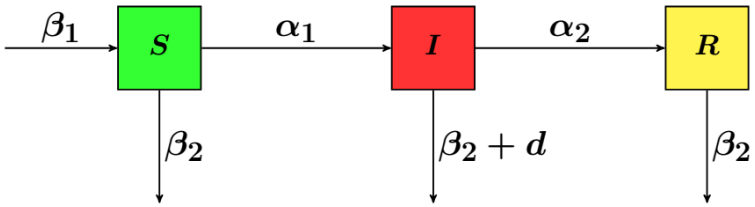

Figure 1.3: Transition diagram of the SIR model of malaria.

Figure 1.3 can be explained using the mass action law and a set of differential equations.

$$S' = \beta_1 - (\alpha_1 + \beta_2)S \tag{1.3}$$

$$I' = \alpha_1 S - (\alpha_2 + \beta_2 + d)I \tag{1.4}$$

$$R' = \alpha_2 I - \beta_2 R \tag{1.5}$$

Ngwa and Shu (2000) adopt an immunity model wherein the total population fluctuates and a notably high disease-related death rate is taken into account. This model comprises four human compartments: (i) Susceptible (S_h), (ii) Exposed (E_h), (iii) Infected (I_h), and (iv) Immune (R_h). Additionally, the mosquito component includes three compartments: (i) Susceptible (S_m), (ii) Exposed (E_m) and (iii) Infected (I_m).

To investigate mosquito population dynamics, Parham and Michael propose a model incorporating the concurrent impacts of rainfall and temperature. The human component of the model comprises three compartments (S_h, I_h, R_h) with a fixed latency duration, while the mosquito component includes three compartments (S_m, I_m, R_m). Environmental elements are

incorporated into the model through parameters associated with mosquitoes. Adult mosquito birth rates are modeled as functions influenced by both rainfall and temperature. Additionally, various mosquito-related factors such as mortality rates, biting rates, sporogonic cycle duration and the likelihood of infected mosquitoes surviving during the parasite's incubation time are all temperature-dependent. The significance of this model lies in its ability to demonstrate the variations in the patterns of rainfall not only impact vector abundance but also play a crucial role in governing malaria endemicity, invasion and extinction. Nevertheless, in situations where sufficient rainfall supports vector development and survival, temperature primarily influences the pathogen life cycle, exerting a more significant impact on the rate of disease spread.

Describing the fundamental process of infectious agent transmission in the host population is essential in epidemiological compartment models. When a pathogen emerges within a host community, individuals are classified based on factors such as parasite density and infection type. Following the convention established by Kermack and McKendrick (1927), these categories are denoted by the standard notations S, E, I and R. The susceptible group constitutes a fraction of the population vulnerable to infection, while the exposed E class represents individuals infected but incapable of transmitting the infection during the latent period. The infectious I class comprises individuals who propagate the infection through interactions with susceptible individuals. Lastly, those recovering from the infection constitute the R class.

1.6. Modeling of Dengue

Dengue is acknowledged as a highly perilous illness with the potential for fatal outcomes. The disease results from one of four identified strains of the flavivirus, specifically DEN-1, DEN-2, DEN-3 and DEN-4. Transmission primarily occurs through female Aedes aegypti mosquitoes and in certain instances, Aedes albopictus can also be implicated in transmitting the disease. The modes of transmission include the transfer of the disease from adult female mosquitoes to their offspring, mechanical transmission from a non-infected human and passing on from a transmissible mosquito to a healthy person.

1.6.1. Basic SIR Model for Dengue Fever

A basic mathematical model for dengue fever can be constructed using the SIR (Susceptible-Infectious-Recovered) framework. In this model, the citizenry is divided within three compartments: (i) susceptible $S(t)$, (ii) infectious $I(t)$ and (iii) recovered $R(t)$. Individuals

move from the susceptible to the infectious compartment upon infection and then to the recovered compartment after they have improved from the disease and gained invulnerability.

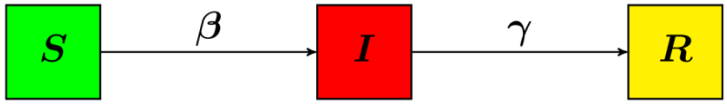

Figure 1.4: Transition diagram of the SIR model of dengue fever.

The framework comprises the subsequent set of differential equations:

$$S' = -\beta SI \tag{1.6}$$

$$I' = \beta SI - \gamma I \tag{1.7}$$

$$R' = \gamma I \tag{1.8}$$

Notations:

β: The rate at which transmission occurs from susceptible individuals to those who have become infected.

γ: The rate at which infected individuals recover and are classified as recovered individuals.

The basic SIR model assumes constant population size and homogeneous mixing within the population. This model yields insights into the dynamics of the disease, such as the potential for outbreaks, the impact of different interventions (such as vaccination or vector control) and the eventual establishment of immunity in the population. The model's parameters β and γ can be estimated based on available data and can vary based on factors such as the mosquito population density, human behavior and climate conditions.

1.7. Main Terms Used in the Thesis

1.7.1. Stability Analysis

Stability analysis is a fundamental aspect of understanding the behavior of mathematical models in epidemiology. It helps determine the conditions under which a disease-free or endemic equilibrium is stable or unstable, thus providing insights into the long-term behavior of the disease within a population. This section introduces the basic concepts and methodologies used in the stability analysis of epidemiological models.

❖ **Locally Asymptotically Stable**

A system is **locally asymptotically stable** if the following conditions are met:

1. **Equilibrium Point**: There exists an equilibrium point $x = 0$.

2. **Local Stability**: The equilibrium point is stable in the sense of Lyapunov, meaning for every small initial condition $x(0)$ close to $x=0$, the solution $x(t)$ remains close to $x=0$ for all $t \geq 0$.
3. **Asymptotic Stability**: Additionally, $x(t)$ not only remains close to $x=0$ but also tends to $x=0$ as $t \to \infty$.

Mathematically, this means that for any given $\in > 0$, there exists a $\delta > 0$ such that if $\|x(0)\| < \delta$, then $\|x(t)\| < \in$ for all $t \geq 0$, and $\lim_{t\to\infty} x(t) = 0$.

❖ **Globally Asymptotically Stable**

A system is **globally asymptotically stable** if the following conditions are met:

1. **Equilibrium Point**: There exists an equilibrium point $x=0$.
2. **Global Stability**: The equilibrium point is stable in the sense of Lyapunov for any initial condition $x(0)$ in the entire state space, meaning the solution $x(t)$ remains bounded and close to $x=0$ for all $t \geq 0$ regardless of the initial state.
3. **Asymptotic Stability**: Additionally, $x(t)$ tends to $x=0$ as $t \to \infty$ for any initial condition $x(0)$ in the entire state space.

Mathematically, this means that for any initial condition $x(0)$ in the entire state space, $\|x(t)\| \to 0$ as $t \to \infty$.

1.7.1.1. Equilibrium Points

In the context of infectious disease modeling, equilibrium points (also known as steady states) are values of the state variables (e.g., susceptible, infected, and recovered individuals) where the system does not change over time. These can be classified into:

❖ **Disease Free Equilibrium (DFE)**

The disease-free equilibrium is a key concept in epidemiological modeling. It represents a situation where a population is entirely free from a specific infectious disease. In this state, no individuals in the population are infected with the disease, and the transmission of the disease has been effectively controlled or eradicated.

Mathematically, the DFE happens when there is no new contamination in the inhabitants. In epidemiological models, this equilibrium is typically elaborated by a set of equations where the number of new infections is counterbalanced by factors like recovery, immunity, or other mechanisms preventing the disease from spreading.

The DFE is a critical concept because it sheds light on the conditions necessary to prevent or eliminate a disease from a population. It guides public health officials and policymakers in designing effective interventions such as vaccination campaigns and quarantine measures to establish and sustain a disease-free state in a population.

❖ **Endemic Equilibrium (EE)**

In epidemiology, endemic equilibrium describes a situation where an infectious disease maintains a stable and consistent presence within a population for an extended period. At this equilibrium, the disease persists at a relatively constant level, with new infections balanced by recoveries and other factors, resulting in steady disease prevalence.

Mathematically, endemic equilibrium occurs when the number of new the capable of equals the number of recoveries or disease-related deaths. In epidemiological models, this equilibrium is represented by equations that balance the rates of infection and recovery, creating a stable state of disease prevalence.

Importantly, endemic equilibrium doesn't mean that every individual in the population is affected simultaneously; rather it signifies that the disease has become a predictable and stable part of the population's health profile. Factors contributing to endemic equilibrium may include immunity, vaccination, and other interventions that influence disease transmission dynamics within the population.

1.7.1.2. Methods of Stability Analysis

❖ **Linear Stability Analysis**

This method involves linearizing the nonlinear system around the equilibrium point and analyzing the eigenvalues of the resulting Jacobian matrix.

1. **Jacobian Matrix:** The matrix of first-order partial derivatives of the system's equations evaluated at the equilibrium point.
2. **Eigenvalues:** The sign of the real part of the eigenvalues determines stability:
    - If all eigenvalues have negative real parts, the equilibrium is locally asymptotically stable.
    - If any eigenvalue has a positive real part, the equilibrium is unstable.

❖ **Reproduction Number**

The reproduction number is a fundamental concept in epidemiology used to measure the transmission potential of a disease within a population.

Basic Reproduction Number (R_0)

The basic reproduction number R_0 is defined as the average number of secondary infections produced by a single infected individual in a completely susceptible population (i.e., where no one is immune).

- If $R_0 > 1$: Each infected individual, on average, infects more than one other person, leading to the potential for an outbreak or epidemic, as the disease can spread exponentially.
- If $R_0 = 1$: Each infected individual, on average, infects exactly one other person, leading to a steady state where the disease remains in the population at a constant level.
- If $R_0 < 1$: Each infected individual, on average, infects less than one other person, leading to the eventual decline and possible eradication of the disease.

❖ **Lyapunov's Method of Stability**

Lyapunov's method is a widely used technique in control theory to determine the stability of a dynamical system. The method involves constructing a Lyapunov function, a scalar function that provides a measure of the system's energy or a generalized measure of distance from equilibrium.

♦ **Lyapunov's Direct Method**

Basic Concepts:

1. **Lyapunov Function:** A Lyapunov function $V(x)$ is a scalar function that is continuously differentiable and satisfies certain properties to help determine stability.
2. **Equilibrium Point:** The equilibrium point $x = 0$ is the state at which the system does not change, i.e., $\dot{x} = f(x) = 0$.

Steps to Use Lyapunov's Direct Method:

1. **Choose a Candidate Lyapunov Function $V(x)$:**
   - $V(x)$ should be positive definite: $V(x) > 0$ for all $x \neq 0$ and $V(0) = 0$.
2. **Compute the Time Derivative $V(x)$:**
   - Calculate the derivative of $V(x)$ along the system trajectories: $\dot{V}(x) = \frac{dV}{dt} = \nabla V(x).f(x)$.
3. **Analyze the Sign of $\dot{V}(x)$:**

- If $\dot{V}(x)$ is negative definite $\left(\dot{V}(x) < 0 \; for \, all \; x\right)$, the equilibrium at $x = 0$ is **asymptotically stable**.
- If $\dot{V}(x)$ is negative semi-definite $\left(\dot{V}(x) < 0 \; for \, all \; x\right)$, the equilibrium at $x = 0$ is **stable** in the sense of Lyapunov.
- If $\dot{V}(x)$ is positive definite or not negative semi-definite, the equilibrium is **unstable**.

♦ **Lyapunov's Indirect Method (Linearization Method)**

This method is useful when finding a Lyapunov function is difficult, the indirect method (or linearization method) can be used.

Steps to Use Lyapunov's Indirect Method:

1. **Linearize the System Around the Equilibrium Point:**
   - For a nonlinear system $\dot{x} = f(x)$, linearize it around the equilibrium point $x = 0$ to obtain $\dot{x} \approx Ax$, where $A = \frac{\partial f}{\partial x}|_{x=0}$ is the Jacobian matrix.
2. **Analyze the Eigenvalues of the Jacobian Matrix A:**
   - If all eigenvalues of A have negative real parts, the equilibrium point is **asymptotically stable**.
   - If any eigenvalue has a positive real part, the equilibrium point is **unstable**.
   - If eigenvalues have zero real parts or purely imaginary eigenvalues, further analysis is required (the system may be stable, asymptotically stable or unstable).

1.7.2. Population Dynamics

Population dynamics is the branch of ecology that investigates how populations evolve in terms of size, composition and distribution over time and space. It encompasses a wide range of species, from animals to plants and microorganisms, and is essential for comprehending ecological processes and interactions in ecosystems. This field delves into factors such as birth rates, death rates, immigration, and emigration patterns within a population. Environmental factors like resource availability, predation, disease and competition all play a role in population size. Through the study of population dynamics, ecologists and researchers uncover the underlying mechanisms that influence ecosystems, species relationships, and biodiversity. Mathematical models are commonly used to simulate and forecast population changes under different scenarios. These models help scientists grasp complex ecological systems and make predictions about the future dynamics of populations. As a result, population dynamics hold

great importance in fields like conservation biology, wildlife management and the evaluation of the effects of human activities on natural ecosystems.

1.7.3. Latent Period

The latent period in mathematical modeling, commonly employed in epidemiology and other disciplines refers to the time lapse between an initial event or exposure and the appearance of a specific effect or outcome. In epidemiological modeling, it denotes the duration between a person contracting a pathogen, such as a virus, and the point at which they become infectious or display symptoms. This period signifies the time during which the pathogen replicates within the host but has not yet reached a detectable or transmissible level. Represented mathematically as τ in equations, the choice of an appropriate latent period value is pivotal for accurately modeling the transference of communicable diseases, influencing the timing and scale of outbreaks in addition to the efficacy of the control plan.

1.7.4. Prevention and Control Measure

In mathematical modeling, a control measure refers to interventions, strategies, or actions implemented to manage a specific phenomenon, like infectious disease spread, environmental pollution or economic fluctuations. These measures manipulate mathematical model parameters to achieve goals, such as reducing transmission rates or stabilizing conditions. In infectious disease modeling, control measures include vaccinations, quarantine and social distancing, often altering parameters like transmission rates. Researchers use these adjustments to simulate and assess the effectiveness of different strategies in containing disease spread. Control measures aid policymakers and public health officials in making informed decisions during outbreaks or crises with mathematical models helping evaluate their impact and select efficient strategies to minimize adverse effects.

1.7.5. Compartment Analysis

Compartmental analysis in mathematical modeling involves breaking down a complex system into interconnected compartments, with each representing a specific subpopulation or state variable. This approach is widely used in fields like epidemiology, pharmacokinetics, ecology and economics to study various processes. Using differential equations, researchers describe how variables within each compartment change over time, capturing interactions and flows between them. By mathematically modeling these relationships, scientists gain insights into the system's behavior, predict outcomes and explore different scenarios. Compartmental

analysis simplifies the study of complex systems by dividing them into manageable parts, facilitating mathematical analysis of interactions and dynamics.

1.7.6. Application to Specific Models

- **HIV/AIDS Model**

  For the HIV/AIDS transmission model, we identify the equilibrium points by setting the differential equations to zero and solving for the state variables. We then perform linear stability analysis by evaluating the Jacobian matrix at these points. The basic reproduction number R_0 is derived, and its implications on stability are discussed.

- **Malaria Model**

  In the malaria model, the stability of the DFE and EE is analyzed through similar procedures. The role of the mosquito population in transmission dynamics is considered and vector control measures are evaluated in terms of their impact on R_0 and equilibrium stability.

- **Dengue Fever Model**

  For dengue fever, which often involves multiple serotypes the model's complexity increases. Stability analysis includes evaluating the impact of cross-immunity and the role of vector control. The conditions for the stability of multiple equilibria are explored and R_0 is calculated for each serotype.

1.8. Mathematical Preliminaries

Mathematical modeling of infectious diseases relies on various analytical techniques to understand and predict the dynamics of disease spread. This section introduces three fundamental methods used in the stability analysis of epidemiological models: the Jacobian method, the next generation technique and the Routh-Hurwitz condition. These methods provide essential tools for determining the stability of equilibrium points and understanding the behavior of disease transmission within a population.

1.8.1. Jacobian Method

The Jacobian method is a crucial analytical tool used to study the local stability of equilibrium points in nonlinear differential equations, which are often used to model the transmission dynamics of infectious diseases. This method involves linearizing the system around the equilibrium points and analyzing the resulting linear system to determine stability.

1. Formulation of the Model

Consider a general system of ordinary differential equations (ODEs) representing an epidemiological model:

$$\frac{dX}{dt} = F(X),$$

where $X = (x_1, x_2, ..., x_n)$ is a vector of state variables (e.g., susceptible, infected and recovered individuals) and $F(X) = (F_1(X), F_2(X), ..., F_n(X))$ is a vector of nonlinear functions describing the rates of change of these state variables.

2. Determination of Equilibrium Points

Equilibrium points (or steady states) of the system are found by setting the time derivatives to zero:

$F(X) = 0$.

Solving this system of equations provides the equilibrium points $X^* = (x_1^*, x_2^*, ..., x_3^*)$.

3. Linearization around the Equilibrium Point

To analyze the stability of an equilibrium point X^*, the system is linearized around X^* by computing the Jacobian matrix J of the system at X^*. The Jacobian matrix, defined as the matrix of first-order partial derivatives of F evaluated at X^*, is given by

$$J = \left[\frac{\partial F_i}{\partial x_j}\right]_{X=X^*}, \text{ where } 1 \le i, j \le n .$$

This matrix encapsulates the local behavior of the system around the equilibrium and is used to determine the stability of the equilibrium by analyzing its eigenvalues.

1.8.2. Next Generation Techniques

This technique is utilized to calculate the fundamental reproduction number within the context of epidemiological models. To provide a brief explanation, consider an autonomous method with non-negative starting conditions represented as:

$$y_j' = f_j(y) = F_j(y) - V_j(y) \text{ for } j = 1, 2, 3.....m \qquad (1.9)$$

where $V_j = V_j^- - V_j^+$.

Let Y be the collection of all the system's equilibrium points that are free of sickness (1.9), defined as $\{y \ge 0 : y_j = 0\}$ for $j = 1,2,.....m$. Here, $y = (y_1, y_2, ...y_m)^t$, with $y_j \ge 0$ indicating the total number of people in each infectious illness model segment.

The method involves the following conditions:

a) If $y \geq 0$, then F_j, V_j^-, and V_j^+ are all greater than or equal to 0.

b) If $y_j = 0$, it implies $V_j^- = 0$, especially for $y \in Y$ where $V_j^- = 0$ for $j = 1, 2, ...m$.

c) $F_j = 0$ for $j > m$.

d) For $y \in Y$, $F_j(y) = 0$, and $V_j(y) = 0$ for all $j = 1, 2, ...m$.

e) If $F(y) = 0$, then all the eigenvalues of $Df(y_0)$ have negative real parts,

where $F_j(y)$ represents new infections in the j^{th} partition, V_j^+ is the transition rate of individuals into the j^{th} compartment, and V_j^- is the transition rate of individuals leaving the j^{th} compartment.

1.8.3. Routh-Hurwitz Conditions

The stability of systems of ordinary differential equations is assessed based on the roots of a polynomial. This analysis centers on a linear system of equations represented in vector form, given by

$$\frac{d\bar{z}}{dt} = A\bar{z} \tag{1.10}$$

where A represents the coefficient matrix resulting from the linearization of nonlinear terms. Solutions are obtained by assuming

$$\bar{z} = z_0 e^{\lambda_1 t} \tag{1.11}$$

where z_0 is a constant vector, and the eigenvalues λ_1 can be identified as the solutions to the characteristic equation

$$|A - \lambda_1 I| = 0 \tag{1.12}$$

with I being the identity matrix. The stability of the solution $z = 0$ is determined by the location of roots λ_1 in the complex plane. If all the roots lie in the left hand complex plane $(\Re e(\lambda_1) < 0 \ \textit{for all roots})$, then the solution $z = 0$ is stable and it decays exponentially as t approaches zero. This indicates stability to small perturbations.

For a system of nth order, the characteristic polynomial can be represented as

$$P(\lambda_1) = \lambda_1^{\,n} + k_1 \lambda_1^{\,n-1} + ... + k_n \tag{1.13}$$

where the coefficient $k_1, k_2, ..., k_n$ are all real. It is crucial to establish conditions on these coefficients to ensure that the zeros of $P(\lambda_1)$ have $\Re e(\lambda_1) < 0$. The Routh-Hurwitz conditions

provide essential and satisfactory criteria for stability and one of these conditions, in conjuction with $k_n > 0$, is

$$D_1 = k_1 > 0,\ D_2 = \begin{vmatrix} k_1 & k_3 \\ 1 & k_2 \end{vmatrix} > 0,\ D_3 = \begin{vmatrix} k_1 & k_3 & k_5 \\ 1 & k_2 & k_4 \\ 0 & k_1 & k_3 \end{vmatrix} > 0,\ \ldots\ldots$$

$$D_i = \begin{vmatrix} k_1 & k_3 & k_5 & . & . & . \\ 1 & k_2 & k_4 & . & . & . \\ 0 & k_1 & k_3 & . & . & . \\ . & . & . & . & . & . \\ 0 & 0 & 0 & . & . & k_i \end{vmatrix} > 0,\ i = 1, 2, 3, ..., n. \tag{1.14}$$

1.9. Numerical Methods

Analytically solving a set of differential equations might be difficult at times. To address this issue, numerical techniques are used, which provide solutions that, while not accurate, are close to the analytical solutions. In our computational research, we used the MATLAB software, which allows us to evaluate approximation results using a variety of numerical approaches.

♦ **Runge-Kutta Method**

In the field of numerical analysis, Runge-Kutta methods stand out as a crucial family of iterative methods, both implicit and explicit, utilized for temporal discretization in approximating solutions of ordinary differential equations (ODE). These methods are precisely designed to deliver increased accuracy and possess the benefit of necessitating only function values at specific points within subintervals.

Researchers widely adopt the Runge-Kutta numerical technique to solve sets of differential equations and determine transient probabilities of system states due to its precision, reliability, and ease of programming. Among the frequently utilized Runge-Kutta methods in mathematical modeling, RK4 is particularly noteworthy. It combines simplicity with effectiveness.

To calculate transient state probabilities using the fourth-order Runge-Kutta method, a MATLAB programme is developed employing the ode45 routine. This iterative procedure involves the following steps:

$$\Pi_i = \Pi_{i-1} + \frac{1}{6}(V_1 + 2V_2 + 2V_3 + V_4) \tag{1.15}$$

where

$$V_1 = cf(t_{i-1}, \Pi_{i-1}),\ V_2 = cf\left(t_{i-1}, \frac{1}{2}h, \Pi_{i-1} + \frac{1}{2}V_1\right),\ V_3 = cf\left(t_{i-1}, \frac{1}{2}h, \Pi_{i-1} + \frac{1}{2}V_2\right),$$

$$V_4 = cf(t_{i-1} + h, \Pi_{i-1} + V_3).$$

♦ **Eigen Values and Eigen Vectors**

An eigenvalue λ signifies a scalar factor by which an eigenvector $\vec{v}$ is scaled when the transformation matrix A is applied to it.

Mathematically, for a square matrix A, an eigenvalue λ and its corresponding eigenvector $\vec{v}$ satisfy the equation

$$A\vec{v} = \lambda\vec{v} \tag{1.16}$$

where $\vec{v}$ is a non-zero vector.

- **How Do We Calculate the Eigen Values and Eigen Vectors**

Determining eigenvalues involves solving the characteristic equation for a given square matrix A, which is obtained by subtracting λ times the identity matrix from A. The characteristic equation is represented as

$$\det(A - \lambda I) = 0 \tag{1.17}$$

where $\det$ denotes the determinant, λ represents the eigenvalue, and I is the identity matrix. Solving this equation yields the eigenvalues for A. Once the eigenvalues are identified, eigenvectors can be found by substituting each eigenvalue back into the equation

$$(A - \lambda I)\vec{v} = 0 \tag{1.18}$$

where $\vec{v}$ is the eigenvector corresponding to the respective eigenvalue. This process allows us to calculate both the eigenvalues and eigenvectors, providing essential insights into the behavior of the matrix in linear transformations and system dynamics.

♦ **Adaptive Neuro-Fuzzy Inference System (ANFIS)**

The Adaptive Neuro-Fuzzy Inference System (ANFIS) is a hybrid intelligent system that combines the learning capabilities of neural networks with the reasoning capabilities of fuzzy logic. This integration allows ANFIS to leverage the strengths of both techniques, making it a powerful tool for modeling complex systems and computing numerical results.

- **Overview of ANFIS**

ANFIS operates by constructing a fuzzy inference system within the framework of adaptive networks. The system consists of a set of fuzzy if-then rules with appropriate membership functions to generate the stipulated output. The key components of ANFIS include:

Fuzzy Logic: Provides a way to represent uncertain and imprecise information through linguistic variables and fuzzy sets.

Neural Networks: Utilized for learning from data and adjusting the membership functions and fuzzy rules to optimize the performance of the system.

- **Structure of ANFIS**

In Figure 1.5, the architecture of ANFIS, which consists of five layers: the input, fuzzy, normalization, rule, and output layers, is depicted. This combined system integrates the advantages of both fuzzy logic and neural networks, making it suitable for various applications, including control systems, pattern recognition, and prediction.

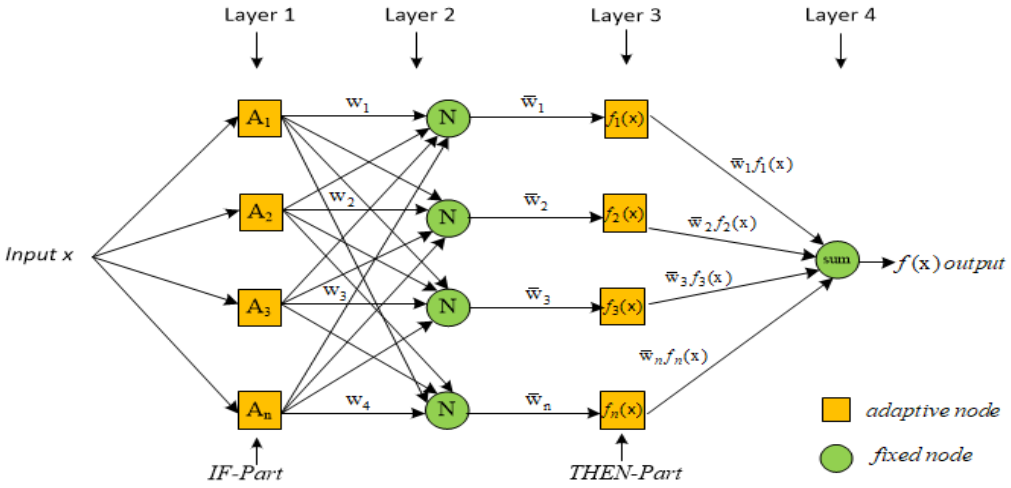

Figure 1.5: ANFIS Architecture

The ANFIS architecture typically comprises five layers:

Input Layer: Accepts the input variables.

Fuzzy Layer: Converts crisp inputs into fuzzy sets using predefined membership functions.

Normalization Layer: Normalizes the firing strengths of the rules.

Rule Layer: Contains fuzzy if-then rules that describe the relationship between input and output variables.

Output Layer: Converts the fuzzy outputs back into crisp values.

- **Application of ANFIS in This Thesis**

In this thesis, ANFIS is specifically employed to compute numerical results for the HIV transmission dynamics explored in Chapter 3. The use of ANFIS offers several advantages:

Modeling Nonlinear Relationships: ANFIS is adept at capturing complex nonlinear relationships between variables, which is essential in epidemiological modeling.

Data-Driven Approach: ANFIS can learn from data, making it possible to refine the models based on empirical observations and improve the accuracy of predictions.

Flexibility: The system can adapt to various scenarios by adjusting the fuzzy rules and membership functions, thus accommodating the diverse nature of disease transmission dynamics.

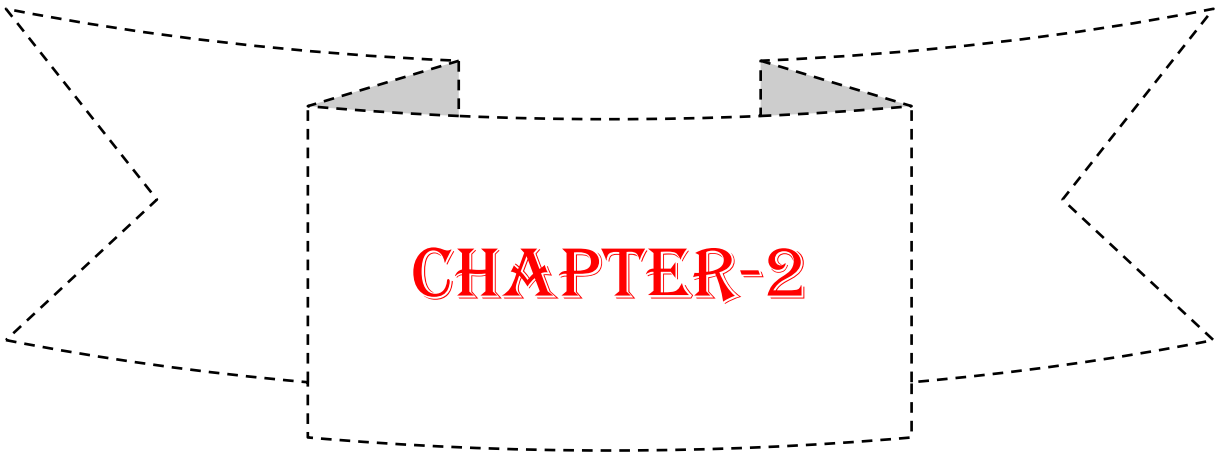

Stability Analysis of HIV/AIDS Transmission: A Mathematical Model for Sex Labourers

Keywords: HIV/AIDS, Sex Labourers, Reproduction Number, Stability Analysis and Infective Compartments.

Chapter 2: Stability Analysis of HIV/AIDS Transmission: A Mathematical Model for Sex Labourers

2.1. Introduction

The exploration of epidemics and critical illnesses has been steeped in a profound historical context, punctuated by a diverse array of mathematical models crucial for comprehending the propagation and underlying causes of epidemic outbreaks. These models serve as indispensable tools in understanding the intricate dynamics of diseases that can be transmitted through various means, including infection or sexual contact between susceptible individuals and those already infected. Among these, Sexually Transmitted Diseases (STDs) stand as a pressing concern, with the Human Immunodeficiency Virus (HIV), capable of progressing to Acquired Immunodeficiency Syndrome (AIDS), emerging as one of the most perilous and widely spread diseases globally.

This chapter embarks on a nuanced exploration into the dynamics of HIV/AIDS transmission with a specific lens trained on female sex workers, an inherently vulnerable population segment. It intricately dissects the multifaceted compartments within populations, unraveling the complexities and subtleties of disease spread within this context. Beyond mere observation, this analysis delves into the underlying mechanisms governing the interplay between different population strata, shedding light on the unique challenges and dynamics inherent in the transmission and persistence of HIV/AIDS within this specific demographic.

Understanding the transmission dynamics of HIV/AIDS among female sex workers necessitates a multidimensional approach that transcends conventional epidemiological models. It demands an acute awareness of socio-cultural determinants, healthcare access disparities, behavioral patterns and economic factors influencing the spread and persistence of this disease within this vulnerable cohort. By contextualizing mathematical modeling within the intricate web of socio-economic and behavioral determinants, this chapter seeks to unravel not only the quantitative aspects of disease spread but also the qualitative facets that underpin its persistence.

Furthermore, this analysis seeks to examine the efficacy of various intervention strategies within the realm of mathematical modeling. By simulating scenarios and interventions through mathematical models, the chapter aims to forecast the potential impact of preventive measures, healthcare access improvements, and behavioral interventions on curbing HIV/AIDS transmission among female sex workers. This predictive aspect of mathematical modeling stands as a testament to its applicability not only in understanding the present state but also in

projecting potential trajectories and outcomes based on hypothetical interventions, thereby guiding policymakers and healthcare professionals in formulating evidence-based strategies.

This approach goes beyond traditional epidemiological studies, aiming to merge mathematical rigor with an understanding of the multifaceted realities faced by female sex workers. It endeavors to provide a holistic framework that integrates mathematical modeling with socio-economic and behavioral insights, not only to comprehend the transmission dynamics but also to devise targeted interventions that address the specific needs and challenges faced by this marginalized population, fostering a more inclusive and effective approach in combating the spread of HIV/AIDS.

In this chapter, we introduce a mathematical model that explores the active nature of HIV/AIDS transmission within the realm of female sex workers, taking into account various distinct population compartments. The subsequent sections are structured as follows: Section 2.2 provides a detailed literature and Section 2.3 provides a comprehensive overview of the assumptions, notations and model description. Moving on to Section 2.4, we delve into the analysis of the model. Section 2.5 showcases numerical illustrations and finally in Section 2.6, we draw a summary and conclusion based on our findings.

2.2. Literature Review

Building on the rich history of epidemic modeling, various researchers have made significant contributions to our understanding of HIV/AIDS transmission dynamics. Mukandavire and Garira (2007) crafted a sex-structured mathematical model tailored to examine HIV/AIDS transmission within heterosexual populations, offering insights into the complexity of such transmission dynamics. Wu and Tan (2000) took a steady-state approach, enabling the estimation of AIDS cases and the number of infectious individuals across various stages, employing Kalman recursion to enhance our grasp of the epidemic. Cai *et al.,* (2009) delved into an HIV/AIDS outbreak mock-up incorporating treatment options, shedding light on the potential impact of medical care on sickness dynamics. Jain *et al.,* (2010) provided a detailed analysis of the active way of behaving of T-lymphocyte cells in the surroundings of Human Immunodeficiency Virus type 1 (HIV-1) contamination. Additionally, Singh *et al.,* (2013) observed the intricate transmission dynamics of malaria, tuberculosis (mTB), HIV/AIDS, and their co-infections. Singh *et al.,* (2016) performed an extensive examination of a mathematical model, specifically centering on the influence of treatment within the framework of the HIV/AIDS epidemic. In a distinct study, Kaur *et al.,* (2014) explored a nonlinear model, underscoring the pivotal involvement of female intercourse workers in the

transmission dynamics of the HIV/AIDS epidemic. Huo and Feng (2013) advanced our understanding by constructing an HIV/AIDS epidemic model that accounts for various latent stages and treatment possibilities. Ali *et al.*, (2019) developed a nonlinear compartmental model, investigating the influence of media coverage on infectious disease control and prevention.

Continuing to expand our understanding of HIV/AIDS transmission dynamics, several researchers have introduced novel epidemic models with unique compartments and factors. Huo *et al.,* (2016) innovatively incorporated a modern compartment, known as the treatment compartment (T), into their HIV/AIDS epidemic model, providing valuable insights into the dynamics of treatment interventions. Furthermore, Huo *et al.,* (2018) formulated an SEIS outbreak version, taking into consideration the effect of means of communication and emphasizing its role in shaping public perception and response to the epidemic. Jia and Qin (2017) described an HIV/AIDS epidemic model with a standard nonlinear prevalence rate and treatment, contributing to the exploration of diverse transmission dynamics. Biswas and Pal (2017) introduced a comprehensive nonlinear mathematical model that considers vaccination and antiretroviral treatment, aiming to elucidate the model's insights and analyze the boundedness of its solutions. Their research extended our knowledge about intervention strategies. Moreover, Wu and Zhao (2021) collected data to investigate the worldwide dimensions of the HIV/AIDS epidemic and to scrutinize its transmission within the demographic of men who engage in sexual activity with other men. Lastly, Kumar *et al.,* (2021) ventured into creating a numerical model of HIV/AIDS transference dynamics, incorporating the impact of mindfulness and analyzing the model with three distinct singular & non-singular fractional operators, thus expanding the range of factors considered in understanding epidemic spread.

In recent years, several significant contributions have been made to the field of HIV/AIDS modeling and epidemiology. Wattanasirikosone and Modnak (2022) presented an innovative mathematical model employing a distinctive approach that specifically addressed two separate categories: individuals with HIV and those with AIDS. Notably, they introduced a controlled class involving treated patients under monitoring, some of whom could potentially transmit the disease. Most recently, Izadi *et al.,* (2023) conducted a cross-sectional survey among female sex workers in various cities in Iran to estimate HIV infection prevalence and high-risk behaviors. Subsequently, Das *et al.,* (2023) developed a mathematical model that considers time delays and co-infection dynamics within the context of TB, HIV, and AIDS. Moreover, Gurski and Hoffman (2023) introduced an autonomous population model that accounts for the

possibility of infection from casual or long-term partners, whether initially infected or newly infected since the partnership began. In that identical year, Zhai *et al.*, (2023) developed a stochastic HIV/AIDS model that incorporated protection awareness among susceptible individuals within a total population. These studies collectively contribute to our understanding of HIV/AIDS epidemiology and modeling.

2.3. Mathematical Model

In this model, we assume that individuals enter the susceptible class, comprising males, females, and female sex workers, primarily through processes like birth. Initially, the transmission dynamics involve susceptible males getting infected at a rate determined by the infective classes of females and female sex workers. Similarly, susceptible females and female sex workers acquire infections through the transmission rate associated with infected males. Subsequently, individuals in the HIV-infected classes of males, females and female sex workers progress to their respective AIDS classes. The total population engaged in sexual activity at a given time t, denoted as $N(t)$, is categorized into twelve distinct and non-overlapping groups. These groups include the HIV-susceptible class of males, females and female sex workers (S_m, S_f, S_w), HIV slow-infective classes of males, females and female sex workers (I_{m1}, I_{f1}, I_{w1}), HIV fast-infective classes of males, females and female sex workers (I_{m2}, I_{f2}, I_{w2}), and the full-blown AIDS class of males, females and female sex workers (A_m, A_f, A_w). Recruitment rates for the male, female and female sex-worker populations are denoted as Δ_1, Δ_2 and Δ_3, respectively. Transmission rates from infective groups of females and female sex workers to susceptible groups of males, respectively, are represented by $\alpha_{mfi}, \alpha_{mwi}$; $i = 1,2$. The current evaluation is focused on determining the transmission rate from infected males to susceptible females, and female sex workers are denoted as $\alpha_{fmi}, \alpha_{wmi}$; $i = 1,2$. Rates of progression from the HIV slow-infective category in males, females and female sex workers to the fast-infective HIV category, respectively, are denoted as δ_{m1}, δ_{f1} and δ_{w1}. Progression rates from HIV-infected individuals of male, female, and female sex workers to the respective AIDS classes are denoted as ρ_{mi}, ρ_{fi} and ρ_{wi}; $i = 1,2$. The natural death rate constant is denoted as σ, while m, f and w denote the disease-induced mortality rate in AIDS classes, respectively. The transition diagram depicting the developed model is illustrated in Figure 2.1. These specified variables, parameters and assumptions lead to a deterministic system of non-linear differential equations describing the model.

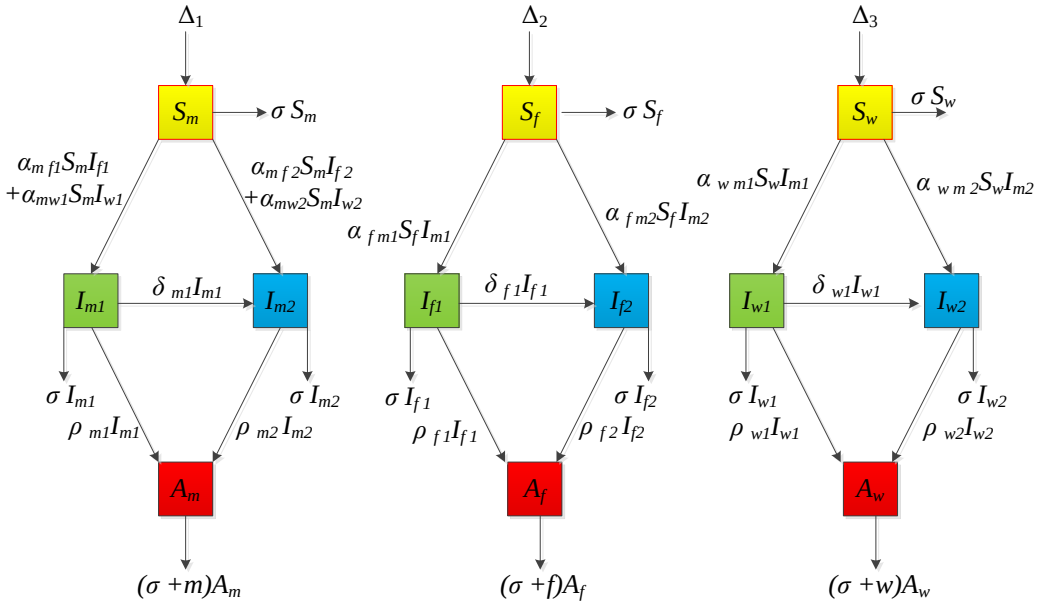

Figure 2.1: Effective model of HIV/AIDS transmission.

Table 2.1: Definition of state parameters use in the model

Symbols	Description
$\Delta_1, \Delta_2, \Delta_3$	Birth rates in different susceptible classes of males, females and female sex workers, respectively.
$\alpha_{mfi}, \alpha_{mwi};\ i = 1,2$	The speed at which infection spreads from infectious groups of females and female sex workers to the vulnerable group of males, correspondingly.
$\alpha_{fmi}, \alpha_{wmi};\ i = 1,2$	The current evaluation is focused on determining the transmission rate from infected males to susceptible females and female sex workers.
$\delta_{m1}, \delta_{f1}, \delta_{w1}$	Rates of progression from the HIV slow-infective category in males, females and female sex workers to the fast-infective HIV category, respectively.
$\rho_{mi}, \rho_{fi}, \rho_{wi};\ i = 1,2$	Progression rates from HIV-infected groups of men, women and female sex workers to their corresponding stages of AIDS.
σ	Constant mortality rates over time.
$m,\ f, w$	The mortality rate resulting from the disease in the AIDS classes, respectively.

2.3.1. Model Equations

The relevant model equations are given as following:

I. Male compartment

$$S'_m = \Delta_1 - \alpha_{mf1}S_mI_{f1} - \alpha_{mf2}S_mI_{f2} - \alpha_{mw1}S_mI_{w1} - \alpha_{mw2}S_mI_{w2} - \sigma S_m \tag{2.1}$$

$$I'_{m1} = \alpha_{mf1}S_mI_{f1} + \alpha_{mw1}S_mI_{w1} - (\rho_{m1} + \delta_{m1} + \sigma)I_{m1} \tag{2.2}$$

$$I'_{m2} = \alpha_{mf2} S_m I_{f2} + \alpha_{mw2} S_m I_{w2} + \delta_{m1} I_{m1} - (\rho_{m2} + \sigma) I_{m2} \quad (2.3)$$

$$A'_m = \rho_{m1} I_{m1} + \rho_{m2} I_{m2} - (\sigma + m) A_m \quad (2.4)$$

II. Female compartment

$$S'_f = \Delta_2 - \alpha_{fm1} S_f I_{m1} - \alpha_{fm2} S_f I_{m2} - \sigma S_f \quad (2.5)$$

$$I'_{f1} = \alpha_{fm1} S_f I_{m1} - (\rho_{f1} + \delta_{f1} + \sigma) I_{f1} \quad (2.6)$$

$$I'_{f2} = \alpha_{fm2} S_f I_{m2} + \delta_{f1} I_{f1} - (\rho_{f2} + \sigma) I_{f2} \quad (2.7)$$

$$A'_f = \rho_{f1} I_{f1} + \rho_{f2} I_{f2} - (\sigma + f) A_f \quad (2.8)$$

III. Female sex-worker compartment

$$S'_w = \Delta_3 - \alpha_{wm1} S_w I_{m1} - \alpha_{wm2} S_w I_{m2} - \sigma S_w \quad (2.9)$$

$$I'_{w1} = \alpha_{wm1} S_w I_{m1} - (\rho_{w1} + \delta_{w1} + \sigma) I_{w1} \quad (2.10)$$

$$I'_{w2} = \alpha_{wm2} S_w I_{m2} + \delta_{w1} I_{w1} - (\rho_{w2} + \sigma) I_{w2} \quad (2.11)$$

$$A'_w = \rho_{w1} I_{w1} + \rho_{w2} I_{w2} - (\sigma + w) A_w \quad (2.12)$$

To simplify the system of equations, let's consider the following substitutions:

$$\nu_1 = \rho_{m1} + \delta_{m1} + \sigma, \nu_2 = \rho_{m2} + \sigma, \nu_3 = \rho_{f1} + \delta_{f1} + \sigma, \nu_4 = \rho_{f2} + \sigma, \nu_5 = \rho_{w1} + \delta_{w1} + \sigma,$$

$$\nu_6 = \rho_{w2} + \sigma, \nu_7 = \sigma + m, \nu_8 = \sigma + f \text{ and } \nu_9 = \sigma + w.$$

In a manner that facilitates the rewriting of equations (2.1)-(2.12),

$$S'_m = \Delta_1 - \alpha_{mf1} S_m I_{f1} - \alpha_{mf2} S_m I_{f2} - \alpha_{mw1} S_m I_{w1} - \alpha_{mw2} S_m I_{w2} - \sigma S_m \quad (2.13)$$

$$I'_{m1} = \alpha_{mf1} S_m I_{f1} + \alpha_{mw1} S_m I_{w1} - \nu_1 I_{m1} \quad (2.14)$$

$$I'_{m2} = \alpha_{mf2} S_m I_{f2} + \alpha_{mw2} S_m I_{w2} + \delta_{m1} I_{m1} - \nu_3 I_{m2} \quad (2.15)$$

$$A'_m = \rho_{m1} I_{m1} + \rho_{m2} I_{m2} - \nu_7 A_m \quad (2.16)$$

$$S'_f = \Delta_2 - \alpha_{fm1} S_f I_{m1} - \alpha_{fm2} S_f I_{m2} - \sigma S_f \quad (2.17)$$

$$I'_{f1} = \alpha_{fm1} S_f I_{m1} - \nu_3 I_{f1} \quad (2.18)$$

$$I'_{f2} = \alpha_{fm2} S_f I_{m2} + \delta_{f1} I_{f1} - \nu_4 I_{f2} \quad (2.19)$$

$$A_f' = \rho_{f1} I_{f1} + \rho_{f2} I_{f2} - \nu_8 A_f \tag{2.20}$$

$$S_w' = \Delta_3 - \alpha_{wm1} S_w I_{m1} - \alpha_{wm2} S_w I_{m2} - \sigma S_w \tag{2.21}$$

$$I_{w1}' = \alpha_{wm1} S_w I_{m1} - \nu_5 I_{w1} \tag{2.22}$$

$$I_{w2}' = \alpha_{wm2} S_w I_{m2} + \delta_{w1} I_{w1} - \nu_6 I_{w2} \tag{2.23}$$

$$A_w' = \rho_{w1} I_{w1} + \rho_{w2} I_{w2} - \nu_9 A_w \tag{2.24}$$

The overall population at any given moment is symbolized as N.

2.3.2. Positivity of the Solutions

Lemma 2.3.1: For $t \geq 0$, all configurations of the framework (2.13)-(2.24) are ultimately constrained within the compact subset.

$$\Pi = \left\{ S_m(t), S_f(t), S_w(t), I_{m1}(t), I_{m2}(t), I_{f1}(t), I_{f2}(t), I_{w1}(t), I_{w2}(t), A_m(t), A_f(t), A_w(t) \in \Re_+^{12} : N \leq \frac{\Lambda}{\mu} \right\}.$$

Proof: Consider the solution $\left(S_m(t), S_f(t), S_w(t), I_{m1}(t), I_{m2}(t), I_{f1}(t), I_{f2}(t), I_{w1}(t), I_{w2}(t), A_m(t), A_f(t), A_w(t)\right)$ with positive initial conditions. Consequently, we obtain:

$$N = S_m + S_f + S_w + I_{m1} + I_{m2} + I_{f1} + I_{f2} + I_{w1} + I_{w2} + A_m + A_f + A_w \tag{2.25}$$

Adding the framework of conditions (2.13)-(2.24), we have

$$\frac{dN}{dt} = (\Delta_1 + \Delta_2 + \Delta_3) - \sigma N - (mA_m + fA_f + wA_w) \leq \Delta - \sigma N \tag{2.26}$$

Here, $\Delta = \Delta_1 + \Delta_2 + \Delta_3$, signify the whole birth rate of the population under consideration. It is mentioned that

$$N(t) \leq \frac{\Delta}{\sigma}(1 - e^{\sigma t}) + N_0 e^{-\sigma t} \tag{2.27}$$

where $N(0)$ represents the initial values of the entire population. Therefore, as $\lim_{t \to \infty} \sup N(t) \leq \frac{\Delta}{\sigma}$. It becomes evident that all the arrangement of framework (2.13)-(2.24) that initiate in $\Re_+^{12}$ are confined within the specified region Π.

2.4. Analysis of the Model

2.4.1. Disease-Free Equilibrium (DFE) and the Basic Reproduction Number

Assuming the right-hand side of the system of equations (2.13)-(2.24) is zero, then we get,

$$\left.\begin{aligned}
&\Delta_1 - \alpha_{mf1} S_m I_{f1} - \alpha_{mf2} S_m I_{f2} - \alpha_{mw1} S_m I_{w1} - \alpha_{mw2} S_m I_{w2} - \sigma S_m = 0\\
&\alpha_{mf1} S_m I_{f1} + \alpha_{mw1} S_m I_{w1} - \nu_1 I_{m1} = 0\\
&\alpha_{mf2} S_m I_{f2} + \alpha_{mw2} S_m I_{w2} + \delta_{m1} I_{m1} - \nu_3 I_{m2} = 0\\
&\rho_{m1} I_{m1} + \rho_{m2} I_{m2} - \nu_7 A_m = 0\\
&\Delta_2 - \alpha_{fm1} S_f I_{m1} - \alpha_{fm2} S_f I_{m2} - \sigma S_f = 0\\
&\alpha_{fm1} S_f I_{m1} - \nu_3 I_{f1} = 0\\
&\alpha_{fm2} S_f I_{m2} + \delta_{f1} I_{f1} - \nu_4 I_{f2} = 0\\
&\rho_{f1} I_{f1} + \rho_{f2} I_{f2} - \nu_8 A_f = 0\\
&\Delta_3 - \alpha_{wm1} S_w I_{m1} - \alpha_{wm2} S_w I_{m2} - \sigma S_w = 0\\
&\alpha_{wm1} S_w I_{m1} - \nu_5 I_{w1} = 0\\
&\alpha_{wm2} S_w I_{m2} + \delta_{w1} I_{w1} - \nu_6 I_{w2} = 0\\
&\rho_{w1} I_{w1} + \rho_{w2} I_{w2} - \nu_9 A_w = 0
\end{aligned}\right\} \qquad (2.28)$$

If we set $I_{m1} = I_{m2} = I_{f1} = I_{f2} = I_{w1} = I_{w2} = A_m = A_f = A_w = 0$ in equation (2.28), it is evident that the model reaches a state of disease-free equilibrium, defined as:

$$E_0 = \left(S_m^0, S_f^0, S_w^0, I_{m1}^0, I_{m2}^0, I_{f1}^0, I_{f2}^0, I_{w1}^0, I_{w2}^0, A_m^0, A_f^0, A_w^0\right) = \left(\frac{\Delta_1}{\sigma}, \frac{\Delta_2}{\sigma}, \frac{\Delta_3}{\sigma}, 0,0,0,0,0,0,0,0,0\right)$$

As per the findings of Van den Driessche and Watmough (2002), the model reproduction number can be computed using the next-generation technique. This approach involves delineating the frameworks F^* and V^*, which individually characterize the introduction of new infections and the transfer of individuals out of infective compartments.

$$F^* = \begin{pmatrix}
\alpha_{mf1} S_m I_{f1} + \alpha_{mw1} S_m I_{w1}\\
\alpha_{mf2} S_m I_{f2} + \alpha_{mw2} S_m I_{w2}\\
\alpha_{fm1} S_f I_{m1}\\
\alpha_{fm2} S_f I_{m2}\\
\alpha_{wm1} S_w I_{m1}\\
\alpha_{wm2} S_w I_{m2}\\
0\\
0\\
0
\end{pmatrix} \quad \text{and} \quad V^* = \begin{pmatrix}
\nu_1 I_{m1}\\
\nu_2 I_{m2} - \delta_{m1} I_{m1}\\
\nu_3 I_{f1}\\
\nu_4 I_{f2} - \delta_{f1} I_{f1}\\
\nu_5 I_{w1}\\
\nu_6 I_{w2} - \delta_{w1} I_{w1}\\
\nu_7 A_m - \rho_{m1} I_{m1} - \rho_{m2} I_{m2}\\
\nu_8 A_f - \rho_{f1} I_{f1} - \rho_{f2} I_{f2}\\
\nu_9 A_w - \rho_{w1} I_{w1} - \rho_{w2} I_{w2}
\end{pmatrix}$$

Now, computing partial derivatives of F^* and V^* we have

$$F = \begin{pmatrix} 0 & 0 & \alpha_{mf1}\frac{\Delta_1}{\sigma} & 0 & \alpha_{mw1}\frac{\Delta_1}{\sigma} & 0 & 0 & 0 & 0 \\ 0 & 0 & 0 & \alpha_{mf2}\frac{\Delta_1}{\sigma} & 0 & \alpha_{mw2}\frac{\Delta_1}{\sigma} & 0 & 0 & 0 \\ \alpha_{fm1}\frac{\Delta_2}{\sigma} & 0 & 0 & 0 & 0 & 0 & 0 & 0 & 0 \\ 0 & \alpha_{fm2}\frac{\Delta_2}{\sigma} & 0 & 0 & 0 & 0 & 0 & 0 & 0 \\ \alpha_{wm1}\frac{\Delta_3}{\sigma} & 0 & 0 & 0 & 0 & 0 & 0 & 0 & 0 \\ 0 & \alpha_{wm2}\frac{\Delta_3}{\sigma} & 0 & 0 & 0 & 0 & 0 & 0 & 0 \\ 0 & 0 & 0 & 0 & 0 & 0 & 0 & 0 & 0 \\ 0 & 0 & 0 & 0 & 0 & 0 & 0 & 0 & 0 \\ 0 & 0 & 0 & 0 & 0 & 0 & 0 & 0 & 0 \end{pmatrix} \quad (2.29)$$

$$V = \begin{pmatrix} \nu_1 & 0 & 0 & 0 & 0 & 0 & 0 & 0 & 0 \\ -\delta_{m1} & \nu_2 & 0 & 0 & 0 & 0 & 0 & 0 & 0 \\ 0 & 0 & \nu_3 & 0 & 0 & 0 & 0 & 0 & 0 \\ 0 & 0 & -\delta_{f1} & \nu_4 & 0 & 0 & 0 & 0 & 0 \\ 0 & 0 & 0 & 0 & \nu_5 & 0 & 0 & 0 & 0 \\ 0 & 0 & 0 & 0 & -\delta_{w1} & \nu_6 & 0 & 0 & 0 \\ -\rho_{m1} & -\rho_{m2} & 0 & 0 & 0 & 0 & \nu_7 & 0 & 0 \\ 0 & 0 & -\rho_{f1} & -\rho_{f2} & 0 & 0 & 0 & \nu_8 & 0 \\ 0 & 0 & 0 & 0 & -\rho_{w1} & -\rho_{w2} & 0 & 0 & \nu_9 \end{pmatrix} \quad (2.30)$$

and then we have

$$FV^{-1} = \begin{pmatrix} 0 & 0 & \frac{\alpha_{mf1}}{\nu_3}\frac{\Delta_1}{\sigma} & 0 & \frac{\alpha_{mw1}}{\nu_5}\frac{\Delta_1}{\sigma} & 0 & 0 & 0 & 0 \\ 0 & 0 & \frac{\alpha_{mf2}\delta_{f1}}{\nu_3\nu_4}\frac{\Delta_1}{\sigma} & \frac{\alpha_{mf2}}{\nu_4}\frac{\Delta_1}{\sigma} & \frac{\alpha_{mw2}\varepsilon_{w1}}{\nu_5\nu_6}\frac{\Delta_1}{\sigma} & \frac{\alpha_{mw2}}{\nu_6}\frac{\Delta_1}{\sigma} & 0 & 0 & 0 \\ \frac{\alpha_{fm1}}{\nu_1}\frac{\Delta_2}{\sigma} & 0 & 0 & 0 & 0 & 0 & 0 & 0 & 0 \\ \frac{\alpha_{fm2}\delta_{m1}}{\nu_1\nu_2}\frac{\Delta_2}{\sigma} & \frac{\alpha_{fm2}}{\nu_2}\frac{\Delta_2}{\sigma} & 0 & 0 & 0 & 0 & 0 & 0 & 0 \\ \frac{\alpha_{wm1}}{\nu_1}\frac{\Delta_3}{\sigma} & 0 & 0 & 0 & 0 & 0 & 0 & 0 & 0 \\ \frac{\alpha_{wm2}\delta_{m1}}{\nu_1\nu_2}\frac{\Delta_3}{\sigma} & \frac{\alpha_{wm2}}{\nu_2}\frac{\Delta_3}{\sigma} & 0 & 0 & 0 & 0 & 0 & 0 & 0 \\ 0 & 0 & 0 & 0 & 0 & 0 & 0 & 0 & 0 \\ 0 & 0 & 0 & 0 & 0 & 0 & 0 & 0 & 0 \\ 0 & 0 & 0 & 0 & 0 & 0 & 0 & 0 & 0 \end{pmatrix} \quad (2.31)$$

The reproductive number of the model, represented as R_0, is derived as

$$R_0 = \sqrt{\frac{\Delta_1\{\Delta_2(\alpha_{mf1}\alpha_{fm1}v_2v_4 - \alpha_{mf2}\alpha_{fm2}v_1v_3)v_5v_6 + \Delta_3(\alpha_{mw1}\alpha_{wm1}v_2v_6 - \alpha_{mw2}\alpha_{wm2}v_1v_5)v_3v_4\}}{\sigma^2 v_1v_2v_3v_4v_5v_6}} \qquad (2.32)$$

Theorem 2.4.1: The local asymptotic stability of the disease-free equilibrium E_0 in the system (2.13)-(2.24) is established when $R_0 < 1$, and it becomes unstable otherwise.

Proof: The Jacobian matrix of the presented system at the disease-free equilibrium is expressed as:

$$J(E_0) = \begin{pmatrix}
-\sigma & 0 & 0 & 0 & 0 & -\alpha_{mf1}\frac{\Delta_1}{\sigma} & -\alpha_{mf2}\frac{\Delta_1}{\sigma} & 0 & 0 & -\alpha_{mw1}\frac{\Delta_1}{\sigma} & -\alpha_{mw2}\frac{\Delta_1}{\sigma} & 0 \\
0 & -v_1 & 0 & 0 & 0 & \alpha_{mf1}\frac{\Delta_1}{\sigma} & 0 & 0 & 0 & \alpha_{mw1}\frac{\Delta_1}{\sigma} & 0 & 0 \\
0 & \delta_{m1} & -v_2 & 0 & 0 & 0 & \alpha_{mf2}\frac{\Delta_1}{\sigma} & 0 & 0 & 0 & \alpha_{mw2}\frac{\Delta_1}{\sigma} & 0 \\
0 & \rho_{m1} & \rho_{m2} & -v_7 & 0 & 0 & 0 & 0 & 0 & 0 & 0 & 0 \\
0 & -\alpha_{fm1}\frac{\Delta_2}{\sigma} & -\alpha_{fm2}\frac{\Delta_2}{\sigma} & 0 & -\sigma & 0 & 0 & 0 & 0 & 0 & 0 & 0 \\
0 & \alpha_{fm1}\frac{\Delta_2}{\sigma} & 0 & 0 & 0 & -v_3 & 0 & 0 & 0 & 0 & 0 & 0 \\
0 & 0 & \alpha_{fm2}\frac{\Delta_2}{\sigma} & 0 & 0 & \delta_{f1} & -v_4 & 0 & 0 & 0 & 0 & 0 \\
0 & 0 & 0 & 0 & 0 & \rho_{f1} & \rho_{f2} & -v_8 & 0 & 0 & 0 & 0 \\
0 & -\alpha_{wm1}\frac{\Delta_3}{\sigma} & -\alpha_{wm2}\frac{\Delta_3}{\sigma} & 0 & 0 & 0 & 0 & 0 & -\sigma & 0 & 0 & 0 \\
0 & \alpha_{wm1}\frac{\Delta_3}{\sigma} & 0 & 0 & 0 & 0 & 0 & 0 & 0 & -v_5 & 0 & 0 \\
0 & 0 & \alpha_{wm2}\frac{\Delta_3}{\sigma} & 0 & 0 & 0 & 0 & 0 & 0 & \delta_{w1} & -v_6 & 0 \\
0 & 0 & 0 & 0 & 0 & 0 & 0 & 0 & 0 & \rho_{w1} & \rho_{w2} & -v_9
\end{pmatrix} \qquad (2.33)$$

$$\text{Trace}\,[J(E_0)] = -(3\sigma + v_1 + v_2 + v_3 + v_4 + v_5 + v_6 + v_7 + v_8 + v_9) < 0$$

$$\text{Det}\,[J(E_0)] = \sigma^3 v_7 v_8 v_9 \left(v_5\alpha_{mf1}\alpha_{fm1}\frac{\Delta_1\Delta_2}{\sigma^2} + v_3\alpha_{mw1}\alpha_{wm1}\frac{\Delta_1\Delta_3}{\sigma^2} - v_1v_3v_5 \right)$$
$$\times \left(v_6\alpha_{mf2}\alpha_{fm2}\frac{\Delta_1\Delta_2}{\sigma^2} + v_4\alpha_{mw2}\alpha_{wm2}\frac{\Delta_1\Delta_3}{\sigma^2} - v_2v_4v_6 \right) > 0$$

$$\Rightarrow \frac{v_5\alpha_{mf1}\alpha_{fm1}\frac{\Delta_1\Delta_2}{\sigma^2} + v_3\alpha_{mw1}\alpha_{wm1}\frac{\Delta_1\Delta_3}{\sigma^2}}{v_1v_3v_5} < 1 \text{ or } \frac{v_6\alpha_{mf2}\alpha_{fm2}\frac{\Delta_1\Delta_2}{\sigma^2} + v_4\alpha_{mw2}\alpha_{wm2}\frac{\Delta_1\Delta_3}{\sigma^2}}{v_2v_4v_6} < 1$$

$$\Rightarrow \frac{v_5\alpha_{mf1}\alpha_{fm1}\frac{\Delta_1\Delta_2}{\sigma^2} + v_3\alpha_{mw1}\alpha_{wm1}\frac{\Delta_1\Delta_3}{\sigma^2}}{v_1v_3v_5} + \frac{v_6\alpha_{mf2}\alpha_{fm2}\frac{\Delta_1\Delta_2}{\sigma^2} + v_4\alpha_{mw2}\alpha_{wm2}\frac{\Delta_1\Delta_3}{\sigma^2}}{v_2v_4v_6} < 1$$

$\Rightarrow R_0^2 < 1 \Rightarrow R_0 < 1.$

Therefore, the local asymptotic stability of the disease-free equilibrium E_0 in the system (2.13)-(2.24) is established when $R_0 < 1$, and it becomes unstable otherwise.

2.4.2. Global Stability of the Disease Free Equilibrium

In Theorem 2.4.1, we have established the local asymptotic stability of the fixed point E_0 when $R_0 < 1.$ In this segment, we enumerate conditions that ensure the global asymptotic stability of the disease-free state. The set of conditions for the framework (2.13)-(2.24) can be formulated as:

$$\frac{dM}{dt} = A(M,\ N)\,,\ \frac{dN}{dt} = B(M,\ N)\,, B(Y,\ 0) = 0 \qquad (2.34)$$

where $M = S = (S_m, S_f, S_w)^T$, $M \in \Re_+^3$ and $N = (I_{m1}, I_{m2}, I_{f1}, I_{f2}, I_{w1}, I_{w2}, A_m, A_f, A_w,)^T$,

$N \in \Re_+^9$ denotes the number of susceptible and HIV/AIDS-infected people. The disease-free equilibrium is determined by:

$$E_0 = (M^*,0) = \left(\frac{\Delta_1}{\sigma}, \frac{\Delta_2}{\sigma}, \frac{\Delta_3}{\sigma}, 0,0,0,0,0,0,0,0,0\right).$$

To confirmation the world wide stability, the subsequent situations should be satisfied

(i) For $\frac{dM}{dt} = A(M,0)$, M^* is globally asymptotically stable,

(ii) $B(M,N) = CN - \widehat{B}(M,N), B(M,N) \geq 0$ for $(M,N) \in \Pi$

In this context, designate $C = D_Z B(M^*,0)$ as an M-matrix and Π as the domain where the model holds biological significance. If the conditions (i) and (ii) are met by the system (2.34), the subsequent theorem is applicable.

Theorem 2.4.2: The equilibrium point $E_0 = (M^*,0)$ demonstrates global asymptotic stability within the system described by equations (2.13)-(2.24) when $R_0 < 1$ and the conditions specified in (2.34) are met.

Proof: Considering equations (2.13)-(2.24) along with the conditions in (2.34), we obtain:

$$A(M,\ 0) = \Gamma - \sigma S,$$

$$B(M,\ N) = C\,N - \widehat{B}(M,\ N) \qquad (2.35)$$

Here $\Gamma = (\Delta_1, \Delta_2, \Delta_3)^T$ and

$$C = \begin{pmatrix} -\nu_1 & 0 & \alpha_{mf1}S_m^0 & 0 & \alpha_{mw1}S_m^0 & 0 & 0 & 0 & 0 \\ \delta_{m1} & -\nu_2 & 0 & \alpha_{mf2}S_m^0 & 0 & \alpha_{mw2}S_m^0 & 0 & 0 & 0 \\ \alpha_{fm1}S_f^0 & 0 & -\nu_3 & 0 & 0 & 0 & 0 & 0 & 0 \\ 0 & \alpha_{fm2}S_f^0 & \delta_{f1} & -\nu_4 & 0 & 0 & 0 & 0 & 0 \\ \alpha_{wm1}S_w^0 & 0 & 0 & 0 & -\nu_5 & 0 & 0 & 0 & 0 \\ 0 & \alpha_{wm2}S_w^0 & 0 & 0 & \delta_{w1} & -\nu_6 & 0 & 0 & 0 \\ \rho_{m1} & \rho_{m2} & 0 & 0 & 0 & 0 & -\nu_7 & 0 & 0 \\ 0 & 0 & \rho_{f1} & \rho_{f2} & 0 & 0 & 0 & -\nu_8 & 0 \\ 0 & 0 & 0 & 0 & \rho_{w1} & \rho_{w2} & 0 & 0 & -\nu_9 \end{pmatrix}$$

Then

$$\widehat{B}(M,N) = \begin{pmatrix} \widehat{B}_1(M,N) \\ \widehat{B}_2(M,N) \\ \widehat{B}_3(M,N) \\ \widehat{B}_4(M,N) \\ \widehat{B}_5(M,N) \\ \widehat{B}_6(M,N) \\ \widehat{B}_7(M,N) \\ \widehat{B}_8(M,N) \\ \widehat{B}_9(M,N) \end{pmatrix} = \begin{pmatrix} \alpha_{mf1}(S_m^0 - S_m)I_{f1} + \alpha_{mw1}(S_m^0 - S_m)I_{w1} \\ \alpha_{mf2}(S_m^0 - S_m)I_{f2} + \alpha_{mw2}(S_m^0 - S_m)I_{w2} \\ \alpha_{fm1}(S_f^0 - S_f)I_{m1} \\ \alpha_{fm2}(S_f^0 - S_f)I_{m2} \\ \alpha_{wm1}(S_w^0 - S_w)I_{m1} \\ \alpha_{wm2}(S_w^0 - S_w)I_{m2} \\ 0 \\ 0 \\ 0 \end{pmatrix} \tag{2.36}$$

Here, $S_m^0 \geq S_m, S_f^0 \geq S_f$ and $S_w^0 \geq S_w$, hence it is clear that $\widehat{B}(M,N) \geq 0 \ \forall \ (M,N) \in \Re_+^9$. Furthermore, it is evident that the matrix C qualifies as an M-matrix due to the non-negativity of all its diagonal elements. Consequently, this establishes the global stability of the disease-free equilibrium point (E_0).

2.4.3. Endemic Equilibrium (EE)

The framework (2.13)-(2.24) encompasses a distinctive endemic equilibrium point $E^* = (S_m^*, S_f^*, S_w^*, I_{m1}^*, I_{m2}^*, I_{f1}^*, I_{f2}^*, I_{w1}^*, I_{w2}^*, A_m^*, A_f^*, A_w^*)$ given by:

$$S_m^* = \frac{\Delta_1}{\alpha_{mf1}I_{f1}^* + \alpha_{mf2}I_{f2}^* + \alpha_{mw1}I_{w1}^* + \alpha_{mw2}I_{w2}^* + \sigma}, \ S_f^* = \frac{\Delta_2}{\alpha_{fm1}I_{m1}^* + \alpha_{fm2}I_{m2}^* + \sigma},$$

$$S_w^* = \frac{\Delta_3}{\alpha_{wm1} I_{m1}^* + \alpha_{wm2} I_{m2}^* + \sigma},\ I_{f1}^* = \frac{\alpha_{fm1} I_{m1}^* S_f^*}{\nu_3},\ I_{f2}^* = \frac{\alpha_{fm2} I_{m2}^* S_f^* + \delta_{f1} I_{f1}^*}{\nu_4},$$

$$I_{w1}^* = \frac{\alpha_{wm1}\, I_{m1}^*\, S_w^*}{\nu_5},\ I_{w2}^* = \frac{\alpha_{wm2}\, I_{m2}^*\, S_w^* + \delta_{w1}\, I_{w1}^*}{\nu_6},\ A_m^* = \frac{\rho_{m1}\, I_{m1}^* + \rho_{m2}\, I_{m2}^*}{\nu_7},$$

$$A_f^* = \frac{\rho_{f1}\, I_{f1}^* + \rho_{f2}\, I_{f2}^*}{\nu_8},\ A_w^* = \frac{\rho_{w1}\, I_{w1}^* + \rho_{w2}\, I_{w2}^*}{\nu_9}.$$

Theorem 2.4.3: The global asymptotic stability of the endemic equilibrium E^* in the system (2.13)-(2.24) is affirmed for $R_0 > 1$.

Proof: To demonstrate the global stability of the endemic equilibrium, consider the Lyapunov function Y as

$$Y = P(S_m - S_m^* \ln S_m) + Q(S_f - S_f^* \ln S_f) + R(S_w - S_w^* \ln S_w) + S(I_{m1} - I_{m1}^* \ln I_{m1}) + T(I_{m2} - I_{m2}^* \ln I_{m2})$$
$$+U\ (I_{f1} - I_{f1}^* \ln I_{f1}) + V(I_{f2} - I_{f2}^* \ln I_{f2}) + W(I_{w1} - I_{w1}^* \ln I_{w1}) + X(I_{w2} - I_{w2}^* \ln I_{w2}) \qquad (2.37)$$

The derivative of Y is

$$Y' = P\left(1 - \frac{S_m^*}{S_m}\right) S_m' + Q\left(1 - \frac{S_f^*}{S_f}\right) S_f' + R\left(1 - \frac{S_w^*}{S_w}\right) S_w' + S\left(1 - \frac{I_{m1}^*}{I_{m1}}\right) I_{m1}' + T\left(1 - \frac{I_{m2}^*}{I_{m2}}\right) I_{m2}'$$
$$+U\left(1 - \frac{I_{f1}^*}{I_{f1}}\right) I_{f1}' + V\left(1 - \frac{I_{f2}^*}{I_{f2}}\right) I_{f2}' + W\left(1 - \frac{I_{w1}^*}{I_{w1}}\right) I_{w1}' + X\left(1 - \frac{I_{w2}^*}{I_{w2}}\right) I_{w2}'$$

$$= P\left(1 - \frac{S_m^*}{S_m}\right)\left(\Delta_1 - \alpha_{mf1} S_m I_{f1} - \alpha_{mf2} S_m I_{f2} - \alpha_{mw1} S_m I_{w1} - \alpha_{mw2} S_m I_{w2} - \sigma S_m\right)$$
$$+ Q\left(1 - \frac{S_f^*}{S_f}\right)\left(\sigma_2 - \alpha_{fm1} S_f I_{m1} - \alpha_{fm2} S_f I_{m2} - \sigma S_f\right) + R\left(1 - \frac{S_w^*}{S_w}\right)\begin{pmatrix}\Delta_3 - \alpha_{wm1} S_w I_{m1} - \alpha_{wm2} S_w I_{m2} \\ - \sigma S_w\end{pmatrix}$$
$$+ S\left(1 - \frac{I_{m1}^*}{I_{m1}}\right)\left(\alpha_{mf1} S_m I_{f1} + \alpha_{mw1} S_m I_{w1} - p_1 I_{m1}\right) + T\left(1 - \frac{I_{m2}^*}{I_{m2}}\right)\begin{pmatrix}\alpha_{mf2} S_m I_{f2} + \alpha_{mw2} S_m I_{w2} \\ + \delta_{m1} I_{m1} - p_2 I_{m2}\end{pmatrix}$$
$$+ U\left(1 - \frac{I_{f1}^*}{I_{f1}}\right)\left(\alpha_{fm1} S_f I_{m1} - p_3 I_{f1}\right) + V\left(1 - \frac{I_{f2}^*}{I_{f2}}\right)\left(\alpha_{fm2} S_f I_{m2} + \delta_{f1} I_{f1} - p_4 I_{f2}\right)$$
$$+ W\left(1 - \frac{I_{w1}^*}{I_{w1}}\right)\left(\alpha_{wm1} S_w I_{m1} - p_5 I_{w1}\right) I_{w1}' + X\left(1 - \frac{I_{w2}^*}{I_{w2}}\right)\left(\alpha_{wm2} S_w I_{m2} + \delta_{w1} I_{w1} - p_6 I_{w2}\right) \qquad (2.38)$$

The framework of conditions (2.13)-(2.24) satisfies the subsequent relation on the equilibrium point

$$\Delta_1 = \alpha_{mf1} S_m^* I_{f1}^* + \alpha_{mf2} S_m^* I_{f2}^* + \alpha_{mw1} S_m^* I_{w1}^* + \alpha_{mw2} S_m^* I_{w2}^* + \sigma S_m^*,$$

$\Delta_2 = \alpha_{fm1} S_f^* I_{m1}^* + \alpha_{fm2} S_f^* I_{m2}^* + \sigma S_f^*$, $\Delta_3 = \alpha_{wm1} S_w^* I_{m1}^* + \alpha_{wm2} S_w^* I_{m2}^* + \sigma S_w^*$,

$$v_1 = \frac{\alpha_{mf1} S_m^* I_{f1}^* + \alpha_{mw1} S_m^* I_{w1}^*}{I_{m1}^*},\ v_2 = \frac{\alpha_{mf2} S_m^* I_{f2}^* + \alpha_{mw2} S_m^* I_{w2}^* + \delta_{m1} I_{m1}^*}{I_{m2}^*},$$

$$v_3 = \frac{\alpha_{fm1} S_f^* I_{m1}^*}{I_{f1}^*},\ v_4 = \frac{\alpha_{fm2} S_f^* I_{m2}^* + \delta_{f1} I_{f1}^*}{I_{f2}^*},\ v_5 = \frac{\alpha_{wm1} S_w^* I_{m1}^*}{I_{w1}^*},\ v_6 = \frac{\alpha_{wm2} S_w^* I_{m2}^* + \delta_{w1} I_{w1}^*}{I_{w2}^*},$$

Substituting all these values in (2.38), we get

$$\begin{aligned}
Y' = {} & P\left(1 - \frac{S_m^*}{S_m}\right)\left[\begin{array}{l}\alpha_{mf1} S_m^* I_{f1}^* + \alpha_{mf2} S_m^* I_{f2}^* + \alpha_{mw1} S_m^* I_{w1}^* + \alpha_{mw2} S_m^* I_{w2}^* + \sigma S_m^* \\ -\left(\alpha_{mf1} S_m I_{f1} + \alpha_{mf2} S_m I_{f2} + \alpha_{mw1} S_m I_{w1} + \alpha_{mw2} S_m I_{w2} + \sigma S_m\right)\end{array}\right] \\
& + Q\left(1 - \frac{S_f^*}{S_f}\right)\left[\alpha_{fm1} S_f^* I_{m1}^* + \alpha_{fm2} S_f^* I_{m2}^* + \sigma S_f^* - \left(\alpha_{fm1} S_f I_{m1} + \alpha_{fm2} S_f I_{m2} + \sigma S_f\right)\right] \\
& + R\left(1 - \frac{S_w^*}{S_w}\right)\left[\alpha_{wm1} S_w^* I_{m1}^* + \alpha_{wm2} S_w^* I_{m2}^* + \sigma S_w^* - \left(\alpha_{wm1} S_w I_{m1} + \alpha_{wm2} S_w I_{m2} + \sigma S_w\right)\right] \\
& + S\left(1 - \frac{I_{m1}^*}{I_{m1}}\right)\left(\alpha_{mf1} S_m I_{f1} + \alpha_{mw1} S_m I_{w1} - \frac{\alpha_{mf1} S_m^* I_{f1}^* + \alpha_{mw1} S_m^* I_{w1}^*}{I_{m1}^*} I_{m1}\right) \\
& + T\left(1 - \frac{I_{m2}^*}{I_{m2}}\right)\left(\alpha_{mf2} S_m I_{f2} + \alpha_{mw2} S_m I_{w2} + \delta_{m1} I_{m1} - \frac{\alpha_{mf2} S_m^* I_{f2}^* + \alpha_{mw2} S_m^* I_{w2}^* + \delta_{m1} I_{m1}^*}{I_{m2}^*} I_{m2}\right) \\
& + U\left(1 - \frac{I_{f1}^*}{I_{f1}}\right)\left(\alpha_{fm1} S_f I_{m1} - \frac{\alpha_{fm1} S_f^* I_{m1}^*}{I_{f1}^*} I_{f1}\right) + V\left(1 - \frac{I_{f2}^*}{I_{f2}}\right)\left(\begin{array}{l}\alpha_{fm2} S_f I_{m2} + \delta_{f1} I_{f1} \\ -\dfrac{\alpha_{fm2} S_f^* I_{m2}^* + \delta_{f1} I_{f1}^*}{I_{f2}^*} I_{f2}\end{array}\right) \\
& + W\left(1 - \frac{I_{w1}^*}{I_{w1}}\right)\left(\alpha_{wm1} S_w I_{m1} - \frac{\alpha_{wm1} S_w^* I_{m1}^*}{I_{w1}^*} I_{w1}\right) + X\left(1 - \frac{I_{w2}^*}{I_{w2}}\right)\left(\begin{array}{l}\alpha_{wm2} S_w I_{m2} + \delta_{w1} I_{w1} \\ -\dfrac{\alpha_{wm2} S_w^* I_{m2}^* + \delta_{w1} I_{w1}^*}{I_{w2}^*} I_{w2}\end{array}\right)
\end{aligned}$$

Using the following variable substitutions

$$\frac{S_m}{S_m^*} = u_1, \frac{S_f}{S_f^*} = u_2, \frac{S_w}{S_w^*} = u_3, \frac{I_{m1}}{I_{m1}^*} = x_1, \frac{I_{m2}}{I_{m2}^*} = x_2, \frac{I_{f1}}{I_{f1}^*} = y_1, \frac{I_{f2}}{I_{f2}^*} = y_2, \frac{I_{w1}}{I_{w1}^*} = z_1, \frac{I_{w2}}{I_{w2}^*} = z_2,$$

the derivative of Y reduces to

$$Y' = -P\sigma S_m^* \frac{(1-u_1)^2}{u_1} - Q\sigma S_f^* \frac{(1-u_2)^2}{u_2} - R\sigma S_w^* \frac{(1-u_3)^2}{u_3}$$

$$+ P\left(1 - \frac{1}{u_1}\right)\left[\alpha_{mf1} S_m^* I_{f1}^* (1 - u_1 y_1) + \alpha_{mf2} S_m^* I_{f2}^* (1 - u_1 y_2) + \alpha_{mw1} S_m^* I_{w1}^* (1 - u_1 z_1) + \alpha_{mw2} S_m^* I_{w2}^* (1 - u_1 z_2)\right]$$

$$+Q\left(1-\frac{1}{u_2}\right)\left[\alpha_{fm1}S_f^*I_{m1}^*(1-u_2x_1)+\alpha_{fm2}S_f^*I_{m2}^*(1-u_2x_2)\right]+R\left(1-\frac{1}{u_3}\right)\begin{bmatrix}\alpha_{wm1}S_w^*I_{m1}^*(1-u_3x_1)\\+\alpha_{wm2}S_w^*I_{m2}^*(1-u_3x_2)\end{bmatrix}$$

$$+S\left(1-\frac{1}{x_1}\right)\left[\alpha_{mf1}S_m^*I_{f1}^*(u_1y_1-x_1)+\alpha_{mw1}S_m^*I_{w1}^*(u_1z_1-x_1)\right]+T\left(1-\frac{1}{x_2}\right)\begin{bmatrix}\alpha_{mf2}S_m^*I_{f2}^*(u_1y_2-x_2)\\+\alpha_{mw2}S_m^*I_{w2}^*(u_1z_2-x_2)\\+\delta_{m1}I_{m1}^*(x_1-x_2)\end{bmatrix}$$

$$+U\left(1-\frac{1}{y_1}\right)\left[\alpha_{fm1}S_f^*I_{m1}^*(u_2x_1-y_1)\right]+V\left(1-\frac{1}{y_2}\right)\left[\alpha_{fm2}S_f^*I_{m2}^*(u_2x_2-y_2)+\delta_{f1}I_{f1}^*(y_1-y_2)\right]$$

$$+W\left(1-\frac{1}{z_1}\right)\left[\alpha_{wm1}S_w^*I_{m1}^*(u_3x_1-z_1)\right]+X\left(1-\frac{1}{z_2}\right)\left[\alpha_{wm2}S_w^*I_{m2}^*(u_3x_2-z_2)+\delta_{w1}I_{w1}^*(z_1-z_2)\right]$$

$$=-P\sigma S_m^*\frac{(1-u_1)^2}{u_1}-Q\sigma S_f^*\frac{(1-u_2)^2}{u_2}-R\sigma S_w^*\frac{(1-u_3)^2}{u_3}+Z(n_1,n_2,n_3,n_4,n_5,n_6,n_7,n_8,n_9) \quad (2.39)$$

where

$$\begin{aligned}
Z=\;&P\alpha_{mf1}S_m^*I_{f1}^*+P\alpha_{mf2}S_m^*I_{f2}^*+P\alpha_{mw1}S_m^*I_{w1}^*+P\alpha_{mw2}S_m^*I_{w2}^*+Q\alpha_{fm1}S_f^*I_{m1}^*+Q\alpha_{fm2}S_f^*I_{m2}^*\\
&+R\alpha_{wm1}S_w^*I_{m1}^*+R\alpha_{wm2}S_w^*I_{m2}^*+S\alpha_{mf1}S_m^*I_{f1}^*+S\alpha_{mw1}S_m^*I_{w1}^*+T\alpha_{mf2}S_m^*I_{f2}^*+T\alpha_{mw2}S_m^*I_{w2}^*\\
&+T\delta_{m1}I_{m1}^*+U\alpha_{fm1}S_f^*I_{m1}^*+V\alpha_{fm2}S_f^*I_{m2}^*+V\delta_{f1}I_{f1}^*+W\alpha_{wm1}S_w^*I_{m1}^*+X\alpha_{wm2}S_w^*I_{m2}^*+X\delta_{w1}I_{w1}^*\\
&+u_1y_1\left(-P\alpha_{mf1}S_m^*I_{f1}^*+S\alpha_{mf1}S_m^*I_{f1}^*\right)+u_1y_2\left(-P\alpha_{mf2}S_m^*I_{f2}^*+T\alpha_{mf2}S_m^*I_{f2}^*\right)\\
&+u_1z_1\left(-P\alpha_{mw1}S_m^*I_{w1}^*+S\alpha_{mw1}S_m^*I_{w1}^*\right)+u_1z_2\left(-P\alpha_{mw2}S_m^*I_{w2}^*+T\alpha_{mw2}S_m^*I_{w2}^*\right)\\
&+u_2x_1\left(-Q\alpha_{fm1}S_f^*I_{m1}^*+U\alpha_{fm1}S_f^*I_{m1}^*\right)+u_2x_2\left(-Q\alpha_{fm2}S_f^*I_{m2}^*+V\alpha_{fm2}S_f^*I_{m2}^*\right)\\
&+u_3x_1\left(-R\alpha_{wm1}S_w^*I_{m1}^*+W\alpha_{wm1}S_w^*I_{m1}^*\right)+u_3x_2\left(-R\alpha_{wm2}S_w^*I_{m2}^*+X\alpha_{wm2}S_w^*I_{m2}^*\right)\\
&+x_1\left(Q\alpha_{fm1}S_f^*I_{m1}^*+R\alpha_{wm1}S_w^*I_{m1}^*-S\alpha_{mf1}S_m^*I_{f1}^*-S\alpha_{mw1}S_m^*I_{w1}^*+T\delta_{m1}I_{m1}^*\right)\\
&+x_2\left(Q\alpha_{fm2}S_f^*I_{m2}^*+R\alpha_{wm2}S_w^*I_{m2}^*-T\alpha_{mf2}S_m^*I_{f2}^*-T\alpha_{mw2}S_m^*I_{w2}^*-T\delta_{m1}I_{m1}^*\right)\\
&+y_1\left(P\alpha_{mf1}S_m^*I_{f1}^*-U\alpha_{fm1}S_f^*I_{m1}^*+V\delta_{f1}I_{f1}^*\right)+y_2\left(P\alpha_{mf2}S_m^*I_{f2}^*-V\alpha_{fm2}S_f^*I_{m2}^*-V\delta_{f1}I_{f1}^*\right)\\
&+z_1\left(P\alpha_{mw1}S_m^*I_{w1}^*-W\alpha_{wm1}S_w^*I_{m1}^*+X\delta_{w1}I_{w1}^*\right)+z_2\left(P\alpha_{mw2}S_m^*I_{w2}^*-X\alpha_{wm2}S_w^*I_{m2}^*-X\delta_{w1}I_{w1}^*\right)\\
&-\frac{u_1y_1}{x_1}\left(S\alpha_{mf1}S_m^*I_{f1}^*\right)-\frac{u_1y_2}{x_2}\left(T\alpha_{mf2}S_m^*I_{f2}^*\right)-\frac{u_1z_1}{x_1}\left(S\alpha_{mw1}S_m^*I_{w1}^*\right)-\frac{u_1z_2}{x_2}\left(T\alpha_{mw2}S_m^*I_{w2}^*\right)\\
&-\frac{u_2x_1}{y_1}\left(U\alpha_{fm1}S_f^*I_{m1}^*\right)-\frac{u_2x_2}{y_2}\left(V\alpha_{fm2}S_f^*I_{m2}^*\right)-\frac{u_3x_1}{z_1}\left(W\alpha_{wm1}S_w^*I_{m1}^*\right)-\frac{u_3x_2}{z_2}\left(X\alpha_{wm2}S_w^*I_{m2}^*\right)\\
&-\frac{x_1}{x_2}\left(T\delta_{m1}I_{m1}^*\right)-\frac{y_1}{y_2}\left(V\delta_{f1}I_{f1}^*\right)-\frac{z_1}{z_2}\left(X\delta_{w1}I_{w1}^*\right)-\frac{1}{u_1}\begin{pmatrix}P\alpha_{mf1}S_m^*I_{f1}^*+P\alpha_{mf2}S_m^*I_{f2}^*\\+P\alpha_{mw1}S_m^*I_{w1}^*+P\alpha_{mw2}S_m^*I_{w2}^*\end{pmatrix}
\end{aligned}$$

$$-\frac{1}{u_2}\left(Q\alpha_{fm1}S_f^*I_{m1}^*+Q\alpha_{fm2}S_f^*I_{m2}^*\right)-\frac{1}{u_3}\left(R\alpha_{wm1}S_w^*I_{m1}^*+R\alpha_{wm2}S_w^*I_{m2}^*\right) \quad (2.40)$$

In arrange to decide the values of $P,Q,R,S,T,U,V,W,$ and X, by making the coefficient $u_1y_1,u_1y_2,u_1z_1,u_1z_2,u_2x_1,u_2x_2,u_3x_1$ and u_3x_2 identical to zero, we get $P=S=T$, $Q=U=V$ and $R=W=X$

Advance by choosing $P=Q=R=S=T=U=V=W=X=1$ in (2.40), we get

$$Z=\alpha_{mf1}S_m^*I_{f1}^*\left(2+y_1-x_1-\frac{u_1y_1}{x_1}-\frac{1}{u_1}\right)+\alpha_{mf2}S_m^*I_{f2}^*\left(2+y_2-x_2-\frac{u_1y_2}{x_2}-\frac{1}{u_1}\right)$$

$$+\alpha_{mw1}S_m^*I_{w1}^*\left(2+z_1-x_1-\frac{u_1z_1}{x_1}-\frac{1}{u_1}\right)+\alpha_{mw2}S_m^*I_{w2}^*\left(2+z_2-x_2-\frac{u_1z_2}{x_2}-\frac{1}{u_1}\right)$$

$$+\alpha_{fm1}S_f^*I_{m1}^*\left(2+x_1-y_1-\frac{u_2x_1}{y_1}-\frac{1}{u_2}\right)+\alpha_{fm2}S_f^*I_{m2}^*\left(2+x_2-y_2-\frac{u_2x_2}{y_2}-\frac{1}{u_2}\right)$$

$$+\alpha_{wm1}S_w^*I_{m1}^*\left(2+x_1-z_1-\frac{u_3x_1}{z_1}-\frac{1}{u_3}\right)+\alpha_{wm2}S_w^*I_{m2}^*\left(2+x_2-z_2-\frac{u_3x_2}{z_2}-\frac{1}{u_3}\right)$$

$$+\delta_{m1}I_{m1}^*\left(1+x_1-x_2-\frac{x_1}{x_2}\right)+\delta_{f1}I_{f1}^*\left(1+y_1-y_2-\frac{y_1}{y_2}\right)+\delta_{w1}I_{w1}^*\left(1+z_1-z_2-\frac{z_1}{z_2}\right)$$

Since the arithmetic imply is more than or identical to the geometric imply, we have

$2+y_1-x_1-\frac{u_1y_1}{x_1}-\frac{1}{u_1}\le 0$ for $u_1,x_1,y_1>0$ and $2+y_1-x_1-\frac{u_1y_1}{x_1}-\frac{1}{u_1}=0$, if and only if $u_1=1,x_1=y_1$. Also the expressions

$$\left(2+y_2-x_2-\frac{u_1y_2}{x_2}-\frac{1}{u_1}\right),\left(2+z_1-x_1-\frac{u_1z_1}{x_1}-\frac{1}{u_1}\right),\left(2+z_2-x_2-\frac{u_1z_2}{x_2}-\frac{1}{u_1}\right),$$
$$\left(2+x_1-y_1-\frac{u_2x_1}{y_1}-\frac{1}{u_2}\right),\left(2+x_2-y_2-\frac{u_2x_2}{y_2}-\frac{1}{u_2}\right),\left(2+x_1-z_1-\frac{u_3x_1}{z_1}-\frac{1}{u_3}\right),$$
$$\left(2+x_2-z_2-\frac{u_3x_2}{z_2}-\frac{1}{u_3}\right),\left(1+x_1-x_2-\frac{x_1}{x_2}\right),\left(1+y_1-y_2-\frac{y_1}{y_2}\right)\text{and}\left(1+z_1-z_2-\frac{z_1}{z_2}\right)$$

are less than or equal to zero if and only if $u_1=u_2=u_3=1$ and $x_1=x_2=y_1=y_2=z_1=z_2$. Therefore, $Y'\le 0$ for $u_1,u_2,u_3,x_1,x_2,y_1,y_2,z_1,z_2>0$ in Π. The equality $Y'=0$ holds if and only if $u_1=u_2=u_3=1$ and $x_1=x_2=y_1=y_2=z_1=z_2$. Applying LaSalle's invariance principle (1976), we can deduce that the endemic equilibrium E^* of the system (2.13)-(2.24) achieves global asymptotic stability when $R_0>1$.

2.5. Numerical Simulation

To validate the analytical findings, a program is created using MATLAB software. The default parameters selected for this purpose are as follows:

$\Delta_1 = 90,\quad \Delta_2 = 40,\quad \Delta_3 = 30,\quad \alpha_{mf1} = 0.00005,\quad \alpha_{mf2} = 0.00002,\quad \alpha_{mw1} = 0.00001,$

$\alpha_{mw2} = 0.00003,\quad \alpha_{fm1} = 0.00002,\quad \alpha_{fm2} = 0.00002,\quad \alpha_{wm1} = 0.00003,\quad \alpha_{wm2} = 0.00004,$

$\sigma = 0.0745,\quad \rho_{m1} = 0.500,\quad \rho_{m2} = 0.09,\quad \rho_{f1} = 0.25,\quad \rho_{f2} = 0.57,\quad \rho_{w1} = 0.30,\quad \rho_{w2} = 0.54,$

$m = f = w = 0.123,\ \delta_{m1} = 0.03,\ \delta_{f1} = 0.04,\ \delta_{w1} = 0.01.$

Figures 2.2, 2.3 and 2.4 depict the variants of susceptible classes, infective classes and full-blown AIDS classes of populations with time t. It is located that during all of the figures, the population of susceptible classes increases and then it goes to the equilibrium point, where the infective classes and full-blown AIDS classes of males, females and female sex workers, respectively, decreases and then it goes to be stable for a fixed value of $R_0 = 0.1086 < 1,$ while in any other case, instability is observed.

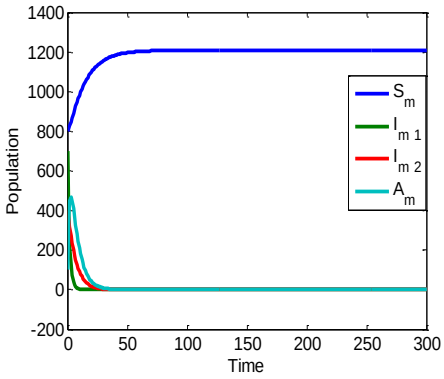

Figure 2.2: Disease free equilibrium of susceptible, infective and the full-blown AIDS classes for males.

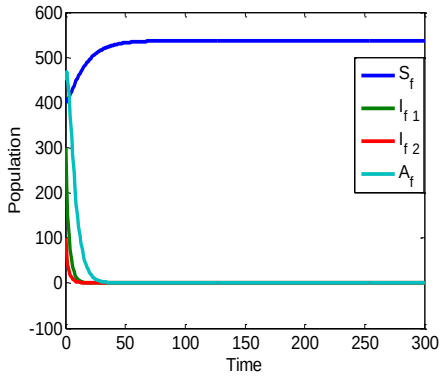

Figure 2.3: Disease free equilibrium of susceptible, infective and the full-blown AIDS classes for females.

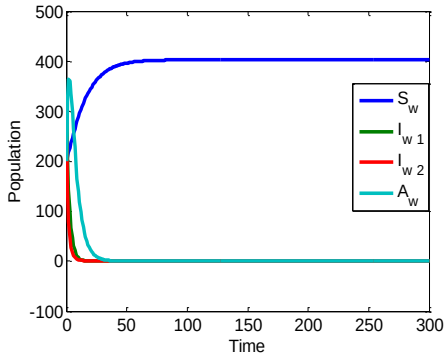

Figure 2.4: Disease free equilibrium of susceptible, infective and the full- blown AIDS classes for female sex workers.

For Figures 2.5, 2.6 and 2.7, the default set of parameters chosen is as follows:

$\Delta_1 = 80$, $\Delta_2 = 60$, $\Delta_3 = 50$, $\alpha_{mf1} = 0.00005$, $\alpha_{mf2} = 0.0002$, $\alpha_{mw1} = 0.0001$, $\alpha_{mw2} = 0.0003$, $\alpha_{fm1} = 0.0002$, $\alpha_{fm2} = 0.0002$, $\alpha_{wm1} = 0.0003$, $\alpha_{wm2} = 0.0004$, $\sigma = 0.0743$, $\rho_{m1} = 0.107261$, $\rho_{m2} = 0.0924$, $\rho_{f1} = 0.25$, $\rho_{f2} = 0.27$, $\rho_{w1} = 0.30$, $\rho_{w2} = 0.24$, $m = f = w = 0.123$, $\delta_{m1} = 0.03$, $\delta_{f1} = 0.05$, $\delta_{w1} = 0.02$.

Figures 2.5, 2.6 and 2.7 depict the variants of susceptible classes, infective classes and full-blown AIDS classes of populations with time. It is located that during all of the figures, the population of susceptible classes increases, and then it goes to the equilibrium point, where the infective classes and full-blown AIDS classes of males, females and female sex workers, respectively, decreases and then it goes to be stable for a fixed value of $R_0 = 1.6235 > 1$, while in any other case, instability is observed.

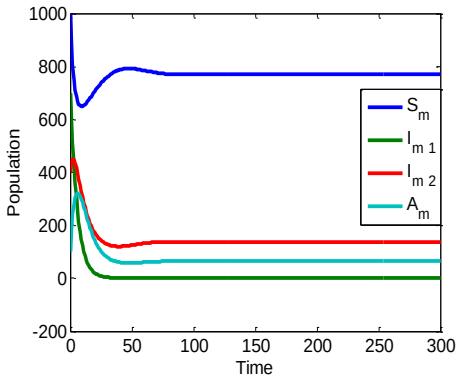

Figure 2.5: Endemic equilibrium of susceptible, infective and the full-blown AIDS classes for males.

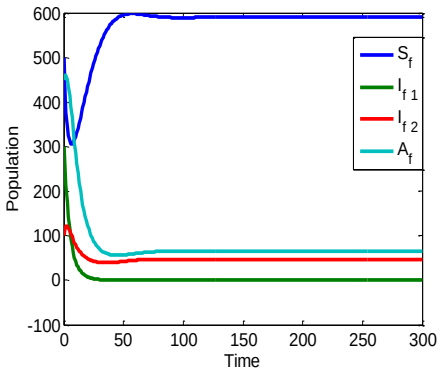

Figure 2.6: Endemic equilibrium of susceptible, infective and the full-blown AIDS classes for females.

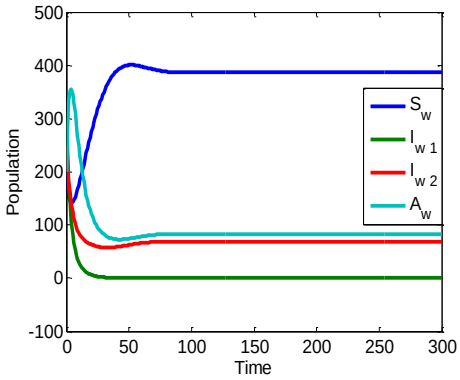

Figure 2.7: Endemic equilibrium of susceptible, infective and the full- blown AIDS classes for female sex workers.

2.6. Summary and Concluding Remarks

In this chapter, we have conducted an in-depth examination of a nonlinear mathematical model describing the transmission dynamics of HIV/AIDS, placing particular emphasis on its effects within the community of female sex workers. Our model has enabled us to delve into

the dynamics of this complex epidemic, examining two critical equilibria: the disease-free equilibrium and the endemic equilibrium.

Our mathematical analysis reveals that the stability of the disease-free equilibrium is contingent upon the value of the reproduction number, denoted as R_0. Our findings demonstrate that when $R_0 < 1$, both local and global asymptotic stability characterize the disease-free equilibrium. Conversely, when R_0 exceeds unity, the disease-free equilibrium becomes unstable, signifying the potential for the disease to persist and spread within the population.

Furthermore, we have employed the Lyapunov characteristic to investigate the worldwide stability of the endemic equilibrium. Our findings reveal that the endemic equilibrium is stable when R_0 exceeds unity, reinforcing the significance of this threshold value in understanding the persistence of the epidemic.

In our numerical simulations, a significant correlation has been identified between the infection rate originating from infective classes of females and female sex workers and the population of susceptible males. Specifically, as the rate of infection increases, the number of susceptible males decreases, underscoring the importance of intervention strategies targeting these specific populations.

Additionally, to visually illustrate our findings, we have provided several key figures:

- Figure 2.2: Disease-Free Equilibrium of Males
- Figure 2.3: Disease-Free Equilibrium of Females
- Figure 2.4: Disease-Free Equilibrium of Female Sex-Workers
- Figure 2.5: Endemic Equilibrium of Males
- Figure 2.6: Endemic Equilibrium of Females
- Figure 2.7: Endemic Equilibrium of Female Sex-Workers

These figures serve as valuable visual aids, providing a graphical representation of the equilibria and dynamics discussed in this research.

In conclusion, our study provides valuable insights into the dynamics of HIV/AIDS transmission among female sex workers, emphasizing the role of mathematical modeling in understanding and mitigating the epidemic. By exploring the equilibria and stability conditions of our model and examining numerical results, we contribute to the body of knowledge essential for formulating effective prevention and control measures.

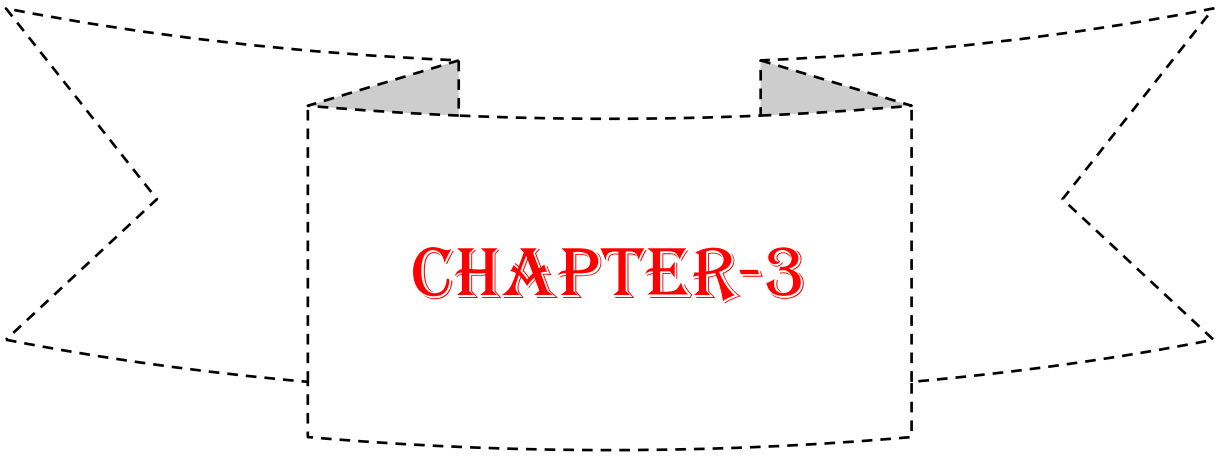

Study of HIV Transmission Dynamics using SEIRS Epidemic Model

Section 3A: Analyzing HIV Transmission Dynamics with Media Awareness

Section 3B: Analyzing the Co-infection Dynamics of HIV/AIDS-TB with Media Awareness

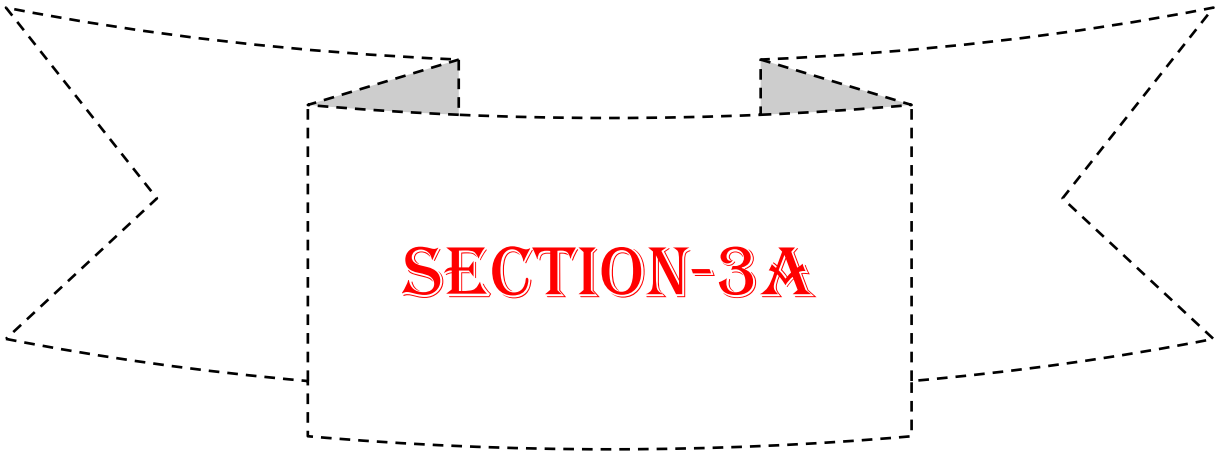

Analyzing HIV Transmission Dynamics with Media Awareness

Keywords: SEIRS Epidemic Model, Reproduction Number, Endemic Equilibrium, Stability Analysis and Adaptive Neuro-Fuzzy Inference System.

Chapter 3: Study of HIV Transmission Dynamics using SEIRS Epidemic Model

This chapter presents a comprehensive examination of disease transmission dynamics in two distinct sections. The first section scrutinizes the intricate dynamics of HIV transmission, specifically exploring the influence of media awareness on its spread within populations. Understanding the interplay between media awareness and HIV transmission is crucial to formulating targeted strategies for prevention and intervention. The second section shifts focus to the complex co-infection dynamics of HIV/AIDS & TB, considering the influence of media awareness on disease dynamics. Investigating the intersection of media influence and co-infection dynamics sheds light on the nuanced interactions between these diseases, offering insights essential for tailored intervention approaches. Both sections aim to provide an integral comprehension of disease transmission and the impact of media awareness on public health strategies, significantly contributing to the discourse on controlling and managing these critical health challenges.

Section 3A: Analyzing HIV Transmission Dynamics with Media Awareness

3A.1. Introduction

HIV is an acronym for Human Immunodeficiency Virus, which causes HIV infection. In many cases HIV can go unnoticed for about a decade before it is detected and by that time the person is more likely to develop Acquired Immunodeficiency Syndrome (AIDS). Unlike other viruses, HIV is difficult to eliminate from the human system partly due to its complex nature. Treatment for HIV can only attempt to make life more comfortable for the patient as there is no cure for it yet making it an epidemic. As per the World Health Organization (WHO), HIV attacks a human innate immunity system by weakening it thus failing to fight contamination of any kind.

Consequently, the human body is highly infected with viruses, various infections and tumours eventually leading to AIDS and death. Since HIV is a virus, it needs a host cell to carry out its toxic operations in the immune system. The origin of HIV has been traced back to a chimpanzee in Central Africa, where humans came into contact with the infected blood of these chimpanzees when they hunted them for meat. Several studies suggest that HIV likely spread from apes to humans in the late 1800s. Over time, the virus spread across Africa and subsequently to other parts of the world, including the US, where it has been known to exist since at least the mid-1970s.

When an infectious disease such as AIDS or HIV starts to spread in a region, it becomes the responsibility of the disease control department to prevent the disease from happening at all costs. The first step is to provide relevant knowledge through the media so that people know how to protect themselves from coming into contact with the disease and what steps to take if they are infected. The more preventive knowledge people have the more likely it is to prevent the disease from spreading across towns or states. Media coverage, such as news channels, newspapers, online social media platforms and educational enlightenment provided in schools and colleges, participates in the huge responsibility of spreading consciousness about the disease as per a recent statistical analysis on HIV and AIDS awareness strategies. One of the critical factors in preventing the AIDS epidemic is public awareness. The chances of people being aware of AIDS increased by 4.67 and 77.73 times for educated men and women respectively rather than uneducated individuals. This proves that providing substantial knowledge about the disease in educational institutions is critical to spreading awareness. Moreover, individuals who engage in daily television (T.V) viewing exhibit an 8.6 times higher likelihood of being informed regarding AIDS compared to those who never view television. These findings underscore the importance of investigating how disease spread dynamics are influenced by media coverage and educational efforts.

The spread of probably the most severe and highly contagious Severe Acute Respiratory Syndrome (SARS) in 2003 in Beijing, China, stimulated an emergency response globally. This emergency highlighted the need for an effective and efficient emergency response to reduce the impacts of such an infectious disease outbreak. The lack of understanding of SARS led to panic in the population. So when the disease control department and government officials announced and shared information about SARS, people responded positively by wearing masks on the streets, reducing close contact with others, reposting new cases to hospitals, etc. Mass Communication Media and education play vital roles in risk communication. These results indicated that releasing prevention knowledge had changed people's health habits.

In this section, we propose a novel approach based on the ANFIS to model the transmission dynamics of HIV using a SEIRS epidemic model. The ANFIS is a hybrid computational model that combines the advantages of artificial neural networks and fuzzy logic and has been successfully applied in a wide range of fields, including engineering, finance, medicine and crisis management (Keshavarz & Torkian, 2018; Perveen *et al.*, 2019; Tan *et al.*, 2011; Yadollahpour *et al.*, 2018; Lakovic, 2020). Our proposed ANFIS-based SEIRS model aims to capture the complex nonlinear interactions among different compartments of the HIV epidemic and predict future trends under different scenarios. The decision to employ the SEIRS model in

studying HIV transmission is motivated by the necessity to comprehensively represent the disease's multifaceted dynamics, including its prolonged incubation period and the potential for reinfection post-recovery, which are often overlooked in existing models. By incorporating the recovered class, our proposed model uniquely addresses these facets of HIV dynamics. Additionally, integrating media influence allows us to provide a holistic understanding of disease transmission, shedding light on previously unexplored dimensions that impact spread and inform more effective control strategies.

This section is structured as follows: Section 3A.2 provides detailed literature on the transmission dynamics of HIV with an SEIRS epidemic model. The mathematical model is covered in section 3A.3. The subsequent sections cover the analysis of the model (Section 3A.4) and the Adaptive Neuro-Fuzzy Inference System (ANFIS) in section 3A.5. A numerical illustration is given in section 3A.6. Finally, summary and concluding remarks are drawn within the last section, 3A.7.

3A.2. Literature Review

Mathematical modeling studies have been conducted to examine how media coverage and psychology can influence the transference and command of infectious diseases in specific populations or regions. In a study conducted by Liu *et al.,* in 2007, a three-partition model, which included individuals exposed (E), infectious (I) and hospitalized (H), was employed to survey the psychological mechanisms associated with various instances of emerging infectious disease outbreaks. The simplification of the imitation involved the supposition that the overall dimensions of the inhabitants remained constant during the spread of the disease. Another study by Cui *et al.,* (2006) extended the classical SEI model by incorporating a new incidence function that considers media coverage's impact on disease transmission and control.

Cai *et al.,* (2009) conducted an investigation into an HIV/AIDS outbreak replica incorporating cure. Jain *et al.,* (2010) studied the dynamics behavior of T-lymphocyte cells with a human immunodeficiency virus type 1 (HIV-I) infection. Huo and Feng (2013) develop an HIV/AIDS outbreak system incorporating various target phases and therapy options. Yang *et al.,* (2023) investigate an edge-based SEIR epidemic model that accounts for both sexual and non-sexual transmission routes.

Huo *et al.,* (2016) introduce a novel HIV/AIDS epidemic model that incorporates a modern section, namely the treatment section (T). Sing *et al.,* (2016) undertake a study using a arithmetical replica to evaluate the transmission dynamics of the HIV/AIDS outbreak, including treatment. Sing *et al.,* (2019) propose an SEIR mathematical model to elucidate the

transmission dynamics of malaria. Ali *et al.,* (2019) devise a nonlinear compartment model to evaluate the impact of media reporting on the control and prevention of infectious diseases. Huo *et al.,* (2018) expand a SEIS outbreak representation that is more realistic by incorporating the influence of media, fundamental reproductive number, and illustrating the firmness of both ailment-free and native symmetry states. Jia and Qin (2017) define an HIV/AIDS epidemic model with a standard nonlinear prevalence rate and treatment. Biswas and Pal (2017) develop a nonlinear mathematical model for HIV/AIDS transmission dynamics, considering vaccination and antiretroviral treatment and demonstrating the existence and boundedness of its solutions. Wu and Zhao (2021) collected data to examine the worldwide dimensions of the HIV/AIDS epidemic and to scrutinize its transmission within the demographic of men who engage in sexual activity with other men. Kumar *et al.,* (2021) present a numerical simulation of HIV/AIDS transference dynamics in the presence of cognizance campaigns, employing a copy with three distinct operators. According to a study by Luxi *et al.,* (2021) on the global impact of the COVID-19 vaccine within the initial year, the vaccination significantly changed the path of the pandemic. It saved tens of millions of lives worldwide. However, the benefit was limited in these situations because of limited vaccine accessibility in low-income countries, underscoring the importance of global vaccine equity and comprehensive coverage. A mathematical study was conducted by Riyapan *et al.,* (2021) to comprehensively examine the dynamics of COVID-19 transmission during the pandemic in Bangkok, Thailand. The study looked at the use of masks as one of the ways of slowing the COVID-19 spread. Modification of the SEIR model to include the symptomatically infected, asymptomatically infected, and quarantined was made in this study.

In the latest, there has been an increase in using ANFIS to model various diseases. Many studies have investigated the effectiveness of this approach in understanding disease spread and developing intervention strategies. Deif *et al.,* (2021) propose an ANFIS approach to rapidly detect COVID-19 cases using commonly available laboratory blood tests. Rise and Ershadi (2022) propose an uncertain SEIAR model to analyze the socioeconomic impacts of infectious diseases based on uncertain behaviours of social and practical subsystems in countries. The proposed model considers different subsystems, including healthcare systems, transportation, contacts, and capacities of food and pharmaceutical networks for sensitivity analysis. An ANFIS model is also designed to predict countries gross domestic product (GDP) and determine the economic impacts of infectious diseases. A COVID-19 forecasting system using ANFIS was discussed by Ly Kim Tien (2021).

In recent times, there has been an increase in utilizing the Adaptive Neuro-Fuzzy Inference System (ANFIS) to model various diseases and understand disease spread, leading to the development of effective intervention strategies. However, few studies specifically address the SEIRS Epidemic Model with software support considering social media's role in the spread of HIV/AIDS. It is crucial to provide a mathematical model examining the transmission dynamics of a SEIRS epidemic model for HIV, emphasizing the influence of media. In light of the analysis gap, the purpose of the current article is to fill the void by presenting an arithmetical copy to examine the transmission dynamics of a SEIRS outbreak model for HIV, with a specific emphasis on the impact of media. Moreover, this study focuses on employing ANFIS to address the SEIRS epidemic model for HIV, which has not been extensively explored in the existing literature. By developing an SEIRS epidemic model for HIV with incorporated features, this research aimed to regulate the fundamental reproduction number and look into the ailment-free and native equilibria. The contributions of this study, along with relevant articles in the literature, are summarized in Table 3A.1. The present studies formulates a structure of distinct calculations for each population group, including the susceptible, uncover, contaminated and convalesce classes, utilizing the Runge-Kutta IV order method. The calculation of the fundamental reproduction number is performed, and the examination of the ailment-free and native states is established.

Table 3A.1: Comparative Analysis of HIV Transmission Dynamics: Unveiling Gaps and Innovations via an SEIRS Epidemic Model with ANFIS Validation.

Author	**Specific features considered**						
	Epidemic Model	HIV	Reproduction Number	Disease-Free Equilibrium	Endemic Equilibrium	Stability Analysis	ANFIS
Cai *et al*., (2009)	✓	✓	✓	✓	✗	✓	✗
Huo & Feng (2013)	✓	✓	✓	✓	✓	✓	✗
Kaur *et al*., (2014)	✗	✓	✓	✓	✓	✓	✗
Biswas *&Pal* (2017)	✓	✓	✓	✓	✗	✓	✗
Jia & Qin (2017)	✓	✓	✓	✓	✓	✓	✗
Huo *et al*., (2018)	✓	✓	✓	✓	✓	✓	✗
Singh *et al*., (2019)	✗	✗	✗	✓	✓	✓	✗
Ali *et al*., (2019)	✗	✓	✓	✓	✗	✓	✗
Wu & Zhao (2021)	✓	✓	✓	✓	✗	✓	✗
Meng & Zhu (2022)	✓	✗	✓	✓	✗	✓	✗
Proposed Model	✓	✓	✓	✓	✓	✓	✓

3A.3. Mathematical Model

3A.3.1. System Description

In the proposed model it is going to be analyzed the population dynamics for transmission of HIV through SEIR model applying ANFIS techniques. It is assumed in the model that the four compartments are used to divide the total population i.e. $S(t)$, $E(t), I(t)$ and $R(t)$. $S(t)$ denotes the count of capable of humans; $E(t)$ signifies the count of person reveal to the contaminated but incapable of transmitting it; $I(t)$ signifies the count of infected persons suspect able of transference of the ailment; and $R(t)$ appear for the count of person who have convalesce due to the impact of media. Additionally, the variable $M(t)$ signifies the number of messages provided by all individuals regarding the epidemic disease at a time t. To account for natural and disease-related mortality, the model considers the long-term outbreak of the disease. The susceptible individuals are assumed to have a recruitment rate Λ.

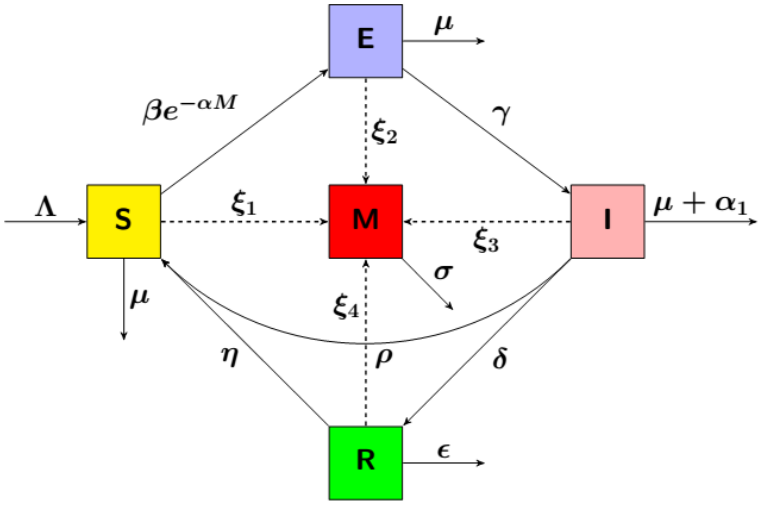

Figure 3A.1: SEIRS epidemic model dynamics with the added control of the media.

The SEIRS epidemic model with media effect incorporates various frame work that influence the transmission vital of the ailment. These parameters include the natural death rate μ and disease-related death rate α_1 of the respective population groups. During an epidemic season, individuals can also send messages about the disease at rates represented by parameters ξ_1, ξ_2, ξ_3 and ξ_4. The transference estimate β in the middle of the capable of and contaminated humans is affected by changes in public behavior after reading messages, resulting in a reduction factor $e^{-\alpha M}$. A parameter determines the effectiveness of ailment associated news on the transference estimate α, while a parameter appear for the transference coefficient from

exposure to contaminated humans γ. The parameter captures the transference estimate from contaminated individuals to capable of individuals ρ. Finally, the estimate at which news become out of date is represented by a parameter σ. A parameter defines the transmission rate of the infected class δ, and the rate at which the recovered class forms the susceptible class is captured by a parameter η. The mortality rate within the recovered class is denoted as ε. Collectively, these parameters serve as the foundation for the SEIRS epidemic model with media influence, providing insights into the intricate dynamics of disease transmission.

The diagram in Figure 3A.1 gives rise to a set of ODEs, outlined as follows:

$$\left.\begin{aligned} S' &= \Lambda + \rho I - \beta S I e^{-\alpha M} - \mu S + \eta R \\ E' &= \beta S I e^{-\alpha M} - \gamma E - \mu E \\ I' &= \gamma E - \rho I - (\mu + \alpha_1) I - \delta I \\ R' &= \delta I - \eta R - \varepsilon R \\ M' &= \xi_1 S + \xi_2 E + \xi_3 I + \xi_4 R - \sigma M \end{aligned}\right\} \qquad (3A.1)$$

3A.3.2. Basic Properties

We will illustrate that all variables in the system of equations (3A.1) remain non-negative for every $t > 0$. This demonstration is crucial to establish the epidemiological significance of the system of equations (3A.1). Consequently, the following lemmas are derived.

3A.3.3. Positivity of the Solutions

Lemma 3A.3.1: States that the attracting region ψ, defined by

$$\psi = \left\{ (S, E, I, R, M) \in \Re_+^5 : 0 \le S, E, I, R \le N \le \frac{\Lambda}{\mu}, 0 \le M \le \frac{\Lambda(\xi_1 + \xi_2 + \xi_3 + \xi_4)}{\sigma(\mu)} \le R \le \frac{\delta}{\eta\varepsilon} \right\}, \text{with}$$

beginning situation $S(0) \ge 0$, $E(0) \ge 0$, $I(0) \ge 0$, $R(0) \ge 0$ and $M(0) \ge 0$, is positive invariant for system (3A.1). This region attracts all solutions that begin within the interior of the positive values for t.

Proof: By summing the first four equations in the system (3A.1), we obtain:

$$N' = \Lambda - \mu N - \alpha_1 I \le \Lambda - \mu N$$

Thus, it follows

$$0 \le N \le \frac{\Lambda}{\mu} + N(0) e^{-\mu t},$$

where the first population is indicated by $N(0)$.

Therefore, $\limsup_{t \to \infty} N \le \frac{\Lambda}{\mu}$.

Moreover, the fifth equation in the system (3A.1) leads us to the conclusion that,

$$M' \leq \frac{(\xi_1 + \xi_2 + \xi_3 + \xi_4)\Lambda}{\mu} - \sigma M,$$

and then,

$$0 \leq M \leq \frac{(\xi_1 + \xi_2 + \xi_3 + \xi_4)\Lambda}{\sigma\mu} + M(0)e^{-\sigma t},$$

where the initial value of the media message is indicated by $M(0)$.

Thus, $\limsup_{t\to\infty} M \leq \frac{(\xi_1 + \xi_2 + \xi_3 + \xi_4)\Lambda}{\mu}$.

3A.4. Analysis of the Model

To analyze the model mathematically, the following disease-free equilibrium points were derived.

3A.4.1. Disease-Free Equilibrium (DFE) and Basic Reproductive Number

If we assume that R.H.S of the system of equation (3A.1) is zero, then we get,

$$\left.\begin{aligned} &\Lambda + \rho I - \beta SIe^{-\alpha M} - \mu S + \eta R = 0 \\ &\beta SIe^{-\alpha M} - \gamma E - \mu E = 0 \\ &\gamma E - \rho I - (\mu + \alpha_1)I - \delta I = 0 \\ &\delta I - \eta R - \varepsilon R = 0 \\ &\xi_1 S + \xi_2 E + \xi_3 I + \xi_4 R - \sigma M = 0 \end{aligned}\right\} \quad (3A.2)$$

If we substitute $E = I = R = 0$ into equation (3A.2), it becomes evident that the model exhibits a disease-free equilibrium, represented by:

$$E_0 = (S_0, 0, 0, 0, M_0) = \left(\frac{\Lambda}{\mu}, 0, 0, 0, \frac{\xi_1\Lambda}{\mu\sigma}\right). \quad (3A.3)$$

Continuing our analysis, we aim to determine a key parameter, the fundamental reproductive number (R_0), for the structure (3A.1) utilizing the next-generation method. In this context, we define the new infection matrix $F(x)$ and the transfer matrix $V(x)$. Consider the state vector as $x = (S,\ E,\ I,\ R,\ M)$ and the representation of the structure (3A.1) can be expressed as:

$x' = F(x) - V(x)$

where,

$$F(x)=\begin{bmatrix}0\\ \beta SIe^{-\alpha M}\\ 0\\ 0\\ 0\end{bmatrix},\quad V(x)=\begin{bmatrix}\beta SIe^{-\alpha M}+\mu S-\Lambda-\rho I-\eta R\\ \gamma E+\mu E\\ \rho I+(\mu+\alpha_1)I+\delta I-\gamma E\\ \eta R+\varepsilon R-\delta I\\ \sigma M-\xi_1 S-\xi_2 E-\xi_3 I-\xi_4 R\end{bmatrix}$$

At the disease-free equilibrium E_0, the respective Jacobian matrices of $F(x)$ and $V(x)$ are,

$$DF(E_0)=\begin{bmatrix}0&0&0&0&0\\0&0&\beta S_0 e^{-\alpha M_0}&0&0\\0&0&0&0&0\\0&0&0&0&0\\0&0&0&0&0\end{bmatrix},$$

$$DV(E_0)=\begin{bmatrix}\mu&0&\beta S_0 e^{-\alpha M_0}-\rho&-\eta&0\\0&\mu+\gamma&0&0&0\\0&-\gamma&\rho+\mu+\alpha_1+\delta&0&0\\0&0&-\delta&\eta+\varepsilon&0\\-\xi_1&-\xi_2&-\xi_3&-\xi_4&\sigma\end{bmatrix}$$

$$|(E_0)|=\begin{vmatrix}\mu&0&\beta S_0 e^{-\alpha M_0}-\rho&-\eta&0\\0&\mu+\gamma&0&0&0\\0&-\gamma&\rho+\mu+\alpha_1+\delta&0&0\\0&0&-\delta&\eta+\varepsilon&0\\-\xi_1&-\xi_2&-\xi_3&-\xi_4&\sigma\end{vmatrix}$$

$$|(E_0)|=(\mu\sigma)(\gamma+\mu)(\rho+\mu+\alpha_1+\delta)(\eta+\varepsilon)$$

$$DV(E_0)^{-1}=\begin{pmatrix}\frac{1}{\mu}&p_{12}&p_{13}&\frac{\eta}{\mu(\eta+\varepsilon)}&0\\0&\frac{1}{\gamma+\mu}&0&0&0\\0&p_{32}&\frac{1}{(\rho+\mu+\alpha_1+\delta)}&0&0\\0&p_{42}&p_{43}&\frac{1}{(\eta+\varepsilon)}&0\\\frac{-\xi_1}{\mu\sigma}&p_{52}&p_{53}&p_{54}&\frac{1}{\sigma}\end{pmatrix}$$

where,

$$p_{12}=\frac{-\gamma}{\mu(\gamma+\mu)(\rho+\mu+\alpha_1+\delta)}\left[(\beta S_0 e^{-\alpha M_0}-\rho)-\frac{\eta\delta}{\eta+\varepsilon}\right]$$

$$p_{13} = \frac{1}{\mu(\rho+\mu+\alpha_1+\delta)}\left[\frac{\eta\delta}{\eta+\varepsilon} - \left(\beta S_0 e^{-\alpha M_0} - \rho\right)\right]$$

$$p_{32} = \frac{\gamma}{(\gamma+\mu)(\rho+\mu+\alpha_1+\delta)}$$

$$p_{42} = \frac{\gamma\delta}{(\gamma+\mu)(\rho+\mu+\alpha_1+\delta)(\eta+\varepsilon)}$$

$$p_{43} = \frac{\delta}{(\rho+\mu+\alpha_1+\delta)(\eta+\varepsilon)}$$

$$p_{52} = \frac{(\eta+\varepsilon)\left[\mu\xi_2(\rho+\mu+\alpha_1+\delta)+\gamma\left(\mu\xi_3-\beta S_0 e^{-\alpha M_0}\xi_1\right)\right]+\gamma\delta(\eta\xi_1+\mu\xi_4)}{\sigma(\gamma+\mu)(\rho+\mu+\alpha_1+\delta)(\eta+\varepsilon)}$$

$$p_{53} = \frac{\mu\xi_3(\eta+\varepsilon)+\delta(\eta\xi_1+\mu\xi_4)-\mu\xi_1\eta}{\mu\sigma(\rho+\mu+\alpha_1+\delta)(\gamma+\mu)(\eta+\varepsilon)}$$

$$p_{54} = \frac{-(\xi_1\eta+\xi_4\mu)}{\mu\sigma(\eta+\varepsilon)}$$

$$DF(E_0)DV(E_0)^{-1} = \begin{bmatrix} 0 & 0 & 0 & 0 & 0 \\ 0 & \dfrac{\gamma\left(\beta S_0 e^{-\alpha M_0}\right)}{(\gamma+\mu)(\rho+\mu+\alpha_1+\delta)} & \dfrac{\left(\beta S_0 e^{-\alpha M_0}\right)}{(\rho+\mu+\alpha_1+\delta)} & 0 & 0 \\ 0 & 0 & 0 & 0 & 0 \\ 0 & 0 & 0 & 0 & 0 \\ 0 & 0 & 0 & 0 & 0 \end{bmatrix}$$

Therefore, the reproductive number R_0 is given as

$$R_0 = \gamma\left(DF(E_0)DV(E_0)^{-1}\right) = \max\left(|\lambda|; \lambda \in \phi\left(DF(E_0)DV(E_0)^{-1}\right)\right), \tag{3A.4}$$

where $\gamma(.)$ and $\phi(.)$ represents the spectral radius and largest eigenvalues, respectively.

Then, the fundamental reproductive number (R_0) is given by

$$R_0 = \frac{\beta\gamma\Lambda e^{\frac{-\alpha\xi_1\Lambda}{\mu\sigma}}}{\mu(\gamma+\alpha_1)(\rho+\mu+\alpha_1+\delta+\delta\varepsilon+\eta\delta)} \tag{3A.5}$$

$$R_{01} = \frac{\Lambda\gamma\Theta}{(\mu+\gamma)(\rho+\mu+\alpha_1)-\gamma\rho} \tag{3A.6}$$

$$R_P = R_{01}e^{1-R_{01}} \tag{3A.7}$$

where,

$$\Theta = -\frac{\alpha}{\mu\gamma\sigma}\left(\xi_1\gamma\delta - \xi_1(\mu+\gamma)(\delta+\mu+\alpha_1) + \mu\xi_2(\delta+\mu+\alpha_1) + \mu\xi_3\gamma\right) + \delta(\eta+\varepsilon) \tag{3A.8}$$

Remark: Clearly, can be checked that: $R_{01} > 0 \Leftrightarrow \Theta > 0$, $R_{01} < 0 \Leftrightarrow \Theta < 0$, $R_{01} = 0 \Leftrightarrow \Theta = 0$.

3A.4.2. Stability Analysis of Disease-Free Equilibrium

Theorem 3A.4.1: Disease-free equilibrium E_0 of the above system of equation (3A.1) is globally asymptotically stable if $R_0 < 1$, and is unstable if $R_0 > 1$.

Proof: At the DFE point E_0, the Jacobian matrix of the above system of equation (3A.1) is

$$\begin{vmatrix} \lambda+\mu & 0 & \beta\frac{\Lambda}{\mu}e^{\frac{-\alpha\xi_1\Lambda}{\mu\sigma}}-\rho & -\eta & 0 \\ 0 & \lambda+(\gamma+\mu) & -\beta\frac{\Lambda}{\mu}e^{\frac{-\alpha\xi_1\Lambda}{\mu\sigma}} & 0 & 0 \\ 0 & -\gamma & \lambda+(\rho+\mu+\alpha_1+\delta) & 0 & 0 \\ 0 & 0 & -\delta & \lambda+(\eta+\varepsilon) & 0 \\ -\xi_1 & -\xi_2 & -\xi_3 & -\xi_4 & \lambda+\sigma \end{vmatrix} = 0$$

then,

$$(\lambda+\mu)(\lambda+\sigma)(\lambda+(\eta+\mu))\left((\lambda+(\gamma+\mu))(\lambda+(\rho+\mu+\alpha_1+\delta))-\gamma\beta\frac{\Lambda}{\mu}e^{\frac{-\alpha\xi_1\Lambda}{\mu\sigma}}\right)=0 \quad \text{(3A.9)}$$

Thus, the three eigenvalues of the equation (3A.9) are $\lambda_1 = -\mu, \lambda_2 = -\sigma$ and $\lambda_3 = -(\eta+\varepsilon)$ and the others are determined by

$$(\lambda+(\gamma+\mu))(\lambda+(\rho+\mu+\alpha_1+\delta))-\gamma\beta\frac{\Lambda}{\mu}e^{\frac{-\alpha\xi_1\Lambda}{\mu\sigma}}=0$$

$$\lambda^2+(\rho+\mu+\alpha_1+\delta)\lambda+(\gamma+\mu)\lambda+(\gamma+\mu)(\rho+\mu+\alpha_1+\delta)-\gamma\beta\frac{\Lambda}{\mu}e^{\frac{-\alpha\xi_1\Lambda}{\mu\sigma}}=0$$

$$\lambda^2+(\gamma+\rho+\delta+2\mu+\alpha_1)\lambda+(\gamma+\mu)(\rho+\mu+\alpha_1+\delta)-\frac{\mu(\gamma+\mu)(\rho+\mu+\alpha_1+\delta)R_0}{\mu}=0$$

$$\Rightarrow \lambda^2+(\gamma+\rho+\delta+2\mu+\alpha_1)\lambda+(\gamma+\mu)(\rho+\mu+\alpha_1+\delta)(1-R_0)=0$$

Then we have

$$\lambda_4+\lambda_5=(\gamma+\rho+\delta+2\mu+\alpha_1)<0$$

$$\lambda_4\lambda_5=(\gamma+\mu)(\rho+\mu+\alpha_1+\delta)(1-R_0)$$

Hence, in the case where $R_0 < 1$, the ailment-free symmetry point E_0 demonstrates local asymptotic stability, while it becomes unstable if R_0 exceeds 1.

Next, a Lyapunov function is presented

$$V(S,E,I,R,M)=e^{\frac{-\alpha\xi_1\Lambda}{\mu\sigma}}\gamma E(t)+(\gamma+\mu)I(t)+(\eta+\varepsilon)R(t) \quad \text{(3A.10)}$$

Using the expression for R_0 in (3A.5) and differentiating (3A.10), we have

$$V'(S,E,I,R,M) = e^{\frac{-\alpha\xi_1\Lambda}{\mu\sigma}}\gamma E'(t) + (\gamma+\mu)I'(t) + (\eta+\varepsilon)R'(t)$$

$$= e^{\frac{-\alpha\xi_1\Lambda}{\mu\sigma}}\gamma(\beta SIe^{-\alpha M} - \gamma E - \mu E) + (\gamma+\mu)\left(\gamma E - \rho I - (\alpha_1+\mu+\delta)I\right) + (\eta+\varepsilon)(\delta I - \eta R - \varepsilon R)$$

$$= e^{\frac{-\alpha\xi_1\Lambda}{\mu\sigma}}\gamma\beta SIe^{-\alpha M} - e^{\frac{-\alpha\xi_1\Lambda}{\mu\sigma}}\gamma^2 E + \mu\gamma E - e^{\frac{-\alpha\xi_1\Lambda}{\mu\sigma}}\gamma\mu E - \mu\rho I - \mu^2 I - \mu\alpha_1 I - \mu\delta I + \gamma^2 E - \rho\gamma I$$
$$- \gamma\mu I - \gamma\alpha_1 I - \gamma\delta I + \eta\delta I - \eta^2 R - \eta\varepsilon R + \varepsilon\delta I - \eta\varepsilon R - \varepsilon^2 R$$

$$\le \frac{\Lambda}{\mu}e^{\frac{-\alpha\xi_1\Lambda}{\mu\sigma}}\gamma\beta Ie^{-\alpha M} - e^{\frac{-\alpha\xi_1\Lambda}{\mu\sigma}}\gamma^2 E + \mu\gamma E - e^{\frac{-\alpha\xi_1\Lambda}{\mu\sigma}}\gamma\mu E - \mu\rho I - \mu^2 I - \mu\alpha_1 I - \mu\delta I + \gamma^2 E - \rho\gamma I$$
$$- \gamma\mu I - \gamma\alpha_1 I - \gamma\delta I + \eta\delta I - \eta^2 R - 2\eta\varepsilon R + \varepsilon\delta I - \varepsilon^2 R$$

$$\le \frac{\Lambda}{\mu}e^{\frac{-\alpha\xi_1\Lambda}{\mu\sigma}}\gamma\beta I - e^{\frac{-\alpha\xi_1\Lambda}{\mu\sigma}}\gamma^2 E + \mu\gamma E - e^{\frac{-\alpha\xi_1\Lambda}{\mu\sigma}}\gamma\mu E - \mu\rho I - \mu^2 I - \mu\alpha_1 I - \mu\delta I + \gamma^2 E - \rho\gamma I - \gamma\mu I$$
$$- \gamma\alpha_1 I - \gamma\delta I + \eta\delta I - \eta^2 R - 2\eta\varepsilon R + \varepsilon\delta I - \varepsilon^2 R$$

$$\le \frac{\Lambda}{\mu}e^{\frac{-\alpha\xi_1\Lambda}{\mu\sigma}}\gamma\beta I - \mu\rho I - \mu^2 I - \mu\alpha_1 I - \rho\gamma I - \mu\delta I - \gamma\mu I - \gamma\alpha_1 I + \eta\delta I - \gamma\delta I - \eta^2 R - 2\eta\varepsilon R$$
$$+ \varepsilon\delta I - \varepsilon^2 R$$

$$= \frac{\Lambda}{\mu}e^{\frac{-\alpha\xi_1\Lambda}{\mu\sigma}}\gamma\beta I - (\rho+\alpha_1+\mu+\delta)\ (\gamma+\mu)\ I + (\eta\delta+\delta\varepsilon)\ I$$

$$= (\gamma+\mu)(\rho+\mu+\alpha_1+\delta+\delta\varepsilon+\eta\delta)I(R_0-1).$$

Thus, $R_0 \le 1$ guarantees that $\frac{dV}{dt}(S,E,I,R,M) \le 0\ \forall t > 0$, therefore $V(S,E,I,R,M)$ is bounded and decreasing. Therefore $\lim_{t\to\infty} V(S,E,I,R,M)$ exists. By LaSalle's Invariance principle (1976), the global asymptotic stability of DFE E_0 can be guaranteed when $R_0 < 1$.

3A.4.3. Endemic Equilibrium (EE)

Theorem 3A.4.2: States that the set of equations in system (3A.1) exhibits

(i) Endemic equilibrium point E_1^* is positive; when $R_0 > \max(1, R_{01})$;

(ii) Endemic equilibrium point E_2^* is positive; when $R_p = R_0 < \min(1, R_{01})$;

(iii) Two separate positive endemic equilibrium points, denoted as E_3^* and E_4^*, occur when $R_p < R_0 < \min(1, R_{01})$; where R_0, R_{01}, R_p and Θ are defined by equations (3A.5)-(3A.8) and

$E_i^* = (S_i^*, E_i^*, I_i^*, R_i^*, M_i^*)$; $i = 1,2,3,4,5$

Proof: Suppose that $P^* = (S^*, E^*, I^*, R^*, M^*)$ represents a solution to equation (3A.2), wherein,

$$\left.\begin{aligned} &\Lambda + \rho I^* - \beta S^* I^* e + \eta R^* - \mu S^* = 0 \\ &\beta S^* I^* e^{-\alpha M} - \gamma E^* - \mu E^* = 0 \\ &\gamma E^* - \rho I^* - (\mu + \alpha_1) I^* - \delta I^* = 0 \\ &\delta I^* - \eta R^* - \varepsilon R^* = 0 \\ &\xi_1 S^* + \xi_2 E^* + \xi_3 I^* + \xi_4 R^* - \sigma M^* = 0 \end{aligned}\right\} \quad (3A.11)$$

In this context, we assume S^*, E^*, I^*, R^*, M^* can be represented as linear function of I^* respectively,

$$S^* = \frac{\Lambda}{\mu} + \left(-\frac{(\mu+\gamma)(\mu+\alpha_1+\delta)}{\mu\gamma} \right) I^* \quad (3A.12)$$

$$E^* = \frac{(\delta+\mu+\alpha_1)}{\gamma} I^* \quad (3A.13)$$

$$R^* = \frac{\delta+\mu+\alpha_1+\delta\varepsilon+\eta\delta}{\varepsilon\gamma} I^* \quad (3A.14)$$

$$M^* = \frac{\xi_1\Lambda}{\mu\sigma} + \frac{I^*}{\mu\sigma\gamma} \begin{pmatrix} \xi_1\gamma\delta - \xi_1(\mu+\alpha_1+\gamma)(\varepsilon+\alpha_1+\delta) \\ + \mu\xi_2(\varepsilon+\alpha_1+\mu+\delta) + \mu\xi_3(\delta+\gamma) + \mu\xi_3\eta\delta \end{pmatrix} \quad (3A.15)$$

Combining equations (3A.12)-(3A.15) with the first equation (3A.11), we obtain:

$$\left(\left(1 - \frac{(\mu+\gamma)(\delta+\mu+\alpha_1)}{\Lambda\gamma} - \frac{\delta}{\Lambda} \right) I^* \right) R_0 = e^{-\Theta I^*} \quad (3A.16)$$

Now, by equations (3A.6) and (3A.16), we have

$$R_0 - \frac{R_0}{R_{01}} \Theta I - e^{-\Theta I^*} = 0 \quad (3A.17)$$

Here we denote, $H(I) = R_0 - \frac{R_0}{R_{01}} \Theta I - e^{-\Theta I^*}$ (3A.18)

By equation (3A.18), we get,

$$H(0) = R_0 - 1, H(\infty) = -\infty, H'(I) = -\frac{R_0}{R_{01}} \Theta I - \Theta e^{-\Theta I^*},$$

$$H'(0) = -\frac{R_0}{R_{01}} \Theta + \Theta, \; H''(I) = -\Theta^2 e^{-\Theta I},$$

(i) While $R_0 > 1, H(0) = R_0 - 1 > 0,$ and $H(\infty) < 0, if \;\; \Theta \neq 0,$

$H''(I) = -\Theta^2 e^{-\Theta I} < 0,$ obtain.

$H'(I) < H'(0)$, specifically $\Theta e^{-\Theta I} < \Theta$,

$$H'(I) = -\frac{R_0}{R_{01}}\Theta + \Theta e^{-\Theta I} < \Theta\left(1 - \frac{R_0}{R_{01}}\right)$$

when $R_0 > R_{01}$, then the single positive result for $H(I) = 0$ exists.

If $\Theta = 0$, by equation (3A.16), we get

$$I^* = \frac{\Lambda\gamma}{(\mu+\gamma)(\delta+\mu+\alpha_1) - \delta\gamma}\left(1 - \frac{1}{R_0}\right) \tag{3A.19}$$

Similarly, when $R_0 > 1$, $I > 0$. Thus, the endemic equilibrium $E_1^* = \left(S_1^*, E_1^*, I_1^*, R_1^*, M_1^*\right)$ can be obtained.

(ii) When $R_0 < 1, H(0) = R_0 - 1 < 0,$ and $H(\infty) < 0.$ We assume that $H'(I) = 0$ then $I = \frac{1}{\Theta}\ln\frac{R_{01}}{R_0}.$

When $R_0 < R_{01}, I$ takes on positive values. Additionally, I serves as a positive solution to $H(I) = 0 \Leftrightarrow R_0 = R_p$. Consequently, the endemic equilibrium $E_2^* = \left(S_2^*, E_2^*, I_2^*, R_2^*, M_2^*\right).$

(iii) Building upon the findings in (ii), when $R_0 > R_p$, and $H(I) = 0$ two outcomes arise. Therefore, the endemic equilibria $E_i^* = \left(S_i^*, E_i^*, I_i^*, R_i^*, M_i^*\right);\ \ i = 1,2,3,4,5$ can be derived.

3A.5. Adaptive Neuro-Fuzzy Inference System

In Figure 3A.2, the architecture of ANFIS, which consists of five layers: the input, fuzzy, normalization, rule and output layers, is depicted. This combined system integrates the advantages of both fuzzy logic and neural networks, making it suitable for various applications, including control systems, pattern recognition, and prediction.

Input Layer: The input layer of ANFIS consists of the input variables that are fed into the system. These input variables can be continuous or discrete, and membership functions represent them.

Fuzzy Layer: The ANFIS fuzzy layer performs the computation of membership degrees for each input variable within each fuzzy set. This layer utilizes fuzzy logic rules on the input variables, which are expressed through fuzzy sets. These fuzzy sets are characterized by membership functions, detailing the extent of membership for each input variable in each respective fuzzy set.

Normalization Layer: The normalization layer of ANFIS is responsible for normalizing the firing strengths of the fuzzy sets. This layer ensures that the total of the firing strengths of all the fuzzy sets equals one.

Rule Layer: The rule layer of ANFIS is responsible for computing the degree of activation of each rule. The rules are defined by combining the fuzzy sets in the antecedent part and the output variable in the consequent part. The degree of activation of each rule is computed by multiplying the firing strengths of the fuzzy sets in the antecedent part.

Output Layer: The output layer of ANFIS is responsible for computing the final output of the system. This layer computes the weighted average of the output values of all the rules. The weight of each rule is proportional to the degree of activation of that rule.

In summary, ANFIS is a hybrid system that combines fuzzy logic and neural networks. Its architecture consists of five layers: the input, fuzzy, normalization, rule and output layer. ANFIS can be used for various applications, such as control systems, pattern recognition and prediction. The choice of employing the ANFIS for numerical simulation in this section is founded on its prowess in capturing the intricate nonlinear dynamics inherent in HIV transmission within the SEIRS model. The complexity of HIV transmission, characterized by multifaceted interactions and behavioural nuances, demands a modeling approach capable of handling nonlinear systems effectively. ANFIS stands out for its adaptability, adeptness in modeling nonlinearities and capacity to capture the intricate relationships among variables such as media impact and disease spread dynamics. Furthermore, ANFIS's robust validation process ensures the reliability and accuracy of simulation outcomes, establishing it as an optimal choice for comprehensively addressing the complexities within HIV transmission dynamics.

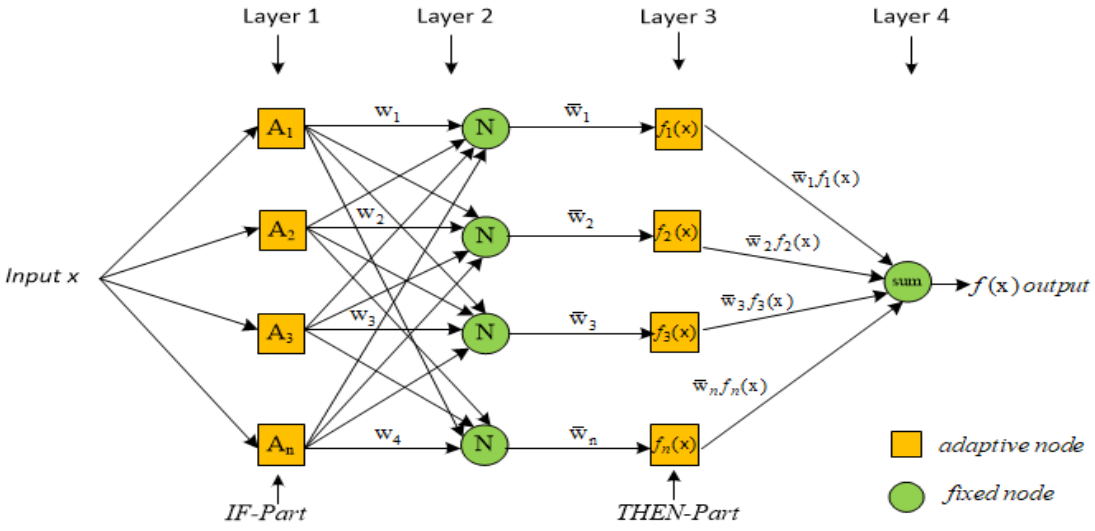

Figure 3A.2: ANFIS Architecture.

3A.6. Numerical Simulation

To verify the logical result obtained in the preceding segment, arithmetical simulations were performed. To perform numerical computations, the governing equations of the system are answered by making use of the 4th-order Runge-Kutta method within the MATLAB software. The 'ode45' function, a built-in feature in MATLAB, is used for this purpose. In order to evaluate the feasibility of the FI-based controller and validate the data, we employ the ANFIS approach within MATLAB's fuzzy logic toolbox. The ANFIS results are obtained by using a Gaussian membership function for five linguistic variables: 'very low', 'low', 'moderate', 'high' and 'very high'. The membership function for x is displayed in Figure 3A.3.

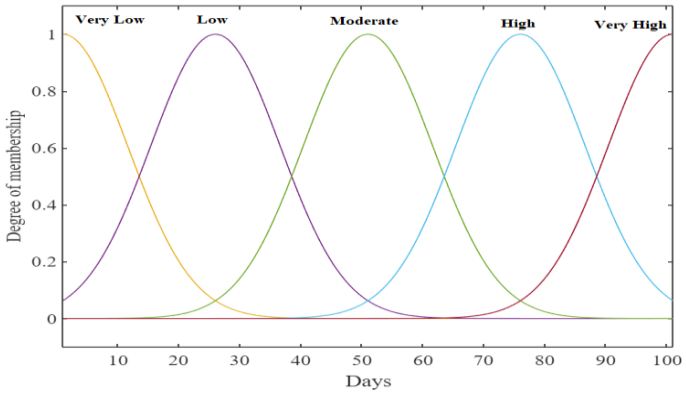

Figure 3A.3: Degree of membership function for input variable "Days".

For Figure 3A.4, the default set of parameters is fixed as:

$\Lambda = 0.8,\ \alpha = 0.08,\ \mu = 0.0001,\ \varepsilon = 0.4,\ \alpha_1 = 0.002,\ \xi_1 = 0.99,\ \xi_2 = 0.4,\ \xi_3 = 0.8,\ \xi_4 = 0.12,$
$\beta = 0.4,\ \rho = 0.7,\ \gamma = 0.1,\ \delta = 0.5,\ \eta = 0.0004,\ \sigma = 0.0006.$

Figure 3A.4 illustrates how the different categories of individuals and messages vary over time. The graph shows that the numbers of susceptible, exposed, infected and recovered individuals and messages remain constant for a fixed value of $R_0 = 0.2381 < 1,$ but become unstable otherwise.

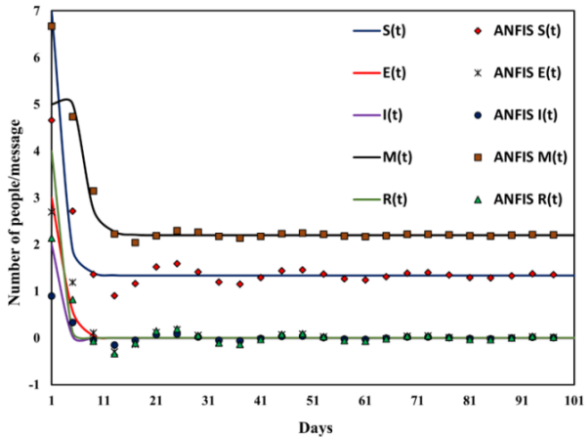

Figure 3A.4: Stability analysis: Disease-free equilibrium under $R_0 = 0.2381 < 1$.

For Figure 3A.5, the default parameter values are set as follows:

$\Lambda = 0.8,\ \alpha = 0.072,\ \mu = 0.2,\ \varepsilon = 0.2,\ \alpha_1 = 0.02,\ \xi_1 = 0.6,\ \xi_2 = 0.8,\ \xi_3 = 0.8,\ \xi_4 = 0.12,\ \beta = 9,$
$\rho = 0.006,\ \gamma = 0.4,\ \delta = 0.5,\ \eta = 0.4,\ \sigma = 0.8.$

Here Figure 3A.5 illustrates how the different categories of individuals and messages vary over time. The graph shows that the numbers of susceptible, exposed, infected and recovered individuals and messages remain constant for a fixed value of $R_0 = 1.5917 > 1$, but become unstable otherwise.

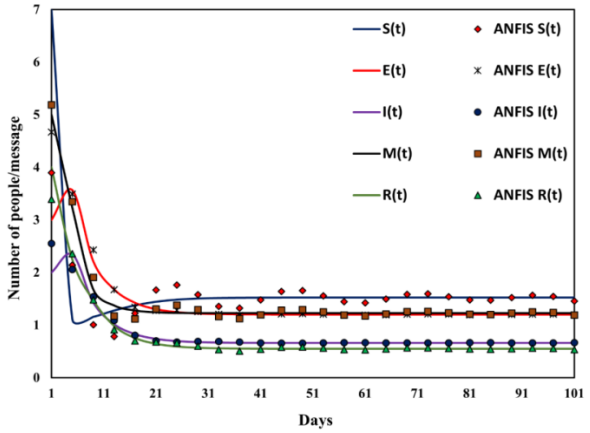

Figure 3A.5: Stability analysis: Endemic equilibrium under $R_0 = 1.5917 > 1$.

3A.A. Summary and Concluding Remarks

In conclusion, this study has successfully developed a mathematical model to analyze the transmission dynamics of an SEIRS epidemic model for HIV, with a specific focus on the influence of media. Through the formulation of a structure of distinctive calculations of elected by the susceptible, exposed, infected and recovered population groups, a comprehensive understanding of the disease spread dynamics has been achieved. The computation of the fundamental reproductive number has yielded significant understandings regarding the gravity and scope of the epidemic, whereas the analysis of the equilibrium states in which the disease is present and absent has illuminated the system's long-term dynamics.

Furthermore, the stability analysis has demonstrated that the disease-free equilibrium is both locally and globally asymptotically stable, indicating the potential for effective disease control measures. To validate the findings, numerical simulations were conducted utilizing the innovative Adaptive Neuro-Fuzzy Inference System (ANFIS), showcasing the practical applicability of the proposed model.

The outcomes of this study contribute to the presented body of understanding on SEIRS epidemic models and provide valuable insights for HIV transmission dynamics. The results underscore the significance of media influence and the necessity for comprehensive intervention strategies. By understanding the underlying mechanisms governing disease spread, policymakers and healthcare professionals can make informed decisions to mitigate the impact of HIV.

Moreover, the inclusion of visual representations adds clarity to the results. Figure 3A.3 illustrates the Degree of membership function for the input variable "Days" assisting in visualizing the credit of time on the vital of the ailment. Additionally, Figure 3A.4 demonstrates that the ailment-free symmetry (E_0) is firm when (R_0) is below the critical threshold $(R_0 = 0.2381 < 1)$, highlighting the potential for disease control. Figure 3A.5 shows that the native symmetry (E^*) is firm when (R_0) exceeds this threshold $(R_0 = 1.5917 > 1)$, emphasizing the importance of maintaining (R_0) below this level for effective prevention.

Overall, this research serves as a stepping stone for further investigations into the modeling and analysis of complex epidemic systems. Future studies may consider additional factors and refine the mathematical models to enhance the accuracy and applicability of the findings. The ultimate goal is to develop effective strategies for disease prevention, control, and management, using insights gained from this study as a foundation for informed decision-making.

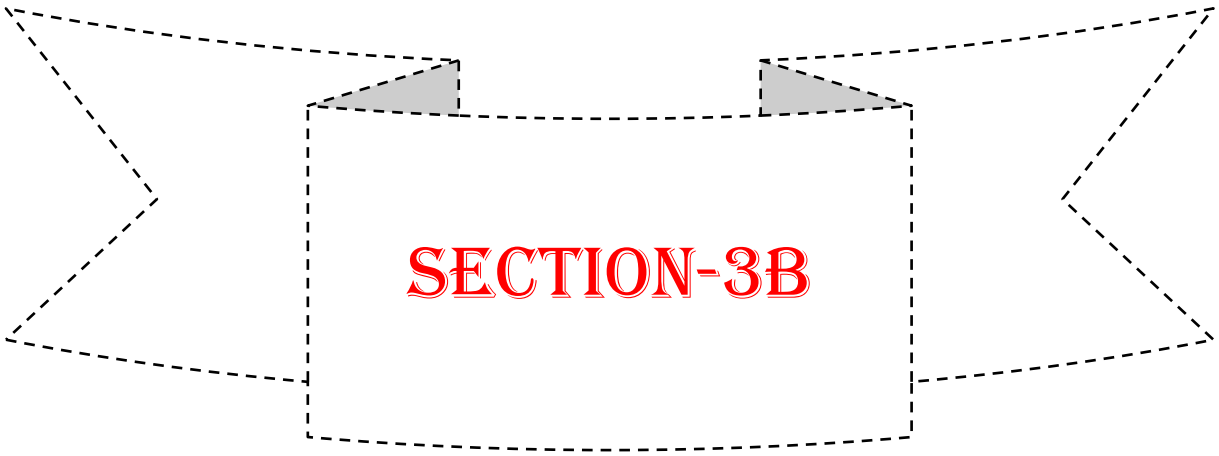

Analyzing the Co-infection Dynamics of HIV/AIDS-TB with Media Awareness

Keywords: HIV/AIDS-TB, Co-infection, Equilibrium Points and Stability Analysis.

Chapter 3: Study of HIV Transmission Dynamics using SEIRS Epidemic Model

Section 3B: Analyzing the Co-infection Dynamics of HIV/AIDS-TB with Media Awareness

3B.1. Introduction

HIV/AIDS and TB co-infection represent a complex and intertwined health challenge, intertwining their impacts on global morbidity and mortality rates, particularly in resource-constrained regions. The synergistic relationship between these two diseases amplifies their severity, underscoring the critical need to comprehend their interactions for effective prevention, management, and control strategies.

This section endeavors to construct a comprehensive model that captures the dynamics of HIV/AIDS and TB co-infection. The model incorporates distinct classes representing different disease states and interventions: susceptible individuals, those infected with TB, individuals undergoing treatment for TB infection, the recovered population, HIV-infected individuals, and those progressing to AIDS.

The global burden of HIV/AIDS and tuberculosis co-infection is substantial, especially in regions where both diseases coexist, exacerbating challenges faced by healthcare systems and communities. Notably, the World Health Organization (WHO) highlights a significant proportion of TB cases occurring in individuals living with HIV/AIDS, substantially increasing the risk of TB infection progressing to active disease. Conversely, TB infection significantly impacts the progression and severity of HIV/AIDS, complicating treatment outcomes and long-term health for co-infected individuals.

Despite advancements in medical science and public health interventions targeting each disease independently, the intricate behaviour of Tuberculosis and HIV/AIDS co-infection persists as a formidable obstacle. This necessitates a comprehensive modeling approach that integrates epidemiological observations, immunological insights, and computational simulations to capture the nuanced interactions between these diseases and their impact on diverse populations.

The proposed model encompasses distinct classes representing various disease states and interventions, including susceptibility to both HIV/AIDS and TB, active TB infection, treatment for infected individuals, the recovered population, HIV-infected individuals, and those progressing to AIDS. By incorporating these classes, the model aims to simulate the

intricate dynamics of co-infection, elucidating critical factors influencing disease propagation and evaluating potential strategies for mitigating their combined impact.

The subsequent sections will delineate the conceptual framework of this model, detailing the parameters, methodologies, and interactions characterizing the different disease states and interventions. Moreover, this section will discuss the implications of the model in informing public health policies, clinical interventions, and future research directions aimed at addressing this pressing global health challenge.

This section is structured as follows: Section 3B.2 provides detailed literature on the transmission dynamics of HIV/AIDS-TB co-infection model. The model description is covered in section 3B.3. The subsequent sections cover the mathematical analysis of equilibrium points (Section 3B.4). Finally, summary and concluding remarks are drawn within the last section, 3B.5.

3B.2. Literature Review

HIV/AIDS and TB co-infection create a lethal synergy, exacerbating the progression and severity of each disease. Individuals living with HIV face a significantly heightened risk, being 16 times extra probable to develop TB compared to those without HIV. This co-infection presents a critical public health concern, with TB emerging as the primary reason of death among people existing with HIV. Without proper treatment, mortality rates are strikingly high, affecting nearly all HIV-positive individuals with TB and approximately 60% of HIV-negative individuals diagnosed with TB.

The World Health Organization's (WHO) 2022 report highlighted the devastating impact of TB, attributing 1.3 million deaths to this disease, of which 167,000 were associated with HIV-TB co-infection. Efforts to combat this dual burden of disease have led to significant advancements in understanding transmission dynamics, treatment strategies, and the role of various interventions.

Several studies have explored the multifaceted aspects of infectious disease dynamics and intervention strategies. Greenhalagh and Das (1995) formulated SIR mathematical models for epidemics, considering population density's influence on contact rates and background death rates. Bhunu *et al.,* (2008) delved into the effects of chemoprophylaxis in TB treatment, advocating a holistic approach to intervention strategies.

Media's role in raising awareness and its impact on disease dynamics has also garnered attention. Khan *et al.,* (1997) conducted a statistical analysis of media and the importance of education in raising AIDS awareness amongst Bangladeshi married people, emphasizing the

influence of media coverage on disease understanding. Cui *et al.,* (2008) examined the influence of media coverage on the transmission and management of infectious diseases such as SARS.

In the realm of HIV-TB co-infection modeling, various approaches have been undertaken. Kirschner (1999) constructed a model elucidating HIV-1 and TB coinfection within a host. Huo *et al.,* (2016) introduced the treatment class in an HIV-AIDS co-infection model. Building upon this, Bhunu *et al.,* (2009) comprehensively considered TB and HIV transmission dynamics, incorporating treatment aspects for both diseases. Roeger *et al.,* (2009) assumed sexually inactive TB-infected persons in the phase of activity of the disease in their co-infection model. Silva and Torres (2014) integrated TB and AIDS treatments in their model for individuals afflicted with either or both diseases.

However, despite these advancements, gaps persist in understanding the influence of media awareness on disease dynamics, treatment outcomes, and overall public health strategies in the context of HIV/AIDS and TB co-infection.

3B.3. Model Description

To investigate the impact of awareness on the control and prevention of HIV/AIDS-TB co-infection, we examine a population denoted by $N(t)$ at time t, with a constant recruitment rate represented by Λ. This entire population is categorized into six sub-classes: susceptible $S(t)$, tuberculosis-infected $T(t)$, individuals undergoing treatment for tuberculosis $M(t)$, those who have recovered post-treatment $R(t)$, HIV-infected $H(t)$, and AIDS-infected $A(t)$. The transition from susceptible to tuberculosis-infected occurs at a rate denoted by ξ_1, representing the contact rate before media alert. The term $\xi(T)=\left(\xi_1-\xi_1'\frac{T}{m+T}\right)$ signifies the reduced value of the tuberculosis transmission rate after media alert, measuring the spread of TB infection from infected to susceptible individuals. When $m=0$, the transmission rate remains constant. The potential of the disease to spread and the population's awareness of each susceptible member are both related to the contact transmission rate. The effect of publicity on the transmission of contact is reflected in the parameter m. The transition from susceptible to HIV-infected takes place at a rate denoted by ξ_2 before media alert. The reduced value of the HIV transmission rate after media awareness is given by $\xi(H)=\left(\xi_2-\xi_2'\frac{H}{n+H}\right)$. The effect of publicity on HIV infection spread through contact is reflected in parameter n. The TB class

population is infected by HIV at a rate ξ_3. Since TB is a curable disease, individuals in the TB class undergo treatment at a rate γ, followed by recovery at a rate δ. Fully recovered individuals re-enter the susceptible class at a rate λ. It is assumed that no effective anti-HIV treatment is available within the population, resulting in some members of the HIV class progressing to full-blown AIDS at a rate ρ. Once AIDS develops in an individual, no awareness can contribute to a cure. The population is assumed to experience a constant death rate represented by μ, where α denotes the disease-induced death rate. Figure 3B.1 shows the model flow of this biological structure.

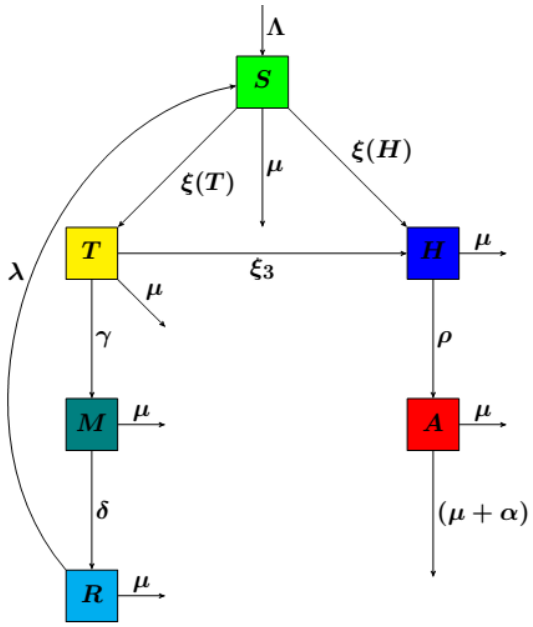

Figure 3B.1: Epidemiological modeling of HIV-TB co-infection.

The mathematical model is expressed through this system of nonlinear differential equations.

$$S' = \Lambda - \left(\xi_1 - \xi_1' \frac{T}{m+T}\right)\frac{ST}{N} - \left(\xi_2 - \xi_2' \frac{H}{n+H}\right)\frac{SH}{N} + \lambda R - \mu S \tag{3B.1}$$

$$T' = \left(\xi_1 - \xi_1' \frac{T}{m+T}\right)\frac{ST}{N} - \xi_3 \frac{TH}{N} - (\gamma + \mu)T \tag{3B.2}$$

$$H' = \left(\xi_2 - \xi_2' \frac{H}{n+H}\right)\frac{SH}{N} + \xi_3 \frac{TH}{N} - (\rho + \mu)H \tag{3B.3}$$

$$M' = \gamma T - (\delta + \mu)M \tag{3B.4}$$

$$R' = \delta M - (\lambda + \mu)R \tag{3B.5}$$

$$A' = \rho H - (\mu + \alpha)A \tag{3B.6}$$

Since $N(t)=S(t)+T(t)+H(t)+M(t)+R(t)+A(t)$, the above set of equations (3B.1)-(3B.6) can be modified as:

$$N' = \Lambda - \mu N - \alpha A \tag{3B.7}$$

$$T' = \left(\xi_1 - \xi_1' \frac{T}{m+T}\right)\frac{(N+T+H+M+R+A)}{N}T - \xi_3 \frac{TH}{N} - (\mu+\gamma)T \tag{3B.8}$$

$$H' = \left(\xi_2 - \xi_2' \frac{H}{n+H}\right)\frac{(N+T+H+M+R+A)}{N}H + \xi_3 \frac{TH}{N} - (\mu+\rho)H \tag{3B.9}$$

$$M' = \gamma T - (\delta+\mu)M \tag{3B.10}$$

$$R' = \delta M - (\lambda+\mu)R \tag{3B.11}$$

$$A' = \rho H - (\mu+\alpha)A \tag{3B.12}$$

Lemma 3B.3.1: The viable range Ω is delineated by

$$\Omega = \left\{(S(t),T(t),H(t),M(t),R(t),A(t)) \in \Re_+^6 : N(t) \le \frac{\Lambda}{\mu}\right\}$$

with initial conditions $S(0) \ge 0,\ T(0) \ge 0,\ H(0) \ge 0,\ M(0) \ge 0,\ R(0) \ge 0,\ A(0) \ge 0$ is positively invariant for system of equations (3B.1)-(3B.6).

Proof: Adding the equations of system (3B.1)-(3B.6), we obtain

$$\frac{dN}{dt} = \Lambda - \mu(S+T+H+M+R+A) - \alpha A$$

$$\frac{dN}{dt} \le \Lambda - \mu N. \tag{3B.13}$$

On solving equation (3B.13), we have

$$0 \le N(t) \le \frac{\Lambda}{\mu} + N(0)\, e^{-\mu t},$$

where the preliminary values of the entire population are denoted by $N(0)$. Thus $\lim_{t\to+\infty} \sup N(t) \le \frac{\Lambda}{\mu}$. It implies that the region $\Omega = \left\{(S(t),T(t),H(t),M(t),R(t),A(t)) \in \Re_+^6 : N(t) \le \frac{\Lambda}{\mu}\right\}$ is a positively invariant set for system (3B.1)-(3B.6).

3B.4. Analysis of the Model

The examination of the model has been done by evaluating the equilibrium points.

3B.4.1. Equilibrium Points

To obtain the equilibrium points, we set left-hand sides of all equations (3B.7)-(3B.12) to zeros, so that we get

$$\Lambda - \mu N - \alpha A = 0 \tag{3B.14}$$

$$\left(\xi_1 - \xi_1' \frac{T}{m+T}\right)\frac{(N+T+H+M+R+A)}{N}T - \xi_3 \frac{TH}{N} - (\gamma+\mu)T = 0 \tag{3B.15}$$

$$\left(\xi_2 - \xi_2' \frac{H}{n+H}\right)\frac{(N+T+H+M+R+A)}{N}H + \xi_3 \frac{TH}{N} - (\rho+\mu)H = 0 \tag{3B.16}$$

$$\gamma T - (\delta+\mu)M = 0 \tag{3B.17}$$

$$\delta M - (\lambda+\mu)R = 0 \tag{3B.18}$$

$$\rho H - (\mu+\alpha)A = 0 \tag{3B.19}$$

Using equations (3B.14)-(3B.19), the four possible equilibrium points are obtained as follows:

(i) The diseases free equilibrium point $E_0(\overline{N},0,0,0,0,0)$ exists for all parameter values as

$$\overline{N} = \frac{\Lambda}{\mu}, \overline{T} = 0,\ \overline{H} = 0,\ \overline{M} = 0,\ \overline{R} = 0,\ \overline{A} = 0$$

(ii) The HIV/AIDS infection-free equilibrium point $E_1(N^*,T^*,0,0,0,0)$ is given by

$$N^* = \frac{\Lambda}{\mu},\ M^* = 0,\ R^* = 0,\ H^* = 0,\ A^* = 0, K_1 T^{*2} + K_2 T^* + K_3 = 0$$

where, $K_1 = -\frac{\mu}{\Lambda}(\xi_1 - \xi_1'),\ K_2 = -\frac{\mu}{\Lambda} m(\xi_1 - \xi_1') - (\gamma+\mu), K_3 = m(\xi_1 - (\gamma+\mu))$

we know that $K_3 > 0$, if $\xi_1 - (\gamma+\mu) > 0$, the hence system has unique HIV/AIDS free equilibrium point.

(iii) The TB infection-free equilibrium point $E_2(\hat{N},0,0,0,\hat{H},\hat{A})$ is

$$\hat{N} = \frac{1}{\mu}\left(\Lambda - \frac{\alpha\rho\hat{H}}{\mu+\alpha}\right), \hat{T} = 0, \hat{M} = 0, \hat{R} = 0, \hat{A} = \frac{\rho\hat{H}}{\mu+\alpha}, P_1\hat{H}^2 + P_2\hat{H} + P_3 = 0$$

where

$$P_1 = -(\xi_2 - \xi_2')\left(\frac{\rho}{\mu+\alpha}\left(\frac{1+\mu}{\mu}\right) + 1 - \frac{\alpha\rho(\mu+\rho)}{\mu(\mu+\alpha)}\right),$$

$$P_2 = -\frac{n\xi_2\rho}{\mu+\alpha}\left(\frac{1+\mu}{\mu}\right) - n\xi_2 + (\xi_2 - \xi_2')\frac{\Lambda}{\mu} + \frac{n\alpha\rho(\mu+\rho)}{\mu(\mu+\alpha)},$$

$$P_3 = \frac{n\Lambda}{\mu}(\xi_2 - (\mu+\rho)) + \frac{\Lambda}{\mu}(\mu+\rho).$$

Clearly $P_3 > 0$, if $\xi_2 > (\mu+\rho)$, then the system has unique TB infection-free equilibrium point.

(iv) The endemic co-infection equilibrium point $E_3(\tilde{N}, \tilde{T}, \tilde{M}, \tilde{R}, \tilde{H}, \tilde{A})$ is given by

$$\tilde{N} = \frac{1}{\mu}\left(\Lambda - \frac{\alpha\rho\tilde{H}}{\mu+\alpha}\right),\ \tilde{M} = \frac{\gamma}{\mu+\delta}\tilde{T}\ ,\tilde{R} = \frac{\delta}{\mu+\lambda}\tilde{M}\ ,\ \tilde{A} = \frac{\rho}{\mu+\alpha}\tilde{H}\ ,$$

$$\tilde{T} = \frac{\frac{\Lambda}{\mu}[(\xi_1 - \xi_1' p_T) - (\mu+\gamma)] - \left[(\xi_1 - \xi_1' p_T)\left(\frac{\mu+\alpha+\rho}{\mu+\alpha}\right) + \xi_3 + \alpha\rho\left\{\frac{(\xi_1 - \xi_1' p_T) - (\gamma+\mu)}{\mu(\alpha+\mu)}\right\}\right]\tilde{H}}{(\xi_1 - \xi_1' p_T)}$$

$$\tilde{H} = \frac{\frac{\Lambda}{\mu}\left[\{(\xi_2 - \xi_2' p_H) - (\mu+\gamma)\} + \left(\frac{\xi_3 - (\xi_2 - \xi_2' p_H)}{(\xi_1 - \xi_1' p_T)}\right)\{(\xi_1 - \xi_1' p_T) - (\gamma+\mu)\}\right]}{\frac{\xi_3(\mu+\alpha+\rho)}{\mu+\alpha} + \xi_3\left(\frac{\xi_3 - (\xi_2 - \xi_2' p_H)}{(\xi_1 - \xi_1' p_T)}\right) + \frac{\alpha\rho}{\mu(\alpha+\mu)}\left[\begin{matrix}\{(\xi_1 - \xi_1' p_T) - (\gamma+\mu)\} \\ + \{(\xi_2 - \xi_2' p_H) - (\gamma+\mu)\}\end{matrix}\right]}$$

3B.5. Summary and Concluding Remarks

This section marks an extension from the preceding SEIRS epidemic model established in Section 3A, specifically centered on the nuanced exploration of the co-infection dynamics between HIV & TB. Departing from the SEIRS framework, this extension delves into the specialized context of HIV/AIDS & TB co-infection.

While the literature review emphasizes the crucial interplay between HIV & TB, recognizing the pivotal role of treatment in mitigating mortality rates, this section's primary focus lies in advancing our understanding solely within the framework of HIV/AIDS & TB co-infection. Limited alterations and extensions within this specialized context contribute incrementally to unraveling the complexities of co-infection transmission and treatment outcomes.

Nevertheless, this section underscores the imperative for future research to explore uncharted territories, such as the influence of media awareness on disease dynamics within the specialized framework of HIV/AIDS & TB co-infection. By extending and refining this specialized model, it lays the foundation for more targeted interventions and further investigations into this intricate health challenge within diverse populations.

CHAPTER-4

Mathematical Analysis of Malaria Transmission: SEIRS Model with Mosquito Vector Dependency

Keywords: Transmission Dynamics, Stability Analysis, Human and Vector population.

Chapter 4: Mathematical Analysis of Malaria Transmission: SEIRS Model with Mosquito Vector Dependency

4.1. Introduction

Malaria, a profoundly impactful infection, stands as a formidable global challenge affecting countries predominantly in Africa and Asia. Its far-reaching impact encompasses nearly 3 billion individuals across 109 countries. This disease, with its staggering toll, annually accounts for approximately 250 million documented cases, tragically resulting in the loss of 1 million lives, a substantial portion of whom are children under the age of five. Central to the complexity of malaria is the microscopic parasite, plasmodium, which operates exclusively through the transmission by female mosquitoes of the Anopheles genus.

The transference of the malaria parasite occurs through the bite of an infected female Anopheline mosquito, introducing the pathogen into the human bloodstream. Notably, among the numerous plasmodium species including Plasmodium malariae, Plasmodium vivax, Plasmodium ovale, Plasmodium falciparum and Plasmodium knowlesi, the latter two especially P. falciparum stand out for their severe clinical outcomes and prevalence in certain regions. The World Health Organization (WHO) records a staggering toll of 627,000 deaths attributed to malaria in 2013, with nearly 207 million cases officially registered, disproportionately affecting African children, emphasizing the gravity of this disease burden within vulnerable populations.

The battle against malaria extends beyond the epidemiological landscape, intertwining with socio-economic and environmental factors that intricately shape its prevalence and impact. Factors such as inadequate access to healthcare, socio-economic disparities, climate variations affecting mosquito habitats and the emergence of drug-resistant parasite strains significantly contribute to the disease's persistence and exacerbate its impact on vulnerable communities. Understanding these multifaceted influences becomes pivotal in devising comprehensive strategies to combat the spread of malaria.

Moreover, this chapter endeavors to bridge the gap between theoretical models and real-world applicability by exploring the potential implications of the SEIRS model with mosquito vector dependency. Beyond theoretical constructs, the analysis aims to simulate and predict the impact of various intervention strategies, including vector control measures, anti-malarial drug distribution, and socio-economic interventions, within the framework of the mathematical model. By projecting potential outcomes and evaluating the effectiveness of interventions, this approach seeks to offer actionable insights for policymakers, health organizations, and researchers striving to mitigate the burden of malaria. This integrated approach, amalgamating

mathematical rigor with an understanding of ecological, socio-economic and healthcare access factors aims to pave the way for more targeted and impactful interventions, ultimately steering the global fight against malaria towards a path of sustained progress and control.

In this chapter, the authors construct a SEIRS model for humans and a SEI model for mosquitoes, ultimately asserting that the primary defense against such a disease lies within the human immune system. The subsequent structure of the chapter unfolds as follows: Section 4.2 provides a detailed literature and Section 4.3 furnishes a portrayal of the model. The subsequent sections, 4.4 and 4.5, undertake the analysis and numerical simulation, respectively. The chapter concludes with a comprehensive summary and concluding remarks in Section 4.6.

4.2. Literature Review

Various epidemic models have undergone mathematical analysis and have been applied to specific diseases (cf. Gupta *et al.,* 1994; Hethcote, 2000). Ross (1916) was the first to introduce the formulation of an initial arithmetical copy for the transference of jungle fever. Since then, a multitude of models have been devised to examine the intricacies of malaria transmission dynamics. (cf. Chitnis *et al.,* 2006 & 2012; Chamchod and Britton, 2011; Ruan *et al*., 2008; Xiao and Zou, 2013; Li, 2011).

Ngwa and Shu (2000) conducted an examination on a deterministic differential equation model regarding the prevalence of malaria, considering the fluctuating populations of both humans and mosquitoes. This avenue of research has seen extensive exploration, with biologists and mathematicians working collaboratively to gain insights into the primary causes of epidemic spread. Ngwa (2004) addressed the issue by employing a mathematical model, utilizing perturbation analysis and determining that the death rate is nonzero, small and significant.

Chitnis *et al.,* (2006 & 2012) presented a model for infection agents taking into account the influence of immigration and death rates induced by the disease. Exploring the dynamics of malaria transference through arithmetical modeling is an extensive and captivating field of study, where developed models depend on various factors including death rates and environmental considerations. Despite considerable progress, certain areas still require research, such as optimizing malaria cure costs, assessing the role of awareness and examining follow-up cases. Among these areas is the coefficient of the human population, which is dependent on density and warrants further exploration.

Anderson and May (1991) examined mathematical models of infectious agent transmission in human groups. Ghosh *et al.,* (2014) introduce an arithmetical model to study the transmission

of malaria among birds, incorporating alterations in vector behavior. Meanwhile, Forouzannia and Gumel (2015) developed and qualitatively analyzed a novel age-structured deterministic copy in sequence to evaluate the effect of anti-malaria medication on jungle fever transmission. Wang *et al.,* (2016) examined a stage-structured mosquito model to investigate the factors behind the significant mosquito abundance in 2014 and its implications for disease outbreaks.

The exploration of malaria transmission dynamics through mathematical modeling has been an engaging area of research (cf. Chaves *et al*., 2008; Erin *et al.*, 2013). Previous models have taken into account factors such as density-dependent death rates and environmental variables. However, these studies have not extensively investigated the influence of the transmission coefficient on humans, considering the density of mosquitoes.

Mathematical modeling has proven to be a valuable tool for understanding the transmission dynamics of malaria. It not only enhances our comprehension of the disease's dissemination and impact but also aids in devising informed policies to combat malaria (cf. Romero-Leiton and Ibarguen-Mondragon, 2019; Abioye *et al*., 2020; Misra *et al*., 2023). Several notable arithmetical models, such as the SIR model and its derivatives have been applied to malaria transference. These models have been consistently extended and adapted by researchers by incorporating nuanced insights related to malaria dynamics and disease control strategies (cf. Romero-Leiton and Ibarguen-Mondragon, 2019; Ndii and Adi, 2021; Nwankwo and Daniel, 2019; Noeiaghdam and Micula, 2021; Kobe, 2020; Handari *et al.,* 2019).

Ibrahim *et al.,* (2020) introduced a unique conceptual framework that divides the population affected by the ailment into two distinct subgroups: those who lack awareness of their infection and those who have awareness of it. This framework suggests that the rate of expansion for the campaign aimed at increasing awareness is directly linked to the number of individuals who are unaware of their infection. Building on this concept, Al Basir *et al.,* (2021) formulate a comprehensive arithmetical design to investigate jungle fever dynamics, incorporating the impact of interventions based on awareness. Their framework suggests that the level of awareness influences disease transmission rates between vectors and humans, as well as between humans and vectors with control methods capable of elevating this level.

The susceptible population is divided in two groups according to a novel mathematical framework developed by Ndii and Adi (2021): the informed and the uninformed. According to this model, which presents a steady awareness rate, some susceptible individuals who are currently uninformed will eventually become conscious and join the informed group.

Al Basir and Abraha (2023) put forth a deterministic mathematical framework in order to scrutinize the intricacies of malaria and assess the efficacy of interventions involving the use of mosquito nets and insecticides. It is worth mentioning that their framework regards awareness as a dynamic variable that evolves over time. Finally, Tchoumi *et al.,* (2023) formulated a mathematical framework that provides insight into the vitals of jungle fever transmission, considering the susceptibility of hosts and acknowledging the acquisition of partial immunity after infection.

This comprehensive array of mathematical models contributes significantly to our understanding of malaria transmission and the potential strategies to control its spread. These models consider awareness as a pivotal factor in intervention strategies and provide essential comprehension of the complex dynamics of an illness.

4.3. Model Description

In this model, we consider two distinct population categories: Human and Vector (mosquito) population. The overall population size of the human population is represented by N_h, and it is distant divided into four sub-classes: Susceptible human (S_h), Exposed human (E_h), Infected humans (I_h) and Recovered human (R_h).

It's believed that individuals come into the susceptible class through processes such as birth. Following a bite from an infected mosquito, a susceptible human may first become exposed and subsequently may experience infection at varying rates. Infected people recover and join the recovered class after a set amount of time. They eventually regain their susceptibility and revert to the susceptible class.

Likewise, the overall vector population is represented by N_v and categorized into three classes: Susceptible mosquito (S_v), Exposed mosquito (E_v) and Infected mosquito (I_v). Susceptible mosquitoes are added to the population at a rate Λ_2. The mosquito initially transitions to the exposed class, and subsequently, there is a progression of individuals from the exposed class to the infected class over time. The malaria transmission diagram is illustrated in Figure 4.1.

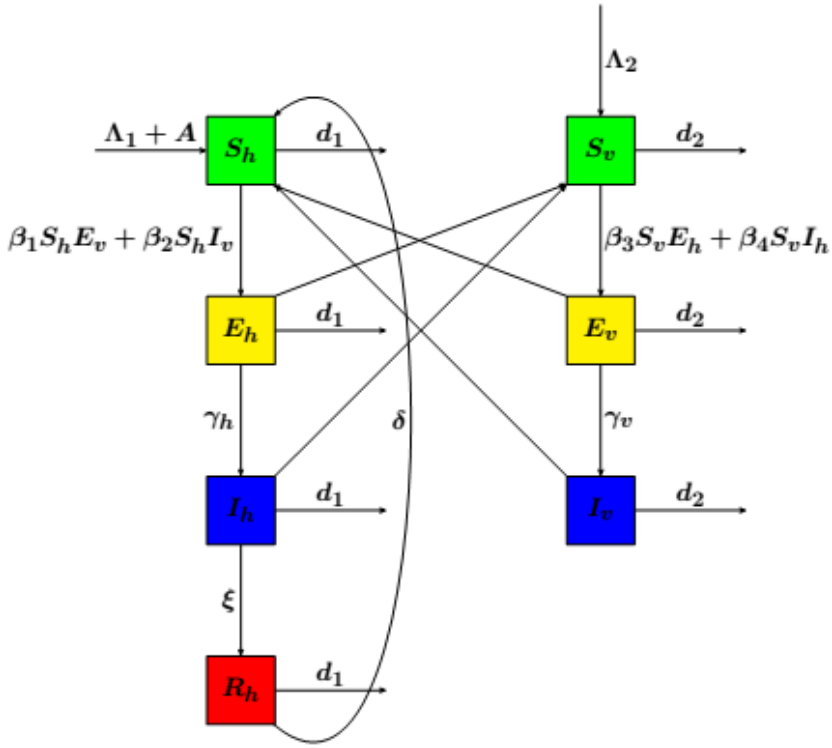

Figure 4.1: Epidemiological modeling of malaria transmission.

Table 4.1: Explanation of state parameters utilized in the model

Symbols	Description
Λ_1	Recruitment rate i.e., human population
Λ_2	The entry rate of the mosquito population, encompassing newly generated vectors
A	The rate of immigration for the human population
β_1	Transmission rate of probability from susceptible humans to exposed vectors (mosquitoes)
β_2	Transmission rate of probability from susceptible humans to infected vectors (mosquitoes)
β_3	The speed at which vulnerable mosquitoes are likely to spread their infection to people who are exposed
β_4	The speed at which virus-carrying mosquitoes are likely to spread their infection to humans
γ_h	Rate at which people become sick after being exposed
γ_v	Rate at which a vector becomes infected after being exposed
δ	The speed at which members of the human population heal completely and become vulnerable once more
ξ	The pace of recovery for people within the human population
$d_1(d_2)$	Mortality rate due to natural causes in the human population (mosquito population), respectively

Two distinct scenarios have been considered in formulating the mathematical model. We will analyze the model in both of the mentioned cases:

Case 1: The transmission probability, denoted as β_1, representing the estimate at which contaminated mosquitoes bite vulnerable humans, is presumed to remain continuous.

Case 2: The likelihood of transmission, denoted as β_1, depends on the solidity of the mosquito inhabitants. It is expressed as $\beta_1 = b_0 + b_1 N_v$, where b_0 and b_1 are constructive continuous.

4.3.1. Governing Equations

The behavior of the model is elucidated by the subsequent set of divergence

$$S_h' = (\Lambda_1 + A) + \delta R_h - (\beta_1 E_v + \beta_2 I_v) S_h - d_1 S_h$$

$$E_h' = (\beta_1 E_v + \beta_2 I_v) S_h - (\gamma_h + d_1) E_h$$

$$I_h' = \gamma_h E_h - (\xi + d_1) I_h$$

$$R_h' = \xi I_h - (\delta + d_1) R_h$$

$$N_h' = \Lambda_1 + A - d_1 N_h \qquad (4.1)$$

$$S_v' = \Lambda_2 - (\beta_3 E_h + \beta_4 I_h) S_v - d_2 S_v$$

$$E_v' = (\beta_3 E_h + \beta_4 I_h) S_v - (\gamma_v + d_2) E_v$$

$$I_v' = \gamma_v E_v - d_2 I_v$$

$$N_v' = \Lambda_2 - d_2 N_v$$

4.4. Mathematical Analysis

The formulated mathematical model can be examined under two distinct cases:

Case 1: When $\beta_1 = \beta_0; \beta_0$ is a constant.

Considering $N_h = S_h + E_h + I_h + R_h$ and $N_v = S_v + E_v + I_v$, the system of equations (4.1) can be reformulated in the following manner:

$$E_h' = (\beta_0 E_v + \beta_2 I_v)(N_h - (E_h + I_h + R_h)) - (\gamma_h + d_1) E_h$$

$$I_h' = \gamma_h E_h - (\xi + d_1) I_h$$

$$R_h' = \xi I_h - (\delta + d_1) R_h$$

$$N_h' = \Lambda_1 + A - d_1 N_h \tag{4.2}$$

$$E_v' = (\beta_3 E_h + \beta_4 I_h)(N_v - (E_v + I_v)) - (\gamma_v + d_2)E_v$$

$$I_v' = \gamma_v E_v - d_2 I_v$$

$$N_v' = \Lambda_2 - d_2 N_v$$

The above system's attractive region is

$$\Phi_1 = \{(E_h, I_h, R_h, N_h, E_v, I_v, N_v) : 0 \le E_h + I_h + R_h \le N_h \le \overline{N}_h, 0 \le E_v + I_v \le N_v \le \overline{N}_v\}$$

where $\overline{N}_h = \lim_{t\to\infty} \sup\ N_h = \dfrac{\Lambda_1 + A}{d_1}$ and $\overline{N}_v = \lim_{t\to\infty} \sup\ N_v = \dfrac{\Lambda_2}{d_2}$.

4.4.1. Equilibrium Points and Stability Analysis

Given that, at equilibrium all derivatives become zero,

i.e., $E_h' = I_h' = R_h' = N_h' = E_v' = I_v' = N_v' = 0$,

then the system of equations (4.2) becomes

$$(\beta_0 E_v + \beta_2 I_v)(N_h - (E_h + I_h + R_h)) - (\gamma_h + d_1)E_h = 0$$

$$\gamma_h E_h - (\xi + d_1)I_h = 0$$

$$\xi I_h - (\delta + d_1)R_h = 0$$

$$\Lambda_1 + A - d_1 N_h = 0 \tag{4.3}$$

$$(\beta_3 E_h + \beta_4 I_h)(N_v - (E_v + I_v)) - (\gamma_v + d_2)E_v = 0$$

$$\gamma_v E_v - d_2 I_v = 0$$

$$\Lambda_2 - d_2 N_v = 0$$

Three equilibrium points that hold both physical and biological relevance are as follows:

(i) Equilibrium E_1 signifies the disease-free state exclusive to the human population and is denoted by $\left(0, 0, 0, \dfrac{\Lambda_1 + A}{d_1}, 0, 0, 0\right)$.

(ii) Equilibrium E_2 represents the disease-free state for both human & mosquito populations, expressed as $\left(0, 0, 0, \frac{\Lambda_1 + A}{d_1}, 0, 0, \frac{\Lambda_2}{d_2}\right)$.

(iii) Equilibrium E_3 designates the endemic equilibrium point and is defined as $\left(\tilde{\tilde{E}}_h, \tilde{I}_h, \tilde{R}_h, \tilde{N}_h, \tilde{\tilde{E}}_v, \tilde{I}_v, \tilde{N}_v\right)$, where

$$\tilde{\tilde{E}}_h = \frac{\left(\beta_0 + \frac{\beta_2 \gamma_v}{d_2}\right) E_v \overline{N}_h}{\left(\beta_0 + \frac{\beta_2 \gamma_v}{d_2}\right)\left(1 + \frac{\gamma_h}{d_1 + \xi} + \frac{\gamma_h \xi}{(d_1 + \delta)(d_1 + \xi)}\right)\tilde{\tilde{E}}_v + (d_1 + \gamma_h)}, \tag{4.4}$$

$$\tilde{I}_h = \frac{\gamma_h \tilde{\tilde{E}}_h}{d_1 + \xi}, \quad \tilde{R}_h = \frac{\xi \gamma_h \tilde{\tilde{E}}_h}{(d_1 + \delta)(d_1 + \xi)}, \quad \tilde{N}_h = \frac{\Lambda_1 + A}{d_1}, \tag{4.5}$$

$$\tilde{\tilde{E}}_v = \frac{\left(\beta_3 + \frac{\beta_4 \gamma_h}{d_1 + \xi}\right) \tilde{\tilde{E}}_h \overline{N}_v}{\left(\beta_3 + \frac{\beta_4 \gamma_h}{d_1 + \xi}\right)\left(1 + \frac{\gamma_v}{d_1 + \xi}\right)\tilde{\tilde{E}}_h + (d_2 + \gamma_v)}, \tag{4.6}$$

$$\tilde{I}_v = \frac{\gamma_v \tilde{\tilde{E}}_v}{d_2}, \quad \tilde{N}_v = \frac{\Lambda_2}{d_2}. \tag{4.7}$$

Theorem 4.4.1: The equilibrium point E_1 is stable if all latent roots are negative. The equilibrium E_2 is stable if $p_i (i = 1,2,4) > 0$ and $p_3(p_1 p_2 - p_3) > p_1^2 p_4$, otherwise unstable and the equilibrium E_3 is stable if $q_i (i = 1,3,4,5) > 0$ and $(q_1 q_4 - q_5)(q_1 q_2 q_3 - q_1^2 - q_3^2 - q_1^2 q_4) > q_5 (q_1 q_2 - q_3)^2 + q_1 q_5^2$.

Proof: In accordance with framework (4.2), the overall variational matrix J is

$$J = \begin{pmatrix} -(\beta_0 E_v + \beta_2 I_v) - (\gamma_h + d_1) & -(\beta_0 E_v + \beta_2 I_v) & -(\beta_0 E_v + \beta_2 I_v) & (\beta_0 E_v + \beta_2 I_v) \\ \gamma_h & -d_1 - \xi & 0 & 0 \\ 0 & \xi & -d_1 - \delta & 0 \\ 0 & 0 & 0 & -d_1 \\ \beta_3 (N_v - (E_v + I_v)) & \beta_4 N_v - \beta_4 (E_v + I_v) & 0 & 0 \\ 0 & 0 & 0 & 0 \\ 0 & 0 & 0 & 0 \end{pmatrix}$$

$$\begin{pmatrix} \beta_0(N_h-(E_h+I_h+R_h)) & \beta_2(N_h-(E_h+I_h+R_h)) & 0 \\ 0 & 0 & 0 \\ 0 & 0 & 0 \\ 0 & 0 & 0 \\ -(\beta_3 E_h+\beta_4 I_h)-(\gamma_v+d_2) & -(\beta_3 E_h+\beta_4 I_h) & (\beta_3 E_h+\beta_4 I_h) \\ \gamma_v & -d_2 & 0 \\ 0 & 0 & -d_2 \end{pmatrix}$$

At the equilibrium $E_1=\left(0,0,0,\frac{\Lambda_1+A}{d_1},0,0,0\right)$, the jacobian matrix J_0 is provided as:

$$J_0=\begin{pmatrix} -(\gamma_h+d_1) & 0 & 0 & 0 & \beta_0\left(\frac{\Lambda_1+A}{d_1}\right) & \beta_2\left(\frac{\Lambda_1+A}{d_1}\right) & 0 \\ \gamma_h & -(d_1+\xi) & 0 & 0 & 0 & 0 & 0 \\ 0 & \xi & -(d_1+\delta) & 0 & 0 & 0 & 0 \\ 0 & 0 & 0 & -d_1 & 0 & 0 & 0 \\ 0 & 0 & 0 & 0 & -(d_2+\gamma_v) & 0 & 0 \\ 0 & 0 & 0 & 0 & \gamma_v & -d_2 & 0 \\ 0 & 0 & 0 & 0 & 0 & 0 & -d_2 \end{pmatrix}$$

The derivation of the Jacobian matrix's characteristic polynomial:

$$|J-\lambda I|=0$$

$$\Rightarrow (d_1+\lambda)(d_2+\lambda)^2(d_1+\delta+\lambda)(d_1+\xi+\lambda)(d_1+\gamma_h+\lambda)(d_1+\gamma_v+\lambda)=0$$

Therefore, all of these roots exhibit negativity. Consequently, the equilibrium point E_1 is deemed stable.

At the equilibrium $E_2=\left(0,0,0,\frac{\Lambda_1+A}{d_1},0,0,\frac{\Lambda_2}{d_2}\right)$, the Jacobian matrix J_1 is provided as:

$$J_1=\begin{pmatrix} -(\gamma_h+d_1) & 0 & 0 & 0 & \beta_0\left(\frac{\Lambda_1+A}{d_1}\right) & \beta_2\left(\frac{\Lambda_1+A}{d_1}\right) & 0 \\ \gamma_h & -(d_1+\xi) & 0 & 0 & 0 & 0 & 0 \\ 0 & \xi & -(d_1+\delta) & 0 & 0 & 0 & 0 \\ 0 & 0 & 0 & -d_1 & 0 & 0 & 0 \\ \beta_3\frac{\Lambda_2}{d_2} & \beta_4\frac{\Lambda_2}{d_2} & 0 & 0 & -(\gamma_v+d_2) & 0 & 0 \\ 0 & 0 & 0 & 0 & \gamma_v & -d_2 & 0 \\ 0 & 0 & 0 & 0 & 0 & 0 & -d_2 \end{pmatrix}$$

The derivation of the Jacobian matrix's characteristic polynomial:

$$|J - \lambda I| = 0$$

$$\Rightarrow (d_1 + \lambda)(d_2 + \lambda)(a_1 + \lambda)\{\lambda^4 + \lambda^3 p_1 + \lambda^2 p_2 + \lambda p_3 + p_4\} = 0 \quad (4.8)$$

where

$p_1 = a_2 + a_3 + a_4 + d_2,$

$p_2 = a_2a_3 + a_2a_4 + a_3a_4 + (a_2 + a_3 + a_4)d_2 - \beta_1\beta_3 N_h N_v,$

$p_3 = a_2a_3a_4 + (a_2a_3 + a_2a_4 + a_3a_4)d_2 - \beta_1\beta_4\gamma_h N_h N_v - \beta_1\beta_3(a_2 + d_2)N_h N_v - \beta_1\beta_3\gamma_v N_h N_v,$

$p_4 = a_2a_3a_4d_2 + (a_2a_3 + a_2a_4 + a_3a_4)d_2 - (\beta_1\beta_2\gamma_h d_2 + \beta_2\beta_4\gamma_h\gamma_v + \beta_1\beta_3a_2d_2 + \beta_2\beta_3\gamma_v a_2)N_h N_v,$
and

$a_1 = (d_1 + \delta),\ a_2 = (d_1 + \xi),\ a_3 = (d_1 + \gamma_h),\ a_4 = (d_2 + \gamma_v)$.

The polynomial provided by equation (4.8) yields three negative roots and the coefficients of a bi-quadratic equation ensure every root contains a true unfavorable portion. Therefore, the Routh-Hurwitz conditions, $p_i(i = 1,2,4) > 0$ and $p_3(p_1p_2 - p_3) > p_1^2 p_4$ are satisfied. In these circumstances, the equilibrium point E_2 exhibits local asymptotic stability.

At the equilibrium $E_3 = \left(\tilde{E}_h,\ \tilde{I}_h,\ \tilde{R}_h,\ \tilde{N}_h,\ \tilde{E}_v,\ \tilde{I}_v,\ \tilde{N}_v\right)$, the Jacobian matrix J_2 is provided as:

$$J_2 = \begin{pmatrix} -(\beta_0\tilde{E}_v + \beta_2\tilde{I}_v) - (\gamma_h + d_1) & -(\beta_0\tilde{E}_v + \beta_2\tilde{I}_v) & -(\beta_0\tilde{E}_v + \beta_2\tilde{I}_v) & (\beta_0\tilde{E}_v + \beta_2\tilde{I}_v) \\ \gamma_h & -(d_1 + \xi) & 0 & 0 \\ 0 & \xi & -(d_1 + \delta) & 0 \\ 0 & 0 & 0 & -d_1 \\ \beta_3(\tilde{N}_v - (\tilde{E}_v + \tilde{I}_v)) & \beta_4(\tilde{N}_v - (\tilde{E}_v + \tilde{I}_v)) & 0 & 0 \\ 0 & 0 & 0 & 0 \\ 0 & 0 & 0 & 0 \end{pmatrix}$$

$$\begin{pmatrix} \beta_0(\tilde{N}_h - (\tilde{E}_h + \tilde{I}_h + \tilde{R}_h)) & \beta_2\tilde{N}_h - \beta_2(\tilde{E}_h + \tilde{I}_h + \tilde{R}_h) & 0 \\ 0 & 0 & 0 \\ 0 & 0 & 0 \\ 0 & 0 & 0 \\ -(\beta_3\tilde{E}_h + \beta_4\tilde{I}_h) - (\gamma_v + d_2) & -(\beta_3\tilde{E}_h + \beta_4\tilde{I}_h) & (\beta_3\tilde{E}_h + \beta_4\tilde{I}_h) \\ \gamma_v & -d_2 & 0 \\ 0 & 0 & -d_2 \end{pmatrix}$$

The derivation of the Jacobian matrix's characteristic polynomial:

$$|J - \lambda I| = 0$$

$$\Rightarrow (d_1 + \lambda)(d_2 + \lambda)\{\lambda^5 + \lambda^4 q_1 + \lambda^3 q_2 + \lambda^2 q_3 + \lambda q_4 + q_5\} = 0 \quad (4.9)$$

where

$$q_1 = a_1 + a_2 + a_3 + a_4 + a_5 + a_6 + d_2,$$

$$q_2 = ((a_4 + a_6)d_2 + a_6\gamma_v) + (a_1 + a_2 + a_3 + a_5)(a_4 + a_6 + d_2) + (a_1a_2 + a_1a_3 + a_1a_5 + a_2a_3 + a_2a_5) + a_7a_8\beta_1\beta_3 - \gamma_h a_5,$$

$$q_3 = (a_1 + a_2 + a_3 + a_5)((a_4 + a_6)d_2 + a_6\gamma_v) + (a_1a_2a_3 + a_1a_2a_5) + (a_1a_2 + a_1a_3 + a_1a_5 + a_2a_3 + a_2a_5)(a_4 + a_6 + d_2) + a_7a_8\beta_3(\beta_1d_2 + a_1\beta_1 + a_2\beta_1 + \beta_2\gamma_v) + a_7a_8\beta_1\beta_4 + \gamma_h\xi a_5 - \gamma_h a_5(a_1 + a_4 + a_6 + d_2),$$

$$q_4 = (a_1a_2 + a_1a_3 + a_1a_5 + a_2a_3 + a_2a_5)((a_4 + a_6)d_2 + a_6\gamma_v) + (a_1a_2a_3 + a_1a_2a_5)(a_4 + a_6 + d_2) + \gamma_h\xi a_5(a_4 + a_6 + d_2) + a_7a_8\beta_4(\beta_1d_2 + a_1\beta_1 + \beta_2\gamma_v) + a_7a_8\beta_3(a_1\beta_1d_2 + a_2\beta_1d_2 + a_1a_2\beta_1 + a_1\beta_2\gamma_v + a_2\beta_2\gamma_v) - \gamma_h a_5(a_1(a_4 + a_6 + d_2) + (a_4 + a_6)d_2 + a_6\gamma_v)$$

$$q_5 = (a_1a_2a_3 + a_1a_2a_5)((a_4 + a_6)d_2 + a_6\gamma_v) + \gamma_h\xi a_5((a_4 + a_6)d_2 + a_6\gamma_v) + a_7a_8\beta_4(\beta_1a_1d_2 + \beta_2a_1\gamma_v) + a_7a_8\beta_3(a_1a_2\beta_1d_2 + a_1a_2\beta_2\gamma_v) - \gamma_h a_5((a_4 + a_6)a_1d_2 + a_1a_6\gamma_v)$$

and

$a_1 = (d_1 + \delta)$, $a_2 = (d_1 + \xi)$, $a_3 = (d_1 + \gamma_h)$, $a_4 = (d_2 + \gamma_v)$, $a_5 = (\beta_0E_v + \beta_2I_v)$, $a_6 = (\beta_3E_h + \beta_4I_h)$,

$a_7 = (N_h - (E_h + I_h + R_h))$, $a_8 = (N_v - (E_v + I_v))$.

With two negative roots and coefficients ensuring every root contains a true unfavorable portion, the Routh-Hurwitz conditions, $q_i(i = 1,3,4,5) > 0$ and $(q_1q_4 - q_5)(q_1q_2q_3 - q_1^2 - q_3^2 - q_1^2q_4) > q_5(q_1q_2 - q_3)^2 + q_1q_5^2$ are met. In these circumstances, the equilibrium point E_3 exhibits local asymptotic stability.

Case 2: When $\beta_1 = b_0 + b_1N_v$; b_0 and b_1 is a constant.

Since $N_h = S_h + E_h + I_h + R_h$ and $N_v = S_v + E_v + I_v$ the system of equations (4.1) can be:

$$E_h' = (b_0 + b_1N_v)(N_h - (E_h + I_h + R_h))E_v + \beta_2I_v(N_h - (E_h + I_h + R_h)) - (\gamma_h + d_1)E_h$$

$$I_h' = \gamma_hE_h - (\xi + d_1)I_h$$

$$R_h' = \xi I_h - (\delta + d_1)R_h$$

$$N_h' = \Lambda_1 + A - d_1N_h \qquad (4.10)$$

$$E_v' = (\beta_3E_h + \beta_4I_h)(N_v - (E_v + I_v)) - (\gamma_v + d_2)E_v$$

$$I_v' = \gamma_vE_v - d_2I_v$$

$N_v' = \Lambda_2 - d_2 N_v$

The system's attractive region, as provided by (4.10), is

$\Phi_2 = \{(E_h, I_h, R_h, N_h, E_v, I_v, N_v) : 0 \le E_h + I_h + R_h \le N_h \le \widehat{N}_h, 0 \le E_v + I_v \le N_v \le \widehat{N}_v\}$

where, $\widehat{N}_h = \lim_{t\to\infty} \sup\ N_h = \frac{\Lambda_1 + A}{d_1}$ and $\widehat{N}_v = \lim_{t\to\infty} \sup\ N_v = \frac{\Lambda_2}{d_2}$.

4.4.2. Equilibrium Points and Stability Analysis

Given that, at equilibrium all derivatives become zero,

i.e., $E_h' = I_h' = R_h' = N_h' = E_v' = I_v' = N_v' = 0$,

then the system of equations (4.10) becomes

$$(b_0 + b_1 N_v)(N_h - (E_h + I_h + R_h))E_v + \beta_2 I_v (N_h - (E_h + I_h + R_h)) - (\gamma_h + d_1)E_h = 0$$

$$\gamma_h E_h - (\xi + d_1) I_h = 0$$

$$\xi I_h - (\delta + d_1) R_h = 0$$

$$\Lambda_1 + A - d_1 N_h = 0 \qquad (4.11)$$

$$(\beta_3 E_h + \beta_4 I_h)(N_v - (E_v + I_v)) - (\gamma_v + d_2)E_v = 0$$

$$\gamma_v E_v - d_2 I_v = 0$$

$$\Lambda_2 - d_2 N_v = 0$$

Three equilibrium points that hold both physical and biological relevance are as follows:

(i) When the open to person inhabitants is contaminated, then the sickness free parity only for the human inhabitants is $P_1 = \left(E_h', 0, 0, \frac{\Lambda_1 + A}{d_1}, 0, 0, 0\right)$.

(ii) When the open to person inhabitants is only contaminated, then the sickness free parity for both human and mosquito inhabitants is $P_2 = \left(E_h', 0, 0, \frac{\Lambda_1 + A}{d_1}, 0, 0, \frac{\Lambda_2}{d_2}\right)$.

(iii) Endemic equilibrium point is $P_3 = \left(\tilde{E}_h, \tilde{I}_h, \tilde{R}_h, \tilde{N}_h, \tilde{E}_v, \tilde{I}_v, \tilde{N}_v\right)$, where

$$E_h' = \frac{\left(b_0 + b_1\frac{\Lambda_2}{d_2} + \frac{\beta_2\gamma_v}{d_2}\right)\tilde{E}_v\frac{\Lambda_1 + A}{d_1}}{\left(b_0 + b_1\frac{\Lambda_2}{d_2} + \frac{\beta_2\gamma_v}{d_2}\right)\left(1 + \frac{\gamma_h}{d_1+\xi} + \frac{\gamma_h\xi}{(d_1+\xi)(d_1+\delta)}\right)\tilde{E}_v + (d_1+\gamma_h)}, \tag{4.12}$$

$$\tilde{E}_h = \frac{\left((b_0 + b_1N_v) + \frac{\beta_2\gamma_v}{d_2}\right)\tilde{E}_v\hat{N}_h}{\left((b_0 + b_1N_v) + \frac{\beta_2\gamma_v}{d_2}\right)\left(1 + \frac{\gamma_h}{d_1+\xi} + \frac{\gamma_h\xi}{(d_1+\xi)(d_1+\delta)}\right)\tilde{E}_v + (d_1+\gamma_h)}, \tag{4.13}$$

$$\tilde{I}_h = \frac{\gamma_h\tilde{E}_h}{d_1+\xi},\ \ \tilde{R}_h = \frac{\xi\gamma_h\tilde{E}_h}{(d_1+\xi)(d_1+\delta)}, \tilde{N}_h = \frac{\Lambda_1 + A}{d_1}, \tag{4.14}$$

$$\tilde{E}_v = \frac{\left(\beta_3 + \frac{\beta_4\gamma_h}{d_1+\xi}\right)\tilde{E}_h\hat{N}_v}{\left(\beta_3 + \frac{\beta_4\gamma_h}{d_1+\xi}\right)\left(1 + \frac{\gamma_v}{d_1+\xi}\right)\tilde{E}_h + (d_2+\gamma_v)}, \tag{4.15}$$

$$\tilde{I}_v = \frac{\gamma_v\tilde{E}_v}{d_2}, \tilde{N}_v = \frac{\Lambda_2}{d_2}. \tag{4.16}$$

Theorem 4.4.2: The equilibrium point P_1 is stable if all latent roots are negative. The equilibrium P_2 is stable if $m_i(i=1,2,4)>0$ and $m_3(m_1m_2 - m_3) > m_1^2m_4$, otherwise unstable and the equilibrium P_3 is stable if $s_i(i=1,3,4,5)>0$ and $(s_1s_4 - s_5)(s_1s_2s_3 - s_1^2 - s_3^2 - s_1^2s_4) > s_5(s_1s_2 - s_3)^2 + s_1s_5^2$.

Proof: In accordance with framework (4.2), the overall variational matrix M is

$$M = \begin{pmatrix} -(b_0 + b_1N_v)E_v - \beta_2I_v - (\gamma_h + d_1) & -(b_0 + b_1N_v)E_v - \beta_2I_v & -(b_0 + b_1N_v)E_v - \beta_2I_v \\ \gamma_h & -(d_1+\xi) & 0 \\ 0 & \xi & -(d_1+\delta) \\ 0 & 0 & 0 \\ \beta_3N_v - \beta_3(E_v + I_v) & \beta_4N_v - \beta_4(E_v + I_v) & 0 \\ 0 & 0 & 0 \\ 0 & 0 & 0 \end{pmatrix}$$

$$\begin{pmatrix} (b_0+b_1N_v)E_v+\beta_2 I_v & (b_0+b_1N_v)(N_h-(E_h+I_h+R_h)) & \beta_2(N_h-(E_h+I_h+R_h)) & 0 \\ 0 & 0 & 0 & 0 \\ 0 & 0 & 0 & 0 \\ -d_1 & 0 & 0 & 0 \\ 0 & -(\beta_3E_h+\beta_4I_h)-(\gamma_v+d_2) & -(\beta_3E_h+\beta_4I_h) & (\beta_3E_h+\beta_4I_h) \\ 0 & \gamma_v & -d_2 & 0 \\ 0 & 0 & 0 & -d_2 \end{pmatrix}$$

At the equilibrium point $P_1=\left(E_h',0,0,\frac{\Lambda_1+A}{d_1},0,0,0\right)$, the variational matrix M_0 is given by

$$M_0=\begin{pmatrix} -(\gamma_h+d_1) & 0 & 0 & 0 & b_0\left(\frac{\Lambda_1+A}{d_1}-E_h'\right) & \beta_2\left(\frac{\Lambda_1+A}{d_1}-E_h'\right) & 0 \\ \gamma_h & -d_1-\xi & 0 & 0 & 0 & 0 & 0 \\ 0 & \xi & -\delta-d_1 & 0 & 0 & 0 & 0 \\ 0 & 0 & 0 & -d_1 & 0 & 0 & 0 \\ 0 & 0 & 0 & 0 & -(\beta_3E_h'+d_2+\gamma_v) & -\beta_3E_h' & \beta_3E_h' \\ 0 & 0 & 0 & 0 & \gamma_v & -d_2 & 0 \\ 0 & 0 & 0 & 0 & 0 & 0 & -d_2 \end{pmatrix}$$

The derivation of the Jacobian matrix's characteristic polynomial:

$$|J-\lambda I|=0$$

$$\Rightarrow (d_1+\lambda)(d_2+\lambda)(d_1+\delta+\lambda)(d_1+\xi+\lambda)(d_1+\gamma_h+\lambda)[((\beta_3E_h'+\gamma_v+d_2)+\lambda)(d_2+\lambda)+\beta_3E_h'\gamma_v]=0$$

$$\Rightarrow (d_1+\lambda)(d_2+\lambda)(d_1+\delta+\lambda)(d_1+\xi+\lambda)(d_1+\gamma_h+\lambda)[\lambda^2+\{(\beta_3E_h'+\gamma_v+d_2)+d_2\}\lambda+(\beta_3E_h'+\gamma_v+d_2)d_2+\beta_3E_h'\gamma_v]=0$$

Clearly, the negative nature of the five roots in the aforementioned equation is evident and the remaining two roots are derived through quadratic equations.

At the equilibrium $P_2=\left(E_h',\,0,\,0,\,\frac{\Lambda_1+A}{d_1},\,0,\,0,\,\frac{\Lambda_2}{d_2}\right)$, the Jacobian matrix M_1 is provided as:

$$M_1=\begin{pmatrix} -(\gamma_h+d_1) & 0 & 0 & 0 & \left(b_0+b_1\frac{\Lambda_2}{d_2}\right)\left(\frac{\Lambda_1+A}{d_1}-E_h'\right) & \beta_2\left(\frac{\Lambda_1+A}{d_1}-E_h'\right) & 0 \\ \gamma_h & -(d_1+\xi) & 0 & 0 & 0 & 0 & 0 \\ 0 & \xi & -(d_1+\delta) & 0 & 0 & 0 & 0 \\ 0 & 0 & 0 & -d_1 & 0 & 0 & 0 \\ \beta_3\frac{\Lambda_2}{d_2} & \beta_4\frac{\Lambda_2}{d_2} & 0 & 0 & -(\beta_3E_h'+\gamma_v+d_2) & -\beta_3E_h' & \beta_3E_h' \\ 0 & 0 & 0 & 0 & \gamma_v & -d_2 & 0 \\ 0 & 0 & 0 & 0 & 0 & 0 & -d_2 \end{pmatrix}$$

The derivation of the Jacobian matrix's characteristic polynomial:

$$\left|J-\lambda I\right|=0$$

$$\Rightarrow (d_1+\lambda)(d_2+\lambda)(a_1+\lambda)\left\{\lambda^4+\lambda^3 m_1+\lambda^2 m_2+\lambda m_3+m_4\right\}=0 \qquad (4.17)$$

where,

$$m_1=a_1+a_2+a_3+a_4+d_2,$$

$$m_2=a_2a_3+a_2a_4+a_3a_4+a_4d_2+a_2d_2+a_3d_2+(a_2+a_3+a_4)d_2+\gamma_v\beta_3E_h' -\beta_3N_v(b_0+b_1N_v)(N_h-E_h'),$$

$$m_3=a_2a_3a_4+(a_2a_3+a_2a_4+a_3a_4)d_2+(a_2+a_3)\beta_3\gamma_vE_h'+\beta_3N_v(a_2+d_2)(b_0+b_1N_v)(N_h-E_h') -\beta_2\beta_3\gamma_vN_v(N_h-E_h')-\beta_4\gamma_hN_v(b_0+b_1N_v)(N_h-E_h'),$$

$$m_4=a_2a_3a_4d_2+a_2a_3\beta_3\gamma_vE_h'+a_2d_2\beta_3N_v(b_0+b_1N_v)(N_h-E_h')+\beta_2\beta_3\gamma_va_2N_v(N_h-E_h') -\beta_4\gamma_hd_2N_v(b_0+b_1N_v)(N_h-E_h')-\beta_4\gamma_h\gamma_vN_v(N_h-E_h'),$$

and

$$a_1=(d_1+\delta),\ a_2=(d_1+\xi),\ a_3=(d_1+\gamma_h),\ a_4=(\beta_3E_h'+\gamma_v+d_2).$$

The polynomial provided by equation (4.17) yields three negative roots and the coefficients of a bi-quadratic equation ensure every root contains a true unfavorable portion. Therefore, the Routh-Hurwitz conditions, $m_i(i=1,2,4)>0$ and $m_3(m_1m_2-m_3)>m_1^2m_4$ are satisfied. In these circumstances, the equilibrium point P_2 exhibits local asymptotic stability.

At the equilibrium $P_3=\left(\tilde{E}_h,\ \tilde{I}_h,\ \tilde{R}_h,\ \tilde{N}_h,\ \tilde{E}_v,\ \tilde{I}_v,\ \tilde{N}_v\right)$, the Jacobian matrix M_2 is provided as:

$$M_2=\begin{pmatrix} -(b_0+b_1\tilde{N}_v)\tilde{E}_v-\beta_2\tilde{I}_v-(\gamma_h+d_1) & -(b_0+b_1\tilde{N}_v)\tilde{E}_v-\beta_2\tilde{I}_v & -(b_0+b_1\tilde{N}_v)\tilde{E}_v-\beta_2\tilde{I}_v \\ \gamma_h & -(d_1+\xi) & 0 \\ 0 & \xi & -(d_1+\delta) \\ 0 & 0 & 0 \\ \beta_3(\tilde{N}_v-(\tilde{E}_v+\tilde{I}_v)) & \beta_4(\tilde{N}_v-(\tilde{E}_v+\tilde{I}_v)) & 0 \\ 0 & 0 & 0 \\ 0 & 0 & 0 \end{pmatrix}$$

$$\begin{pmatrix} (b_0+b_1\tilde{N}_v)\tilde{E}_v+\beta_2\tilde{I}_v & (b_0+b_1\tilde{N}_v)(\tilde{N}_h-(\tilde{E}_h+\tilde{I}_h+\tilde{R}_h)) & \beta_2(\tilde{N}_h-(\tilde{E}_h+\tilde{I}_h+\tilde{R}_h)) & 0 \\ 0 & 0 & 0 & 0 \\ 0 & 0 & 0 & 0 \\ -d_1 & 0 & 0 & 0 \\ 0 & -(\beta_3\tilde{E}_h+\beta_4\tilde{I}_h)-(\gamma_v+d_2) & -(\beta_3\tilde{E}_h+\beta_4\tilde{I}_h) & (\beta_3\tilde{E}_h+\beta_4\tilde{I}_h) \\ 0 & \gamma_v & -d_2 & 0 \\ 0 & 0 & 0 & -d_2 \end{pmatrix}$$

The derivation of the Jacobian matrix's characteristic polynomial:

$$|J - \lambda I| = 0$$

$$\Rightarrow (d_1 + \lambda)(d_2 + \lambda)\{\lambda^5 + \lambda^4 s_1 + \lambda^3 s_2 + \lambda^2 s_3 + \lambda s_4 + s_5\} = 0 \quad (4.18)$$

where

$$s_1 = a_1 + a_2 + a_3 + a_4 + a_5 + a_6 + d_2,$$

$$s_2 = ((a_4 + a_6)d_2 + a_6\gamma_v) + (a_1 + a_2 + a_3 + a_5)(a_4 + a_6 + d_2) + (a_1a_2 + a_1a_3 + a_1a_5 + a_2a_3 + a_2a_5) + a_7a_8a_9\beta_3 - \gamma_h a_5,$$

$$s_3 = (a_1 + a_2 + a_3 + a_5)((a_4 + a_6)d_2 + a_6\gamma_v) + (a_1a_2a_3 + a_1a_2a_5) + (a_1a_2 + a_1a_3 + a_1a_5 + a_2a_3 + a_2a_5)(a_4 + a_6 + d_2) + a_7a_8\beta_3(a_9d_2 + a_1a_9 + a_2a_9 + \beta_2\gamma_v) + a_7a_8a_9\beta_4 + \gamma_h\xi a_5 - \gamma_h a_5(a_1 + a_4 + a_6 + d_2),$$

$$s_4 = (a_1a_2 + a_1a_3 + a_1a_5 + a_2a_3 + a_2a_5)((a_4 + a_6)d_2 + a_6\gamma_v) + (a_1a_2a_3 + a_1a_2a_5)(a_4 + a_6 + d_2) + \gamma_h\xi a_5(a_4 + a_6 + d_2) + a_7a_8\beta_4(a_9d_2 + a_1a_9 + \beta_2\gamma_v) + a_7a_8\beta_3(a_1a_9d_2 + a_2a_9d_2 + a_1a_2a_9 + a_1\beta_2\gamma_v + a_2\beta_2\gamma_v) - \gamma_h a_5(a_1(a_4 + a_6 + d_2) + (a_4 + a_6)d_2 + a_6\gamma_v),$$

$$s_5 = (a_1a_2a_3 + a_1a_2a_5)((a_4 + a_6)d_2 + a_6\gamma_v) + \gamma_h\xi a_5((a_4 + a_6)d_2 + a_6\gamma_v) + a_7a_8\beta_4(a_1a_9d_2 + \beta_2a_1\gamma_v) + a_7a_8\beta_3(a_1a_2a_9d_2 + a_1a_2\beta_2\gamma_v) - \gamma_h a_5((a_4 + a_6)a_1d_2 + a_1a_6\gamma_v),$$

and

$$a_1 = (d_1 + \delta), a_2 = (d_1 + \xi), a_3 = (d_1 + \gamma_h), a_4 = (d_2 + \gamma_v), a_5 = (b_0 + b_1N_v)E_v + \beta_2 I_v,$$
$$a_6 = (\beta_3 E_h + \beta_4 I_h), a_7 = (N_h - (E_h + I_h + R_h)), a_8 = (N_v - (E_v + I_v)), a_9 = b_0 + b_1N_v.$$

With two negative roots and coefficients ensuring every root contains a true unfavorable portion, the Routh-Hurwitz conditions, $s_i(i = 1,3,4,5) > 0$ and $(s_1s_4 - s_5)(s_1s_2s_3 - s_1^2 - s_3^2 - s_1^2s_4) > s_5(s_1s_2 - s_3)^2 + s_1s_5^2$ are met. In these circumstances, the equilibrium point P_3 exhibits local asymptotic stability.

4.5. Numerical Simulation

Numerical simulations supporting the analytical results stated in Section 4.4 are presented in this section. For this purpose, the Runge-Kutta fourth-order method is used to perform the sensitivity analysis. The data set for case 1 was as follows:

$\beta_1 = 0.00000029$, $\beta_2 = 0.00000021$, $\beta_3 = 0.00000015$, $\beta_4 = 0.00000009$, $d_1 = 0.00012$, $d_2 = 0.0085$, $\Lambda_1 = 0.00012$, $\Lambda_2 = 0.0085$, $\delta = 0.00146$, $\xi = 0.0085$, $\gamma_h = 0.012$, $\gamma_v = 0.015$, $A = 12$ and initial values are:

$E_h = 500$, $I_h = 4181.8$, $R_h = 209.2$, $N_h = 20000$, $E_v = 14000$, $I_v = 30000$, $N_v = 963400$

which draw inspiration from Hazarika and Bhattacharjee (2011) as well as Ghosh *et al.*, (2005).

In a similar vein, the parameter values for case 2 are determined as follows:

$b_0 = 0.00012$, $b_1 = 0.00000006$, $\beta_2 = 0.00000021$, $\beta_3 = 0.000024$, $\beta_4 = 000000009$,

$d_1 = 0.00012$, $d_2 = 0.0085$, $\Lambda_1 = 0.00012$, $\Lambda_2 = 0.00085$, $\delta = 0.000146$, $\xi = 0.012$,

$\gamma_h = 0.012$, $\gamma_v = 0.015$, $A = 10$ and initial values are:

$E_h = 50$, $I_h = 101.5$, $R_h = 10.9$, $N_h = 402.8$, $E_v = 300$, $I_v = 602.3$, $N_v = 1188.8$

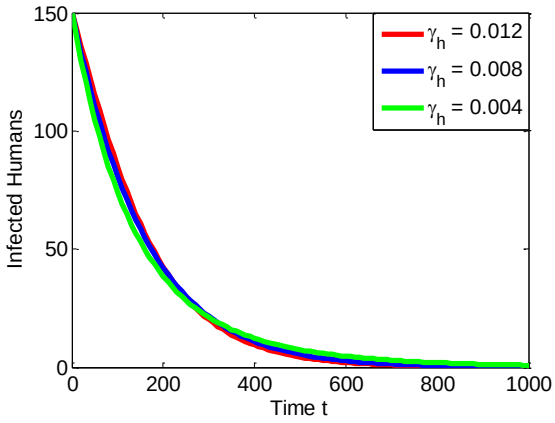

Figure 4.2: Variant in the proportion of I_h for different progression rates γ_h.

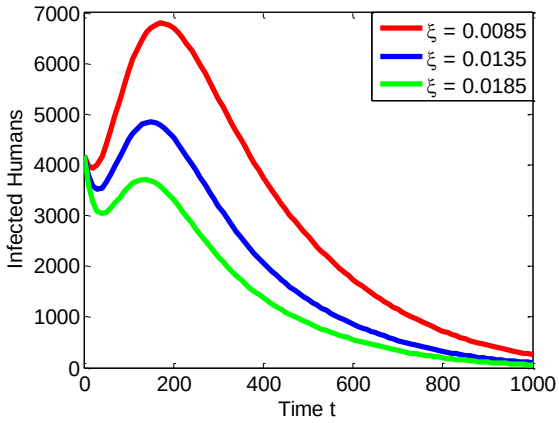

Figure 4.3: Variant in the proportion of I_h for different recovery rates ξ.

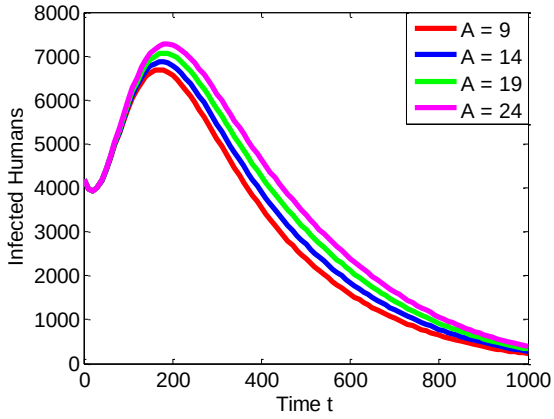

Figure 4.4: Variant in the proportion of I_h for different immigration constant A.

The impact of the progression rate, denoted as γ_h, on the infected human population I_h is illustrated in Figure 4.2. Firstly, when γ_h is lower, the corresponding infected human inhabitants is also lower. However, with the passage of time the influence of γ_h on I_h under goes a reversal. Figure 4.3 demonstrates that an increase in the recovery rate ξ leads to a decrease in I_h.

Figure 4.4 illustrates the influence of the immigration constant A on the contaminated human inhabitants I_h. As A increases, I_h also shows an increase. Additionally, I_h rises with a higher

rate of immunity loss among recovered humans, represented by the parameter δ as depicted in Figure 4.5.

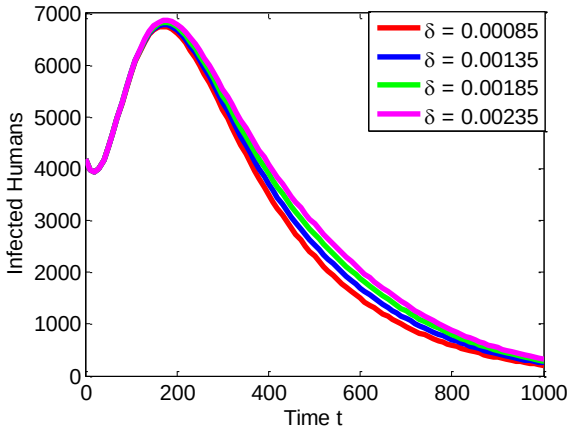

Figure 4.5: Variant in the proportion of I_h for different immunity loss δ.

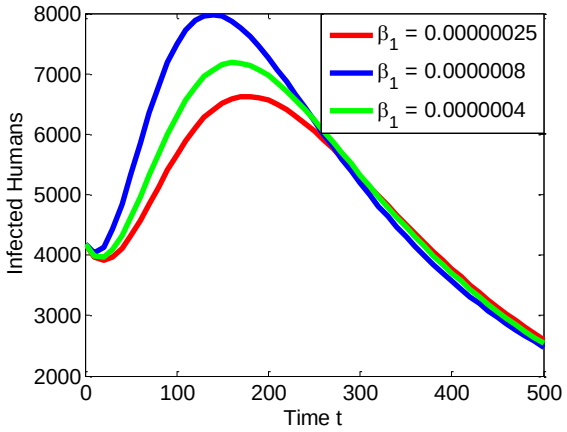

Figure 4.6: Variant in the proportion of I_h for different interaction coefficient β_1.

Figure 4.6 displays the plot of I_h against different values of β_1, indicating the degree to which exposed mosquitoes and susceptible humans interact. The trend indicates that an augmentation in β_1 results in an increase in I_h. Similarly, in Figure 4.7, I_h is graphed against various values of β_2, indicating the degree to which infected mosquitoes and susceptible humans interact. Notably, β_2 follows a comparable trend to β_1 concerning its impact on I_h.

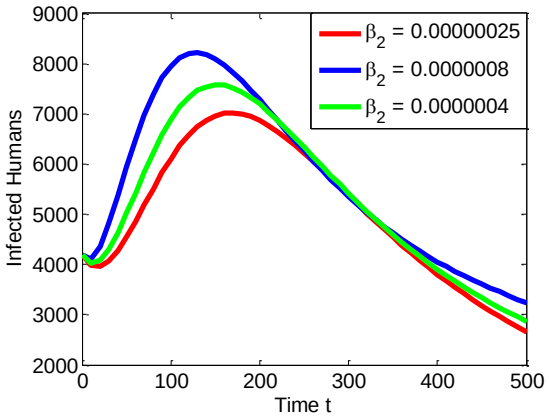

Figure 4.7: Variant in the proportion of I_h for different interaction coefficient β_2.

The Figure 4.8 illustrates the dynamic changes in infection and immunity over time. Initially, the infected human population undergoes an increase, followed by a gradual decrease as time progresses. This pattern is attributed to the non-linear terms incorporated into the model. Conversely, the proportion of recovered humans shows an upward trend. This is attributed to the significant raise in the recovery rate when medicinal care is administered to infected individuals.

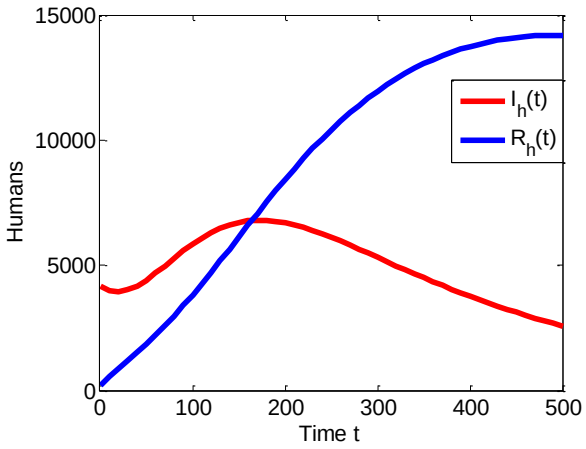

Figure 4.8: Variant in the infective and recovered human population.

The exploration of case 2, wherein β_1 is defined as $\beta_1 = b_0 + b_1 N_v$, is depicted in Figures 4.9 to 4.12. Figure 4.9 demonstrates that a reduction in γ_v leads to an augmentation in I_h.

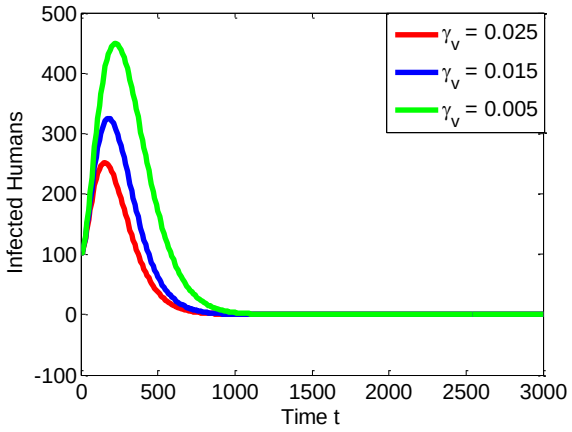

Figure 4.9: Variant in the proportion of I_h for different progression rate γ_v.

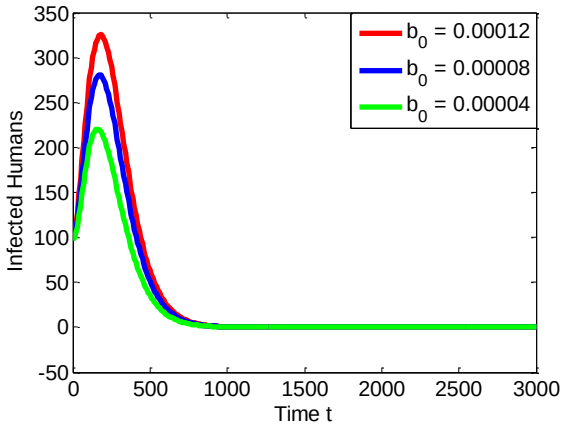

Figure 4.10: Variant in the proportion of I_h for different values b_0.

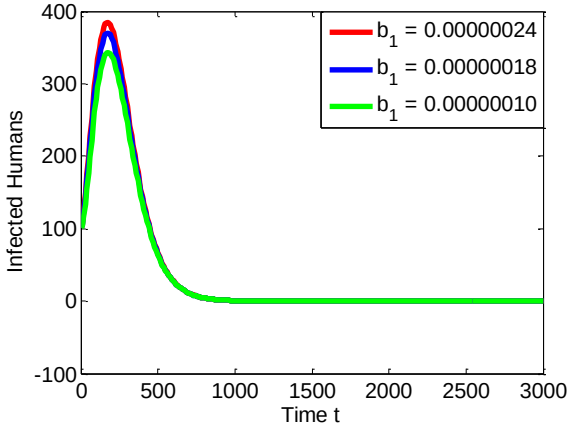

Figure 4.11: Variant in the proportion of I_h for different values b_1.

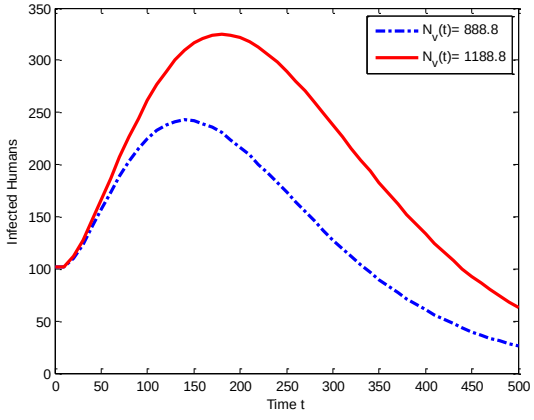

Figure 4.12: Variant in the proportion of I_h for different values N_v.

Figures 4.10 and 4.11 portray the changes in I_h concerning b_0 and b_1. These figures illustrate that the infected human population rises with an increase in both b_0 and b_1. The relationship is further presented in Figure 4.12 for two different values of $N_v(t)$ (888.8, 1188.8). It is observed that when N_v is high, I_h is also high, which is intuitively evident.

4.6. Summary and Concluding Remarks

The dynamics of a malaria epidemic, accounting for human beings and vector populations, were simulated using the SEIRS model that we introduced in this chapter. Our model included an exposed class for both human and mosquito populations, allowing us to gain a more comprehensive understanding of the disease's dynamics.

One of the critical determinants of malaria spread is the transmission coefficient between the human population and infected mosquitoes. Through our numerical analysis, we have uncovered significant insights. We observed that as the immigration constant A and the human population with impunity dropping increase, the number of contaminated persons also rises. These findings are vividly depicted in Figures 4.4 and 4.5, emphasizing the urgency of addressing these factors in malaria control efforts.

In conclusion, our study underscores the essential need for effective control strategies against the malaria vector, which plays a pivotal role in disease outbreaks. Implementing measures such as a robust drainage system and the strategic use of insecticides can substantially contribute to the diminution and control of the mosquito population, thereby curbing the transmission of malaria. These strategies are vital steps towards minimizing the effect of this devastating ailment on human inhabitants.

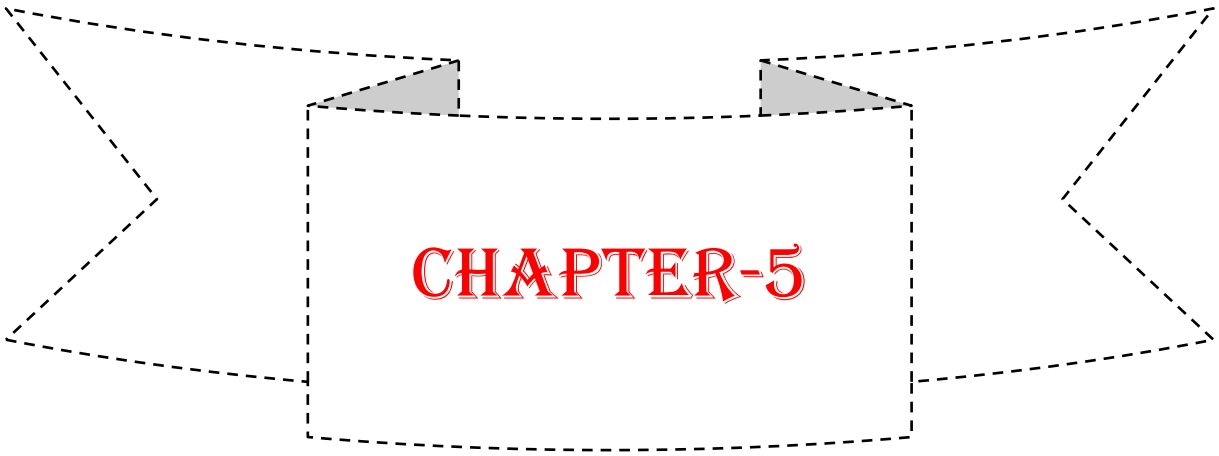

The Study of Dengue Transmission Dynamics through the SEIR Model

Keywords: Transmission Dynamics, Dengue Fever, Disease Free Equilibrium and Stability Analysis.

Chapter 5: The Study of Dengue Transmission Dynamics through the SEIR Model

5.1. Introduction

Dengue, a viral disease transmitted primarily by mosquitoes, stands as a significant global public health concern. This pervasive illness affects over 50% of the global population and poses a substantial threat, potentially leading to severe symptoms and, in rare instances, fatalities. Understanding the complex dynamics of dengue transmission becomes imperative in combating its spread and devising effective control measures. Mathematical models emerge as indispensable tools in unraveling the intricate transmission patterns of dengue, serving as the cornerstone for devising comprehensive strategies aimed at disease containment and prevention. Within the landscape of mathematical modeling, the SEIR (Susceptible-Exposed-Infectious-Recovered) model stands as a pivotal framework for exploring the transmission dynamics of dengue. This chapter extensively delves into the intricacies of the SEIR model, specifically tailored to dissect the transmission patterns of dengue. Emphasizing the multifaceted nature of disease propagation, this model incorporates a logistic function, shedding light on the growth and stability of mosquito populations-an essential factor in the dissemination of the disease. Moreover, the computation of the fundamental reproduction number within this model serves as a critical indicator, elucidating the potential for disease spread within populations.

Beyond the immediate quantification of disease spread, this analysis extends its purview to evaluate the stability of both endemic and disease-free equilibria, offering a glimpse into the long-term behavior of the dengue transmission system. By unraveling the intricate interplay between susceptible, exposed, infectious and recovered individuals within populations, this examination aims to provide not only a snapshot of disease transmission but also valuable insights into the underlying dynamics dictating the ebb and flow of dengue spread.

The significance of these findings lies in their potential to inform and guide the formulation of effective strategies aimed at controlling and preventing the spread of dengue. By synthesizing mathematical rigor with epidemiological insights, this chapter endeavors to offer actionable perspectives that can be instrumental in guiding policymakers, healthcare practitioners, and public health organizations towards implementing targeted interventions and surveillance measures. Ultimately, the overarching goal remains the mitigation of dengue's burden on global health and the enhancement of strategies to protect vulnerable communities from the perils of this viral disease.

In this chapter, we introduce a mathematical model to examine the transmission dynamics of dengue fever. The chapter is structured as follows: Section 5.2 provides a detailed literature and Section 5.3 outlines the model description, system equations, and fundamental properties. Section 5.4 conducts stability analysis, while Section 5.5 presents numerical results to support our model. In Section 5.6, we summarize key findings and highlight future research directions.

5.2. Literature Review

A substantial body of work in disease transmission modeling has yielded valuable insights into various aspects of disease dynamics and the influence of climate factors. Notable among these contributions are the works of J. P. LaSalle (1976), whose comprehensive exploration of stability analysis for dynamical systems serves as a fundamental reference for researchers and practitioners. Singh *et al.,* (2019) present an arithmetical framework that embraces the influence of the mosquito inhabitants in the transmission of malaria, contributing to a greater insight into jungle fever vitals and the effectiveness of vector control strategies. Similarly, Singh *et al.,* (2016) put forward an outbreak representation that examined the transference vital of HIV/AIDS, incorporating various latent stages. The study specifically concentrated on assessing the consequences of treatment, thereby making a valuable contribution to our comprehension of the influence of treatment interventions on the dissemination of the disease. Additionally, Van den Driessche and Watmough (2002) delved into the implications of reproduction numbers for disease transmission models, examining sub-threshold endemic equilibria and offering insights into the stability of endemic & disease-free states within compartmental models.

Building upon this substantial body of work in disease transmission modeling, several researchers have furthered our understanding of the complex interplay between disease dynamics and climate factors. Bal and Sodoudi (2020), in their study focused on dengue occurrences in Kolkata, India and skillfully integrated climate variables into their model, enabling an enhanced grasp of the transmission dynamics of dengue and thus enhancing our knowledge of the intricate relationship between climate and disease spread. In a similar vein, Baylis (2017) investigated the possible effects of weather change on various diseases spread by vectors, emphasizing the critical need to account for climate change effects when assessing the risks and emergence of infectious diseases. Benedum *et al.,* (2018) delved into the statistical modeling of rainfall's effect on dengue transmission in Singapore. Their in-depth analysis of the relationship between rainfall patterns and dengue transmission provided critical insights into the role of environmental variables play in this disease's epidemiology.

In addition, Bhatt *et al.,* (2013) conducted a comprehensive analysis of the worldwide dispersal and load of dengue fever, offering a comprehensive overview of the geographic distribution, incidence and public health impact of dengue, thereby contributing to our understanding of the global epidemiology of the disease. Moreover, Butterworth *et al.,* (2017) investigated the potential implications of varying atmospheric conditions on the transference of dandy fever in the southeastern United States, projecting future changes in transmission dynamics through climate modeling. This work illuminated the vulnerability of the region to climate-driven shifts in disease risk. In a similar vein, Caldwell *et al.*, (2021) investigated the intricate interactions between two continent's worth of mosquito-borne disease dynamics and climate. Their comprehensive analysis of climate variables aimed to unravel the geographic and temporal variations in disease transmission, underscoring the crucial role of climate in influencing disease patterns. Davis *et al.,* (2021) developed a topical index for assessing favorable circumstances, seeking to predict how the dengue virus may adapt to changing climatic conditions. Their innovative modeling approach incorporated climate variables to assess potential changes in vector-borne disease transmission, providing crucial insights into the future implications of weather change on dengue dynamics. Moreover, Ebi and Nealon (2016) conducted a comprehensive review to examine the multifaceted effect of weather swaps on dandy fever. Their study explored the intricate interactions between climate factors and dengue transmission, underscoring the necessity of considering climate change effects when developing strategies for disease prevention and control.

Moreover, Gutierrez *et al.,* (2022) focused their investigation on meteorological indicators associated with dengue epidemics in non-endemic Northwest Argentina. Their study delved into the intricate relationship between meteorological factors and dengue outbreaks, providing valuable insights into the role of weather conditions in dandy fever transference dynamics within a non-endemic region. Huber *et al.,* (2018) undertook an exploration of the impact of periodic weather condition disparity on the suitability of climate for the transference vital of Chikungunya, Zika, & Dengue fever. The study underscored the paramount importance of temperature as a key factor in determining the appropriateness of the transmission of diseases spread by vectors. Similarly, Kakarla *et al.,* (2020) focused on the dengue condition in India and created a model that could be used to determine appropriateness and potential for transmission under both the existing and anticipated scenarios of climate change. Their research yielded priceless insights into how weather change can influence the complex dynamics of dengue transmission in India. In addition, Liu-Helmersson *et al.,* (2016) engaged

in the critical task of projecting dengue transmission in Europe under climate change situations, bringing to the forefront the potential future risks of dengue transmission in Europe, driven by changing climatic conditions and the expansion of Aedes vectors. Marino *et al.,* (2008) concentrated mostly on sensitivity analysis and global uncertainty in systems biology, their methodology although not directly related to dengue offers a valuable approach to understanding and quantifying uncertainties within dengue transmission models. Furthermore using mechanistic models, Mordecai *et al.,* (2017) investigated the consequence of the Kelvin scale on the increase of Chikungunya, Zika, & Dengue fever. Their research deepened our understanding of the association between climate and illness by offering profound insights into the complex interactions between temperature, vector dynamics, and disease transmission. Morin *et al.,* (2013) took an in-depth look at the evidence and implications of climate on dengue transmission, providing a complete analysis of the existing literature on the intricate relationship among weather and dengue and highlighting the pivotal role of climate factors in influencing disease transmission dynamics. Furthermore, Ngonghala *et al.,* (2021) explored the impacts of temperature changes on zika dynamics and control, shedding light on the significance of considering temperature variations when assessing the effectiveness of control strategies for zika and other vector-borne diseases. Collectively, the aforementioned studies have significantly contributed to the advancement of our understanding of the complex mechanisms of disease transmission within the framework of climate change.

Continuing our exploration of the intricate connection among climate and disease transmission, Nuraini *et al.,* (2021) introduced a dengue model based on climate in Indonesia, Semarang, focusing on predicting and analyzing dengue transmission dynamics using climate data. Their findings provided critical insights into the connection between climate variables and dengue occurrences in the study area, contributing to our understanding and prediction of dengue outbreaks in Indonesia. In a broader context, Okais *et al.,* (2010) discussed the methodology of sensitivity analysis for modeling infectious diseases, underscoring the importance of sensitivity analysis in evaluating the robustness and reliability of disease models. This work presented methods and approaches valuable for understanding and quantifying uncertainties in dengue transmission models. Similarly, Okuneye and Gumel (2017) explored a model for malaria transmission dynamics that considered temperature and rainfall dependencies. Their study provided valuable insights into the mathematical modeling of temperature and rainfall effects on disease transmission, contributing to our understanding of climate-driven dynamics in vector-borne diseases, including dengue. The zika virus outbreak in

Brazil was examined by Sadeghieh *et al.,* (2021) in light of both the present and the future environment, offering insights into how the dynamics of disease transmission are contaminated by climate crises. Their research contributes to the expansion of our grip regarding the possible consequences of weather pattern variation on the dissemination and propagation of illnesses facilitated by vectors, such as dengue. Wang *et al.,* (2022) explore the ramifications of severe meteorological phenomena on the occurrence of dengue fever in four nations of the Asian continent, providing valuable perspectives on the association between extraordinary atmospheric events and the prevalence of dengue infection. Williams *et al.,* (2016) provided predictions indicating both heightened and reduced occurrences of dengue under diverse weather transformation scenarios. Finally, Xu *et al.,* (2020) projected future dengue under climate change scenarios, addressing existing knowledge and uncertainties regarding the effect of weather transformation on dengue dynamics. This literature review highlights various studies contributions, covering stability analysis, disease spread models, co-infection dynamics, environmental factors, climate change impacts and mathematical modeling. Collectively, these studies offer a thorough comprehension of the intricate interactions between climate, vectors, and disease dynamics in dengue transmission. Further research is crucial to address remaining uncertainties, enhance modeling approaches, and create efficient plans for controlling and preventing dengue.

5.3. Model Description

In the proposed work, it is going to be analyzed the population dynamics for the spread of dengue disease using the SEIR model. The overall population is categorized into two distinct groups: the human population and the vector population. The total human population is represented by $N_h(t)$ and is further subdivided into four classes: susceptible humans (S_h), exposed humans (E_h), infected humans (I_h) and recovered humans (R_h). Also, the overall vector population at time t is represented by $N_v(t)$ and subdivided into three classes, namely, the susceptible vector (S_v), exposed vector (E_v) and infected vector (I_v).

In this model, we assume that individuals enter the susceptible human class through processes like birth. Upon being bitten by an infected vector, a susceptible human undergoes the stages of exposure and subsequent infection at variable rates. Recovered individuals emerge from the infected class after a specified duration.

Similarly, susceptible vectors are introduced into the population at a certain rate. The vector initially shifts to the exposed class, and over time, individuals progress from the exposed class to the infected class.

Susceptible human populations are recruited at a rate $\left(\lambda - \frac{\gamma N_h}{k}\right)N_h$, where λ is the birth rate, γ is the growth rate and k is the carrying capacity of the human population. Susceptible humans get the virus from an infected vector following an effective constant at the rate $\frac{b\beta_1 I_v S_h}{N_h}$. It is likely that the dengue virus will infect humans through its vector population, represented by number β_1.

Susceptible mosquitoes recruited at rate A and become infectious at rate $\frac{b\beta_2 I_h S_v}{N_h}$ after being contacted by infected humans. The likelihood that the dengue virus will spread through humans into the mosquito population is shown by β_2. ξ_h represents a development rate from exposed class E_h to contaminated class I_h and ξ_v represents a development rate from exposed class E_v to contaminated class I_v. The improvement rate for the human population is δ_h. μ_h denotes the inherent death estimate within the person inhabitants and μ_v represents the inherent death estimate within the vector population. Figure 5.1 illustrates the transmission diagram for the dengue fever model.

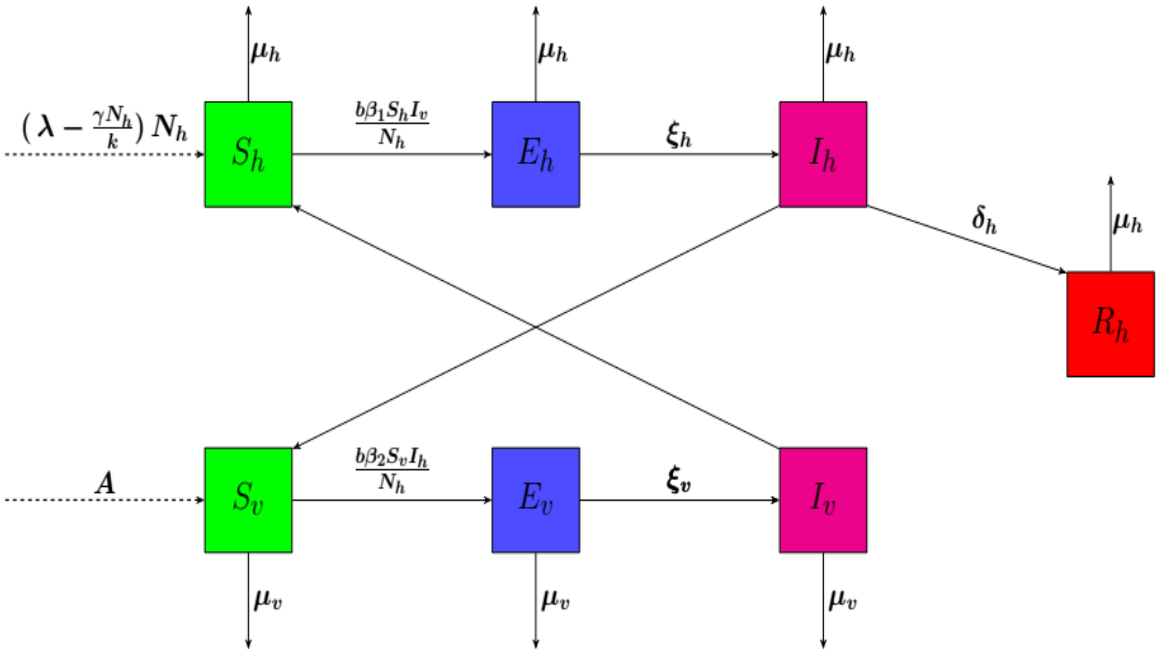

Figure 5.1: Transmission dynamic diagram.

5.3.1. Governing Equations

The model's governing differential equations are formulated by taking into account the relevant inflow and outflow rates for each compartment.

(I) Human population

$$S_h' = \left(\lambda - \frac{\gamma N_h}{k}\right)N_h - \left(\frac{b\beta_1 I_v}{N_h} + \mu_h\right)S_h$$

$$E_h' = \frac{b\beta_1 I_v}{N_h} S_h - (\xi_h + \mu_h) E_h \qquad (5.1)$$

$$I_h' = \xi_h E_h - (\delta_h + \mu_h)\, I_h$$

$$R_h' = \delta_h I_h - \mu_h R_h$$

(II) Vector population

$$S_v' = A - \left(\mu_v + \frac{b\beta_2 I_h}{N_h}\right)S_v$$

$$E_v' = \frac{b\beta_2 I_h}{N_h} S_v - (\xi_v + \mu_v)E_v \qquad (5.2)$$

$$I_v' = \xi_v E_v - \mu_v I_v$$

with initial conditions;

$S_h(t) \geq 0, E_h(t) \geq 0, I_h(t) \geq 0, R_h(t) \geq 0, S_v(t) \geq 0, E_v(t) \geq 0, I_v(t) \geq 0$.

Therefore the total human population and vector population is given by

$N_h = S_h + E_h + I_h + R_h \Rightarrow R_h = N_h - S_h - E_h - I_h$ and

$$N_v = S_v + E_v + I_v = \frac{A}{\mu_v} \Rightarrow S_v = \frac{A}{\mu_v} - E_v - I_v.$$

The system of equations (5.1) and (5.2) can be simplified by letting

$s_h = S_h N_h^{-1}, e_h = E_h N_h^{-1}, i_h = I_h N_h^{-1}, r_h = R_h N_h^{-1}, s_v = S_v N_v^{-1}, e_v = E_v N_v^{-1}$ and

$$i_v = I_v N_v^{-1}. \qquad (5.3)$$

Differentiating the above system of equations (5.3), w.r.t. time

$$\frac{ds_h}{dt} = \frac{1}{N_h}\left(\frac{dS_h}{dt} - s_h \frac{dN_h}{dt}\right) = \lambda - \frac{\gamma N_h}{k} - nb\beta_1 s_h i_v - \gamma\left(1 - \frac{N_h}{k}\right)s_h - \mu_h s_h$$

$$\frac{de_h}{dt} = \frac{1}{N_h}\left(\frac{dE_h}{dt} - e_h\frac{dN_h}{dt}\right) = nb\beta_1 s_h i_v - (\mu_h + \xi_h)e_h - \gamma\left(1 - \frac{N_h}{k}\right)e_h$$

$$\frac{di_h}{dt} = \frac{1}{N_h}\left(\frac{dI_h}{dt} - i_h\frac{dN_h}{dt}\right) = \xi_h e_h - (\mu_h + \delta_h)i_h - \gamma\left(1 - \frac{N_h}{k}\right)i_h$$

$$\frac{dr_h}{dt} = \frac{1}{N_h}\left(\frac{dR_h}{dt} - r_h\frac{dN_h}{dt}\right) = \delta_h i_h - \mu_h r_h - \gamma\left(1 - \frac{N_h}{k}\right)r_h$$

$$\frac{ds_v}{dt} = \frac{1}{N_v}\left(\frac{dS_v}{dt} - s_v\frac{dN_v}{dt}\right) = \mu_v - b\beta_2 s_v i_h - \mu_v s_v$$

$$\frac{de_v}{dt} = \frac{1}{N_v}\left(\frac{dE_v}{dt} - e_v\frac{dN_v}{dt}\right) = b\beta_2 s_v i_h - (\mu_v + \xi_v)e_v$$

$$\frac{di_v}{dt} = \frac{1}{N_v}\left(\frac{dI_v}{dt} - i_v\frac{dN_v}{dt}\right) = \xi_v e_v - \mu_v i_v$$

Hence, the simplified system of equations becomes

$$\frac{ds_h}{dt} = \lambda - \gamma\alpha - nb\beta_1 s_h i_v - \gamma(1-\alpha)s_h - \mu_h s_h$$

$$\frac{de_h}{dt} = nb\beta_1 s_h i_v - (\mu_h + \xi_h)e_h - \gamma(1-\alpha)e_h$$

$$\frac{di_h}{dt} = \xi_h e_h - (\mu_h + \delta_h)i_h - \gamma(1-\alpha)i_h$$

$$\frac{dr_h}{dt} = \delta_h i_h - \mu_h r_h - \gamma(1-\alpha)r_h \qquad (5.4)$$

$$\frac{ds_v}{dt} = \mu_v - b\beta_2 s_v i_h - \mu_v s_v$$

$$\frac{de_v}{dt} = b\beta_2 s_v i_h - (\mu_v + \xi_v)e_v$$

$$\frac{di_v}{dt} = \xi_v e_v - \mu_v i_v$$

where, $\alpha = \frac{N_h}{k}$

5.3.2. Basic Properties

In this portion, we explore essential principles that are pivotal for the subsequent mathematical examination of the provided model.

5.3.2.1. Invariant Region

Considering the replica tracking of swap in the person inhabitants, we assume all variables are changeable and constructive for $t \geq 0$. Thus, the structure of calculations (5.4) is analyzed within a biologically relevant and feasible region denoted as Ω. The following lemma outlines the feasible region for the system (5.4).

Lemma 5.3.1: The solution of the simplified model structure (5.4) is contained in the region $\Omega = \Omega_h \cup \Omega_v \subset \Re_+^4 \times \Re_+^3$.

Proof: To demonstrate that in a proper subset of $\Omega \subset \Re_+^4 \times \Re_+^3$, all possible solutions are uniformly bounded**.** Splitting the system into a human component n_h and a vector component n_v such that $n_h = s_h + e_h + i_h + r_h = 1$ and $n_v = s_v + e_v + i_v = 1$ (5.5)

Consider any solution $\{s_h, e_h, i_h, r_h\}$ in $\Re_+^4$ with non negative initial conditions. By applying Birkhoff and Rota's theorem (1989) to differential inequalities, it can be inferred that

$\lim_{t\to\infty} S_h(t) \leq 1$ (5.6)

It is also similar for the solution of the vector population. $\{s_v, e_v, i_v\} \in \Re_+^3$ that

$\lim_{t\to\infty} S_v(t) \leq 1$ (5.7)

From the system of equation (4), we have:

$n_h' = s_h' + e_h' + i_h' + r_h'$, $n_h' = 0$

Integrating, we get $\Rightarrow n_h = k_1$, where k_1 constant. But, from $n_h = s_h + e_h + i_h + r_h = 1$, it follows that $k_1 = 1$.

Hence; $\Omega_h = \{(s_h, e_h, i_h, r_h) \in \Re_+^4 : s_h + e_h + i_h + r_h = 1\}$.

Similarly: $n_v' = s_v' + e_v' + i_v'$, $n_v' = 0$.

Integrating, we get $\Rightarrow n_v = k_2$. Also, from $n_v = s_v + e_v + i_v = 1$, it follows that $k_2 = 1$.

Hence; $\Omega_v = \{(s_v, e_v, i_v) \in \Re_+^3 : s_v + e_v + i_v = 1\}$.

As a result, we can affirm that the region Ω remains positively invariant, confirming that

the model is well-defined and holds biological significance. Consequently, we can focus on the dynamics produced by the simplified model (5.4) within the Ω region.

5.3.2.2. Positivity of Solutions

Lemma 5.3.2: With the initial conditions proposed in the model to lie in Ω, where

$$\Omega = \left\{ \left(s_h, e_h, i_h, r_h, s_v, e_v, i_v \right) \in \Re_+^7 : s_h \geq 0, e_h \geq 0, i_h \geq 0, r_h \geq 0, s_v \geq 0, e_v \geq 0, i_v \geq 0 \right\}.$$

Then the solution set $\left\{ s_h(t), e_h(t), i_h(t), r_h(t), s_v(t), e_v(t), i_v(t) \right\}$ of the simplified model system (4) is positive for all time $t \geq 0$.

Proof: By using the simplified model structure (5.4), from the first equation we have

$$\frac{ds_h}{dt} = \lambda - \gamma\alpha - nb\beta_1 s_h i_v - \gamma(1-\alpha)s_h - \mu_h s_h$$

$$= \lambda - \gamma\alpha - nb\beta_1 s_h i_v - \gamma s_h - \gamma\alpha s_h - \mu_h s_h$$

$$\geq -(\gamma + \mu_h)s_h$$

Integration with initial condition, we have

$$t = 0, s(0) = s_0$$

$$s_h(t) \geq s_h(0)e^{-(\gamma+\mu_h)t} \geq 0$$

The second equation of the simplified model system (5.4), we have

$$\frac{de_h}{dt} = nb\beta_1 s_h i_v - (\mu_h + \xi_h)e_h - \gamma(1-\alpha)e_h$$

$$= nb\beta_1 s_h i_v - \mu_h e_h - \xi_h e_h - \gamma e_h - \gamma\alpha e_h$$

$$\geq -(\gamma + \mu_h + \xi_h)e_h$$

Integrating with initial condition, we have

$$t = 0,\ e(0) = e_0$$

$$e_h(t) \geq e_h(0)e^{-(\gamma+\mu_h+\xi_1)t} \geq 0$$

Similarly, the remaining equations of the simplified system (5.4) are also positive $\forall\ t > 0$. Thus if we consider the third equation

$$\frac{di_h}{dt} = \xi_h e_h - (\mu_h + \delta_h)i_h - \gamma(1-\alpha)i_h$$

$$= \xi_h e_h - \mu_h i_h - \delta_h i_h - \gamma i_h - \alpha i_h$$

$$\geq -(\gamma + \mu_h + \delta_h) i_h$$

The integration will gives $i_h(t) \geq i_h(0) e^{-(\gamma+\mu_h+\delta_h)t} \geq 0$.

Now we consider the fourth equation

$$\frac{dr_h}{dt} = \delta_h i_h - \mu_h r_h - \gamma r_h + \gamma \alpha r_h$$

$$\geq -(\gamma + \mu_h) r_h$$

The integration will gives $r_h(t) \geq r_h(0) e^{-(\gamma+\mu_h)t} \geq 0$.

Also

$$\frac{ds_v}{dt} = \mu_v - b\beta_2 s_v i_h - \mu_v s_v \geq -\mu_v s_v$$

The integration will gives $s_v(t) \geq s_v(0) e^{-\mu_v t} \geq 0$.

and

$$\frac{de_v}{dt} = b\beta_2 s_v i_h - (\mu_v + \xi_v) e_v \geq -(\mu_v + \xi_v) e_v$$

The integration will gives $e_v(t) \geq e_v(0) e^{-(\mu_v+\xi_v)t} \geq 0$.

Lastly;

$$\frac{di_v}{dt} = \xi_v e_v - \mu_v i_v \geq -\mu_v i_v$$

The integration will gives $i_v(t) \geq i_v(0) e^{-\mu_v t} \geq 0$.

Therefore the solution set $\{s_h(t), e_h(t), i_h(t), r_h(t), s_v(t), e_v(t), i_v(t)\}$ of the simplified model system (5.4) is positive for all time $t \geq 0$.

5.4. Analysis of the Model

This segment is dedicated to computing the symmetry states, particularly the disease-free equilibrium (DFE) and the endemic equilibrium (EE). Additionally, we conduct a firmness examination by calculating the fundamental reproduction number.

5.4.1. Disease Free Equilibrium (DFE) and Basic Reproduction Number

The simplified system of equation (5.4) has a disease free equilibrium given by

$$E_0 = \left(s_h^0, e_h^0, i_h^0, r_h^0, s_v^0, e_v^0, i_v^0\right) = (1,0,0,0,1,0,0)$$

The assessment of the direct firmness of the ailment-free symmetry state relies on the procreation figure, following the methodology outlined in Anderson and May (1988). To delve into the regional firmness of this symmetry, we employ the next-generation concept, as elucidated by Alexander *et al.,* (2005) and Mushayabasa *et al.,* (2011). To facilitate this, we introduce matrices F^* and V^*, designed to introduction recently developed infections and the transition of persons out of contaminated sections. The derivations proceed as follows:

$$F^* = \begin{pmatrix} nb\beta_1 s_h i_v \\ \xi_h e_h \\ b\beta_2 s_v i_h \\ \xi_v e_v \end{pmatrix} \quad \text{and} \quad V^* = \begin{pmatrix} \gamma(1-\alpha)e_h + (\xi_h + \mu_h)e_h \\ \gamma(1-\alpha)i_h + (\delta_h + \mu_h)i_h \\ (\xi_v + \mu_v)e_v \\ \mu_v i_v \end{pmatrix}$$

Once the partial derivatives of F^* and V^* at E_0 are calculated, the corresponding matrices are

$$F = \begin{pmatrix} 0 & 0 & 0 & nb\beta_1 \\ \xi_h & 0 & 0 & 0 \\ 0 & b\beta_2 & 0 & 0 \\ 0 & 0 & \xi_v & 0 \end{pmatrix} \text{ and}$$

$$V = \begin{pmatrix} \gamma(1-\alpha)+(\xi_h + \mu_h) & 0 & 0 & 0 \\ 0 & \gamma(1-\alpha)+(\delta_h + \mu_h) & 0 & 0 \\ 0 & 0 & (\xi_v + \mu_v) & 0 \\ 0 & 0 & 0 & \mu_v \end{pmatrix}$$

Consider the following matrix

$$FV^{-1} = \begin{pmatrix} 0 & 0 & 0 & \dfrac{nb\beta_1}{\gamma(1-\alpha)+(\xi_h + \mu_h)} \\ \dfrac{\xi_h}{\gamma(1-\alpha)+(\delta_h + \mu_h)} & 0 & 0 & 0 \\ 0 & \dfrac{b\beta_2}{(\xi_v + \mu_v)} & 0 & 0 \\ 0 & 0 & \dfrac{\xi_v}{\mu_v} & 0 \end{pmatrix}$$

Thus the reproduction number R_0, is obtained as

$$R_0 = \sqrt{\frac{n\, b^2\, \xi_h\, \xi_v \beta_1\, \beta_2}{((1-\alpha)\gamma + (\delta_h\ +\ \mu_h))((1-\alpha)\gamma + (\xi_h\ +\ \mu_h))(\xi_v\ +\ \mu_v)\mu_v}}. \tag{5.8}$$

5.4.2. Local Stability of Disease-Free Equilibrium

In this segment, we consider the local stability of the DFE. They are presented in Theorem 5.4.1.

Theorem 5.4.1: The local asymptotic stability of the disease-free equilibrium E_0 in the system (5.4) is established when $R_0 < 1$, and it becomes unstable otherwise.

Proof: The Jacobian matrix of the model system (5.4) at E_0 is given by

$$J(E_0) = \begin{pmatrix} -\gamma(1-\alpha)-\mu_h & 0 & 0 & 0 & 0 & 0 & -nb\beta_1 \\ 0 & -\gamma(1-\alpha)-(\xi_h+\mu_h) & 0 & 0 & 0 & 0 & nb\beta_1 \\ 0 & \xi_h & -\gamma(1-\alpha)-(\delta_h+\mu_h) & 0 & 0 & 0 & 0 \\ 0 & 0 & \delta_h & -\gamma(1-\alpha)-\mu_h & 0 & 0 & 0 \\ 0 & 0 & -b\beta_2 & 0 & -\mu_v & 0 & 0 \\ 0 & 0 & b\beta_2 & 0 & 0 & -(\xi_v+\mu_v) & 0 \\ 0 & 0 & 0 & 0 & 0 & \xi_v & -\mu_v \end{pmatrix}$$

Trace $[J(E_0)] = -(2\mu_v + a_1 + a_2 + a_3 + a_4 + a_5) < 0$

where, $a_1 = -[\gamma(1-\alpha) + \mu_h]$, $a_2 = -[\gamma(1-\alpha) + (\mu_h + \xi_h)]$, $a_3 = -[\gamma(1-\alpha) + (\mu_h + \delta_h)]$,

$a_4 = -[\gamma(1-\alpha) + \mu_h]$, and $a_5 = -(\mu_v + \xi_v)$.

$$\text{Det}[J(E_0)] = \left(-\gamma(1-\alpha) - \mu_h - \lambda\right)^2 \left(-\mu_v - \lambda\right) \begin{bmatrix} \left(\gamma(1-\alpha) + (\mu_h + \xi_h) + \lambda\right)\left(\gamma(1-\alpha) + (\mu_h + \delta_h) + \lambda\right) \\ \left((\mu_v + \xi_v) + \lambda\right)\left(\mu_v + \lambda\right) - nb^2\beta_1\beta_2\xi_h\xi_v \end{bmatrix}.$$

For $\text{Det}[J(E_0)] > 0$,

$$\Rightarrow \left[\left(\gamma(1-\alpha) + (\mu_h + \xi_h) + \lambda\right)\left(\gamma(1-\alpha) + (\mu_h + \delta_h) + \lambda\right)\left((\mu_v + \xi_v) + \lambda\right)\left(\mu_v + \lambda\right) - nb^2\beta_1\beta_2\xi_h\xi_v\right] > 0,$$

$$\Rightarrow \frac{nb^2\, \xi_h\, \xi_v\, \beta_1\, \beta_2}{\left(\gamma(1-\alpha) + (\xi_h + \mu_h) + \lambda\right)\left(\gamma(1-\alpha) + (\delta_h + \mu_h) + \lambda\right)\left((\xi_v + \mu_v) + \lambda\right)\left(\lambda + \mu_v\right)} < 1,$$

$$\Rightarrow \mathrm{R}_0^2 < 1 \Rightarrow R_0 < 1.$$

This shows that the disease free equilibrium point E_0 is locally asymptotically stable if $R_0 < 1$, otherwise unstable.

5.4.3. Global Stability of Disease-Free Equilibrium

In this segment, we assess worldwide firmness by applying a comparison theorem outlined in Lakshmikantham *et al.*, (1989) and Mushayabasa *et al.*, (2011).

Theorem 5.4.2: The global asymptotic stability of the ailment-free symmetry E_0 in the order (5.4) is established when $R_0 < 1$, and it becomes unsteady or else.

Proof: The behavior of the varying signifying the contaminated part in the order (5.4) can be stated as follows:

$$\begin{pmatrix} \frac{de_h}{dt} \\ \frac{di_h}{dt} \\ \frac{de_v}{dt} \\ \frac{di_v}{dt} \end{pmatrix} = (F - V)\begin{pmatrix} e_h \\ i_h \\ e_v \\ i_v \end{pmatrix} - F_i \begin{pmatrix} e_h \\ i_h \\ e_v \\ i_v \end{pmatrix} \tag{5.9}$$

where

$$\begin{pmatrix} \frac{de_h}{dt} \\ \frac{di_h}{dt} \\ \frac{de_v}{dt} \\ \frac{di_v}{dt} \end{pmatrix} = (F - V)\begin{pmatrix} -(\mu_h + \xi_h) - \gamma(1-\alpha) + nb\beta_1 \\ -(\mu_h + \delta_h) - \gamma(1-\alpha) + \xi_h \\ -(\mu_v + \xi_v) + b\beta_2 \\ \xi_v - \mu_v \end{pmatrix} - F_i \begin{pmatrix} e_h \\ i_h \\ e_v \\ i_v \end{pmatrix}$$

Thus

$$\begin{pmatrix} \frac{de_h}{dt} \\ \frac{di_h}{dt} \\ \frac{de_v}{dt} \\ \frac{di_v}{dt} \end{pmatrix} \leq (F - V)\begin{pmatrix} e_h \\ i_h \\ e_v \\ i_v \end{pmatrix} \tag{5.10}$$

Given that every eigenvalue of the matrix $F-V$ possesses a negative real component, the stability of the linearized differential inequality (5.10) is ensured when R_0 is less than 1. Therefore $(e_h, i_h, e_v, i_v) \to (0, 0, 0, 0)$ as $t \to \infty$. Substituting $e_h = i_h = e_v = i_v = 0$, in (5.4) gives $s_h(t) \to s_h(0)$ as $t \to \infty$ and $s_v(t) \to s_v(0)$ as $t \to \infty$. Hence, the DFE (E_0) is globally asymptotically stable for $R_0 < 1$ and unstable if $R_0 > 1$.

5.4.4. Endemic Equilibrium (EE)

The system (5.4) attains an endemic equilibrium point, which is given by:

$$\lambda - \gamma\alpha - nb\beta_1 s_h^* i_v^* - \gamma(1-\alpha)s_h^* - \mu_h s_h^* = 0 \quad (5.11)$$

$$nb\beta_1 s_h^* i_v^* - (\mu_h + \xi_h)e_h^* - \gamma(1-\alpha)e_h^* = 0 \quad (5.12)$$

$$\xi_h e_h^* - (\mu_h + \delta_h)i_h^* - \gamma(1-\alpha)i_h^* = 0 \quad (5.13)$$

$$\delta_h i_h^* - \mu_h r_h^* - \gamma(1-\alpha)r_h^* = 0 \quad (5.14)$$

$$\mu_v - b\beta_2 s_v^* i_h^* - \mu_v s_v^* = 0 \quad (5.15)$$

$$b\beta_2 s_v^* i_h^* - (\mu_v + \xi_v)e_v^* = 0 \quad (5.16)$$

$$\xi_v e_v^* - \mu_v i_v^* = 0 \quad (5.17)$$

Adding (5.11) and (5.12), we get

$$e_h^* = \frac{(\lambda - \gamma\alpha)(1 - s_h^*)}{(\lambda - \gamma\alpha + \xi_h)} \quad (5.18)$$

From (5.13), $e_h^* = \dfrac{(\lambda - \gamma\alpha + \delta_h)i_h^*}{\xi_h}$ (5.19)

From (5.14), $r_h^* = \dfrac{\delta_h i_h^*}{(\lambda - \gamma\alpha)}$ (5.20)

From (5.15), $i_h^* = \dfrac{\mu_v i_v^*}{b\beta_2(1 - i_v^*)}$ (5.21)

From (5.11), $i_v^* = \dfrac{(\lambda - \gamma\alpha)(1 - s_h^*)}{nb\beta_1 s_h^*}$ (5.22)

From (5.17), $e_v^* = \dfrac{\mu_v i_v^*}{\xi_v}$ (5.23)

Put the value of i_v^* and i_h^* in equation (5.21) and (5.19), we get

Therefore, $i_h^* = \dfrac{\mu_v(\lambda - \gamma\alpha)(1 - s_h^*)}{nb^2\beta_1\beta_2 s_h^* - b\beta_2(\lambda - \gamma\alpha)(1 - s_h^*)}$ (5.24)

and $e_h^* = \dfrac{(\lambda-\gamma\alpha+\xi_h)\mu_v(\lambda-\gamma\alpha)(1-s_h^*)}{nb^2\beta_1\beta_2\xi_h s_h^* - b\beta_2\xi_h(\lambda-\gamma\alpha)(1-s_h^*)}$ (5.25)

Equating equations (5.18) and (5.25), we get

$$\frac{(1-s_h^*)(\lambda-\gamma\alpha)}{(\lambda-\gamma\alpha+\xi_h)} = \frac{\mu_v(\lambda-\gamma\alpha+\delta_h)(\lambda-\gamma\alpha)(1-s_h^*)}{nb^2\xi_h\beta_1\beta_2 s_h^* - b\beta_2\xi_h(\lambda-\gamma\alpha)(1-s_h^*)}$$

$$\Rightarrow nb^2\xi_h\beta_1\beta_2 s_h^*(1-s_h^*)(\lambda-\gamma\alpha) - b\beta_2\xi_h(1-s_h^*)^2(\lambda-\gamma\alpha)^2 = (\lambda+\delta_h-\gamma\alpha)(\lambda+\xi_h-\gamma\alpha) \times \mu_v(1-s_h^*)(\lambda-\gamma\alpha)$$

$$\Rightarrow \left[nb^2\xi_h\beta_1\beta_2 s_h^* - b\,\xi_h\beta_2(1-s_h^*)(\lambda-\gamma\alpha)\right] = (\lambda+\xi_h-\gamma\alpha)(\lambda+\delta_h-\gamma\alpha)\mu_v$$

$$\Rightarrow \left[n\,b^2\xi_h\,\beta_1\,\beta_2 + b\,\beta_2\,\xi_h(\lambda-\gamma\alpha)\right]s_h^* - b\beta_2\xi_h(\lambda-\gamma\alpha) = (\lambda+\xi_h-\gamma\alpha)(\lambda+\delta_h-\gamma\alpha)\mu_v$$

$$\Rightarrow s_h^* = \frac{b\beta_2(\lambda-\gamma\alpha)\xi_h + \mu_v(\lambda+\xi_h-\gamma\alpha)(\lambda+\delta_h-\gamma\alpha)}{b\beta_2\xi_h[nb\beta_1+(\lambda-\gamma\alpha)]}$$

Put the value of s_h^* in equation (5.18), we get

$$i_h^* = \frac{(\lambda-\gamma\alpha)}{(\lambda+\xi_h-\gamma\alpha)}\left[1 - \frac{b\beta_2\xi_h(\lambda-\gamma\alpha)+(\lambda+\xi_h-\gamma\alpha)\mu_v(\lambda+\delta_h-\gamma\alpha)}{b\beta_2[nb\beta_1+(\lambda-\gamma\alpha)]\xi_h}\right]$$

$$i_h^* = \frac{(\lambda-\gamma\alpha)}{(\lambda+\xi_h-\gamma\alpha)}\left[\frac{b\beta_2\xi_h[nb\beta_1+(\lambda-\gamma\alpha)]-b\beta_2\xi_h(\lambda-\gamma\alpha)-(\lambda+\xi_h-\gamma\alpha)(\lambda+\delta_h-\gamma\alpha)\mu_v}{b\beta_2\xi_h[nb\beta_1+(\lambda-\gamma\alpha)]}\right]$$

$$i_h^* = \frac{(\lambda-\gamma\alpha)}{(\lambda+\xi_h-\gamma\alpha)}\left[\frac{b\beta_2\xi_h[nb\beta_1+2(\lambda-\gamma\alpha)]-(\lambda+\xi_h-\gamma\alpha)(\lambda+\delta_h-\gamma\alpha)\mu_v}{b\beta_2[nb\beta_1+(\lambda-\gamma\alpha)]\xi_h}\right]$$

$$i_h^* = \frac{(\lambda-\gamma\alpha)}{(\lambda+\xi_h-\gamma\alpha)}\left[\frac{nb^2\xi_h\beta_1\beta_2 + 2(\lambda-\gamma\alpha)b\beta_2\xi_h - (\lambda+\xi_h-\gamma\alpha)(\lambda+\delta_h-\gamma\alpha)\mu_v}{nb^2\xi_h\beta_1\beta_2 + b\beta_2(\lambda-\gamma\alpha)\xi_h}\right]$$

Put the value of i_h^* in equation (5.19) and (5.20), we get

$$e_h^* = \frac{(\lambda+\delta_h-\gamma\alpha)}{\xi_h}\times \frac{(\lambda-\gamma\alpha)}{(\lambda+\xi_h-\gamma\alpha)}\left[\frac{nb^2\xi_h\beta_1\beta_2 + 2\xi_h(\lambda-\gamma\alpha)b\beta_2 - (\lambda+\xi_h-\gamma\alpha)\mu_v(\lambda+\delta_h-\gamma\alpha)}{nb^2\xi_h\beta_1\beta_2 + b\beta_2(\lambda-\gamma\alpha)\xi_h}\right]$$

and

$$r_h^* = \frac{\delta_h}{(\lambda+\xi_h-\gamma\alpha)}\left[\frac{nb^2\xi_h\beta_1\beta_2 + 2\xi_h(\lambda-\gamma\alpha)b\beta_2 - (\lambda+\xi_h-\gamma\alpha)\mu_v(\lambda+\delta_h-\gamma\alpha)}{nb^2\xi_h\beta_1\beta_2 + b\beta_2(\lambda-\gamma\alpha)\xi_h}\right]$$

Put the value of s_h^* in equation (5.22), we get

$$i_v^* = \frac{(\lambda-\gamma\alpha)\left[1-\frac{b\beta_2\xi_h(\lambda-\gamma\alpha)+(\lambda+\xi_h-\gamma\alpha)\mu_v(\lambda+\delta_h-\gamma\alpha)}{b\beta_2[nb\beta_1+(\lambda-\gamma\alpha)]\xi_h}\right]}{nb\beta_1\left[\frac{b\beta_2\xi_h(\lambda-\gamma\alpha)+(\lambda+\xi_h-\gamma\alpha)\mu_v(\lambda+\delta_h-\gamma\alpha)}{b\beta_2[nb\beta_1+(\lambda-\gamma\alpha)]\xi_h}\right]}$$

$$\Rightarrow i_v^* = \frac{(\lambda-\gamma\alpha)\left[\frac{b\beta_2[nb\beta_1+(\lambda-\gamma\alpha)]\xi_h-b\beta_2(\lambda-\gamma\alpha)\xi_h+(\lambda+\xi_h-\gamma\alpha)\mu_v(\lambda+\delta_h-\gamma\alpha)}{b\beta_2[nb\beta_1+(\lambda-\gamma\alpha)]\xi_h}\right]}{nb\beta_1\left[\frac{b\beta_2\xi_h(\lambda-\gamma\alpha)+(\lambda+\xi_h-\gamma\alpha)\mu_v(\lambda+\delta_h-\gamma\alpha)}{b\beta_2[nb\beta_1+(\lambda-\gamma\alpha)]\xi_h}\right]}$$

$$\Rightarrow i_v^* = \frac{(\lambda-\gamma\alpha)}{nb\beta_1}\left[\frac{b\beta_2[nb\beta_1+(\lambda-\gamma\alpha)]\xi_h-b\beta_2(\lambda-\gamma\alpha)\xi_h+(\lambda+\xi_h-\gamma\alpha)\mu_v(\lambda+\delta_h-\gamma\alpha)}{b\beta_2(\lambda-\gamma\alpha)\xi_h+(\lambda+\xi_h-\gamma\alpha)\mu_v(\lambda+\delta_h-\gamma\alpha)}\right]$$

Put the value of i_v^* in equation (5.23), we get

$$e_v^* = \frac{(\lambda-\gamma\alpha)\mu_v}{nb\beta_1\xi_v}\left[\frac{b\beta_2[nb\beta_1+(\lambda-\gamma\alpha)]\xi_h-b\beta_2(\lambda-\gamma\alpha)\xi_h+(\lambda+\xi_h-\gamma\alpha)\mu_v(\lambda+\delta_h-\gamma\alpha)}{b\beta_2\xi_h(\lambda-\gamma\alpha)+(\lambda+\xi_h-\gamma\alpha)\mu_v(\lambda+\delta_h-\gamma\alpha)}\right]$$

and

$$s_v^* = \frac{nb\beta_1\mu_v(\lambda+\xi_h-\gamma\alpha)(\lambda+\delta_h-\gamma\alpha)+2b\beta_2\xi_h(\lambda-\gamma\alpha)^2-\mu_v(\lambda-\gamma\alpha)(\lambda+\xi_h-\gamma\alpha)(\lambda+\delta_h-\gamma\alpha)}{nb\beta_1(b\beta_2\xi_h(\lambda-\gamma\alpha)+\mu_v(\lambda+\xi_h-\gamma\alpha)(\lambda+\delta_h-\gamma\alpha))}$$

5.4.5. Global Stability of Endemic Equilibrium

We discuss the overall firmness of the native symmetry in this sub-section.

Theorem 5.4.3: The world wide tangent firmness of the native symmetry E^* in the system (5.4) is established when $R_0 > 1$, and it becomes unstable otherwise.

Proof: Consider a Lyapunov function V as a means of demonstrating the global stability of endemic equilibrium.

$$V = \left\{s_h - s_h^*\left(1+\ln\frac{s_h}{s_h^*}\right)\right\} + \left\{s_v - s_v^*\left(1+\ln\frac{s_v}{s_v^*}\right)\right\} + \left\{e_h - e_h^*\left(1+\ln\frac{e_h}{e_h^*}\right)\right\} + \left\{e_v - e_v^*\left(1+\ln\frac{e_v}{e_v^*}\right)\right\}$$
$$+ \left\{i_h - i_h^*\left(1+\ln\frac{i_h}{i_h^*}\right)\right\} + \left\{i_v - i_v^*\left(1+\ln\frac{i_v}{i_v^*}\right)\right\} + \left\{r_h - r_h^*\left(1+\ln\frac{r_h}{r_h^*}\right)\right\} \qquad (5.26)$$

The derivation of V is

$$V' = \left(1-\frac{s_h^*}{s_h}\right)s_h' + \left(1-\frac{s_v^*}{s_v}\right)s_v' + \left(1-\frac{e_h^*}{e_h}\right)e_h' + \left(1-\frac{e_v^*}{e_v}\right)e_v' + \left(1-\frac{i_h^*}{i_h}\right)i_h' + \left(1-\frac{i_v^*}{i_v}\right)i_v' + \left(1-\frac{r_h^*}{r_h}\right)r_h' = 0$$

Since,

$$s_h' = \lambda - \gamma\alpha - nb\beta_1 s_h i_v - (\lambda - \gamma\alpha)\, s_h$$

$$e_h' = nb\beta_1 s_h i_v - (\lambda - \gamma\alpha + \xi_h)\, e_h$$

$$i_h' = \xi_h e_h - (\lambda - \gamma\alpha + \delta_h)\, i_h$$

$$r_h' = \delta_h i_h - (\lambda - \gamma\alpha)\, r_h$$

$$s_v' = \mu_v - b\beta_2 s_v i_h - \mu_v s_v$$

$$e_v' = b\beta_2 s_v i_h - (\mu_v + \xi_v)\, e_v$$

$$i_v' = \xi_v e_v - \mu_v i_v$$

Then

$$V' = \left(\frac{s_h - s_h^*}{s_h}\right)\left(\lambda - \gamma\alpha - nb\beta_1 s_h i_v - (\lambda - \gamma\alpha)s_h\right) + \left(\frac{e_h - e_h^*}{e_h}\right)\left(nb\beta_1 s_h i_v - (\lambda - \gamma\alpha + \xi_h)e_h\right)$$

$$+ \left(\frac{i_h - i_h^*}{i_h}\right)\left(\xi_h e_h - (\lambda - \gamma\alpha + \delta_h)i_h\right) + \left(\frac{r_h - r_h^*}{r_h}\right)\left(\delta_h i_h - (\lambda - \gamma\alpha)r\right) + \left(\frac{s_v - s_v^*}{s_v}\right)\left(\mu_v - b\beta_2 s_v i_h - \mu_v s_v\right)$$

$$+ \left(\frac{e_v - e_v^*}{e_v}\right)\left(b\beta_2 s_v i_h - (\mu_v + \xi_v)e_v\right) + \left(\frac{i_v - i_v^*}{i_v}\right)\left(\xi_v e_v - \mu_v i_v\right)$$

$$= \left(\frac{s_h - s_h^*}{s_h}\right)\left[\lambda - \gamma\alpha - \left\{nb\beta_1\left(i_v - i_v^*\right) + (\lambda - \gamma\alpha)\right\}\left(s_h - s_h^*\right)\right] + \left(\frac{e_h - e_h^*}{e_h}\right)\left\{\begin{matrix} nb\beta_1\left(s_h - s_h^*\right)\left(i_v - i_v^*\right) \\ -(\lambda - \gamma\alpha + \xi_h)\left(e_h - e_h^*\right)\end{matrix}\right\}$$

$$+ \left(\frac{i_h - i_h^*}{i_h}\right)\left\{\xi_h\left(e_h - e_h^*\right) - (\lambda - \gamma\alpha + \delta_h)\left(i_h - i_h^*\right)\right\} + \left(\frac{r_h - r_h^*}{r_h}\right)\left\{\delta_h\left(i_h - i_h^*\right) - (\lambda - \gamma\alpha)\left(r_h - r_h^*\right)\right\}$$

$$+ \left(\frac{s_v - s_v^*}{s_v}\right)\left[\mu_v - \left\{b\beta_2\left(i_h - i_h^*\right) + \mu_v\right\}\left(s_v - s_v^*\right)\right] + \left(\frac{e_v - e_v^*}{e_v}\right)\left\{b\beta_2\left(i_h - i_h^*\right)\left(s_v - s_v^*\right) - (\mu_v + \xi_v)\left(e_v - e_v^*\right)\right\}$$

$$+ \left(\frac{i_v - i_v^*}{i_v}\right)\left\{\xi_v\left(e_v - e_v^*\right) - \mu_v\left(i_v - i_v^*\right)\right\}$$

$$= -(\lambda - \gamma\alpha)\frac{\left(s_h - s_h^*\right)^2}{s_h} + \frac{\left(s_h - s_h^*\right)}{s_h}\left[(\lambda - \gamma\alpha) - nb\beta_1\left(i_v - i_v^*\right)\left(s_h - s_h^*\right)\right] - (\lambda - \gamma\alpha + \xi_h)\frac{\left(e_h - e_h^*\right)^2}{e_h}$$

$$+ \frac{\left(e_h - e_h^*\right)}{e_h}\left\{nb\beta_1\left(s_h - s_h^*\right)\left(i_v - i_v^*\right)\right\} - (\lambda - \gamma\alpha + \delta_h)\frac{\left(i_h - i_h^*\right)^2}{i_h} + \frac{\left(i_h - i_h^*\right)}{i_h}\left\{\xi_h\left(e_h - e_h^*\right)\right\}$$

$$-(\lambda-\gamma\alpha)\frac{(r_h-r_h^*)^2}{r_h}+\frac{(r_h-r_h^*)}{r_h}\{\delta_h(i_h-i_h^*)\}-\mu_v\frac{(s_v-s_v^*)^2}{s_v}+\frac{(s_v-s_v^*)}{s_v}[\mu_v-b\beta_2(i_h-i_h^*)(s_v-s_v^*)]$$

$$-(\mu_v+\xi_v)\frac{(e_v-e_v^*)^2}{e_v}+\frac{(e_v-e_v^*)}{e_v}\{b\beta_2(i_h-i_h^*)(s_v-s_v^*)\}-\mu_v\frac{(i_v-i_v^*)^2}{i_v}+\frac{(i_v-i_v^*)}{i_v}\{\xi_v(e_v-e_v^*)\}$$

$$=-(\lambda-\gamma\alpha)\frac{(s_h-s_h^*)^2}{s_h}+(\lambda-\gamma\alpha)-(\lambda-\gamma\alpha)\frac{s_h^*}{s_h}-(nb\beta_1 i_v-nb\beta_1 i_v^*)\frac{(s_h-s_h^*)^2}{s_h}$$

$$-(\lambda-\gamma\alpha+\xi_h)\frac{(e_h-e_h^*)^2}{e_h}+\frac{(e_h-e_h^*)}{e_h}(nb\beta_1 s_h i_v-nb\beta_1 s_h i_v^*-nb\beta_1 s_h^* i_v+nb\beta_1 s_h^* i_v^*)$$

$$-(\lambda-\gamma\alpha+\delta_h)\frac{(i_h-i_h^*)^2}{i_h}+\frac{(i_h-i_h^*)}{i_h}(\xi_h e_h-\xi_h e_h^*)-(\lambda-\gamma\alpha)\frac{(r_h-r_h^*)^2}{r_h}+\frac{(r_h-r_h^*)}{r_h}(\delta_h i_h-\delta_h i_h^*)$$

$$-\mu_v\frac{(s_v-s_v^*)^2}{s_v}+\mu_v-\mu_v\frac{s_v^*}{s_v}-b\beta_2 i_h\frac{(s_v-s_v^*)^2}{s_v}+b\beta_2 i_h^*\frac{(s_v-s_v^*)^2}{s_v}-(\mu_v+\xi_v)\frac{(e_v-e_v^*)^2}{e_v}$$

$$+\frac{(e_v-e_v^*)}{e_v}\{b\beta_2(i_h s_v-i_h s_v^*-s_v i_h^*+s_v^* i_h^*)\}-\mu_v\frac{(i_v-i_v^*)^2}{i_v}+\frac{(i_v-i_v^*)}{i_v}(\xi_v e_v-\xi_v e_v^*)$$

$$=-(\lambda-\gamma\alpha)\frac{(s_h-s_h^*)^2}{s_h}+(\lambda-\gamma\alpha)-(\lambda-\gamma\alpha)\frac{s_h^*}{s_h}-nb\beta_1 i_v\frac{(s_h-s_h^*)^2}{s_h}+nb\beta_1 i_v^*\frac{(s_h-s_h^*)^2}{s_h}$$

$$-(\lambda-\gamma\alpha+\xi_h)\frac{(e_h-e_h^*)^2}{e_h}+nb\beta_1 s_h i_v-nb\beta_1 s_h i_v^*-nb\beta_1 s_h^* i_v+nb\beta_1 s_h^* i_v^*-nb\beta_1 s_h i_v\frac{e_h^*}{e_h}$$

$$+nb\beta_1 s_h i_v^*\frac{e_h^*}{e_h}+nb\beta_1 s_h^* i_v\frac{e_h^*}{e_h}-nb\beta_1 s_h^* i_v^*\frac{e_h^*}{e_h}-(\lambda-\gamma\alpha+\delta_h)\frac{(i_h-i_h^*)^2}{i_h}+\xi_h e_h-\xi_h e_h^*$$

$$-\xi_h e_h\frac{i_h^*}{i_h}+\xi_h e_h^*\frac{i_h^*}{i_h}-(\lambda-\gamma\alpha)\frac{(r_h-r_h^*)^2}{r_h}+\delta_h i_h-\delta_h i_h^*-\delta_h i_h\frac{r_h^*}{r_h}+\delta_h i_h^*\frac{r_h^*}{r_h}-\mu_v\frac{(s_v-s_v^*)^2}{s_v}$$

$$+\mu_v-\mu_v\frac{s_v^*}{s_v}-b\beta_2 i_h\frac{(s_v-s_v^*)^2}{s_v}+b\beta_2 i_h^*\frac{(s_v-s_v^*)^2}{s_v}-(\mu_v+\xi_v)\frac{(e_v-e_v^*)^2}{e_v}+b\beta_2 i_h s_v-b\beta_2 i_h s_v^*$$

$$-b\beta_2 s_v i_h^*+b\beta_2 s_v^* i_h^*-b\beta_2 i_h s_v\frac{e_v^*}{e_v}+b\beta_2 i_h s_v^*\frac{e_v^*}{e_v}+b\beta_2 s_v i_h^*\frac{e_v^*}{e_v}-b\beta_2 s_v^* i_h^*\frac{e_v^*}{e_v}-\mu_v\frac{(i_v-i_v^*)^2}{i_v}$$

$$+\xi_v e_v-\xi_v e_v^*-\xi_v e_v\frac{i_v^*}{i_v}+\xi_v e_v^*\frac{i_v^*}{i_v}=0$$

Separate positive and negative terms such that

$$G = nb\beta_1 i_v^* \frac{(s_h - s_h^*)^2}{s_h} + b\beta_2 i_h^* \frac{(s_v - s_v^*)^2}{s_v} + nb\beta_1 s_h i_v + nb\beta_1 s_h^* i_v^* + nb\beta_1 s_h i_v^* \frac{e_h^*}{e_h} + nb\beta_1 s_h^* i_v \frac{e_h^*}{e_h}$$

$$+ \xi_h e_h + \xi_h e_h^* \frac{i_h^*}{i_h} + \delta_h i_h + \delta_h i_h^* \frac{r_h^*}{r_h} + \mu_v + b\beta_2 i_h s_v + b\beta_2 s_v^* i_h^* + b\beta_2 i_h s_v^* \frac{e_v^*}{e_v} + b\beta_2 s_v i_h^* \frac{e_v^*}{e_v} + \xi_v e_v$$

$$+ \xi_v e_v^* \frac{i_v^*}{i_v} + (\lambda - \gamma\alpha)$$

$$H = -(\lambda - \gamma\alpha)\frac{(s_h - s_h^*)^2}{s_h} - nb\beta_1 i_v \frac{(s_h - s_h^*)^2}{s_h} - \mu_v \frac{(s_v - s_v^*)^2}{s_v} - b\beta_2 i_h \frac{(s_v - s_v^*)^2}{s_v}$$

$$-(\lambda - \gamma\alpha + \xi_h)\frac{(e_h - e_h^*)^2}{e_h} - (\lambda - \gamma\alpha + \delta_h)\frac{(i_h - i_h^*)^2}{i_h} - (\lambda - \gamma\alpha)\frac{(r_h - r_h^*)^2}{r_h} - (\mu_v + \xi_v)\frac{(e_v - e_v^*)^2}{e_v}$$

$$- \mu_v \frac{(i_v - i_v^*)^2}{i_v} - (\lambda - \gamma\alpha)\frac{s_h^*}{s_h} - nb\beta_1 s_h i_v \frac{e_h^*}{e_h} - nb\beta_1 s_h^* i_v^* \frac{e_h^*}{e_h} - \xi_h e_h \frac{i_h^*}{i_h} - \delta_h i_h \frac{r_h^*}{r_h} - \mu_v \frac{s_v^*}{s_v} - b\beta_2 i_h s_v \frac{e_v^*}{e_v}$$

$$- b\beta_2 s_v^* i_h^* \frac{e_v^*}{e_v} - \xi_v e_v \frac{i_v^*}{i_v} - nb\beta_1 s_h i_v^* - nb\beta_1 s_h^* i_v - \xi_h e_h^* - \delta_h i_h^* - b\beta_2 i_h s_v^* - b\beta_2 s_v i_h^* - \xi_v e_v^*$$

If G < H then V'will be negative it means that $V' < 0$. It follows that $V' = 0 \Leftrightarrow s_h = s_h^*$, $e_h = e_h^*$, $i_h = i_h^*$, $r_h = r_h^*$, $s_v = s_v^*$, $e_v = e_v^*$ and $i_v = i_v^*$. The maximum invariant set of system (5.4) on the set $\{(s_h^*, e_h^*, i_h^*, r_h^*, s_v^*, e_v^*, i_v^*) : V' = 0\}$ is the singleton(E^*). Thus for system (5.4), the endemic equilibrium E^* is globally asymptotically stable if $G < H$ by LaSalle's invariance principle (1976).

5.5. Numerical Simulation

Applying the technique of Runge-Kutta to a simplified structure of the model (5.4) and using the estimated parameter values given in Table 5.1, the numerical simulations of the study are demonstrated.

Table 5.1: Presents the estimated parameters for the mathematical model of dengue fever.

Parameters	Values	Source
λ	0.00002	Chen and Hsieh (2012)
γ	0.000004	Pande J. (2013)
B	0.33	Adams and Boots (2010)
β_1	0.375	KMTL (2006)
β_2	0.75	KMTL (2006)
ξ_h	0.197	Assumed
ξ_v	0.183	Assumed
μ_h	0.000016	Chen and Hsieh (2012)

μ_v	0.331	Chen and Hsieh (2012)
δ_h	0.142	Adams and Boots (2010)
n	12	Assumed
α	0.637	Pande J. (2013)

Figure 5.2 depicts how the population is distributed across various demographic categories over time.

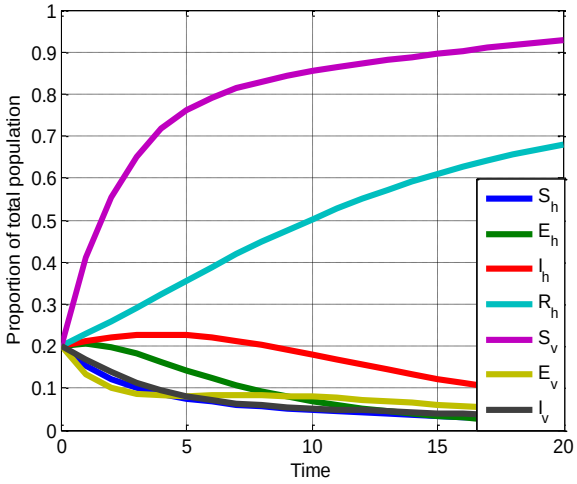

Figure 5.2: Variation of proportion of population at different classes.

The portion of the sensitive human inhabitants declines with time when it comes to the equilibrium point, as shown in Figure 5.2. This decline is primarily attributed to many individuals becoming infected, often due to a lack of awareness about dengue, and also because of a decrease or shortage in human carrying capacity. The exposed human population, as well as the infective human population, initially increases with time but eventually declines due to disease-induced deaths and other natural causes as some individuals recover and transition to the recovery class. As a result, the percentage of the recovered human population rises. Meanwhile, the proportion of sensitive vector populations increases while that of exposed and infective vector populations decreases over time.

Figures 5.3 to 5.9 depict the variations in terms of proportions susceptible humans, exposed humans, infected humans, recovered humans, susceptible vectors, exposed vector and infective vectors for various biting rates denoted as b.

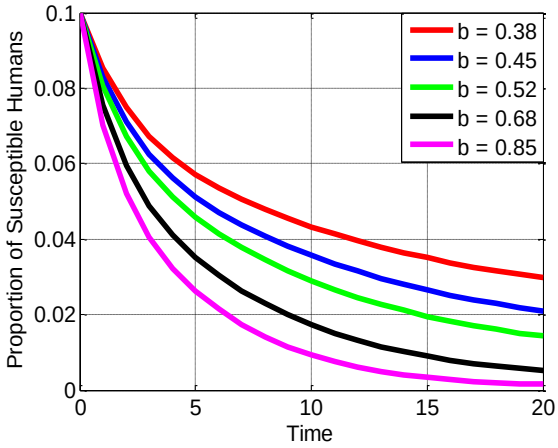

Figure 5.3: Variation in the susceptible human population for varying biting rates b.

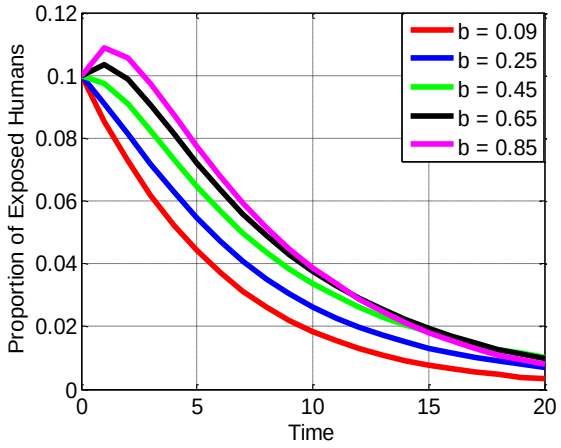

Figure 5.4: Variation in the exposed human population for varying biting rates b.

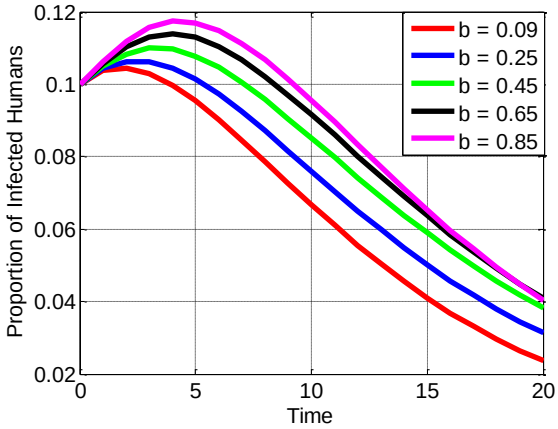

Figure 5.5: Variation in the infected human population for varying biting rates b.

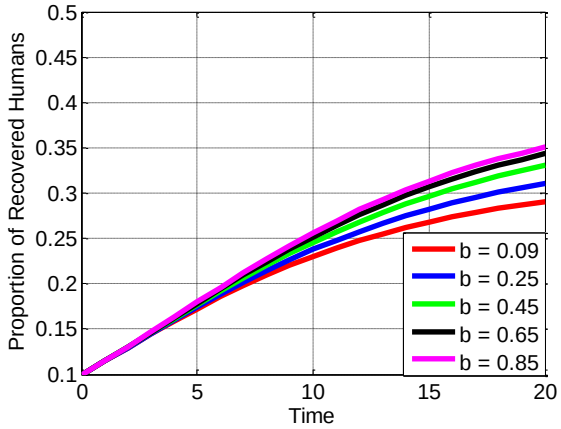

Figure 5.6: Variation in the recovered human population for varying biting rates b.

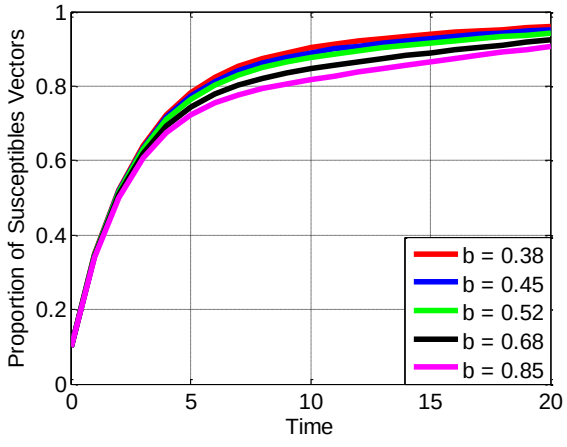

Figure 5.7: Variation in the susceptible vector population for varying biting rates b.

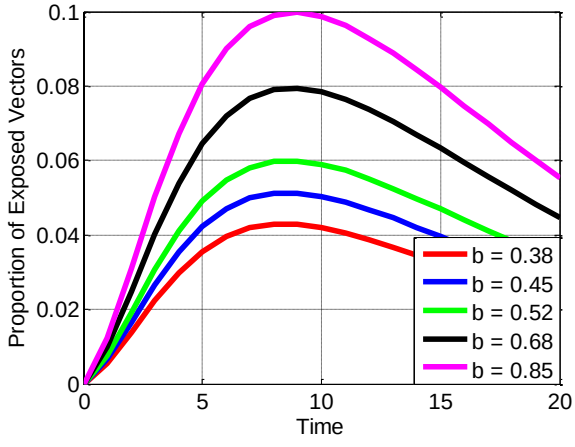

Figure 5.8: Variation in the exposed vector population for varying biting rates b.

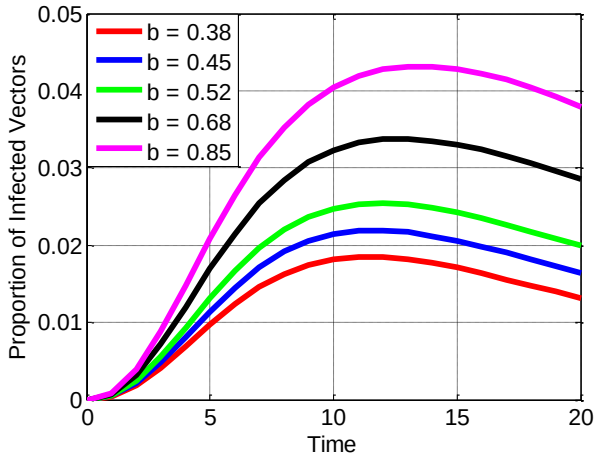

Figure 5.9: Variation in the infected vector population for varying biting rates b.

In Figure 5.3, a notable trend is the decline in the susceptible human population as the biting rate rises. In contrast, as we observe in Figures 5.4, 5.5 and 5.6, a rise in the biting rate corresponds to a rise in the part of the exposed, infected and recuperated human population. Furthermore, when the rate of biting rises, there is a noticeable reduction in the proportion of susceptible vector populations. Conversely, a rise in the biting rate is associated with a rise in the proportions of exposed vector populations and infected vector populations, which is evident in Figures 5.8 and 5.9, correspondingly.

Figures 5.10 to 5.16 illustrate the changes in terms of proportions of susceptible, exposed, infected, and recovered human inhabitants in relation to susceptible, exposed, and infected vector populations. These variations are observed for different virtues of the transference likelihood from vectors to the person population, denoted as β_1.

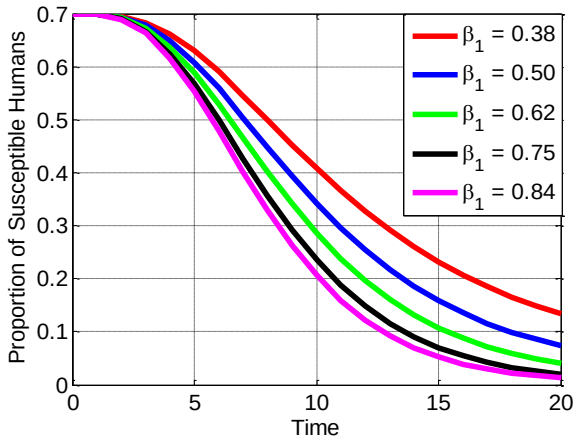

Figure 5.10: Variation in the proportion of susceptible human for different transmission probability rates β_1.

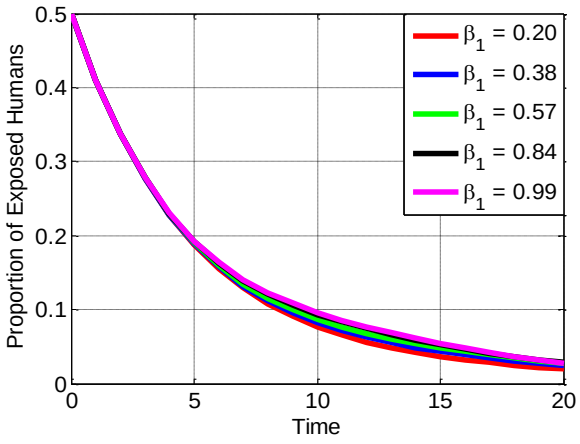

Figure 5.11: Variation in the proportion of exposed human for different transmission probability rates β_1.

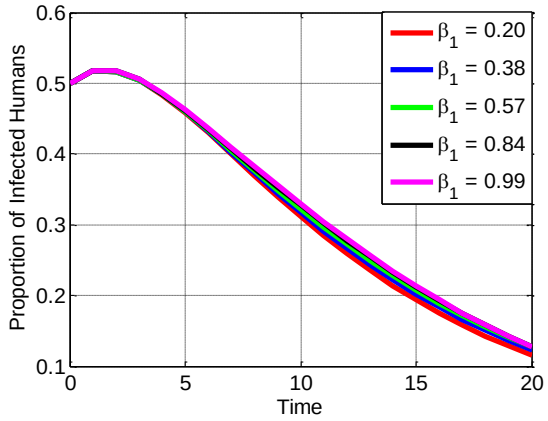

Figure 5.12: Variation in the proportion of infected human for different transmission probability rates β_1.

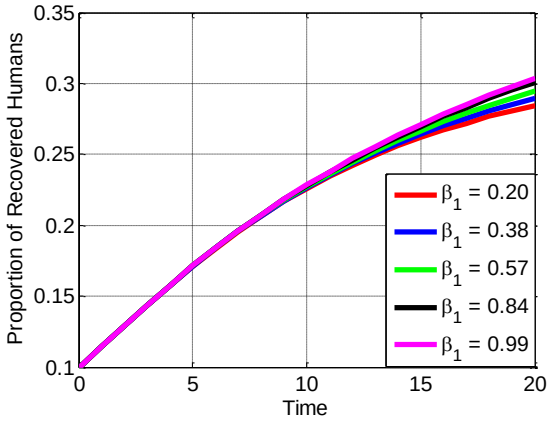

Figure 5.13: Variation in the proportion of recovered human for different transmission probability rates β_1.

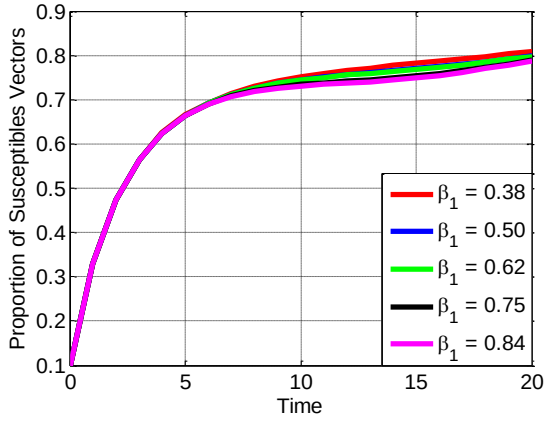

Figure 5.14: Variation in the proportion of susceptible vector population for different transmission probability rates β_1.

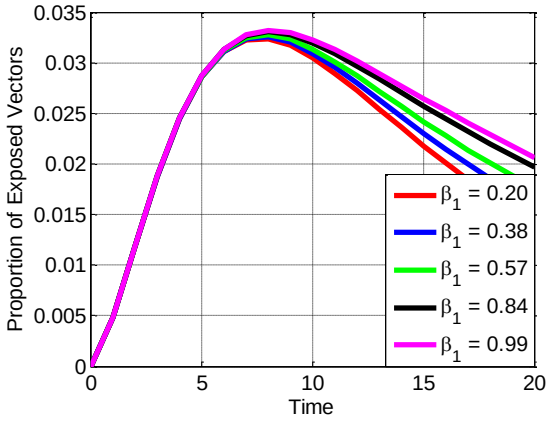

Figure 5.15: Variation in the proportion of exposed vector population for different transmission probability rates β_1.

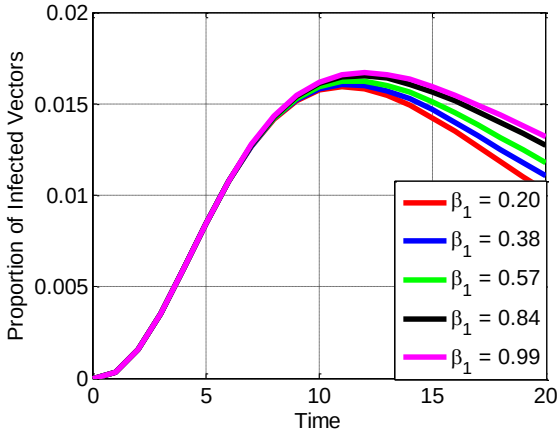

Figure 5.16: Variation in the proportion of infected vector population for different transmission probability rates β_1.

In Figures 5.10, 5.11, 5.12 and 5.13, it is clear that an augmentation in the transference likelihood of the toxic from the bearing to the human population results in observable patterns. As this probability rises, the amount of sensitive individuals in the human population decreases

significantly as more individuals become infected. Simultaneously, the sum of uncovering and contaminating individuals in the personage inhabitant increases. Furthermore, the proportion of the recovered human population also rises as individuals successfully recover from the disease.

In Figure 5.14, it is evident that the proportion of susceptible vectors decreases as the transference of likeliness viruses from vectors to person populations gets larger. Simultaneously, the ratio of exposed as well as infected vector populations increases with the rising transmission probability of viruses from vectors to human populations. These trends are further illustrated in Figures 5.15 and 5.16, correspondingly.

Figures 5.17 to 5.23 display the variations in the portion of susceptible human, exposed human, infected human, and recovered human inhabitants in relation to susceptible vector, exposed vector and infected vector inhabitants. These visual representations are generated for a range of different values of the transference probability from the human to the vector population, denoted as β_2.

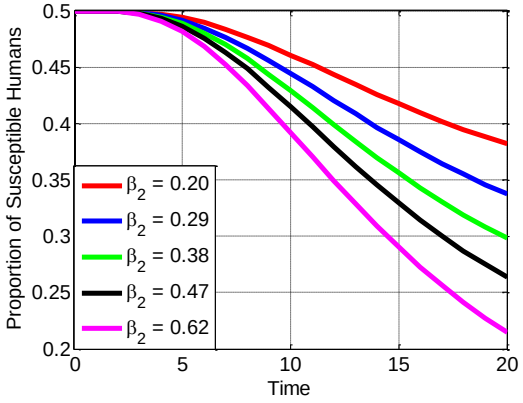

Figure 5.17: Variation in the proportion of susceptible human population for different transmission probability rates β_2.

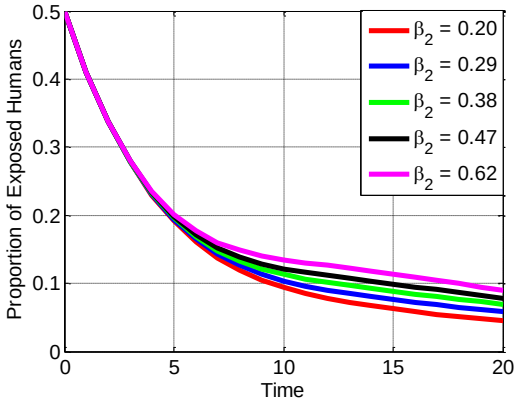

Figure 5.18: Variation in the proportion of exposed human population for different transmission probability rates β_2.

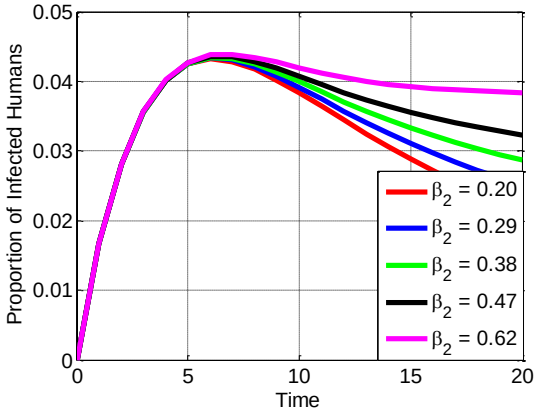

Figure 5.19: Variation in the proportion of infected human population for different transmission probability rates β_2.

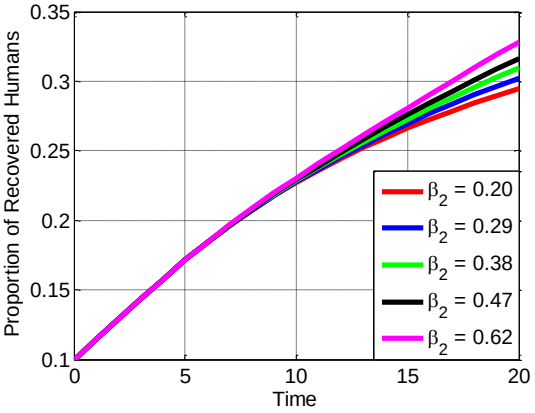

Figure 5.20: Variation in the proportion of recovered human population for different transmission probability rates β_2.

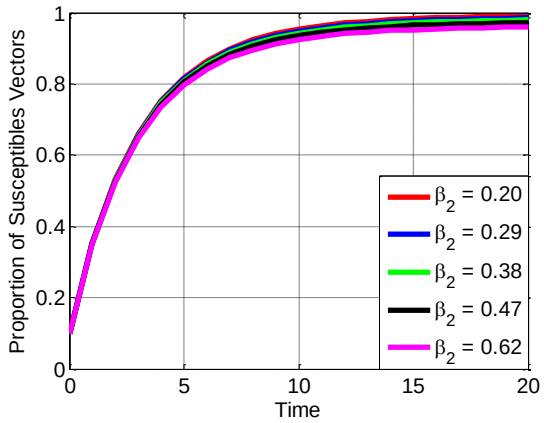

Figure 5.21: Variation in the proportion of susceptible vector population for different transmission probability rates β_2.

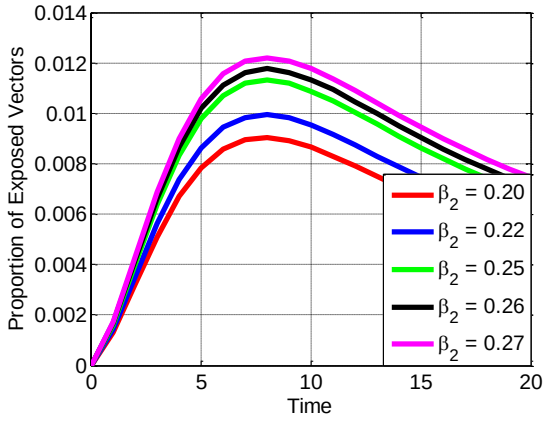

Figure 5.22: Variation in the proportion of exposed vector population for different transmission probability rates β_2.

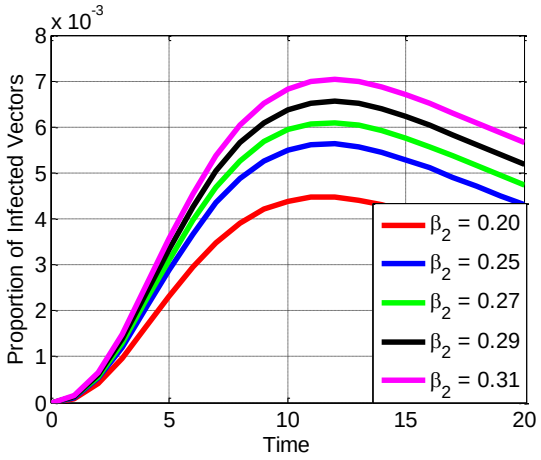

Figure 5.23: Variation in the proportion of infected vector population for different transmission probability rates β_2.

In Figures 5.17, 5.18, 5.19, and 5.20, it is noticeable that as the transference likelihood of the virus from the human to the vector population rises, discernible trends emerge. As this probability rises, the amount of sensitive individuals in the human population decreases significantly, as more individuals become infected. Simultaneously, the number of uncovered and contaminated individuals in the population increases, and the proportion of the recovered human population also rise as individuals successfully recover from the disease.

A similar pattern can be observed in Figure 5.21. The proportion of vectors that are susceptible decreases as the likelihood of the virus being transmitted from human to vector population increases. At the same time, the percentages of vector populations that are exposed and infected increase as the likelihood of the virus being transmitted from the human to the bearing inhabitants rises, as shown in numbers 5.22 and 5.23, respectively.

Figures 5.24 and 5.25 illustrate the variations in the portion of uncovered and contaminated person populations, respectively. These figures display these variations for a range of different values of the progression rate denoted as ξ_h.

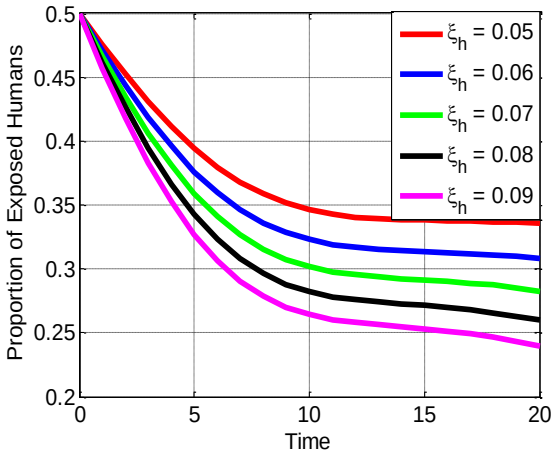

Figure 5.24: Variation in the proportion of exposed human population for different progression rates ξ_h.

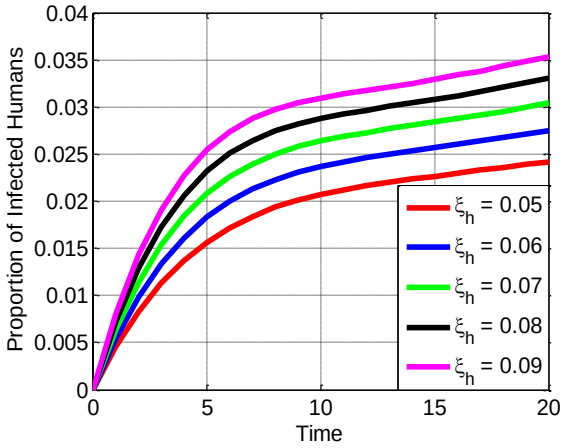

Figure 5.25: Variation in the proportion of infected human population for different progression rates ξ_h.

In Figure 5.24, it is observed that the exposed human population decreases as the progression rate denoted as (ξ_h), increases, whereas with an increase in the progression rate (ξ_h), the proportion of the infected human population also increases, as indicated in Figure 5.25.

Furthermore, Figures 5.26 and 5.27 present the variations in the proportions of exposed vector and infected vector populations. These figures demonstrate these variations for a range of different values of the progression rate, referred to as ξ_v.

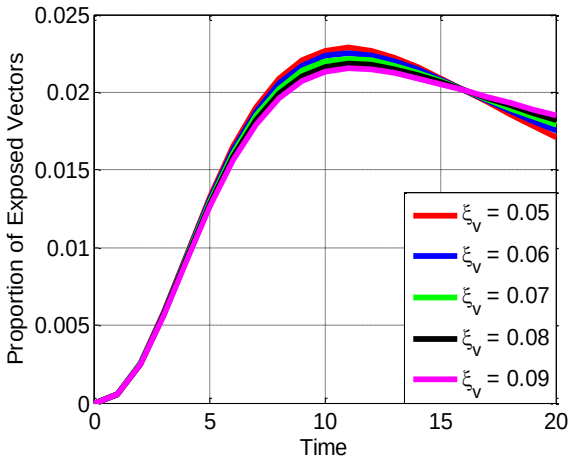

Figure 5.26: Variation in the proportion of exposed vector population for different progression rates ξ_v.

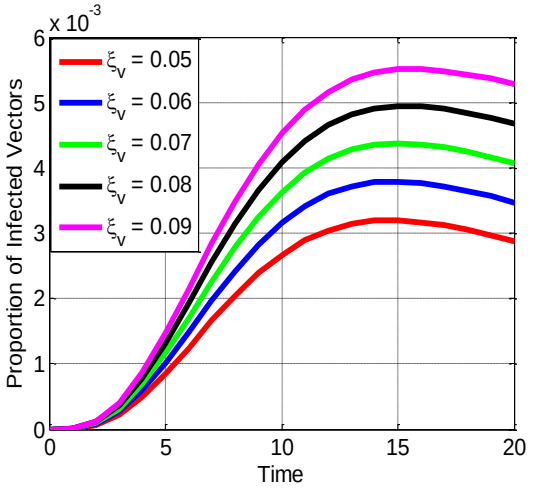

Figure 5.27: Variation in the proportion of infected vector population for different progression rates ξ_v.

In Figure 5.26, it is observed that the exposed vector population decreases as the progression rate (ξ_v) increases while the increase of progression rate (ξ_v) the proportion of infected vector population increases as it is indicated in Figure 5.27.

5.6. Summary and Concluding Remarks

In this chapter, an arithmetical replica has been constructed that effectively represents the transmission of dengue through the utilization of a SEIR framework. By incorporating a logistic function to represent the extension and survival of the mosquito inhabitants, which relies on the human inhabitants for sustenance, our model offers a comprehensive understanding of the complex interplay between the vector and human populations in the spread of dengue.

Through our analysis, we determined the basic reproduction number, denoted by R_0, which serves as a critical indicator of disease transmission potential. Our findings revealed that the disease free equilibrium is regionally firm when $R_0 < 1$, indicating that the disease can be effectively controlled and eliminated under certain conditions. Conversely, when it exceeds one, the disease-free equilibrium becomes unstable, suggesting the potential for sustained transmission within the population.

Moreover, we performed stability assessment for both the states of the system in which there is no disease and the states in which the disease is present. This examination enabled us to investigate the long-term dynamics of the system and determine the circumstances under which the disease can endure or diminish. These observations are crucial for guiding the enhancement of a focused strategy for the management and prevention of the disease.

Overall, our research provides valuable contributions to the understanding of dengue transmission dynamics. By employing mathematical modeling techniques and considering the logistical human population and exposed class, we have shed light on the complex interplay between the mosquito vector and human host. These insights can assist policymakers, healthcare professionals, and researchers in formulating effective measures to combat dengue, mitigate its impact, and ultimately reduce its burden on affected communities.

However, it is crucial to recognize that our model, like any mathematical representation, simplifies the complexity of real-world dynamics. Further research and data collection are necessary to refine and validate the model, incorporating additional factors such as spatial heterogeneity, environmental influences, and intervention strategies. The implementation of these extensions would significantly contribute to a more comprehensive understanding of the transmission of dengue fever and assist in the development of targeted interventions to manage and prevent this significant public health concern.

In conclusion, our study demonstrates the potential of arithmetical design to elucidate the transmission vitals of dengue. By providing insights into the role of human population and the interaction with the mosquito vector, our findings contribute to the broader body of knowledge aimed at controlling and mitigating the impact of dengue, ultimately working towards a future with reduced disease prevalence and improved public health outcomes.

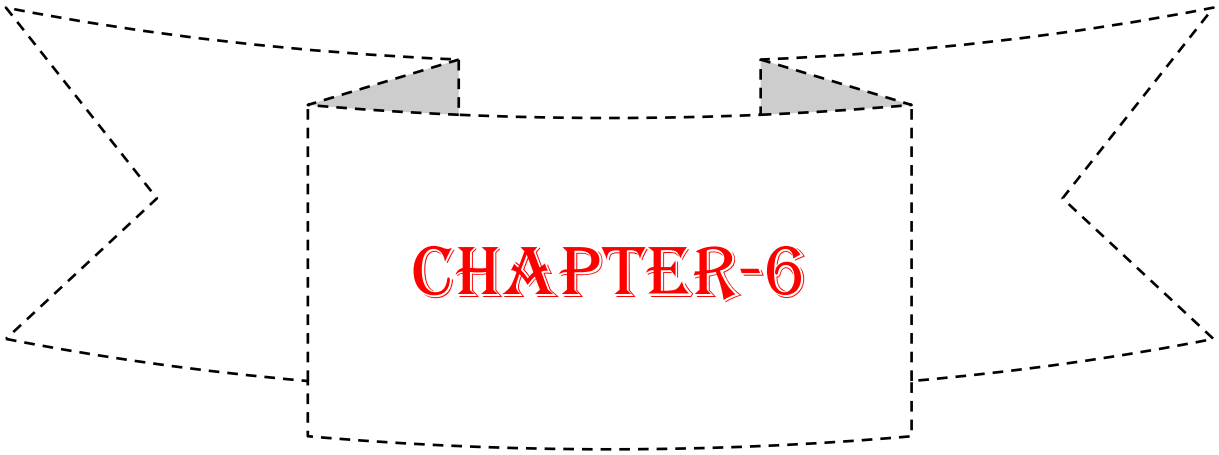

Conclusion and Future Scope

6.1 Conclusion
6.2 Future Scope
6.3 Limitations and Areas for Improvement

Chapter 6: Conclusion and Future Scope

In the forthcoming chapter, a concise overview of significant findings that align with the proposed objectives has been provided. Furthermore, deliberations on potential avenues for future investigation, suggestions, and recommendations within the realm of the research conducted in this thesis are presented.

6.1. Conclusion

In conclusion, this thesis has embarked on a journey to unravel the intricate dynamics of HIV/AIDS, Malaria, and Dengue fever through the lens of mathematical modeling. By developing and analyzing various mathematical models, we have delved into the transmission dynamics of these diseases, providing valuable insights that bridge the gap between theoretical constructs and real-world clinical applicability.

The stability analysis conducted in Chapter 2, focusing on HIV/AIDS transmission among sex workers, highlighted the pivotal role of the reproduction number in determining disease eradication. The stability analysis of both disease-free equilibrium and endemic equilibrium offered a comprehensive understanding of the system's dynamics.

Chapter 3 extended the exploration, considering the impact of media awareness on HIV transmission dynamics. The findings not only established the asymptotic stability of the disease-free equilibrium but also introduced an innovative hybrid soft computing approach for numerical simulations, enhancing the robustness of our analysis.

In Chapter 4, the SEIRS model with mosquito vector dependency sheds light on the transmission dynamics of malaria. The sensitivity analysis emphasized crucial factors in combating the disease, such as targeting pesticide use and improving drainage systems.

Lastly, Chapter 5 explored the transmission dynamics of dengue through an SEIR model, providing insights into the disease's potential for transmission and contributing to the formulation of effective control and prevention strategies.

6.2. Future Scope

The comprehensive exploration of disease dynamics within this thesis opens avenues for future research and development. The derived mathematical models serve as a foundation for further refinement and extension. The following directions could be pursued in future studies:

Refinement of Models: Further refinement and validation of the existing models, incorporating additional parameters and complexities, to enhance the accuracy of predictions and broaden the applicability of the models.

Exploration of Additional Factors: Investigate new factors influencing disease dynamics, such as socio-economic conditions, geographical variations, and evolving treatment strategies.

Dynamic Media Impact: Extend the analysis of media awareness impact on disease transmission, exploring dynamic changes in media influence over time and its implications for public health interventions.

Incorporation of Treatment Dynamics: Expand the models to incorporate detailed treatment dynamics, considering evolving medical interventions, drug resistance patterns, and the impact of vaccination programs.

Comparative Analysis: Conduct comparative analyses between different regions or populations, accounting for diverse demographics and healthcare infrastructures, to tailor intervention strategies according to specific contexts.

Collaborative Research: Foster collaboration between mathematicians, biologists, healthcare professionals, and policymakers to ensure a multidisciplinary approach in addressing the complexities of disease dynamics.

By venturing into these avenues, future research can build upon the foundation laid by this thesis, advancing our understanding of disease dynamics and contributing to the development of targeted strategies for disease control and management on a global scale.

6.3. Limitations and Areas for Improvement

In reflecting on the research presented in this thesis, several limitations and areas for improvement can be identified:

Simplifying Assumptions: The models developed often rely on simplifying assumptions about disease transmission dynamics and population interactions, which may not fully capture the complexities observed in real-world scenarios.

Parameter Uncertainty: The parameter values used in the models are largely derived from existing literature or assumed due to lack of empirical data in certain contexts. This uncertainty could affect the accuracy and generalizability of the findings.

Model Validation: While the models undergo rigorous mathematical analysis, there is limited validation against real-world data. More empirical validation and sensitivity analysis would strengthen the robustness of the results.

Scope and Generalizability: The focus on specific populations and diseases (e.g., sex workers in HIV/AIDS transmission) may limit the generalizability of the findings to broader populations or different epidemiological contexts.

Dynamic Factors: The models do not fully incorporate dynamic factors such as behavioral changes, migration patterns, or evolving treatment strategies, which are crucial in shaping disease transmission dynamics over time.

Data Availability: Limited availability of local epidemiological data in some regions restricts the ability to tailor models to specific geographical contexts, potentially overlooking region-specific nuances.

Technological Assumptions: The use of specific numerical methods and modeling frameworks may introduce inherent biases or limitations that influence the outcomes and interpretations of the study.

Communication of Findings: The thesis could benefit from clearer articulation of the practical implications and actionable insights derived from the mathematical models for public health policies and interventions.

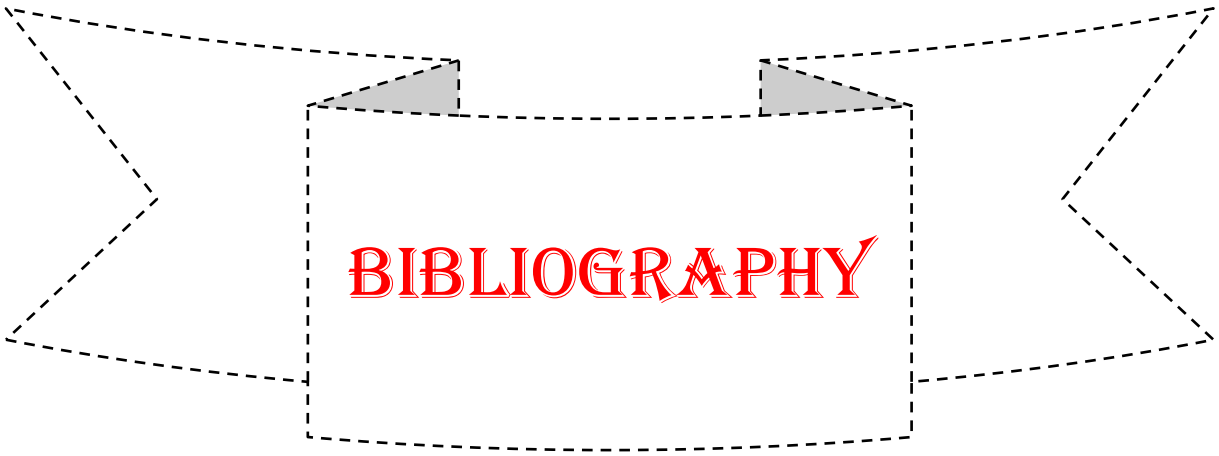
BIBLIOGRAPHY

1. **Abioye, A. I., Ibrahim, M. O., Peter, O. J. and Ogunseye, H. A. (2020).** Optimal control on a mathematical model of malaria, Scientific Bulletin, Series A: Applied Mathematics and Physics, Vol. 83, No. 3, pp. 178-190.
2. **Adams, B. and Boots, M. (2010).** How important is vertical transmission in mosquitoes for the persistence of dengue? Insights from a mathematical model, Epidemics, Vol. 2, No. 1, pp. 1-10.
3. **Al Basir, F. and Abraha, T. (2023).** Mathematical Modelling and Optimal Control of Malaria Using Awareness-Based Interventions, Mathematics, Vol. 11, No. 7, 1687.
4. **Al Basir, F., Banerjee, A. and Ray, S. (2021).** Exploring the effects of awareness and time delay in controlling malaria disease propagation, International Journal of Nonlinear Sciences and Numerical Simulation, Vol. 22, No. 6, pp. 665-683.
5. **Alexander, M. E. and Moghadas, S.M. (2005).** Bifurcation analysis of an SIRS epidemic model with generalized incidence, SIAM Journal on Applied Mathematics, Vol. 65, No. 5, pp. 1794-1816.
6. **Ali, S., Raina, A. A., Iqbal, J. and Mathur, R. (2019).** Mathematical modeling and stability analysis of HIV/AIDS-TB co-infection, Palestine Journal of Mathematics, Vol. 8, No. 2, pp. 380-391.
7. **Anderson, R. M. and May, R. M. (1988).** Epidemiological parameters of HIV transmission, Nature, Vol. 333, pp. 514-519.
8. **Anderson, R.M. and May, R.M. (1991).** Infectious diseases of humans, Oxford, Oxford University Press.
9. **Augiar, M., Kooi, B. W., Rocha, F., Ghaffari, P. and Stollenwerk, N. (2013).** How much complexity is needed to describe the fluctuations observed in dengue hemorrhagic fever incidence data, Ecological Complexity, Vol. 16, pp. 31-40.
10. **Bakary, T., Boureima, S. and Sado, T. (2018).** A mathematical model of malaria transmission in a periodic environment, Journal of Biological Dynamic, Vol. 12, No. 1, pp. 400-432.
11. **Bal, S. and Sodoudi, S. (2020).** Modeling and prediction of dengue occurrences in Kolkata, India, based on climate factors, International Journal of Biometeorology, Vol. 64, No. 8, pp. 1379-1391.
12. **Baylis, M. (2017).** Potential impact of climate change on emerging vector-borne and other infections in the UK, Environmental Health, Vol. 16, No. 112, pp. 45-76.
13. **Benedum, C. M., Seidahmed, O. M. E., Eltahir, E. A. B. and Markuzon, N. (2018).** Statistical modeling of the effect of rainfall flushing on dengue transmission in Singapore, PLOS Neglected Tropical Diseases, Vol. 12, No. 12, e0006935.
14. **Bhatt, S., Gething, P. W., Brady, O. J., Messina, J. P., Farlow, A. W., Moyes, C. L., Drake, J. M., Brownstein, J. S., Hoen, A. G., Sankoh, O., Myers, M. F., George, D. B., Jaenisch, T., Wint, G. R., Simmons, C. P., Scott, T. W., Farrar, J. J. and Hay, S. I. (2013).** The global distribution and burden of dengue, Nature, Vol. 496, pp. 504-507.

15. **Bhunu, C. P. and Mushayabasa, S. (2013).** Modelling the transmission dynamics of HIV/AIDS and hepatitis C virus co-infection, HIV & AIDS Review, Vol. 12, No. 2, pp. 37-42.
16. **Bhunu, C. P., Garira, W. and Mukandavire, Z. (2009).** Modelling HIV/AIDS and tuberculosis co-infection, Bulletin of Mathematical Biology, Vol. 71, pp. 1745-1780.
17. **Bhunu, C. P., Garira, W., Mukandavire, Z. and Zimba, M. (2008).** Tuberculosis transmission model with chemoprophylaxis and treatment, Bulletin of Mathematical Biology, Vol. 70, pp. 1163-1191.
18. **Birkhoff, G and Rota G. (1989).** Ordinary Differential Equations, 4th Edition, Wily, New York.
19. **Biswas, D. and Pal, S. (2017).** Stability analysis of a nonlinear HIV/AIDS epidemic model with vaccination and antiretroviral therapy, International Journal of Advances in Applied Mathematics and Mechanics, Vol.5, No. 2, pp. 41-50.
20. **Butterworth, M. K., Morin, C. W. and Comrie, A. C. (2017).** An Analysis of the Potential Impact of Climate Change on Dengue Transmission in the Southeastern United States, Environmental Health Perspectives, Vol. 125, No. 4, pp. 579-585.
21. **Cai, L. M., Li, X., Ghosh, M. and Guo, B. (2009).** Stability analysis of an HIV/AIDS epidemic model with treatment, Journal of Computational and Applied Mathematics, Vol. 229, No. 1, pp. 313-323.
22. **Cai, L., Guo, S. and Wang, S. (2014).** Analysis of an extended HIV/AIDS epidemic model with treatment, Applied Mathematics and Computation, Vol. 336, pp. 621-627.
23. **Cai, L., Li, X., Tuncer, N., Martcheva, M. and Lashari, A. A. (2017).** Optimal control of a malaria model with asymptomatic class and super infection, Mathematical Biosciences, Vol. 288, pp. 94-108.
24. **Caldwell, J. M., LaBeaud, A. D., Lambin, E. F., Stewart-Ibarra, A. M., Ndenga, B. A., Mutuku, F. M., Krystosik, A. R., Ayala, E. B., Anyamba, A., Borbor-Cordova, M. J., Damoah, R., Grossi-Soyster, E. N., Heras, F. H., Ngugi, H. N., Ryan, S. J., Shah, M. M., Sippy, R. and Mordecai, E. A. (2021).** Climate predicts geographic and temporal variation in mosquito-borne disease dynamics on two continents, Nature Communications, Vol. 12, No. 1233, pp. 1-13.
25. **Chamchod, F. and Britton, N. F. (2011).** Analysis of a vector-bias model on malaria transmission, Bulletin of Mathematical Biology, Vol.73, No. 3, pp. 639-657.
26. **Chaves, F.L., Kaneko, A., Taleo, G., Pascual, M. and Wilson, L.M. (2008).** Malaria transmission pattern resilience to variability is by insecticide-treated nets, Biomed Central, Vol. 7, pp. 180-190.
27. **Chen, S. C. and Hsieh, M. H. (2012).** Modelling the transmission dynamics of dengue fever: Implication, of temperature effects, The Science of Total Environment, Vol. 431, pp. 385-391.
28. **Chitnis, N., Cushing, J. M. and Hyman, J. M. (2006).** Bifurcation analysis of a mathematical model for malaria transmission, SIAM Journal on Applied Mathematics, Vol. 67, No. 1, pp. 24-45.

29. **Chitnis, N., Hardy, D. and Smith, T. (2012).** A periodically-forced mathematical model for the seasonal dynamics of malaria in mosquitoes, Bulletin of Mathematical Biology, Vol. 74, No. 5, pp. 1098-1124.
30. **Cui, J., Sun, Y. and Zhu, H. (2008).** The impact of media on the control of infectious diseases, Journal of Dynamics and Differential Equations, Vol. 20, No. 1, pp. 31-53.
31. **Cui, J., Takeuchi, Y. and Saito, Y. (2006).** Spreading disease with transport-related infection, Journal of Theoretical Biology, Vol. 239, No. 3, pp. 376-390.
32. **Das, K., Chinnathambi, R., Srinivas, M. N. and Rihan, F.A. (2023).** An analysis of time-delay epidemic model for TB, HIV, and AIDS co-infections, Results in Control and Optimization, Vol. 12, 100263.
33. **Davis, C., Murphy, A. K., Bambrick, H., Devine, G. J., Frentiu, F. D., Yakob, L., Huang, X., Li, Z., Yang, W., Williams, G. and Hu, W. (2021).** A regional suitable conditions index to forecast the impact of climate change on dengue vectorial capacity, Environmental Research, Vol. 195, 110849.
34. **Defeng L. and Wang B. (2013).** A novel time delayed HIV/AIDS model with vaccination & antiretroviral therapy and its stability analysis, Applied Mathematical Modelling, Vol. 37, pp. 4608-4625.
35. **Deif, M., Hammam, R. and Solyman, A. (2021).** Adaptive Neuro-Fuzzy Inference System (ANFIS) for Rapid Diagnosis of COVID-19 Cases Based on Routine Blood Tests, International Journal of Intelligent Engineering & Systems, Vol. 14, No.2, pp. 178-189.
36. **Ebi, K. L. and Nealon, J. (2016).** Dengue in a changing climate, Environmental Research, Vol. 151, pp. 115-123.
37. **Elaiw A. M. and Almuallem N. A. (2015).** Global properties of delayed-HIV dynamics models with differential drug efficacy in co circulating target cells, Applied Mathematics and Computation, Vol. 265, pp. 1067-1089.
38. **Erin, M., Thomas, S., Smith, A. and Chitnis, N. (2013).** Estimating malaria transmission through mathematical models, Trends in Parasitology, Vol. 29, No. 10, pp. 477-482.
39. **Forouzannia, F. and Gumel, A. B. (2014).** Mathematical analysis of an age-structured model for malaria transmission dynamics, Mathematical Biosciences, Vol. 247, pp. 80-94.
40. **Forouzannia, F. and Gumel, A. B. (2015).** Dynamics of an age-structured two-strain model for malaria transmission, Applied Mathematics and Computation, Vol. 250, No. 1, pp. 860-886.
41. **Ghosh, M., Chandra, P., Sinha, P. and Shukla, J. B. (2005).** Modeling the spread of bacterial disease: Effect of service providers from an environmentally degraded region, Applied Mathematics and Computation, Vol. 160, pp. 615-647.
42. **Ghosh, S., Waite, L. J., Clayton, H. D. and Adler, R. F. (2014).** Can antibodies against flies alter malaria transmission in birds by changing vector behaviour, Journal of Theoretical Biology, Vol. 358, pp. 93-101.

43. **Greenhalgh, D. and Das, R. (1995).** Modeling epidemics with variables contact rates, Theoretical Population Biology, Vol. 47, No. 2, pp. 129-179.
44. **Gubler, D. J. (2002).** Epidemic dengue/dengue hemorrhagic fever as public health, social and economic problems in the 21st century, Trends Microbiology, Vol.10, No. 2, pp. 100-103.
45. **Gupta, S., Swinton, J. and Anderson, R. M. (1994).** Theoretical studies of the effects of heterogeneity in the parasite population on the transmission dynamics of malaria, Proceedings of the Royal Society B, Vol. 256, No. 1347, pp. 231-238.
46. **Gurski, K. and Hoffman, K. (2023).** Staged HIV transmission and treatment in a dynamic model with long-term partnerships, Journal of Mathematical Biology, Vol. 86, pp. 1-37.
47. **Gutierrez, J. A., Laneri, K., Aparicio, J. P. and Sibona, G. J. (2022).** Meteorological indicators of dengue epidemics in non-endemic Northwest Argentina, Infectious Disease Modelling, Vol. 7, No. 4, pp. 823-834.
48. **Handari, B. D., Vitra, F., Ahya, R., Nadya, S. T. and Aldila, D. (2019).** Optimal control in a malaria model: Intervention of fumigation and bed nets, Advances in Difference Equations, 497.
49. **Haynatzki, G. R., Gani, J. M. and Rachev, S. T. (2000).** A steady state model for the spread of HIV among drug users, Mathematical and Computer Modelling, Vol. 32, No. 1-2, pp. 181-195.
50. **Hazarika, G. C. and Bhattacharjee, A. (2011).** Analysis of a malaria model with time mosquito-dependent transmission co-efficient for human, Proceeding of the Indian Academy of Science: Mathematical Sciences, Vol. 121, No. 1, pp. 93-109.
51. **Hethcote, H. W. (2000).** The mathematics of infectious diseases, SIAM Review, Vol. 42, No. 4, pp. 599-653.
52. **Huber, J. H., Childs, M. L., Caldwell, J. M. and Mordecai, E. A. (2018).** Seasonal temperature variation influences climate suitability for dengue, chikungunya, and Zika transmission, PLoS Neglected Tropical Diseases, Vol. 12, No. 5, e0006451.
53. **Huo, H. F. and Feng, L. X. (2013).** Global stability for an HIV/AIDS epidemic model with different latent stages and treatment, Applied Mathematical Modelling, Vol. 37, No. 3, pp. 1480-1489.
54. **Huo, H. F., Chen, R. and Wang, X. Y. (2016).** Modelling and stability of HIV/AIDS epidemic model with treatment, Applied Mathematical Modelling, Vol. 40, No. 13-14, pp. 6550-6559.
55. **Huo, H. F., Yang, P. and Xiang, H. (2018).** Stability and bifurcation for an SEIS epidemic model with the impact of media, Physica A: Statistical Mechanics and its Application, Vol. 490, pp. 702-720.
56. **Hyman, J. M. and Stanley, E. A. (1988).** Using mathematical models to understand the AIDS epidemic, Mathematical Bioscience, Vol. 90, No. (1-2), pp. 415-473.
57. **Ibrahim, M. M., Kamran, M. A., Naeem Mannan, M. M., Kim, S. and Jung, I. H. (2020).** Impact of awareness to control malaria disease: A mathematical modeling approach, Complexity, pp. 1-13.

58. **Ida, A., Oharu, S. and Oharu, Y. (2007).** A mathematical approach to HIV infection dynamics, Journal of Computational and Applied Mathematics, Vol. 204, No.1, pp. 172-186.
59. **Izadi, N., Gouya, M. M., Akbarpour, S., Zareie, B., Moradi, Y., Kazerooni, P. A., Mahboobi, M., Mohseni, P. and Moradi, G. (2023).** HIV prevalence and associated factors among female sex workers in Iran: a bio-behavioral survey in 2020, AIDS and Behavior, Vol. 27, pp. 909-918.
60. **Jain, M., Sharma, G. C. and Singh, A. (2010).** Compartment analysis for proliferation rate of T-lymphocytes cells in HIV-1 infection, Mathematics Today, Vol. 26, pp. 40-52.
61. **Jia, J. and Qin, G. (2017).** Stability analysis of HIV/AIDS epidemic model with nonlinear incidence and treatment, Advances in Difference Equation, Vol. 136, pp.1-13.
62. **Jones, L. E., and Perelson, A. S. (2005).** Opportunistic infection as a cause of transient viremia in chronically infected hiv patients under treatment with patients under treatment with HAART, Bulletin of Mathematical Biology, Vol. 67, No. 6, pp.1227-1251.
63. **Kakarla, S. G., Bhimala, K. R., Kadiri, M. R., Kumaraswamy, S. and Mutheneni, S. R. (2020).** Dengue situation in India: Suitability and transmission potential model for present and projected climate change scenarios, Science of the Total Environment, Vol. 739, No. 15, 140336.
64. **Kaur, N., Ghosh, M. and Bhatia, S. S. (2014).** Mathematical analysis of the transmission dynamics of HIV/AIDS: Role of female sex workers, Applied Mathematics & Information Science, Vol. 8, No. 5, pp. 2491-2501.
65. **Kermack, W. O. and McKendrick, A. G. (1927).** A contribution to the mathematical theory of epidemics, Proceedings of the Royal Society of London, Series A, Vol. 115, pp. 700-721.
66. **Keshavarz, Z. and Torkian, H. (2018).** Application of ANN and ANFIS models in determining compressive strength of concrete. Journal of Soft Computing in Civil Engineering, Vol. 2, No. 1, pp. 62-70.
67. **Khan, M. A., Rehman, M., Khanam, P.A., Khuda, B.E., Kane, T.T. and Ashraf, A. (1997).** Awareness of sexually transmitted disease among women and services providers in rural Bangladesh, International Journal of STD and AIDS, Vol. 8, No. 11, pp. 688-696.
68. **King Monkut's Institute of Technology Ladkrabang-KMTL (2006).** Transmission model for dengue disease with and without the effect of extrinsic incubation period, Ladkrabang, Bankok, Thailand, Vol. 6, No. 2, 10520.
69. **Kirschner, D. (1999).** Dynamics of co-infection with M. Tuberculosis and HIV-1, Theoretical Population Biology, Vol. 55, No. 1, pp. 94-109.
70. **Kobe, F. T. (2020).** Mathematical Model of Controlling the Spread of Malaria Disease Using Intervention Strategies, Pure and Applied Mathematics Journal, Vol. 9, No. 6, pp. 101-108.
71. **Korobeinikov, A. (2009).** Global properties of SIR and SEIR epidemic models with the multiple parallel infectious stages, Bulletin of Mathematical Biology, Vol. 71, pp. 75-83.

72. **Kumar, S., Chauhan, R. P., Abdel-Aty, A. H. and Alharthi, M. R. (2021).** A study on transmission dynamics of HIV/AIDS model through fractional operators, Results in Physics, Vol. 22, pp. 103855.
73. **Lakovic, V. (2020).** Crisis management of android botnet detection using adaptive neuro-fuzzy inference system. Annals of Data Science, Vol. 7, No. 2, pp. 347-355.
74. **Lakshmikantham, V., Leela, S., Martynyuk, A. A. (1989).** Stability Analysis of Nonlinear Systems, Marcel Dekker Inc. New York.
75. **LaSalle, J. P. (1976).** The Stability of Dynamical Systems, in: CBMS-NSF Regional Conference Series in Applied Mathematics, SIAM, Philadelphia.
76. **Li, J. (2011).** Malaria model with stage-structured mosquitoes, Mathematical Biosciences and Engineering, Vol. 8, No. 3, pp. 753-768.
77. **Liu, R., Wu, J. and Zhu, H. (2007).** Media/psychological impact on multiple outbreaks of emerging infectious diseases, Computational and Mathematical Methods in Medicine, Vol. 8, pp. 153-164.
78. **Liu-Helmersson, J., Quam, M., Wilder-Smith, A., Stenlund, H., Ebi, K., Massad, E. and Rocklov, J. (2016).** Climate Change and Aedes Vectors: 21st Century Projections for Dengue Transmission in Europe, EBioMedicine, Vol. 7, pp. 267-277.
79. **Luxi, N., Giovanazzi, A., Capuano, A., Crisafulli, S., Cutroneo, P. M., Fantini, M. P. and Trifirò, G. (2021).** COVID-19 vaccination in pregnancy, paediatrics, immune compromised patients, and persons with history of allergy or prior SARS-CoV-2 infection: overview of current recommendations and pre-and post-marketing evidence for vaccine efficacy and safety. Drug safety, Vol. 44, No. 12, pp. 1247-1269.
80. **Ly. K. T. (2021).** A COVID-19 forecasting system using adaptive neuro-fuzzy inference, Finance Research Letters, Vol. 41, pp. 101844.
81. **Marino, S., Hogue, I. B., Ray, C. J. and Kirschner, D. E. (2008).** A methodology for performing global uncertainty and sensitivity analysis in systems biology, Journal of Theoretical Biology, Vol. 254, No. 1, pp. 178-196.
82. **Meng, L. and Zhu, W. (2022).** Analysis of SEIR epidemic patch model with nonlinear incidence rate, vaccination and quarantine strategies, Mathematics and Computers in Simulation, Vol. 200, pp. 489-503.
83. **Misra, A. K., Pal, S. and Gupta, R. K. (2023).** Modeling the Effect of TV and Social Media Advertisements on the Dynamics of Vector-Borne Disease Malaria, International Journal of Bifurcation and Chaos, Vol. 33, No. 3, 2350033.
84. **Mordecai, E. A., Cohen, J. M., Evans, M. V., Gudapati, P., Johnson, L. R., Lippi, C. A., Miazgowicz, K., Murdock, C. C., Rohr, J. R., Ryan, S. J., Savage, V., Shocket, M. S., Stewart Ibarra, A., Thomas, M. B. and Weikel, D. P. (2017).** Detecting the impact of temperature on

transmission of Zika, dengue, and chikungunya using mechanistic models, PLoS Neglected Tropical Diseases, Vol. 11, No. 4, e0005568.

85. **Morin, C. W., Comrie, A. C. and Ernst, K. (2013).** Climate and dengue transmission: evidence and implications, Environmental Health Perspectives, Vol. 121, No. (11-12) pp. 1264-1272.
86. **Mukandavire, Z. and Garira, W. (2007).** Effects of public health educational campaigns and the role of sex workers on the spread of HIV/AIDS among heterosexuals, Theoretical Population Biology, Vol. 72, pp. 346-365.
87. **Mushayabasa, S., Tchuenche, J. M., Bhunu, C. P., Gwasira-Ngarakana, E. (2011).** Modelling gonorrhoea and HIV co-interaction, Biosystems, Vol. 103, No. 1, pp. 27-37.
88. **Naresh, R., Sharma, D. and Tripathi, A. (2009).** Modelling the effect of tuberculosis on the spread of HIV infection in a population with density-dependent birth and death rate, Mathematical and Computer Modelling, Vol. 50, No. 7-8, pp. 1154-1166.
89. **Ndii, M. Z. and Adi, Y. A. (2021).** Understanding the effects of individual awareness and vector controls on malaria transmission dynamics using multiple optimal control, Chaos Solitons & Fractals, Vol. 153, 111476.
90. **Ngonghala, C. N., Ryan, S. J., Tesla, B., Demakovsky, L. R., Mordecai, E. A., Murdock, C. C. and Bonds, M. H. (2021).** Effects of changes in temperature on Zika dynamics and control, Journal of the Royal Society Interface, Vol. 18, No. 178, 20210165.
91. **Ngwa, G. A. (2004).** Modelling the dynamics of endemic malaria in growing populations, Discrete and Continuous Dynamical Systems B, Vol. 4, No. 4, pp. 1173-1202.
92. **Ngwa, G. A. and Shu, W. S. (2000).** A mathematical model for endemic malaria with variable human and mosquito populations, Mathematical and Computer Modelling, Vol. 32, No. 7-8, pp. 747-763.
93. **Noeiaghdam, S. and Micula, S. (2021).** Dynamical Strategy to Control the Accuracy of the Nonlinear Bio-Mathematical Model of Malaria Infection, Mathematics, Vol. 9, No. 9, 1031.
94. **Nuraini, N., Fauzi, I. S., Fakhruddin, M., Sopaheluwakan, A. and Soewono, E. (2021).** Climate-based dengue model in Semarang, Indonesia: Predictions and descriptive analysis, Infectious Disease Modelling, Vol. 6, pp. 598-611.
95. **Nwankwo, A. A. and Daniel, O. (2019).** A mathematical model for the population dynamics of malaria with a temperature dependent control, Differential Equations and Dynamical Systems, Vol. 30, No. 4, pp. 1-30.
96. **Okais, C., Roche, S., Kurzinger, M. L., Riche, B., Bricout, H., Derrough, T., Simondon, F. and Ecochard, R. (2010).** Methodology of the sensitivity analysis used for modeling an infectious disease, Vaccine, Vol. 28, No. 51, pp. 8132-8140.
97. **Okosun, K. O., Makinde, O. D. and Takaidza, I. (2013).** Impact of optimal control on the treatment of HIV/AIDS and screening of unaware infectives, Applied Mathematical Modelling, Vol. 37, pp. 3802-3820.

98. **Okuneye, K. and Gumel, A. B. (2017).** Analysis of a temperature and rainfall dependent model for malaria transmission dynamics, Mathematical Bioscience, Vol. 287, pp. 72-92.
99. **Pande, J. (2013).** Mathematical Modelling of the transmission dynamics of dengue with logistic human population growth, Dar es Salaam.
100. **Perveen, G., Rizwan, M. and Goel, N. (2019).** An ANFIS-based model for solar energy forecasting and its smart grid application. Engineering Reports, Vol. 1, No. 5, 12070.
101. **Rise, Z. R. and Ershadi, M. M. (2022).** Socioeconomic analysis of infectious diseases based on different scenarios using uncertain SEIAR system dynamics with effective subsystems and ANFIS, Journal of Economic and Administrative Sciences.
102. **Riyapan, P., Shuaib, S. E. and Intarasit, A. (2021).** A mathematical model of COVID-19 pandemic: A case study of Bangkok, Thailand. Computational and Mathematical Methods in Medicine, Vol. 2021, No.1, pp. 1-11.
103. **Roeger, L. I. W., Feng, Z. and Castillo-Chavez, C. (2009).** Modeling TB and HIV Co-infections, Mathematical Biosciences and Engineering, Vol. 6, No. 4, pp. 815-837.
104. **Romero-Leiton, J. P. and Ibarguen-Mondragon, E. (2019).** Stability analysis and optimal control intervention strategies of a malaria mathematical model, Applied Sciences, Vol. 21, pp. 184-218.
105. **Ross, R. (1911).** The prevention of malaria 2nd Edition, John Murray, London.
106. **Ross, R. (1916).** An application of the theory of probabilities to the study of a priori pathometry, Proceedings of the Royal Society A, Vol. 92, pp. 204-230.
107. **Ruan, S., Xiao, D. and Beier, J. C. (2008).** On the delayed Ross-Macdonald model for malaria transmission, Bulletin of Mathematical Biology, Vol. 70, No. 4, pp. 1098-1114.
108. **Sadeghieh, T., Sargeant, J. M., Greer, A. L., Berke, O., Dueymes, G., Gachon, P., Ogden, N. H. and Ng, V. (2021).** Zika virus outbreak in Brazil under current and future climate, Epidemics, Vol. 37, 100491.
109. **Sani, A., Kroese, D. P. and Pollett, P. K. (2007).** Stochastic models for the spread of HIV in a mobile heterosexual population, Mathematical Biosciences, Vol. 208, No. 1, pp. 98-124.
110. **Shen, M., Xiao, Y. and Rong L. (2015).** Global stability of an infection-age structured HIV-1 model linking within-host and between-host dynamics, Mathematical Biosciences, Vol. 263, pp. 37-50.
111. **Silva, C. J. and Torres, D.F.M. (2014).** Modeling TB-HIV Syndemic and Treatment, Journal of Applied Mathematics, 248407.
112. **Singh, A., Jain, M. and Sharma, G. C. (2013).** Stability and numerical analysis of malaria mTB-HIV/AIDS co-infection, International Journal of Engineering Transaction A: Basics, Vol. 26, pp. 729-742.
113. **Singh, R., Ali, S., Jain, M. and Raina, A. A. (2019).** Mathematical model for malaria with mosquito-dependent coefficient for human population with exposed class, Journal of National Science Foundation of Sri Lanka, Vol. 47, No. 2, pp. 185-198.

114. **Singh, R., Ali, S., Jain, M. and Rakhee (2016).** Epidemic model of HIV/AIDS transmission dynamics with different latent stages based on treatment, American Journal of Applied Mathematics. Vol. 4, No. 5, pp. 222-234.
115. **Smallbone, K. and Simeonidis, E. (2009).** Flux balance analysis: A geometric perspective, Journal of Theoretical Biology, Vol. 258, No. 2, pp. 311-315.
116. **Smith, R. J. and Wahl, L. M. (2005).** Drug resistance in an immunological model of HIV-1 infection with impulsive drug effects, Bulletin of Mathematical Biology, Vol. 67, pp. 783-813.
117. **Smith, T. A. M. and Mercer, G. N. (2014).** Complex behavior in dengue model with a seasonally varying vector population, Mathematical Biosciences, Vol. 248, pp. 22-30.
118. **Song, X., Zhou, X. and Zhao, X. (2010).** Properties of stability and Hopf bifurcation for a HIV infection model with delay time, Applied Mathematical Modelling, Vol. 34, No. 6, pp. 1511-1523.
119. **Tacconelli, E. and Cataldo, M. A. (2009).** Identifying risk factors for infections: The role of meta-analyses, Infection Disease Clinics North America, Vol. 23, No. 2, pp. 211-224.
120. **Taghikhani, R. and Gumel, A.B. (2018).** Mathematics of dengue transmission dynamics: Roles of vector vertical transmission and temperature fluctuations, Infectious Disease Modelling, Vol. 3, pp. 266-292.
121. **Tan, W. Y. (1991).** Some general stochastic model for the spread of AIDS and some simulation results, Mathematical and Computer Modelling, Vol. 15, No.2, pp. 19-39.
122. **Tan, Z., Quek, C. and Cheng, P. Y. (2011).** Stock trading with cycles: A financial application of ANFIS and reinforcement learning. Expert Systems with Applications, Vol. 38, No. 5, pp. 4741-4755.
123. **Tchoumi, S. Y., Rwezaura, H. and Tchuenche, J. M. (2023).** A mathematical model with numerical simulations for malaria transmission dynamics with differential susceptibility and partial immunity, Healthcare Analytics, Vol. 3, 100165.
124. **Ven den Driessche, P. and Watmough, J. (2002).** Reproduction numbers and sub-threshold endemic equilibria for compartmental models of disease transmission, Mathematical Biosciences, Vol. 180, pp. 29-48.
125. **Wang J., Zhang R. and Kuniya T. (2015).** Global dynamics for a class of age-infection HIV models with nonlinear infection rate, Journal of Mathematical Analysis and Application, Vol. 432, pp. 289-313.
126. **Wang, X., Tang, S. and Cheke, R. A. (2016).** A stage structured mosquito model incorporating effects of precipitation and daily temperature fluctuations, Journal of Theoretical Biology, Vol. 411, No. 21, pp. 27-36.
127. **Wang, Y., Wei, Y., Li, K., Jiang, X., Li, C., Yue, Q., Zee, B. C. and Chong, K. C. (2022).** Impact of extreme weather on dengue fever infection in four Asian countries: A modelling analysis, Environment International, Vol. 169, 107518.

128. **Wattanasirikosone, R. and Modnak, C. (2022).** Analysing transmission dynamics of HIV/AIDS with optimal control strategy and its controlled state, Journal of Biological Dynamics, Vol. 16, No. 1, pp. 499-527.
129. **Williams, C. R., Mincham, G., Faddy, H., Viennet, E., Ritchie, S. A. and Harley, D. (2016).** Projections of increased and decreased dengue incidence under climate change, Epidemiology and Infection, Vol. 144, No. 14, pp. 3091-3100.
130. **World Health Organization (2013).** Fact sheet on the World Malaria Report.
131. **Wu, H. and Tan, W. Y (2000).** Modelling the HIV epidemic: A state-space approach, Mathematical and Computer Modelling, Vol. 32, No. 1-2, pp. 197-215.
132. **Wu, P. and Zhao, H. (2021).** Mathematical analysis of an age-structured HIV/AIDS epidemic model with HAART and spatial diffusion, Nonlinear Analysis Real World Applications, Vol. 60, pp. 103289.
133. **Xiao, Y. and Zou, X. (2013).** Can multiple malaria species co-persist? SIAM Journal on Applied Mathematics, Vol. 73, No. 1, pp. 351-373.
134. **Xu, Z., Bambrick, H., Frentiu, F. D., Devine, G., Yakob, L., Williams, G. and Hu, W. (2020).** Projecting the future of dengue under climate change scenarios: Progress, uncertainties and research needs, PLoS Neglected Tropical Diseases, Vol. 14, No.3, e0008118.
135. **Yadollahpour, A., Nourozi, J., Mirbagheri, S. A., Simancas-Acevedo, E. and Trejo-Macotela, F. R. (2018).** Designing and implementing an ANFIS based medical decision support system to predict chronic kidney disease progression. Frontiers in physiology, Vol. 9, 1753.
136. **Yang, Q., Huo, H. F. and Xiang, H. (2023).** Analysis of an edge-based SEIR epidemic model with sexual and non-sexual transmission routes, Physica A: Statistical Mechanics and its Applications, Vol. 609, pp. 128340.
137. **Yovanna, A., Sanchez, C., Aerts, M., Shkedy, Z., Vickerman, P., Faggiano, F., Salamina, G. and Hens, N. (2013).** A mathematical model for HIV and hepatitis C co-infection and its assessment from a statistical perspective, Epidemics, Vol. 5, pp. 56-66.
138. **Yuan, X., Wang, F., Xue, Y. and Liu, M. (2018).** Global stability of an SIR model with differential infectivity on complex networks, Physica A: Statistical Mechanics and its Applications, Vol. 499, No. 1, pp. 443-456.
139. **Zhai, X., Li, W., Wei, F. and Mao, X. (2023).** Dynamics of an HIV/AIDS transmission model with protection awareness and fluctuations, Chaos, Solitons and Fractals, Vol. 169, 113224.
140. **Zhang, S. and Guo, H. (2018).** Global analysis of age-structured multi-stage epidemic models for infectious diseases, Applied Mathematics and Computation, Vol. 337, No. 15, pp. 214-233.

1. **Shoket Ali,** Ather Aziz Raina, Javid Iqbal and Rinku Mathur (2019): Mathematical Modelling and Stability Analysis of HIV/AIDS-TB Co-infection, Palestine Journal of Mathematics, Vol. 8, No. 2, pp. 380-391. (Scopus Indexed)
2. Ram Singh, **Shoket Ali,** Madhu Jain and Ather Aziz Raina (2019): Mathematical model for malaria with mosquito-dependent coefficient for human population with exposd class, Journal of the National Science Foundation of Sri Lanka, Vol. 47, No. 2, pp. 185-198. (SCIE Indexed)
3. Preety Kalra, **Shoket Ali** and Samuel Ocen (2024): Modelling on COVID-19 Control with Double and Booster-Dose Vaccination, Gene, Vol. 928, 148795. (Elsevier)
4. Preety Kalra and **Shoket Ali** (2024): Analysis of HIV/AIDS Transmission Dynamics among Female Sex Labourers, AIP Conference Proceeding, Vol. 2986, No. 1, pp. 030176(1-17). (Scopus Indexed)
5. Preety Kalra, **Shoket Ali** and Ather Aziz Raina (2024): A Study on Mathematical Modeling of HIV/AIDS, Malaria and Dengue fever, Exploring Medical Statistics: Biostatistics, Clinical Trials, and Epidemiology, IGI Global: International Academic Publisher, ISBN 9798369326558, pp. 279-295. (Scopus Indexed)
6. Ather Aziz Raina, **Shoket Ali,** Preety Kalra and Umar Muhammad Modibbo (2024): Adaptive Neuro-Fuzzy Inference System for Transmission Dynamics of HIV Virus with an SEIRS Epidemic Model, New Mathematics and Natural Computation. (Communicated)
7. Ather Aziz Raina, **Shoket Ali,** Preety Kalra and Umar Muhammad Modibbo (2024): A Mathematical Model of Logistic Human Population Growth and Vector Population for Dengue Transmission Dynamics, Journal of the Egyptian Mathematical Society. (Communicated)
8. **Shoket Ali,** Preety Kalra and Ather Aziz Raina (2024): Study the impact of communicable disease on population dynamics using mathematical modeling, Copyright Office, Government of India, Registration Number L-151985/2024.

Presentation/Participation in the Conferences

1. Presented paper entitled 'Mathematical Modeling in Transmission Dynamics of the spread of HIV/AIDS among female prostitutes' in three days online International Conference on Recent Advances in Computational Mathematics and Engineering, organized by Department of Applied Sciences & Humanities, at B K Birla Institute of Engineering & Technology, Pilani, on March 19-21, 2021.
2. Presented paper entitled 'A SIR Mathematical Model for the spread of Dengue fever and Its Simulations' in two days International Conference on Recent Trends in Multidisciplinary Research (ICORM-2020), organized by Eudoxia Research Centre, India, on September 19-20, 2020.
3. Presented paper entitled 'Mathematical Model for Transmission of HIV/AIDS through sexual contact with recurrence based on treatment' in 3rd National Conference on Recent Trends in Sciences, Social Sciences and Humanities, organized by Govt. Post Graduate College Rajouri, J&K, India, on January 19-20, 2019.
4. Presented paper entitled 'Mathematical Modeling and Analysis of Transmission Dynamics of HIV Virus' in International Conference on Recent Advances in Interdisciplinary Sciences, organized by Department of Electronics, University of Jammu in Collaboration with IEEE EDS Delhi Chapter and IETE Jammu Center on January 11-12, 2019.
5. Presented paper entitled 'Mathematical Modeling and Stability analysis of HIV/AIDS-TB Co-infection' in 5th Annual National Conference in Mathematics on Recent Developments in Algebra and Analysis, organized by Department of Mathematics, GGM Science College, a constituent college of the Cluster University of Jammu, on December 13-14, 2018.
6. Presented paper entitled 'Mathematical Modeling and Stability analysis of HIV/AIDS epidemic model' in National Conference on Recent Advances in Mathematics, organized by Department of Mathematics, Central University of Jammu, Jammu and Kashmir, India, on October 4-5, 2018.
7. Presented paper entitled 'Mathematical Modeling and Stability Analysis of a compartmental model of cell production Systems' in International Conference on Science and Technology: Trends and Challenges (ICSTTC-2018), organized by Faculty of Science, Gujranwala Guru Nanak Khalsa College, Civil Lines, Luddhiana, Punjab, India, on April 16-17th, 2018.
8. Presented paper entitled 'Mathematical Modeling and Stability analysis of Malaria, TB, HIV/AIDS Co-infection' in National Conference on Interdisciplinary Sciences and Humanities, organized by Govt. Post Graduate College Rajouri, J&K, India, on March 22nd, 2018.
9. Presented paper entitled 'Mathematical Modeling and Stability analysis of an SEIRS epidemic model with media' in Two Day National Science Conference, organized by Govt. Degree College Thannamandi, J&K, India, on March 19-20, 2018.

Participation in the Workshops/ Seminars

1. Participated in a National Webinar on "Applications of Mathematics in Recent Times" organized by Department of Mathematics, GHATAL RABINDRA SATABARSIKI MAHAVIDYALAYA, Ghatal, Paschim Medinipur, West Bengal, India, on June 19, 2023.
2. Participated in the 5 days SERB-funded Workshop "Nonlinear Phenomena in Mathematical Biology" (WoNPMB-2022) organized by Department of Applied Sciences, ABV-Indian Institute of Information Technology and Management, Gwalior, on December 19-23, 2022.
3. Participated in Online Three Day International FDP on "Research Methodology & Scientific Tools" organized by Department of Applied Sciences & Humanities, B K Birla Institute of Engineering & Technology, Pilani, Rajasthan, India, on 13th-15th April, 2021.
4. Participated in "Mathematics Seminar on Sciences & Engineering Applications" organized by Department of Mathematics, BITS Mesra, Ranchi, India, on 12th and 13th February, 2021.
5. Participated in a Webinar on "MATHEMATICS IN AICTE THRUST AREAS" organized by Department of Mathematics, Sri Sai Ram Engineering College, West Tambaram, Chennai, on October 10, 2020.
6. Participated in the One Week National E-Workshop on "Research Methodology" jointly organized by Department of Zoology and Department of Commerce, Govt. Lahiri P.G. College, Chirimiri, Koriya (C.G) India, from 8th to 14th September, 2020.
7. Participated in Three Days International Workshop on "Research Methodology in Higher Education" Organized by Department of Applied Sciences, Engineering College Banswara, from 3rd to 5th September, 2020.